

**THE ROLE OF
L31 PROTEINS IN
ACINETOBACTER BAUMANNII
ZINC HOMEOSTASIS**

BY

BETTY SURYAWATI

A thesis submitted for the Degree of Doctor of Philosophy

The School of Biological Sciences

Flinders University

November 2017

TABLE OF CONTENTS

| | |
|-----------------------------------------------------------------------------------------------------|-------------|
| TABLE OF FIGURES | VII |
| TABLE OF TABLES | X |
| ABSTRACT | XI |
| DECLARATION | XIII |
| ACKNOWLEDGMENTS | XIV |
| CONTRIBUTIONS | XV |
| PUBLICATIONS | XVI |
| CHAPTER 1 INTRODUCTION | 1 |
| 1.1 <i>Acinetobacter baumannii</i> is an emerging threat to human health | 2 |
| 1.2 The natural habitat of <i>A. baumannii</i> | 3 |
| 1.2.1 Infections caused by <i>A. baumannii</i> | 4 |
| 1.2.2 Emergence of multidrug resistant <i>A. baumannii</i> | 5 |
| 1.3 Characteristics of <i>A. baumannii</i> that contribute to its pathogenicity and virulence..... | 7 |
| 1.3.1 The ability to survive on biotic and abiotic surfaces | 7 |
| 1.3.2 The formation of pellicles and biofilms..... | 8 |
| 1.3.3 The ability to scavenge iron from an iron-limited environment..... | 11 |
| 1.3.4 Capsule | 12 |
| 1.3.5 Type I and Type IV Pili..... | 13 |
| 1.3.6 Type VI secretion system..... | 14 |
| 1.3.7 Lipooligosaccharides | 14 |
| 1.3.8 Outer membrane protein A..... | 15 |
| 1.3.9 Outer membrane vesicles | 16 |
| 1.4 Nutrient acquisition is crucial for bacterial virulence..... | 16 |
| 1.5 Bacterial metal ions: regulation and transport..... | 17 |
| 1.6 Regulation of Zn ²⁺ in bacterial cells..... | 19 |
| 1.6.1 Zn ²⁺ acquisition in bacterial cells | 21 |
| 1.6.2 Zn ²⁺ -efflux systems in bacterial cells | 23 |
| 1.7 Zn ²⁺ regulation, acquisition and efflux in <i>A. baumannii</i> | 25 |
| 1.8 Zinc plays a significant role in bacterial virulence and the response to oxidative stress | 31 |
| 1.8.1 Zinc in bacterial virulence and pathogenesis | 31 |
| 1.8.2 Zn ²⁺ and oxidative stress..... | 32 |

| | | |
|----------------------------------------------|-------------------------------------------------------------------------------------------------|-----------|
| 1.9 | Ribosomal proteins | 33 |
| 1.9.1 | L31 ribosomal proteins..... | 34 |
| 1.9.2 | L31 proteins and intracellular Zn ²⁺ storage | 35 |
| 1.9.3 | Other ribosomal proteins with Zn ²⁺ -binding motifs..... | 37 |
| 1.10 | Scope of this thesis | 38 |
| CHAPTER 2 MATERIALS AND METHODS | | 40 |
| 2.1 | Reagents, buffers, solutions and growth media..... | 41 |
| 2.2 | Bacterial strains and growth conditions | 41 |
| 2.3 | Bacterial phenotypic assays..... | 49 |
| 2.3.1 | Bacterial growth under Zn ²⁺ -limited and Zn ²⁺ -replete conditions | 49 |
| 2.3.2 | Minimum inhibitory concentration..... | 50 |
| 2.3.3 | Disk diffusion method for antibiotic resistance | 51 |
| 2.3.4 | Static biofilm assay | 51 |
| 2.3.5 | Eukaryotic cell adherence assays | 52 |
| 2.3.6 | Motility assay..... | 52 |
| 2.3.7 | Oxidative stress assay..... | 53 |
| 2.3.8 | Statistical analyses..... | 53 |
| 2.4 | Inductively coupled plasma-mass spectrometry analysis | 53 |
| 2.5 | DNA techniques | 54 |
| 2.5.1 | Plasmid DNA isolation | 54 |
| 2.5.2 | Genomic DNA isolation | 54 |
| 2.5.3 | Quantitation and quality assessment of DNA and RNA | 54 |
| 2.5.4 | Polymerase chain reaction | 55 |
| 2.5.5 | Agarose gel electrophoresis of DNA..... | 61 |
| 2.5.6 | Extraction and purification of DNA from agarose gel | 61 |
| 2.5.7 | Purification of DNA fragments | 61 |
| 2.5.8 | DNA sequencing | 62 |
| 2.6 | RNA Techniques | 62 |
| 2.6.1 | RNA isolation | 62 |
| 2.6.2 | Quantitative reverse transcription-PCR | 62 |
| 2.6.3 | Next-generation RNA sequencing analysis | 63 |
| 2.7 | DNA manipulations | 64 |
| 2.7.1 | Digestion and ligation..... | 64 |
| 2.7.2 | Conjugation | 64 |
| 2.7.3 | Preparation of chemically competent <i>E. coli</i> cells | 65 |
| 2.7.4 | Transformation of chemically competent <i>E. coli</i> cells | 65 |
| 2.7.5 | Preparation of electrocompetent <i>A. baumannii</i> cells..... | 65 |
| 2.7.6 | Transformation of electrocompetent <i>A. baumannii</i> cells..... | 66 |
| 2.7.7 | Construction of <i>A. baumannii</i> mutant strains by gene replacement..... | 66 |

| | | |
|----------------------------------------------------------------------------------------------------------------------------------|-------------------------------------------------------------------------------------------------------------------------------------------|------------|
| 2.7.8 | Generation of complementation strains..... | 68 |
| 2.8 | Bioinformatics analyses | 68 |
| 2.8.1 | Alignments and <i>in silico</i> manipulations..... | 68 |
| 2.8.2 | Genomic DNA analyses..... | 69 |
| 2.8.3 | RNA-seq analyses | 69 |
| 2.8.4 | Clusters of Orthologous Groups analysis | 69 |
| CHAPTER 3 INVESTIGATION OF <i>A. BAUMANNII</i> ATCC 17978 UNDER Zn²⁺-LIMITED CONDITIONS | | 70 |
| 3.1 | Introduction | 71 |
| 3.2 | Results and discussion | 72 |
| 3.2.1 | Optimisation of Zn ²⁺ -limited growth conditions..... | 72 |
| 3.2.2 | Optimisation of metal ion concentration for growth assays | 75 |
| 3.2.3 | The effect of Zn ²⁺ limitation on the bacterial phenotype | 77 |
| 3.2.3.1 | The effect of Zn ²⁺ limitation on <i>A. baumannii</i> motility | 77 |
| 3.2.3.2 | The effect of Zn ²⁺ limitation on biofilm formation in <i>A. baumannii</i> | 79 |
| 3.2.3.3 | The effect of Zn ²⁺ limitation on <i>A. baumannii</i> antibiotic resistance..... | 81 |
| 3.2.4 | Quantitative-reverse-transcriptase PCR measurements of selected <i>A. baumannii</i> genes under Zn ²⁺ -limited conditions..... | 84 |
| 3.2.5 | Global RNA expression changes in <i>A. baumannii</i> during growth in Zn ²⁺ -limited conditions | 84 |
| 3.2.5.1 | Functional categories of genes identified as differentially expressed..... | 87 |
| 3.2.5.2 | Categorisation of genes differentially expressed in response to Zn ²⁺ limitation in <i>A. baumannii</i> | 93 |
| 3.2.5.3 | Restriction of Zn ²⁺ affects the transcription of a number of transporter genes..... | 104 |
| 3.2.5.4 | Zn ²⁺ limitation increases the expression of TonB-dependent receptor genes..... | 106 |
| 3.2.5.5 | The effect of Zn ²⁺ limitation on known Zn ²⁺ -dependent proteins | 107 |
| 3.2.5.6 | The effect of Zn ²⁺ limitation on the transcription of ribosomal proteins | 108 |
| 3.2.5.7 | The effect of Zn ²⁺ -limitation on bacterial metabolism..... | 109 |
| 3.3 | Conclusions | 114 |
| CHAPTER 4 THE ROLE OF RPME1 AND RPME2 IN <i>A. BAUMANNII</i> ATCC 17978 IN Zn²⁺ HOMEOSTASIS AND VIRULENCE..... | | 116 |
| 4.1 | Introduction | 117 |
| 4.2 | Results and Discussion | 119 |

| | | |
|------------------------------------------------------------------------------------------------------------------------|------------------------------------------------------------------------------------------------------------------------------------------------------------------------|------------|
| 4.2.1 | Construction of <i>A. baumannii</i> ATCC 17978 <i>rpmE1</i> and <i>rpmE2</i> mutants and complemented derivatives | 119 |
| 4.2.2 | Growth of <i>A. baumannii</i> $\Delta rpmE1$ and $\Delta rpmE2$ mutants in LB broth | 127 |
| 4.2.3 | Growth of <i>A. baumannii</i> $\Delta rpmE1$ or $\Delta rpmE2$ mutants under Zn ²⁺ -limited conditions..... | 129 |
| 4.2.4 | The effect of <i>rpmE1</i> and <i>rpmE2</i> inactivation on the expression of genes involved in Zn ²⁺ homeostasis | 129 |
| 4.2.5 | The role of <i>rpmE1</i> and <i>rpmE2</i> in intracellular Zn ²⁺ levels in <i>A. baumannii</i> ATCC 17978 | 134 |
| 4.2.6 | Impact of the inactivation of <i>rpmE1</i> or <i>rpmE2</i> on the virulence characteristics of <i>A. baumannii</i> ATCC 17978..... | 136 |
| 4.2.6.1 | The effect of <i>rpmE1</i> or <i>rpmE2</i> inactivation on bacterial susceptibility to antibiotics..... | 138 |
| 4.2.6.2 | The effect of <i>rpmE1</i> or <i>rpmE2</i> inactivation in <i>A. baumannii</i> ATCC 17978 on bacterial motility..... | 140 |
| 4.2.6.3 | The effect of <i>rpmE1</i> or <i>rpmE2</i> inactivation on the ability to form biofilms..... | 143 |
| 4.2.6.4 | The effect of <i>rpmE1</i> or <i>rpmE2</i> inactivation on cellular adherence to eukaryotic cells | 145 |
| 4.2.6.5 | The effect of <i>rpmE1</i> or <i>rpmE2</i> inactivation on the ability of <i>A. baumannii</i> to survive oxidative stress | 145 |
| 4.3 | Conclusions | 149 |
| CHAPTER 5 TRANSCRIPTIONAL EFFECTS AFFORDED BY DELETION OF THE L31 GENES IN <i>A. BAUMANNII</i> ATCC 17978 | | 152 |
| 5.1 | Introduction | 153 |
| 5.2 | Results and Discussion | 154 |
| 5.2.1 | Growth of <i>A. baumannii</i> in both Zn ²⁺ -replete and Zn ²⁺ -limited conditions for RNA-sequencing analysis | 154 |
| 5.2.2 | Global transcriptomic analyses of the ATCC 17978 $\Delta rpmE1$ and $\Delta rpmE2$ mutants..... | 154 |
| 5.2.3 | Effect of the deletion of <i>rpmE1</i> or <i>rpmE2</i> on the <i>A. baumannii</i> ATCC 17978 transcriptome during growth in Zn ²⁺ -replete conditions | 156 |
| 5.2.3.1 | Effect of the inactivation of <i>rpmE1</i> on gene expression in <i>A. baumannii</i> ATCC 17978 grown under Zn ²⁺ -replete conditions | 156 |
| 5.2.3.1.1 | <i>Identification of COG functional categories</i> | <i>161</i> |
| 5.2.3.1.2 | <i>The effect of <i>rpmE1</i> deletion on the expression of Zn²⁺ homeostasis genes during growth in Zn²⁺-replete conditions</i> | <i>163</i> |

| | | |
|----------------------------------|------------------------------------------------------------------------------------------------------------------------------------------------------------|------------|
| 5.2.3.1.3 | <i>The effect of the inactivation of rpmE1 on the expression of the type VI secretion system</i> | 164 |
| 5.2.3.1.4 | <i>The effect of inactivation of rpmE1 on the expression of genes involved in bacterial carbohydrate metabolism</i> | 166 |
| 5.2.3.1.5 | <i>The effect of inactivation of rpmE1 on the expression of genes involved in lipid metabolism</i> | 168 |
| 5.2.3.2 | The effect of inactivation of <i>rpmE2</i> on the transcriptome of <i>A. baumannii</i> ATCC 17978 under Zn ²⁺ -replete conditions | 171 |
| 5.2.3.2.1 | <i>COG functional categories</i> | 175 |
| 5.2.3.2.2 | <i>The effect of deletion of rpmE2 on the heat shock protein HtpG</i> | 177 |
| 5.2.3.3 | Comparison of ATCC 17978 <i>rpmE1</i> and <i>rpmE2</i> inactivated strains under Zn ²⁺ -replete conditions | 178 |
| 5.2.3.4 | Shared and unique genes with altered expression in $\Delta rpmE1$ and $\Delta rpmE2$ mutants in Zn ²⁺ -replete conditions..... | 178 |
| 5.2.4 | The effect of Zn ²⁺ limitation on the transcriptomes of the $\Delta rpmE1$ and $\Delta rpmE2$ mutants | 186 |
| 5.2.4.1 | The effect of inactivation of <i>rpmE1</i> on gene expression in <i>A. baumannii</i> ATCC 17978 grown under Zn ²⁺ -limited conditions | 186 |
| 5.2.4.2 | The effect of inactivation of <i>rpmE2</i> on gene expression in <i>A. baumannii</i> ATCC 17978 when grown under Zn ²⁺ -limited conditions..... | 188 |
| 5.2.4.3 | Shared and unique gene expression changes between the <i>rpmE1</i> and <i>rpmE2</i> mutants grown in Zn ²⁺ -limited conditions | 190 |
| 5.3 | Conclusions | 190 |
| CHAPTER 6 DISCUSSION..... | | 195 |
| 6.1 | Introduction | 196 |
| 6.2 | Development of Zn ²⁺ -limited media | 197 |
| 6.3 | The importance of Zn ²⁺ in <i>A. baumannii</i> ATCC 17978 | 200 |
| 6.4 | The role of RpmE1 and RpmE2 in <i>A. baumannii</i> ATCC 17978 | 205 |
| 6.5 | Conclusions | 209 |

| | |
|----------------------------------------------------------------------------------------------------------------------------------------------------------------|------------|
| APPENDICES | 211 |
| Appendix 1 – Genes significantly up-regulated in <i>A. baumannii</i> ATCC 17978 under Zn ²⁺ -limited conditions (CP000521.1)..... | 212 |
| Appendix 2 – Genes significantly down-regulated in <i>A. baumannii</i> ATCC 17978 under Zn ²⁺ -limited conditions (CP000521.1)..... | 214 |
| Appendix 3 – Genes significantly up-regulated in <i>A. baumannii</i> ATCC 17978 $\Delta rpmE1$ under Zn ²⁺ -replete conditions (CP000521.1)..... | 220 |
| Appendix 4 – Genes significantly down-regulated in <i>A. baumannii</i> ATCC 17978 $\Delta rpmE1$ under Zn ²⁺ -replete conditions (CP000521.1)..... | 221 |
| Appendix 5 – Genes significantly up-regulated in <i>A. baumannii</i> ATCC 17978 $\Delta rpmE1$ under Zn ²⁺ -limited conditions (CP000521.1)..... | 228 |
| Appendix 6 – Genes significantly down-regulated in <i>A. baumannii</i> ATCC 17978 $\Delta rpmE1$ under Zn ²⁺ -limited conditions (CP000521.1)..... | 229 |
| Appendix 7 – Genes significantly up-regulated in <i>A. baumannii</i> ATCC 17978 $\Delta rpmE2$ under Zn ²⁺ -replete conditions (CP000521.1)..... | 231 |
| Appendix 8 – Genes significantly down-regulated in <i>A. baumannii</i> ATCC 17978 $\Delta rpmE2$ under Zn ²⁺ -replete conditions (CP000521.1)..... | 232 |
| Appendix 9 – Genes significantly up-regulated in <i>A. baumannii</i> ATCC 17978 $\Delta rpmE2$ under Zn ²⁺ -limited conditions (CP000521.1)..... | 236 |
| Appendix 10 – Genes significantly down-regulated in <i>A. baumannii</i> ATCC 17978 $\Delta rpmE2$ under Zn ²⁺ -limited conditions (CP000521.1)..... | 237 |
| Appendix 11 – Genes significantly up-regulated in <i>A. baumannii</i> ATCC 17978 under Zn ²⁺ -limited conditions (CP012004)..... | 238 |
| Appendix 12 – Genes significantly down-regulated in <i>A. baumannii</i> ATCC 17978 under Zn ²⁺ -limited conditions (CP012004)..... | 241 |
| Appendix 13 – Genes significantly up-regulated in <i>A. baumannii</i> ATCC 17978 $\Delta rpmE1$ under Zn ²⁺ -replete conditions (CP012004)..... | 246 |
| Appendix 14 – Genes significantly down-regulated in <i>A. baumannii</i> ATCC 17978 $\Delta rpmE1$ under Zn ²⁺ -replete conditions (CP012004)..... | 247 |
| Appendix 15 – Genes significantly up-regulated in <i>A. baumannii</i> ATCC 17978 $\Delta rpmE2$ under Zn ²⁺ -replete conditions (CP012004)..... | 254 |
| Appendix 16 – Genes significantly down-regulated in <i>A. baumannii</i> ATCC 17978 $\Delta rpmE2$ under Zn ²⁺ -replete conditions (CP012004)..... | 255 |
| Appendix 17 – Abbreviations | 261 |
| REFERENCES | 264 |

TABLE OF FIGURES

| | |
|---------------------------------------------------------------------------------------------------------------------------------------------------------------------------------------------------------------|-----|
| Figure 1.1: The mechanism of Zn ²⁺ acquisition and efflux in Gram-negative bacteria | 26 |
| Figure 1.2: The mechanism of Zn ²⁺ acquisition and efflux in Gram-positive bacteria | 27 |
| Figure 1.3: Schematic diagram of a putative Zur box in <i>A. baumannii</i> | 28 |
| Figure 1.4: The mechanism of Zn ²⁺ acquisition and efflux in <i>A. baumannii</i> | 30 |
| Figure 1.5: Mechanism of Zn ²⁺ mobilisation from the RpmE1 L31 ribosomal protein | 36 |
| Figure 3.1: The effect of supplementation of MH media with the metal ions Fe ²⁺ , Mn ²⁺ and Zn ²⁺ on <i>A. baumannii</i> ATCC 17978 growth..... | 74 |
| Figure 3.2: The effect of TPEN on <i>A. baumannii</i> ATCC 17978 growth | 76 |
| Figure 3.3: The effect of supplementation of Zn ²⁺ on <i>A. baumannii</i> ATCC 17978 growth in various M9 media | 78 |
| Figure 3.4: Comparison of biofilm production by <i>A. baumannii</i> ATCC 17978 in Zn ²⁺ -limited and Zn ²⁺ -replete media | 80 |
| Figure 3.5: qRT-PCR expression analysis of selected <i>A. baumannii</i> ATCC 17978 genes during growth in Zn ²⁺ -limited and Zn ²⁺ -replete conditions | 85 |
| Figure 3.6: Overview of the transcriptional responses to Zn ²⁺ limitation in <i>A. baumannii</i> ATCC 17978 | 88 |
| Figure 3.7: Correlation of Log ₂ -based fold changes for six genes showing altered expression in <i>A. baumannii</i> ATCC 17978 grown in Zn ²⁺ -limited conditions | 89 |
| Figure 3.8: Transcriptional changes in <i>A. baumannii</i> ATCC 17978 during growth in Zn ²⁺ -limited conditions relative to Zn ²⁺ -replete conditions, displayed by COG function | 91 |
| Figure 3.9: RNA expression of genes within the A1S_1697-1705 cluster in <i>A. baumannii</i> ATCC 17978 under Zn ²⁺ -limited conditions..... | 110 |
| Figure 3.10: RNA expression of genes within the A1S_1880-1894 cluster in <i>A. baumannii</i> ATCC 17978 under Zn ²⁺ -limited conditions..... | 112 |
| Figure 4.1: Amino acid sequence alignment of RpmE1 and RpmE2 from <i>A. baumannii</i> ATCC 17978 | 118 |
| Figure 4.2: Strategy via homologous recombination for generation of the <i>rpmE</i> mutants..... | 121 |
| Figure 4.3: Schematic showing the position of oligonucleotides used for PCR confirmation of the <i>rpmE1</i> mutation | 124 |
| Figure 4.4: PCR products generated to confirm successful deletion of <i>rpmE1</i> and insertion of the Ery cartridge in <i>A. baumannii</i> ATCC 17978..... | 125 |

| | |
|-------------------------------------------------------------------------------------------------------------------------------------------------------------------------------------------------------------|-----|
| Figure 4.5: PCR products generated to confirm successful deletion of <i>rpmE2</i> and insertion of Ery cartridge in <i>A. baumannii</i> ATCC 17978 | 126 |
| Figure 4.6: The effect of <i>rpmE1</i> and <i>rpmE2</i> inactivation on <i>A. baumannii</i> growth in LB medium | 128 |
| Figure 4.7: The effect of <i>rpmE1</i> inactivation on growth of <i>A. baumannii</i> in Zn^{2+} -replete and Zn^{2+} -limited media | 130 |
| Figure 4.8: The effect of <i>rpmE2</i> inactivation on growth of <i>A. baumannii</i> in Zn^{2+} -replete and Zn^{2+} -limited media | 131 |
| Figure 4.9: Level of intracellular Zn^{2+} in ATCC 17978, $\Delta rpmE1$ and $\Delta rpmE2$ cells grown in Zn^{2+} -replete and Zn^{2+} -limited conditions | 135 |
| Figure 4.10: Level of intracellular Mn^{2+} , Fe^{2+} and Mg^{2+} in ATCC 17978, $\Delta rpmE1$ and $\Delta rpmE2$ cells grown in Zn^{2+} -replete and Zn^{2+} -limited conditions... | 137 |
| Figure 4.11: Assessment of motility of <i>A. baumannii</i> ATCC 17978 WT, $\Delta rpmE1$ and $\Delta rpmE2$ strains carrying the pWH1266 shuttle vector, and $\Delta rpmE1$ carrying pWH <i>rpmE1</i> | 142 |
| Figure 4.12: Biofilm production by <i>A. baumannii</i> ATCC 17978, $\Delta rpmE1$ and $\Delta rpmE2$ strains grown under Zn^{2+} -limited conditions..... | 144 |
| Figure 4.13: Cellular adherence of <i>A. baumannii</i> ATCC 17978, $\Delta rpmE1$ and $\Delta rpmE2$ strains to the pneumocyte cell line type 2 A549 | 146 |
| Figure 4.14: Effect of oxidative stress on the growth of <i>A. baumannii</i> ATCC 17978 $\Delta rpmE1$ and $\Delta rpmE2$ strains..... | 148 |
| Figure 4.15: qRT-PCR expression analyses of selected stress-response genes during growth with/without paraquat | 150 |
| Figure 5.1: Transcriptional changes in the ATCC 17978 $\Delta rpmE1$ mutant in response to growth in Zn^{2+} -replete conditions | 158 |
| Figure 5.2: Correlation of the \log_2 -based fold changes for six genes showing altered expressed in the $\Delta rpmE1$ grown in Zn^{2+} -replete conditions..... | 160 |
| Figure 5.3: Transcriptional changes in the ATCC 17978 $\Delta rpmE1$ mutant relative to WT when both are grown in Zn^{2+} -replete conditions, displayed by COG function | 162 |
| Figure 5.4: RNA expression of genes within the A1S_1292-1310 cluster encoding the T6SS in <i>A. baumannii</i> ATCC 17978 $\Delta rpmE1$ compared to WT under Zn^{2+} -replete conditions | 165 |
| Figure 5.5: RNA expression of genes within the A1S_1699-1705 cluster in <i>A. baumannii</i> ATCC 17978 $\Delta rpmE1$ mutant compared to the WT under Zn^{2+} -replete conditions | 167 |
| Figure 5.6: RNA expression of genes within the A1S_1880-1894 cluster in <i>A. baumannii</i> ATCC 17978 $\Delta rpmE1$ mutant compared to the WT under Zn^{2+} -replete conditions | 169 |

| | |
|--------------------------------------------------------------------------------------------------------------------------------------------------------------------------------------------------------------------------------------------------------|-----|
| Figure 5.7: Correlation of Log ₂ -based fold changes for six genes showing altered expression in the <i>A. baumannii</i> ATCC 17978 $\Delta rpmE2$ mutant grown in Zn ²⁺ -limited and Zn ²⁺ -replete conditions | 173 |
| Figure 5.8: Transcriptional changes in the ATCC 17978 $\Delta rpmE2$ mutant in response to growth in Zn ²⁺ -replete conditions | 174 |
| Figure 5.9: Transcriptional changes in the ATCC 17978 $\Delta rpmE2$ mutant relative to WT when both are grown in Zn ²⁺ -replete conditions, displayed by COG function | 176 |
| Figure 5.10: RNA expression of genes within the T6SS A1S_1292-1310 cluster in <i>A. baumannii</i> ATCC 17978 $\Delta rpmE2$ compared to WT under Zn ²⁺ -replete conditions..... | 179 |
| Figure 5.11: RNA expression of genes within the A1S_1699-1705 cluster in $\Delta rpmE2$ 17978 <i>A. baumannii</i> ATCC 17978 compared to WT under Zn ²⁺ -replete conditions | 180 |
| Figure 5.12: RNA expression of genes within the A1S_1880-1894 cluster in <i>A. baumannii</i> ATCC 17978 $\Delta rpmE2$ compared to WT under Zn ²⁺ -replete conditions..... | 181 |
| Figure 5.13: Comparison of up-regulated genes in the $\Delta rpmE1$ and $\Delta rpmE2$ mutants compared to WT when grown in Zn ²⁺ -replete conditions | 183 |
| Figure 5.14: Comparison of down-regulated genes in the $\Delta rpmE1$ and $\Delta rpmE2$ mutants compared to WT when grown in Zn ²⁺ -replete conditions | 185 |
| Figure 5.15: Transcriptional changes in the ATCC 17978 $\Delta rpmE1$ mutant in response to growth in Zn ²⁺ -limited conditions | 187 |
| Figure 5.16: Transcriptional changes in the ATCC 17978 $\Delta rpmE2$ mutant in response to growth in Zn ²⁺ -limited conditions | 189 |
| Figure 5.17: Comparison of genes down-regulated in $\Delta rpmE1$ and $\Delta rpmE2$ mutants compared to WT when grown in Zn ²⁺ -limited conditions | 191 |
| Figure 5.18: Comparison of genes up-regulated in $\Delta rpmE1$ and $\Delta rpmE2$ mutants compared to WT when grown in Zn ²⁺ -limited conditions | 192 |

TABLE OF TABLES

| | |
|---------------------------------------------------------------------------------------------------------------------------------------------------------------------------------------------------------------------------------------------------|-----|
| Table 2.1: Media, buffers, solutions and reagents..... | 42 |
| Table 2.2: Bacterial strains used in this study | 44 |
| Table 2.3: Plasmids used in this study..... | 46 |
| Table 2.4: Oligonucleotides used in this study..... | 56 |
| Table 3.1: Antibiotic susceptibility of <i>A. baumannii</i> ATCC 17978 grown on MH agar with and without the addition of 30 μ M TPEN | 82 |
| Table 3.2: Validation of transcriptomic data generated from <i>A. baumannii</i> ATCC 17978 grown in Zn^{2+} -limited conditions | 90 |
| Table 3.3: <i>A. baumannii</i> ATCC 17978 genes with altered expression in response to Zn^{2+} -limitation as determined by RNA-seq | 94 |
| Table 4.1: Expression of zinc-associated genes in the $\Delta rpmE1$ and $\Delta rpmE2$ ATCC 17978 strains grown in Zn^{2+} -replete and Zn^{2+} -limited conditions determined by qRT-PCR..... | 133 |
| Table 4.2: Susceptibility of WT <i>A. baumannii</i> ATCC 17978, $\Delta rpmE1$ and $\Delta rpmE2$ strains to various antibiotics..... | 139 |
| Table 4.3: Susceptibility of WT <i>A. baumannii</i> ATCC 17978 and $\Delta rpmE1$ and $\Delta rpmE2$ strains to aminoglycoside antibiotics | 141 |
| Table 5.1: Validation of the transcriptomic data generated from the ATCC 17978 $\Delta rpmE1$ grown in Zn^{2+} -replete conditions by comparison of expression levels determined by RNA-seq and qRT-PCR analysis | 159 |
| Table 5.2: Validation of transcriptomic data generated from the ATCC 17978 $\Delta rpmE2$ mutant grown in Zn^{2+} -limited and Zn^{2+} -replete conditions by comparison of expression levels determined by RNA-seq and qRT-PCR analysis..... | 172 |

ABSTRACT

Acinetobacter baumannii is an important nosocomial pathogen associated with a wide variety of illnesses. Its role as a significant human pathogen has been well established. The ability to cause infections is not only multifactorial but also requires a number of cofactors; one of these factors is the metal ion zinc (Zn^{2+}). The role that Zn^{2+} plays in the pathogenesis of a number of bacteria has been well established and the ability to obtain and control the intracellular concentration of Zn^{2+} is critical for full bacterial virulence. In some bacteria the L31 proteins play a role in this Zn^{2+} homeostasis. Two paralagous genes encode two different L31 ribosomal proteins, RpmE1 and RpmE2, where one protein contains the Zn^{2+} -binding motif (RpmE1, C⁺) and the other does not (RpmE2, C⁻ form). The ability of the bacteria to alternate between these two L31 forms effectively increases the availability of Zn^{2+} during growth in Zn^{2+} -limited media, allowing for Zn^{2+} to be available for use in metabolically critical cell functions. In *A. baumannii*, little is known about the role of Zn^{2+} and if it can assist in colonisation of host niches. Additionally, how RpmE1 and RpmE2 function has not been elucidated. This projects aims to examine the effect of Zn^{2+} limitation on *A. baumannii* and investigate the precise role the L31 ribosomal proteins play in *A. baumannii* intracellular Zn^{2+} and in virulence.

The effect of Zn^{2+} deficiency on *A. baumannii* phenotypes and global gene expression responses were examined. The results revealed that Zn^{2+} limitation affected bacterial growth, biofilm formation, and susceptibility to antibiotics. The RNA-seq transcriptomic analysis revealed that *A. baumannii* showed a strong transcriptional response to Zn^{2+} limitation, predominantly via increased expression of Zn^{2+} -acquisition mechanisms and other ion transporters and receptors. Genes previously known to contain a Zur-binding site were up-regulated, however many genes which do not contain this motif were also affected indicating that these are Zn^{2+} dependant, including genes involved in bacterial virulence. Moreover, many genes were also differentially expressed under these conditions involving diverse processes other than Zn^{2+} acquisition, such as carbohydrate, lipid, secondary

metabolites biosynthesis, transport, and catabolism, and genes involve in energy production and conversion.

To investigate the role of L31 proteins in *A. baumannii* ATCC 17978 two individual deletion mutants ($\Delta rpmE1$ and $\Delta rpmE2$) were constructed. The effects of the inactivation of these genes were examined at a phenotypic and global transcriptional level. The $\Delta rpmE1$ mutant showed changed in multiple bacterial phenotypes, including a slight growth defect in Zn^{2+} -limited medium, a reduction in motility, an impairment in biofilm formation and an increased sensitivity to oxidative stress. The $\Delta rpmE2$ mutant also showed similar changes in phenotypes as except that the motility was not significantly affected. In addition, when grown in Zn^{2+} -limited medium, the the levels of intracellular Zn^{2+} in both mutant strains were 25% lower compared to the parent.

The unique effect of the deletion of *rpmE1* when cells were grown in Zn^{2+} -replete conditions was the reduced expression of the Zur global transcription repressor involved in Zn^{2+} homeostasis. Zur negatively regulates genes that have a Zur-binding site which include *rpmE2*, A1S_0146, A1S_0452, A1S_0453, A1S_2829, A1S_0391, A1S_3411, and A1S_3412. In contrast, in $\Delta rpmE2$ most of the genes encoding ribosomal proteins were highly up-regulated. The RNA-seq analysis revealed that there were a large number of shared genes differentially expressed in both mutants. This included genes involved in; a Type VI secretion system (A1S_1292-1310), lipid metabolism (A1S_1699-1705), carbohydrate metabolism (A1S_1880-1894) and the *csuABABCDE* cluster (A1S_2213-2218). All of these showed decreased expression in both Zn^{2+} -replete and Zn^{2+} -limited conditions. Thus, these alterations show an association between these ribosomal proteins beyond sharing the same function as a part of the ribosomal complex.

In conclusion, the transcriptional changes in response to the deletion of L31 ribosomal proteins showed pleiotropic effects. The data from phenotypic assays, inductively coupled plasma mass spectrometry, and RNA-seq analysis revealed that *rpmE1* and *rpmE2* play significant roles in *A. baumannii* ATCC 17978, not only in response to Zn^{2+} limitation, but also in various bacterial phenotype and virulence features.

DECLARATION

'I certify that this thesis does not incorporate without acknowledgment any material previously submitted for a degree or diploma in any university; and that to the best of my knowledge and belief it does not contain any material previously published or written by another person except where due reference is made in the text.'

Betty Suryawati

16th November 2017

ACKNOWLEDGMENTS

First of all I would like to thank my supervisor Professor Melissa Brown for giving me the opportunity to conduct my PhD project in her lab. Your support and advice throughout the last few years allowed me to get to this stage. I would also like to express my deepest thanks and sincere appreciation to my co-supervisor Dr Uwe Stroehler for his significant help and guidance through out the the project and for completing the thesis. I will never forget your endless support.

I would like to thank to Sylvia, Mohsen, Sarah, Felise, Jenny, Michelle, Hang, Hayden, and Jan who have gave enjoyable experience working in the lab for the last few years. I am thankful to Motiur, Nguyen and Samra for sharing experience; and thanks to Ita, Lina and Aini for our friendship. For my husband, thank you for your understanding, encouragement, and endless support; and for my children: Hasna, Naja, and Faris all of you always give happines and strength for all the time I spent here.

Finally, thanks to Endeavour program which give the scholarship for me to undertake this Phd program in Flinders University.

CONTRIBUTIONS

Dr Shashikanth Marri (Flinders University, Australia) assisted with processing of the transcriptomic data.

Mr Jason Young (Flinders University, Australia) conducted ICP-MS analysis.

PUBLICATIONS

Abstracts:

Suryawati B, Stroehler UH, and Brown MH. The role of L31 ribosomal proteins on *Acinetobacter baumannii* virulence. *BacPath Conference*, Brisbane, Australia October 2013.

Suryawati B, Stroehler UH, and Brown MH. The role of L31 ribosomal proteins on *Acinetobacter baumannii* virulence. *School of Biology Postgraduate Conference 2014*, Flinders University, Adelaide, South Australia, Australia November 2014.

Suryawati B, Stroehler UH, and Brown MH. The role of L31 ribosomal proteins on *Acinetobacter baumannii* zinc homeostasis. *Australian Scientific Meeting (ASM)*, Melbourne, Australia, July 2014.

Suryawati B, Stroehler UH, and Brown MH. The role of L31 ribosomal proteins on *Acinetobacter baumannii* zinc homeostasis. *The 9th International BioMetals Symposium*, Duke University, Durham, North Carolina, USA, July 2014.

Manuscripts:

Suryawati B, Stroehler UH, and Brown MH. The phenotypic and transcriptomic response of *Acinetobacter baumannii* ATCC 17978 to zinc limitation. Manuscript in preparation.

Suryawati B, Stroehler UH, and Brown MH. The role of L31 ribosomal proteins in zinc homeostasis and virulence characteristics of *Acinetobacter baumannii*. Manuscript in preparation.

CHAPTER 1
INTRODUCTION

1.1 *Acinetobacter baumannii* is an emerging threat to human health

The human bacterial pathogen *Acinetobacter baumannii* is a Gram-negative coccobacilli belonging to the gamma-proteobacteria group and the *Acinetobacter* genus. Members of this genus are non-motile, oxidase-negative, non-fermentive that grow in strictly aerobic conditions and their shape varies from rod to coccoidal under different growth conditions (Peleg *et al.* 2008). *A. baumannii* has emerged as one of the leading causes of hospital-acquired infections worldwide (Consales *et al.* 2011; Gentile *et al.* 2014). The pathogenicity of this organism is partly due to its multidrug resistant (MDR) nature and ability to form biofilms on abiotic surfaces, which facilitates long-term persistence in the hospital setting (Espinal *et al.* 2012; Gentile *et al.* 2014; Pour *et al.* 2011). Another factor that has over time enhanced the virulence potential of *A. baumannii* is its ability to undergo genetic exchange, which enables the uptake of genes from other pathogens. The acquisition of antibiotic resistance frequently occurs via horizontal transfer of genes between different species in the environment or in hospital settings (Rumbo *et al.* 2011). Thus, the combination of environmental resilience and the acquisition of a wide range of resistance determinants render *A. baumannii* a successful nosocomial pathogen (Jawad *et al.* 1998; Perez *et al.* 2007).

A. baumannii possesses a number of antibiotic resistance mechanisms and the emergence of MDR *A. baumannii* isolates has increased the number of untreatable infections and the subsequent fatality rate (McConnell *et al.* 2012). The mortality rate for bacteraemia caused by *A. baumannii* ranges from 30% to 60% (Chuang *et al.* 2011; Lee *et al.* 2011). In addition, *A. baumannii* infection inevitably results in longer hospital stays with patients requiring additional treatment, significantly increasing the cost to the health-care system. A study examining infections with carbapenem resistant *A. baumannii* in intensive-care units (ICU) revealed that carbapenem resistant *A. baumannii* was associated with higher mortality, and an increase in both the length and cost of hospital stays (Lemos *et al.* 2014). The higher mortality rate associated with MDR *A. baumannii* is due to the highly limited therapeutic options available for treatment of infected patients

(Lemos *et al.* 2014). Moreover, infections caused by *A. baumannii* which are resistant to all clinically used antibiotics also have been reported (Gulen *et al.* 2015). Overall, the trend of increasing resistance to numerous classes of antibiotics appears to be continuing for this pathogen.

1.2 The natural habitat of *A. baumannii*

Members of the genus *Acinetobacter* are considered ubiquitous organisms as they can be found in many different ecological niches and can also be part of human skin flora (Peleg *et al.* 2008). Despite this, the natural reservoir for the *A. baumannii* species is not clear. *A. baumannii* has been recovered from soil, water, animals, and humans leading some to conclude that *A. baumannii*, like other species within the genus, is ubiquitous in nature (Fournier and Richet 2006). It has been reported that *A. baumannii* (and its close relatives of clinical importance) can be isolated from patients and hospital environmental sources during outbreaks, however, no known natural habitat has been identified for this species outside the clinical setting (Peleg *et al.* 2008). *A. baumannii* is also thought to be part of the normal human flora; a study showed that up to 43% of non-hospitalised individuals were colonised with *Acinetobacter* species (Seifert *et al.* 1997). The most frequently isolated species were *A. Iwoffii* (58%), *A. johnsonii* (20%), *A. junii* (10%) and *Acinetobacter* genomic species 3 (5%). However, *A. baumannii* was found only rarely on humans (Seifert *et al.* 1997).

Using information on ecology, epidemiology and antibiotic resistance phenotype, *Acinetobacter* spp. can be classified into three major overlapping groups (Towner 2009). The first one is the MDR group and includes *A. baumannii* and closely related members of *A. baumannii* complex. These strains have all been isolated from medical environments and equipment, medical personnel and hospitalised patients. Strain typing of *A. baumannii* clinical isolates by various methods showed the genetic diversity among this pathogen (Zarrilli *et al.* 2013). Multilocus sequence typing analysis divided clinical isolates of *A. baumannii* into 59 distinct sequence types (Diancourt *et al.* 2010). Three of these sequence types were comprised of 15 or more strains and were constituted of strains previously

identified as international clone I, II and III (Diancourt *et al.* 2010). The second group represents strains that have been isolated from human and animal skin flora. Included in this group are strains belonging to the species *A. johnsonii*, *A. lwoffii* and *A. radioresistens*. The last group represents strains isolated from the environment, such as soil and water, and mainly comprises strains belonging to the species *A. calcoaceticus*, and *A. johnsonii* (Towner 2009).

1.2.1 Infections caused by *A. baumannii*

Most *A. baumannii* infections occur in health-care settings worldwide and in particular amongst immunocompromised patients admitted to ICUs (Ansaldi *et al.* 2011; Lee *et al.* 2012b). Factors predisposing an individual to infections include previous antibiotic therapy, major surgery, burns, immunosuppression and/or the presence of invasive devices. The majority of *A. baumannii* infections occur in ICUs where *A. baumannii* is responsible for ventilator-associated pneumonia in 4% to 7% of cases (Lazureanu *et al.* 2016; Liu *et al.* 2015).

A. baumannii is associated with a diverse range of infections including bacteremia, ventilator-associated pneumonia, urinary tract infections and surgical site infections (Ansaldi *et al.* 2011). This pathogen can be the cause of meningitis and other central nervous system disease, particularly in patients who have undergone neurological surgery (Ho *et al.* 2007; Ni *et al.* 2015). This bacterium is also the causative agent of serious burn infections (Leseva *et al.* 2013; Tekin *et al.* 2014). Additionally, *A. baumannii* has been identified as the causative agent in osteomyelitis, endocarditis, and soft tissue infections (Chen *et al.* 2015; McConnell *et al.* 2013; Patel *et al.* 2011).

Although most *A. baumannii* infections occur in a clinical setting, there has been evidence that *A. baumannii* also plays an important role in community-acquired infections (Dexter *et al.* 2015; Vila and Pachon 2011). Fatal cases of community-acquired *A. baumannii* pneumonia have occurred in patients with a range of risk factors including; male gender, old age, alcoholism, cancer, cerebrovascular disease, diabetes mellitus, renal disease and liver cirrhosis (Chen *et al.* 2001; Dexter *et al.* 2015). Community-acquired infections of *A. baumannii* have

also resulted in meningitis (Ozaki *et al.* 2009), bacteraemic cellulitis (Chiang *et al.* 2003), urinary tract infections (Solak *et al.* 2011) and septic shock (Eugenin 2013). *A. baumannii* is the most common bacteria isolated from wounds of natural disasters and war survivors (Calhoun *et al.* 2008). A study in the National Naval Medical Centre (USA) on post war wounds in US troops from Iraq and Afghanistan demonstrated that *A. baumannii* was the most prevalent organism isolated, accounting for 63% of all isolates (Eveillard *et al.* 2013). *A. baumannii* was also the most cause of infection, representing of 65%, of the Bali bombing victims admitted to Perth Royal hospital (Australia) (Heath *et al.* 2003).

1.2.2 Emergence of multidrug resistant *A. baumannii*

MDR strains are defined as those that show resistance to at least three different classes of antimicrobial agents. Many *Acinetobacter* spp. exhibit intrinsic resistance to many antibiotics including amoxicillin, narrow-spectrum cephalosporins, ertapenem, trimethoprim and chloramphenicol (Bonnin *et al.* 2013). *A. baumannii* produces β -lactamases encoded either chromosomally or on native (or acquired) plasmids. Resistance to β -lactam antibiotics in *A. baumannii* is mediated by an intrinsic AmpC-type cephalosporinase that is encoded by *blaADC*-like genes (Bou and Martinez-Beltran 2000). AmpC enzymes are class C β -lactamases and confer resistance to all penicillins and extended-spectrum cephalosporins, except cefepime and β -lactam- β -lactamase inhibitor combinations (Jacoby 2009). In addition, along with other Gram-negative pathogens, *A. baumannii* can acquire new resistance genes via plasmids, integrons, and transposons (Misbah *et al.* 2005). The activation of *ampC* mediated by the acquisition of insertion sequences *ISAbal* or *ISAbal25* upstream of this gene, has been known to increase resistance to cephalosporins (Hamidian and Hall 2014). Other β -lactamases, including OXA-23, OXA-24 (and the identical OXA-40), OXA-58, OXA-143 and OXA-235 that are able to hydrolyse carbapenems have been increasingly reported as playing a role in carbapenem resistance in *A. baumannii* (Nigro and Hall 2015).

In addition, metallo β -lactamases (MBL) are a diverse set of β -lactamase enzymes which have also been identified in *A. baumannii* isolates. The MBLs require one or two zinc (Zn) ions in their active sites to catalyse the hydrolysis of all classes of β -lactam antibiotics (Tamilselvi and Mugesh 2008). MBL types in *A. baumannii* can be grouped into the following four types; imipenemase, Verona integron-encoded metallo- β -lactamase (VIM), Seoul imipenemase and New Delhi metallo- β -lactamase (NDM) (Bonnin *et al.* 2013). Furthermore, isolates of *A. baumannii* producing extended spectrum β -lactamases (ESBL) have also been reported (Naas *et al.* 2006). Strains with the PER-1 type of ESBL have been reported in Turkey, Korea and France while strains producing the VEB-1 and CTX-M-2 ESBL types were reported in France and Korea, respectively (Naas *et al.* 2006).

The emergence of MDR *A. baumannii* is not only due to the wide range of β -lactamases that can be produced but also can be attributed to the carriage of many antibiotic resistance mechanisms. Resistance to quinolones and fluoroquinolones in *A. baumannii* occurs as the result of mutations in the DNA gyrase (Coyne *et al.* 2011). In addition, resistance to quinolones can be efflux-mediated involving the resistance nodulation division (RND) efflux pumps AdeABC, AdeIJK and AdeFGH (Coyne *et al.* 2011). Resistance to aminoglycosides in *A. baumannii* can occur via the use of efflux pumps or by the expression of aminoglycoside-modifying enzymes such as acetyl transferases, nucleotidyl transferases, and phosphotransferases (Roca *et al.* 2012). In addition, resistance to aminoglycosides in *A. baumannii* can be spread via the acquisition of the pRAY plasmid harbouring an *aadB*-kanamycin, gentamicin and tobramycin resistance cassette (Nigro and Hall 2016). Resistance to antibiotics within the cycline group has also been reported; tetracycline resistance in *A. baumannii* is mediated by the Tet efflux pumps that confer a high-level resistance to tetracycline but are ineffective against tigecycline (a new member of the cycline family) (Coyne *et al.* 2011). Nevertheless, an increase in the resistance rates to tigecycline has been reported in multiple clones of MDR *A. baumannii* that is likely due to the over-expression of an intrinsic efflux pump (Ade-derivate system) (Chuang *et al.* 2014; Coyne *et al.* 2011). Resistance to the antibiotic colistin, considered to be a last resort treatment for MDR *A. baumannii* infections, is now also being reported worldwide (Cai *et al.* 2012). Alarmingly, both tigecycline and

colistin represent a last treatment choice for infections caused by MDR *A. baumannii*.

1.3 Characteristics of *A. baumannii* that contribute to its pathogenicity and virulence

A. baumannii strains have a number of characteristics that contribute to their pathogenicity. These factors include; its ability to adhere to abiotic and biotic surfaces (Eijkelkamp *et al.* 2011b), the ability to scavenge iron (Fe) in Fe²⁺-limited environments (Eijkelkamp *et al.* 2011a), and the ability to rapidly acquire resistance to antibiotics, via horizontal gene transfer and homologous recombination (Snitkin *et al.* 2011) or by a DNA damage-inducible response (Norton *et al.* 2013). In addition, the type VI secretion system (T6SS), a large protein complex which can transfer substrates across the cell, has been identified in *A. baumannii* genomes (Eijkelkamp *et al.* 2014b). These characteristics have allowed *A. baumannii* to persist in patients and the hospital environment and have led to the global emergence of MDR strains. In addition, *A. baumannii* quickly adapts to new or challenging environments, not only by the horizontal acquisition of genetic traits which is contributing to the evolution of non-MDR ancestors into MDR outbreak strains, but also by recombination events within the genome (Snitkin *et al.* 2011). Investigation of *A. baumannii* genome sequences and a closer inspection of recombined regions indicate that this species can shuffle, add, and/or delete genes, many of which encode important virulence factors including cell surface proteins and O-antigen/capsule (Snitkin *et al.* 2011).

1.3.1 The ability to survive on biotic and abiotic surfaces

A. baumannii has the ability to adhere to eukaryotic cells, which is crucial for initial adherence and subsequent colonisation of host tissue. Interestingly, the capacity to adhere to eukaryotic lung epithelial cells varies significantly between isolates as analysis of strains representing different clonal groups revealed that there are no clonal-specific trends (Eijkelkamp *et al.* 2011b). Adherence is multifactorial with a number of proteins known to play a role. A biofilm-associated

protein (Bap) is involved in the adherence to normal human bronchial epithelial cells and human neonatal keratinocytes (Brossard and Campagnari 2012). A study examining adherence in the *A. baumannii* strain ATCC 19606^T revealed that the outer membrane fibronectin binding protein, outer membrane protein (Omp)A, also plays an important role in the interaction between this bacteria and human lung epithelial cells (Smani *et al.* 2012).

A. baumannii can survive and persist on a range of abiotic surfaces in health-care facilities including floors, doors and curtains. Equipment such as portable X-ray and wheelchairs can be the source of *A. baumannii* infection due to aerolisation of the organism (Munoz-Price *et al.* 2013). Furthermore, adherence and persistence of *A. baumannii* on the surfaces of medical equipment and in-dwelling medical devices, including ventilators or catheters, is common and can result in pneumonia, urinary tracts infections and bacteremia (Brossard and Campagnari 2012). Moreover, abiotic surfaces can be colonised or repeatedly recolonised from reservoirs such as infected patients or the introduction of contaminated equipment into the area (Raad *et al.* 2008). The ability to survive for a prolonged period on dry surfaces, combined with the high level of antibiotic resistance, contribute to persistence of *A. baumannii* and complicates eradication during outbreaks (Brossard and Campagnari 2012). The capacity of this organism to survive and cause disease in the hospital environment can be reduced by the implementation of effective control measures, including environmental decontamination with hypochlorite solution (Villegas and Hartstein 2003) or the use of vaporised hydrogen peroxide in long-term acute care hospital settings (Ray *et al.* 2010).

1.3.2 The formation of pellicles and biofilms

Biofilms consist of a structured community of microorganisms enclosed in a self-produced extracellular polymer matrix. The matrix of the biofilm is responsible for adhesion to both biological and non-biological surfaces, and for maintaining the cohesion of the biofilm. Depending on the microorganisms within the biofilm, the matrix may contain polysaccharides, proteins and extracellular DNA (Wu *et al.* 2013). Clinical isolates of *A. baumannii* have been shown to form a biofilm at the

interface between liquid and solid media as well between liquid media and the air interface; the latter biofilm represents a special form of biofilm known as a pellicle (Giles *et al.* 2015). A critical component of the *A. baumannii* cell needed for biofilm formation is the Csu pili (Harding *et al.* 2013). *A. baumannii* can produce type I pili and type IV pili that are believed to play a role in motility and biofilm formation (Harding *et al.* 2013).

The type I pili are encoded by the *csuABABCDE* chaperone usher complex and the fimbriae gene cluster (A1S_1507-1510 in ATCC 17978) (Harding *et al.* 2013). Expression of *csuABABCDE* is controlled by a two-component regulatory system BfmRS (Tomaras *et al.* 2003). Insertional inactivation of the BfmR response regulator in *A. baumannii* resulted in a loss of expression of the *csuABABCDE* operon, a subsequent loss of pili production and reduced biofilm formation (as measured on a plastic surface) (Tomaras *et al.*, 2008). However, inactivation of BfmRS did not completely abolish biofilm production, indicating that a range of different environmental stimuli could be involved in inducing biofilm formation and that the BfmR regulator may crosstalk with the sensor kinase in other two-component regulator systems (Tomaras *et al.*, 2008). The significant role of *csuABABCDE* in biofilm formation has been also shown using a *csuE* mutant in ATCC 19606^T. This *csuE* mutant produced significantly less biofilm, indicating that expression of the chaperone-usher secretion system is required for pili formation and attachment to plastic surfaces (Tomaras *et al.* 2003). The ATCC 17978 gene cluster A1S_1507-1510, encoding fimbrial biosynthesis proteins is similarly thought to play a role in pellicle formation (Eijkelkamp *et al.* 2014b). The fimbrial gene within this gene cluster (A1S_1507) as well as the *csu* genes, are highly expressed in ATCC 17978 biofilm cells compared to expression in planktonic cells (Rumbo-Feal *et al.* 2013).

The expression of OmpA has also been identified as important in *A. baumannii* ATCC 19606^T for biofilm formation on abiotic surfaces (Gaddy *et al.* 2009). Additionally, the *A. baumannii* protein Bap is expressed on the cell surface and is important for adherence to eukaryotic cells and for mature biofilm formation on various clinical equipment (Brossard and Campagnari 2012; Loehfelm *et al.* 2008). Carbohydrate analysis has confirmed that pellicle matrices contain

carbohydrate-rich material and that the exopolysaccharide produced by *A. baumannii* contributes to pellicle formation (Nait Chabane *et al.* 2014).

Recently, a study using an *A. baumannii* ATCC 17978 hyper-motile strain (17978hm) identified three genes critical for pellicle formation, namely *cpdA* (involved in degradation of cyclic adenosine monophosphate), A1S_0112 and A1S_0115 (required in the production of a secondary metabolite) (Giles *et al.* 2015). A1S_0112 and A1S_0115 mutant strains showed less pellicle formation than the wild-type (WT) strain and the expression of A1S_0112 and A1S_0115 was down-regulated in the *cpdA* mutant (Giles *et al.* 2015). This indicated that these three genes were playing role in pellicle formation. Together, these findings show that biofilm and pellicle formation by *A. baumannii* on abiotic surfaces is a multistep process that involves several cellular structures and functions (Gaddy *et al.* 2009).

Biofilm formation is responsive to changes in specific environmental conditions, including intracellular metal availability (Gaddy *et al.* 2009). A study of MDR *A. baumannii* clinical isolates showed that in the presence of the chelating agent ethylenediaminetetraacetic acid (EDTA) the ability to form biofilms was markedly reduced (Lee *et al.* 2008). A global transcriptomic analysis of ATCC 17978 grown under Fe²⁺-chelated conditions showed that *csu* pili gene expression was reduced indicating that Fe²⁺ availability may also be involved in biofilm formation (Eijkelkamp *et al.* 2011b).

The capacity to form a biofilm increases the resistance of the bacteria to desiccation and to a variety of antibacterial drugs (Greene *et al.* 2016; Gurung *et al.* 2013; Rao *et al.* 2008). In addition, the horizontal transfer of genes is greatly enhanced within biofilm communities, thereby facilitating the spread of antibiotic resistance amongst the bacterial population (Lee *et al.* 2008). Thus, the capability to form biofilms can lead to greater persistence of the bacteria in the medical environment where they are subjected to stresses such as antibiotics and disinfectants. Within the infected host, biofilms also protect bacteria against components of the immune system and thereby enhance the virulence capacity of biofilm producing strains (McConnell *et al.* 2012; Wu *et al.* 2013).

1.3.3 The ability to scavenge iron from an iron-limited environment

One of the requirements for *A. baumannii* survival, successful invasion and colonisation, is the essential micronutrient Fe^{2+} . However, the bioavailability of Fe^{2+} within the host is extremely low due to the host's ability to sequester free Fe^{2+} (Weinberg 2009) leading to the phenomenon known as "nutritional immunity" (Hood 2012; Weinberg 2009). Fe^{2+} acquisition is crucial for persistence of pathogens inside the host and it has been reported that most clinical *A. baumannii* strains have the ability to grow under Fe^{2+} -limiting conditions (Eijkelkamp *et al.* 2011a). *A. baumannii* cells recruit Fe^{2+} by expressing specialised outer membrane proteins that directly bind Fe^{2+} or heme from the extracellular space (Clarke *et al.* 2001; Koster 2005). In addition, most *A. baumannii* strains also possess an active mechanism of Fe^{2+} acquisition that involves siderophores. These molecules are synthesised in the bacterial cell and then secreted into the extracellular space within the host where they scavenge for available Fe^{2+} . Several Fe^{2+} -scavenging siderophores and at least five gene clusters encoding proteins required for siderophore synthesis and transport have been identified (Eijkelkamp *et al.* 2011a). Siderophore receptors present on the cell surface recognise the Fe^{2+} -bound siderophores allowing for their uptake and importation across the outer membrane using the TonB-ExbB-ExbD dependent transport system (Braun and Braun 2002). The Fe^{2+} -bound siderophores, once released, bind to specific binding proteins within the periplasmic space which then deliver free Fe^{2+} or Fe^{2+} -containing compounds to the ATP binding cassette (ABC) transporters in the cytoplasmic membrane (Braun and Braun 2002).

Genes encoding a biosynthesis protein (BasD), a receptor protein (BauA) and an uptake protein (BauD), all required for the biosynthesis of a unique siderophore called acinetobactin are located in a single cluster within the *A. baumannii* genome (Dorsey *et al.* 2004; Yamamoto *et al.* 1994). Fe^{2+} -uptake systems are often regulated by the Fe^{2+} -uptake regulator (Fur) protein (Vassinova and Kozyrev 2000). The Fur protein dimerises in the presence of Fe^{2+} and in this state is capable of binding to palindromic sequences known as the Fur-binding sites or Fur boxes and thereby stops transcription of the associated gene/s (Stojiljkovic *et al.* 1994). In Fe^{2+} -limited

conditions Fe^{2+} bound to Fur dissociates from the protein resulting in derepression of Fe^{2+} -acquisition genes (Hantke 2001b). In *A. baumannii* many genes containing Fur-binding sites were up-regulated during growth under Fe^{2+} -limiting conditions, indicating a significant role of this regulatory protein in *Acinetobacter* responding to Fe^{2+} deprivation (Eijkelkamp *et al.* 2011a).

1.3.4 Capsule

Like many other bacterial pathogens, the *A. baumannii* cell is surrounded by a layer of capsular polysaccharide (CPS) that protects the organism from stressors, such as desiccation and antimicrobial compounds, as well as providing protection from opsonisation and macrophage uptake. A study involving more than 40 *A. baumannii* isolates found that almost all isolates expressed CPS and genomic studies examining a large number of clinical isolates have identified a sequence-variable gene cluster (the K locus) with predicted capsule biosynthesis functions (Geisinger and Isberg 2015). There are many distinct arrangements of a large CPS biosynthesis locus found in *Acinetobacter* spp. genomes, designated the K locus (Hu *et al.* 2013; Kenyon and Hall 2013). These loci also include genes *wza*, *wzb* and *wzc* that encode proteins involved in export of CPS to the cellular surface (Kenyon and Hall 2013). The CPS repeat unit structures of different K loci have also been determined (Kenyon *et al.* 2014a; Kenyon *et al.* 2015; Kenyon *et al.* 2016).

Experiments with capsule-deficient mutants have demonstrated a role for CPS in the growth of *A. baumannii* within soft tissue infection sites in mice (Russo *et al.* 2010). Mutagenesis of a key glycosyltransferase prevented the synthesis of capsule and a lack of protein glycosylation which resulted in abnormal biofilm formation, reduced virulence in mice, as well as loss of motility and reduced resistance against serum killing (Russo *et al.* 2010). In addition, a study of the K locus CPS indicated that capsule contributes to antibiotic resistance in *A. baumannii*; deletion of the K locus in *A. baumannii* resulted in an increase sensitivity to colistin, rifampicin and erythromycin (Geisinger and Isberg 2015). It has also been demonstrated that the induction of capsule production increased

bacterial resistance to complement killing and enhanced its virulence capacity during the course of infection (Geisinger and Isberg 2015).

1.3.5 Type I and Type IV Pili

Pili play an important role in twitching motility, as well as adhesion to inert or living surfaces and hence in the formation of biofilms (Gohl *et al.* 2006). Four distinct pathways for the assembly of bacterial pili have been identified; the chaperone-usher pathway (P and type I pili), extracellular nucleation-precipitation pathway (curli pili), alternate chaperone pathway (CS1 pili), and general secretion pathway (type IV pili) (Gohl *et al.* 2006). Type I pili are the most common structures on the outer surface of Gram-negative bacteria and are frequently involved in adherence. Genome analysis of *A. baumannii* strains has identified four gene clusters encoding type I pili, namely A1S_1507-1510 (fimbriae cluster), A1S_2088-2091 and A1S_2213-2218 (Csu-cluster) in ATCC 17978 and AB57_2003-2007 (P pili cluster) in *A. baumannii* AB0057 (Eijkelkamp *et al.* 2014b). At a proteomic level, it was shown that the P pili proteins, CsuC and CsuD, were relatively highly expressed in cells within pellicles (Marti *et al.* 2011). It is also been suggested that the fimbriae play a role in pellicle formation in *A. baumannii* ATCC 17978 (Eijkelkamp *et al.* 2014b), as A1S_1507 was highly up-regulated in biofilm cells compared to expression in planktonic cells, as were the *csu* genes *csuD*, *csuC* and *csuAB* (Rumbo-Feal *et al.* 2013). Together, these findings show that type I pili play a significant role in *A. baumannii* adherence and biofilm/pellicle formation.

The type IV pili are believed to mediate twitching motility, allowing *Acinetobacter* to spread across solid surfaces. This is based on evidence which shows that mutations in the type IV pili genes led to the loss of both natural transformation and twitching motility in *A. nosocomialis* strain M2 (Harding *et al.* 2013). *A. baumannii* strain ATCC 17978 encodes orthologs for the type IV pili proteins *pilX*, *pilV* and *pilT* as do most pathogenic *A. baumannii* strains. In comparison, the avirulent *Acinetobacter* strain SDF was found to have a number of non-functional type IV pili genes as a result of insertional/deletion events (Eijkelkamp *et al.* 2014b).

1.3.6 Type VI secretion system

The T6SS is a bacterial secretion system widely spread throughout Gram-negative species (Coulthurst 2013). T6SS are complex molecular machines that include a bacteriophage-like cell-puncturing device that delivers effector proteins and virulence factors into target cells (Coulthurst 2013). T6SS can be comprised of at least 13 core proteins, required for both the assembly and function of the T6SS, and is widely conserved across all of the known T6SS (Carruthers *et al.* 2013). However the exact genes within the clusters are varied between species, including the gene order and orientation (Decoin *et al.* 2014).

The T6SS play a wide-ranging role and in some bacterial pathogens contribute to virulence. In *Citrobacter freundii* the T6SS regulates the flagellar system and is involved in host cell adherence and the induction of cytotoxicity in host cells (Carruthers *et al.* 2013). The T6SS have also been identified and characterised for their roles in bacterial competition and pathogenicity (Eijkelkamp *et al.* 2014b). The role of T6SS in bacterial invasion has been shown in *Escherichia coli* (Zhou *et al.* 2012) and *Burkholderia* spp. (Schwarz *et al.* 2014) in which the deletion of key T6SS genes resulted in a reduced ability to invade host cells. Several studies have reported that T6SS in *Burkholderia* (Schwarz *et al.* 2010), *Pseudomonas aeruginosa* (Hood *et al.* 2010), *Vibrio cholera* (MacIntyre *et al.* 2010) and *Pseudomonas fluorescens* (Decoin *et al.* 2014) are used to kill competing bacteria. The role of the T6SS system in *Acinetobacter* spp. appears to be limited to intra- and inter-species competition. The genes (*tssB-tssD*) encoding the T6SS in *A. nosocomialis* strain M2 are required for the killing of *E. coli* via cell-cell contact. This ability would give *Acinetobacter* species expressing T6SS a competitive advantage in a mixed bacterial environment (Carruthers *et al.* 2013).

1.3.7 Lipooligosaccharides

Lipooligosaccharide (LOS) and lipopolysaccharide (LPS) are lipid-carbohydrate surface structures unique to the outer membrane of Gram-negative bacteria. LOS is composed of distinct constituents: the lipid A, which anchors the LOS in the outer-leaflet of the outer membrane, and an oligosaccharide that extends out from the

cell surface (Kenyon *et al.* 2014b). In many bacteria, this carbohydrate structure is further extended with long polysaccharide (O-antigen) repeat units to generate LPS. *A. baumannii* is predicted to only produce LOS as analysis of the genome indicates that the species lacks the key enzyme required for polymerisation of O-antigen (Kenyon and Hall 2013). *A. baumannii* LOS has been shown to play crucial roles in bacterial pathogenesis. It has been revealed that a mutant deficient in LOS production shows a defect in bacterial motile ability (McQueary *et al.* 2012). LOS also contributes in the ability of *A. baumannii* to cause disease in the host, as the administration of an LpxC inhibitor (which affects lipid A biosynthesis), to mice infected with *A. baumannii*, enhances opsonophagocytic killing, reduces serum LOS concentration and inflammation, and protects the mice from lethal infection (Lin *et al.* 2012). On the other hand, the modification of LOS also impact on bacterial survival during desiccation and increased resistance to antimicrobial agents (Weber *et al.* 2016). *A. baumannii* has ability to develop colistin resistance by inactivating lipid A biosynthesis; the complete loss of LOS inhibits the binding of the antibiotic to bacterial outer membrane thereby conferring colistin resistance (Moffat *et al.* 2013).

1.3.8 Outer membrane protein A

The protein, OmpA, is the most dominant protein in the *A. baumannii* outer membrane and contributes to *A. baumannii* virulence. A random transposon mutagenesis screen of *A. baumannii* showed that inactivation of OmpA led to bacterial impairment in inducing apoptosis in a human laryngeal epithelial cell (Choi *et al.* 2005). OmpA seems to be particularly important in the early stages of infection as *A. baumannii* OmpA⁻ mutants show significantly decreased adherence and invasion compared to the WT strain (Choi *et al.* 2008). It was hypothesised that OmpA plays a role in adherence to epithelial cells and disruption of the mucosal lining, allowing penetration and invasion into deeper tissues. There is also evidence that *A. baumannii* OmpA interacts with components of the host's immune system, in particular complement and factor H (Kim *et al.* 2009). Furthermore, OmpA is also believed to play a role in biofilm formation (Gaddy *et al.* 2009). Thus, the role of OmpA in *A. baumannii* virulence appears to be diverse and critical for full virulence.

1.3.9 Outer membrane vesicles

Many Gram-negative bacteria naturally release or “bleb” outer membrane vesicles (OMVs) consisting of outer membrane and periplasmic proteins, phospholipids, LPS/CPS and may also contain ribonuclease (RNAse) or deoxyribonuclease (DNAse) (Ellis and Kuehn 2010). OMVs are thought to play a role in the delivery of virulence factors to host cells, including effector molecules. When co-cultured *in vitro*, *A. baumannii* has been shown to release OMVs that induce apoptosis of host cells in an OmpA-dependent manner (Jin *et al.* 2011). *A. baumannii* OMVs have been shown to be a potent innate immune response inducer in the infected host (Jun *et al.* 2013). OMVs also have a role in horizontal gene transfer by allowing DNA within the vesicle to be transferred between strains (Rumbo *et al.* 2011). Thus, OMVs play a role in virulence via two distinct mechanisms; the direct transfer of effector molecules to eukaryotic cells and the release of DNA including DNA encoding antibiotic resistance determinants.

1.4 Nutrient acquisition is crucial for bacterial virulence

Nutrition, including carbon and energy sources, is a fundamental need for all microorganisms to grow and replicate (Somerville and Proctor 2009). Free-living or symbiotic bacteria can obtain carbon and energy from the environment, whereas pathogenic bacteria derive their carbon and energy by parasitising or destroying a host organism (Somerville and Proctor 2009). Therefore, the acquisition of essential nutrients from the host environment is fundamental for infectious microorganisms (Price *et al.* 2014). Nutrition restriction is an effective part of the host’s innate immune defense against microbial infection (Price *et al.* 2014). Without proper nutritional resources for survival/proliferation in the host, pathogens are incapable of causing disease. To combat this, pathogens have evolved unique metabolic adaptations to adequately respond to various complex nutritional micro-environments (Abu Kwaik and Bumann 2013). Indeed, analysis of *A. baumannii* strain ATCC 19606^T has revealed an ability to utilise a wider range of carbon and nitrogen sources compared to a less virulent *A. calcoaceticus* strain (Peleg *et al.* 2012).

Other micronutrients required by bacteria, including the metal ions Fe^{2+} , Zn^{2+} , copper (Cu^{2+}), and manganese (Mn^{2+}), are also of limited supply in the host (Hood 2012). Limiting the availability of these micronutrients is a process called “nutritional immunity” (see Section 1.3.3) (Hood 2012). Nutritional immunity can even occur within subcellular compartments of the eukaryotic cell. For example, both Fe^{2+} and Mn^{2+} within phagosomes containing engulfed bacteria are limited by the use of efflux systems that pump the ions out into the cytoplasm of the host cell, thereby depriving the phagocytised bacteria (Hood 2012). The host can also respond in other ways; within abscesses infected with *Staphylococcus aureus*, available Zn^{2+} and Mn^{2+} can be reduced by the release of calprotectin from neutrophils (Corbin *et al.* 2008). Therefore, in order to survive in the hostile environment within the host, bacterial pathogens exploit multiple mechanisms to obtain micronutrients. The acquisition of Zn^{2+} by many bacteria is achieved by using a high affinity Zn^{2+} -uptake system. These systems have been identified in many bacterial species including *Campylobacter jejuni*, *Salmonella sp.*, *Neisseria meningitidis*, *E. coli*, and *Yersinia pestis* and have been shown in some species to be required for full virulence (Ammendola *et al.* 2007; Hood *et al.* 2012; Patzer and Hantke 1998; Stork *et al.* 2010). Another metal ion critical for full virulence (*e.g.* in *Streptococcus pneumoniae* and *Staphylococcus*) and survival is Mn^{2+} (McDevitt *et al.* 2011). Bacteria within the genus *Staphylococcus* have Mn^{2+} transporters that are believed to promote Mn^{2+} acquisition during infection (Kehl-Fie *et al.* 2013).

1.5 Bacterial metal ions: regulation and transport

Transition metals, such as Fe^{2+} , Cu^{2+} , Zn^{2+} , nickel (Ni^{2+}) and Mn^{2+} play essential roles in a diversity of biological processes in the cell (Lee *et al.* 2012a), including cofactors for oxidation-reduction reactions, electron transfer, hydrolytic and acid-base chemistry, transcription and replication, and structural proteins (Lee *et al.* 2012a); but an excess of these intracellularly is deleterious to the cells. Moreover, various non-essential and extremely toxic heavy metals and metalloids (including mercury, cadmium (Cd^{2+}), arsenic, and tin) are present in the bacterial environment (Reyes-Caballero *et al.*, 2011). Thus, to be able to utilise these

essentials metal and to discharge the excess and the toxic metals, microorganisms and all cells have developed mechanisms to regulate intracellular metal homeostasis via metal sensor and metal transporters (Ma *et al.* 2009).

Cells restrict the amounts of each metal within their cytoplasm to prevent competition between metals for specific metal-binding proteins. Thus, in this tightly controlled environment, each metal-binding protein competes with other proteins for a limited pool of a specific metal. Cells are able to distinguish the different metals and control their effective intracellular concentration via selective metal transporters and metal responsive transcription mechanisms (Waldron and Robinson 2009). These metal homeostatic systems consist of specific protein-metal coordination complexes that function in uptake, efflux, intracellular trafficking between cell compartments, and storage (Ma *et al.* 2009). The expression of genes encoding these proteins is regulated by metalloregulatory proteins or “metal sensor” proteins which specifically sense one or a small number of metal ions (Reyes-Caballero *et al.* 2011). These transcriptional regulators are classified based on their structural homology. A large number of metal transcriptional regulators have been characterised namely the ArsR/SmtB family (arsenic regulator), MerR (mercuric ion regulator), the CsoR/RcnR family, CopY (Cu regulator), Fur (Fe regulator), Zur (Zn²⁺ regulator), the DtxR family and NikR (Ni regulator) (Brown *et al.* 2003; Iwig *et al.* 2006; Liu *et al.* 2007; Schmitt *et al.* 1992). In addition, proteins from other transcriptional regulator families, including the LysR and OxyR family, the MarR family member protein AdcR, and TetR family member protein SczA, appear to function as metal ions sensors, metal oxyanions or oxidative stress (via dithiol-disulfide exchange chemistry) (Ma *et al.* 2009).

Metalloregulatory proteins control the expression of genes that allow organisms to survive in their hostile microenvironment where there is persistent toxicity or a scarcity of essential metal ions and also the tenuous persistence of heavy metal pollutants (Giedroc and Arunkumar 2007). The intracellular quota or free metal concentration at which a metalloregulator is inhibited or activated to bind to its operator is determined by the threshold or sensitivity (K_{metal}) of the transcriptional response (Reyes-Caballero *et al.* 2011). The reciprocal of the metal affinity constant K_{metal} ($1/ K_{metal}$), defines the ability of the cells to buffer biologically required

transitions metal ions (Reyes-Caballero *et al.* 2011). Thus, the higher the regulator affinity for the cognate metal under particular intracellular conditions, the lower the concentration of bioavailable metal in the cell (Capdevila *et al.* 2016).

Binding of the cognate metal to the metalloregulator regulates the transcription of genes responsible for metal homeostasis (Reyes-Caballero *et al.* 2011). Metal homeostasis is achieved by a balance between metal import and export which determines how many atoms of each metal can be accumulated within the bacterial cell (Waldron and Robinson 2009). This involves metal importers including ABC transporters and NRAMP transporters that transport specific metal ions to the cytosol of bacterial cells (Nevo and Nelson 2006). In contrast, export/efflux of these metal ions is largely performed by Cation Diffusion Facilitator (CDF) proteins (Montanini *et al.* 2007), P-type ATPases, and tripartite RND transporters (Murakami 2008). In Gram-negative bacteria, some metals may be able to diffuse across the outer membrane and into the periplasm compartment through porins, such as OmpF (Nikaido 2003). Other metals, such as Fe^{2+} , are bound to siderophores that are too large for porins, and are therefore brought into the periplasm via energy-coupled importers. This energy is provided by the electrochemical charge gradient of the cytoplasmic membrane and is delivered by the energy-transducing TonB-ExbB-ExbD protein complex (Braun and Braun 2002).

1.6 Regulation of Zn^{2+} in bacterial cells

Zn^{2+} plays a dual role in the cell, as both a structural element (stabilising diverse “Zn-finger” proteins) and a catalytic cofactor (including proteases, phosphatases, deacetylases and esterases) (Blindauer *et al.* 2001; Maret 2013; Palmieri *et al.* 2014). However, Zn^{2+} is toxic to microorganisms at high concentrations (Choudhury and Srivastava 2001), *e.g.* Zn^{2+} toxicity in *Streptococcus pyogenes* results in the impairment of the glycolytic enzymes phosphofructokinase and glyceraldehyde-3-phosphate dehydrogenase which leads to glucose metabolism impairment (Ong *et al.* 2015). Therefore, maintaining a sub-toxic Zn^{2+} concentration is crucial for bacteria to survive in high Zn^{2+} environments

and in order to maintain Zn^{2+} homeostasis, the regulation of Zn^{2+} -transporter genes must be precisely controlled.

As has been discussed above (Section 1.5), the strategies utilised by bacterial cells in response to Zn^{2+} starvation or toxicity are via transcriptional regulation by metal-sensing metalloregulatory proteins and Zn^{2+} efflux and acquisition across cell membranes (Capdevila *et al.* 2016). Zn^{2+} homeostasis in *E. coli*, for example, is controlled by two metalloregulatory proteins, Zur and ZntR (Patzner and Hantke 2000; Wang *et al.* 2012). Zur is a member of the Fur family that in the presence of Zn^{2+} represses the expression of *znuABC*, which encodes a Zn^{2+} -uptake ABC transporter (Hantke 2001a; Outten *et al.* 2001). Conversely, ZntR is a MerR-family regulator that activates the transcription of *zntA*, a gene encoding a P-type ATPase that effluxes Zn^{2+} from the cytoplasm to the periplasm (Capdevila *et al.* 2016). In most bacteria, Zur acts as a global regulator that regulates the expression of a number of genes required to adapt to conditions of Zn^{2+} deprivation. When the intracellular Zn^{2+} concentration falls below a critical threshold, $[\text{metal}]_{\text{free}}/K_{\text{metal}}$ (Zn-replete conditions), the Zn^{2+} -bound form of Zur binds tightly to the operator site thus preventing transcription (Gilston *et al.* 2014). Likewise, when the intracellular "free" Zn^{2+} concentration increases transiently from picomolar to nanomolar levels, ZntR binds Zn^{2+} and allosterically activates transcription of *zntA* in *E. coli* (Capdevila *et al.* 2016; Wang *et al.* 2012).

Under severe Zn^{2+} starvation conditions, a process called " Zn^{2+} sparing" allows bacterial cells to increase the expression of non Zn^{2+} -requiring proteins to replace essential Zn^{2+} -dependent enzymes and proteins, as has been revealed with the ribosomal proteins L31 (Gabriel and Helmann 2009; Nanamiya *et al.* 2004). This strategy ensures that the metabolic functions of key Zn^{2+} -dependent enzymes are maintained under Zn^{2+} -deprived conditions. Another strategy to maintain the function of the Zn^{2+} -dependent enzymes is by utilising a Zn^{2+} chaperone. A recent study showed that the Zn^{2+} chaperon, ZigA, a G3E family GTPase from the COG0523 subfamily and a *zur* regulated gene, impacts on the labile Zn^{2+} pool which allows Zn^{2+} to be liberated in Zn^{2+} -deprived conditions (Nairn *et al.* 2016).

The role of the reduced form of low-molecular-weight thiols, glutathione (GSH) and bacillithiol (BSH) in buffering transition metals has been identified (Helbig *et al.* 2008; Ma *et al.* 2014). GSH is one of the major Zn²⁺-binding molecules in the cytoplasm. The classic view of how the concentration of Zn²⁺ is managed by the cells has been that Zn²⁺ first binds to GSH and an overload of the GSH pool will activate a Zn²⁺-sensor protein, which will then stimulate de-novo synthesis of Zn²⁺ transporters and apo-metal-thionine increasing the capacity for Zn²⁺ extrusion and sequester excess Zn²⁺ (Colvin *et al.* 2010). On the other hand, *Bacillus subtilis* when under the condition of Zn²⁺ excess, BSH has been shown to serve as an intracellular Zn²⁺ buffer as it can temporarily accumulate Zn²⁺ in a low-molecular-weight pool; thus cells lacking BSH are more sensitive to Zn²⁺ stress (Ma *et al.* 2014).

1.6.1 Zn²⁺ acquisition in bacterial cells

Members of the Fur protein family of metal-dependent transcriptional regulators control Fe²⁺-uptake systems and may also act on Mn²⁺- and Zn²⁺-uptake systems, as well as other genes associated with these metals (Hantke 2005). Zur, a Fur-family member, is a metallo-regulatory DNA-binding protein with femtomolar sensitivity to free intracellular Zn²⁺ (Shin *et al.* 2007). It has two conserved domains: an N-terminal DNA-binding motif and a C-terminal dimerisation domain and three metal ion binding sites (Somerville and Proctor 2009). When loaded with Zn²⁺, Zur binds to DNA containing a Zur box that consists of a 19-bp inverted repeat (consensus sequence AAATCGTAATNATTACGATTT) (Gabriel *et al.* 2008). By binding to this Zur box, located within the promoter region of Zur-regulated genes, the Zur protein represses transcription.

Functional Zur homologs have been identified in many bacteria, including *Listeria monocytogenes* (Dalet *et al.* 1999), *S. aureus* (Lindsay and Foster 2001), *Mycobacterium tuberculosis* (Maciag *et al.* 2007), *Streptomyces coelicolor* (Shin *et al.* 2007), *Streptococcus suis* (Feng *et al.* 2008), *Corynebacterium diphtheriae* (Smith *et al.* 2009), *Bacillus subtilis* (Gabriel and Helmann 2009) and *A. baumannii* (Mortensen *et al.* 2014). In *E. coli*, Zur responds to femtomolar levels of free intracellular Zn²⁺ as low as 10⁻¹⁵ M *in vitro* (Porcheron *et al.* 2013) and regulates

ZnuABC (Owen *et al.* 2007; Patzer and Hantke 2000; Smith *et al.* 2009). In *C. diphtheriae*, Zur represses transcription of *cmrA*, *troA*, and *zrg* which are predicted to be involved in Zn²⁺ transport as well as transcription of *zur* itself during growth in Zn²⁺-limited conditions, indicating that the expression of *zur* is autoregulated (Smith *et al.* 2009).

Genetic and biochemical studies in *E. coli* have shown that expression of ZnuABC is repressed in cells containing adequate concentrations of Zn²⁺ via the activity of Zur (Grass *et al.* 2005). Regulation by Zur enables cells to balance Zn²⁺ concentration in the cells (Hantke 2005) and allows cells to precisely respond to changes in the intracellular levels of Zn. Zur also regulates the expression of various ribosomal proteins including YtiA (Panina *et al.* 2003), RpmGC in *B. subtilis* (encoding the L33 paralog designated L33c) (Gabriel and Helmann 2009) and three ribosomal proteins RpmG2, RpmE2 and RpmB2 in *S. coelicolor* (Owen *et al.* 2007). These ribosomal proteins are paralogs of Zn²⁺-containing ribosomes. When required, they function by displacing Zn²⁺-containing ribosomal proteins from the ribosome, allowing for the degradation of the proteins and the release of the Zn²⁺ metal ions (Akanuma *et al.* 2006).

Many bacterial species have two types of Zn²⁺-uptake systems that are used under different conditions (Hantke 2005). During conditions of Zn²⁺-starvation, the high affinity Zn²⁺-uptake systems are up-regulated, while during conditions of moderate Zn²⁺ availability, Zn²⁺ uptake is carried out by low affinity uptake transporters (Hantke 2005). The high-affinity Zn²⁺-uptake systems belong to the ABC transporter family. These transporters consist of three proteins; ZnuA, ZnuB and ZnuC, encoded by the *znuABC* genes (Patzer and Hantke 2000). A number of enterobacterial species including *E. coli*, *Salmonella enterica* Serotype Typhimurium, *S. enterica* Serotype Enteritidis and *Proteus mirabilis* revealed that *znuA*, *znuC*, *znuB* or *znuABC* deletion mutants had decreased Zn²⁺-uptake compared to the parental strains (Porcheron *et al.* 2013). As the system is a P-type ATPase transporter, the energy requirement for transport comes from the hydrolysis of ATP, undertaken by ZnuC. ZnuA is the soluble Zn²⁺-binding periplasmic protein that interacts with the inner membrane permease, ZnuB (Chandra *et al.* 2007). The *znuABC* genes are not only regulated by Zur but also by SoxR. SoxR is part of the SoxRS regulon and

belongs to the MerR family of regulators (Li et al., 2009). The SoxRS regulon responds to oxidative stress and activates the expression of numerous genes including *znuABC* (Brown et al., 2003; Warner and Levy, 2012; (Porcheron *et al.* 2013).

In addition to the high-affinity Zn^{2+} -uptake system, there is a low-affinity Zn^{2+} -uptake system. Little is known about this system but in *E. coli* (Grass *et al.* 2002) and *S. enterica* Serovar Typhimurium (Cerasi *et al.* 2014), *zupT* has been shown to involve in bacterial growth in Zn^{2+} -limiting conditions and it has been suggested that its expression is not regulated by Zur (Cerasi *et al.* 2014). However, ZupT does not specifically import Zn^{2+} but imports a broad range of other metal ions, such as Cd^{2+} , Fe^{2+} , cobalt (Co^{2+}), Cu^{2+} and possibly Mn^{2+} (Grass *et al.* 2005). Moreover, the *zupT* gene was not induced by the presence/absence of metal ions and appears to be constitutively expressed (Grass *et al.* 2005). In the Gram-positive bacterium *B. subtilis*, the membrane protein YciC is also predicted to be involved in a low-affinity transport system for Zn^{2+} (Gaballa and Helmann 1998).

1.6.2 Zn^{2+} -efflux systems in bacterial cells

In conditions where Zn^{2+} is at toxic levels, bacterial cells will express efflux systems and export Zn^{2+} out of the cytoplasm to prevent intracellular overloading (Guilhen *et al.* 2013). As already mentioned, exporters that fall into three families of transport proteins have been identified in bacteria, namely the CDF, RND, and P-type ATPases families (Kolaj-Robin *et al.* 2015). The CDF family is an ubiquitous family of proteins found in all major phyla of living organisms and these proteins have evolved a strong preference for the trafficking of Zn^{2+} ions in many biological systems (Kolaj-Robin *et al.* 2015). Included in the CDF family are the ZitB and YiiP proteins in *E. coli* that utilise the free energy derived from hydrogen influx to export heavy metals ions, including Co^{2+} , Cd^{2+} , Zn^{2+} and Ni^{2+} , from the cytoplasm to the periplasm by translocation across the inner membrane (Porcheron *et al.* 2013). Another CDF transporter, CzcD, has been identified in *Ralstonia eutropha* and functions as a Zn^{2+} exporter (Anton *et al.* 1999) in addition to repressing the Czc system (a Zn^{2+} , Co^{2+} , and Cd^{2+} -efflux system performed by the CzcCB₂A cation-

proton antiporter) by exporting inducing cations (Anton *et al.* 1999). A CDF family transporter, ZntA, which is involved in the resistance to Zn^{2+} and Co^{2+} , has been identified in *S. aureus*, is regulated by ZntR, a *trans*-acting repressor that regulates its own expression, as well as the adjacent gene encoding the transmembrane protein (Singh *et al.* 1999). It has to be noted that the ZntA and ZntR proteins in *E. coli* are different from ZntA and ZntR in *S. aureus*. In *E. coli*, ZntA and ZntR are designated as a transporter and a regulator belonging to the P-type ATPase family of transporters (described below).

The second family of exporters are the P-type ATPase family that are found in both the eukaryote and bacterial cells. These transport proteins are controlled by either MerR/ZntR regulators or by members of the ArsR/SmtB superfamily of repressors. Both types of regulators are also found in connection with other metal transporters (Hantke 2001a). The P-type ATPases perform active ion transport across the membrane by utilising free energy of ATP hydrolysis (Apell 2004). The most striking feature of the P-type ATPases is the presence of 1-6 amino acid motifs, GXXCXXC or (MyH)XXMDH(SyG)XM, at the N-terminus of the protein that act as putative metal-binding domains (Rensing *et al.* 1997). P-type ATPases that export Cd^{2+} and Zn^{2+} have been well characterised in *S. aureus* (encoded by *cadA* and *cadC*), *L. monocytogenes*, *Stenotrophomonas maltophilia* and in *B. subtilis* (Hantke 2001b). ZntA is a P-type ATPase transporter that has been identified in *E. coli*, where ZntA mutants exhibited hypersensitivity to Zn^{2+} and Cd^{2+} but not other metals, suggesting a role in Zn^{2+} and Cd^{2+} homeostasis (Rensing *et al.* 1997). Also, in *E. coli*, it has been suggested that the exporter ZitB contributes to Zn^{2+} homeostasis at low Zn^{2+} concentrations while ZntA is required for growth at higher, toxic concentrations (Grass *et al.* 2001). *zntA* is regulated by ZntR, a MerR-family regulator that binds to the *zntA* promoter to repress transcription (Hantke 2001a). This repression of *zntA* by ZntR prevents *zntA* expression until intracellular Zn^{2+} levels exceeds sub-toxic levels, thus allowing the efflux system to be activated before truly toxic level of Zn^{2+} occurs (Khan *et al.* 2002).

RND efflux systems are composed of a tripartite protein complex consisting of a cytoplasmic membrane-associated protein, a periplasmic membrane fusion protein and an outer-membrane channel protein (Valencia *et al.* 2013). This

structure enables the membrane-spanning complex to export its substrates, including Zn^{2+} , across the cytoplasmic membrane and the outer membrane of Gram-negative bacteria (Guilhen *et al.* 2013). However, RND-type exporters for Zn^{2+} are restricted to a limited number of Gram-negative bacteria (Hantke 2001a). For example, in *Helicobacter pylori* CznABC exports Ni^{2+} , Zn^{2+} and Cd^{2+} (Stahler *et al.* 2006). Two RND efflux systems have been identified in *Caulobacter crescentus*, *czrCBA* that exports Cd^{2+} and Zn^{2+} with a secondary role exporting Co^{2+} , and *nczCBA* that exports Ni^{2+} and Co^{2+} with a secondary role exporting Cd^{2+} and Zn^{2+} (Valencia *et al.* 2013). In *Ralstonia metallidurans* the CzcABC system exports Zn^{2+} , Co^{2+} and Cd^{2+} (Anton *et al.* 1999) and regulation appears to involve the CzcS/CzcR two-component regulatory system (Hantke 2001a). A diagrammatic representation of the Zn^{2+} -uptake and Zn^{2+} -efflux systems in Gram-negative and Gram-positive bacteria are shown in Figures 1.1 and 1.2, respectively.

1.7 Zn^{2+} regulation, acquisition and efflux in *A. baumannii*

Several studies have been conducted to examine Zn^{2+} uptake and regulation in *A. baumannii*, however, the full picture of Zn^{2+} homeostasis and regulation is still poorly understood. To date, no low affinity uptake system has been found in *A. baumannii* and it has been recently shown that *A. baumannii* obtains Zn^{2+} using the high Zn^{2+} -uptake ZnuABC transporter system (Hood *et al.* 2012). Evidence to support this notion comes from studies examining *znuB* mutants. These *A. baumannii znuB* mutants displayed reduced growth compared to the parental strain in Zn^{2+} -limited conditions, indicating that the Znu system is required for optimal growth under Zn^{2+} starvation (Hood *et al.* 2012). A Zur-binding site (Section 1.6.2) has been identified in the intragenic region between *znuA* and *zur* in *A. baumannii* ATCC 17978 (Figure 1.3) (Gaballa and Helmann 1998; Li *et al.* 2009). As with other Gram-negative bacteria, in *A. baumannii* Zn^{2+} acquisition requires the Zn^{2+} ion to cross two membranes and, although there is some diffusion through non-selective, outer membrane porins (Stork *et al.* 2010), another system is required in order to obtain Zn^{2+} under Zn^{2+} -depleted conditions. A diagrammatic

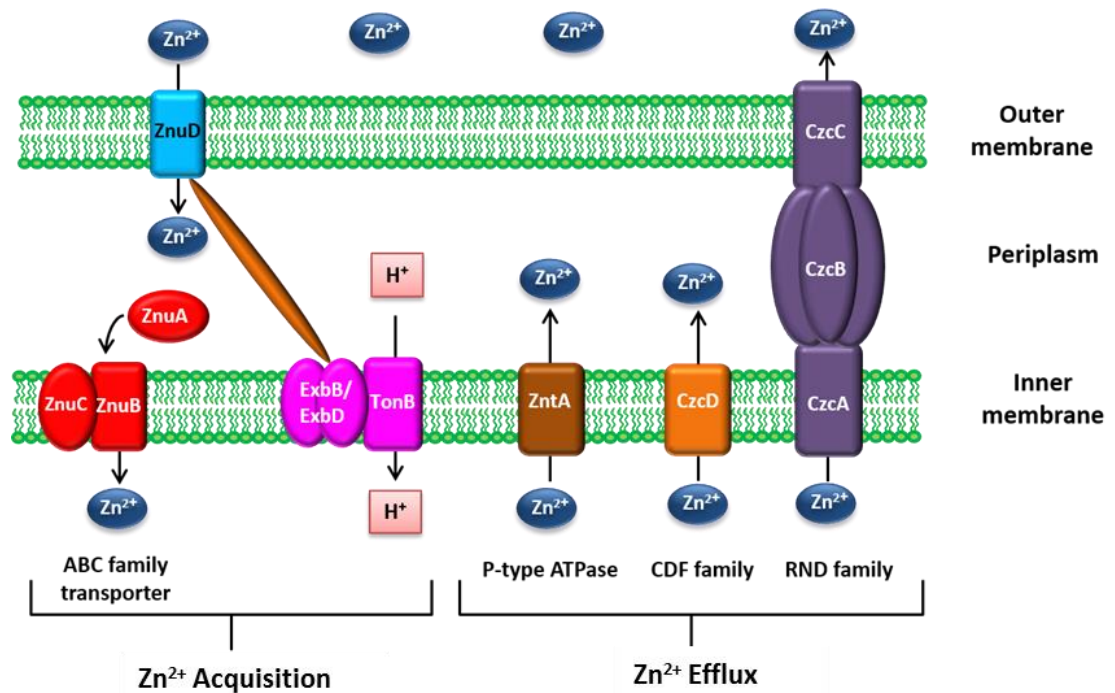


Figure 1.1: The mechanism of Zn²⁺ acquisition and efflux in Gram-negative bacteria

The Zn²⁺-acquisition and efflux systems in Gram-negative bacteria are shown diagrammatically. The dark blue ellipsoids represent Zn²⁺ ions (Zn²⁺). One mechanism of Zn²⁺ import occurs via the Zn²⁺-regulated TonB-dependent outer membrane receptor, ZnuD (cyan). This is energised by a Zn²⁺-regulated TonB-ExbB-ExbD (magenta) system and requires the proton motive force (represented by hydrogen ions, H⁺, pink boxes). Transport to and across the inner membrane is mediated by the ZnuABC transporter (red), an ABC transporter family member. Three types of Zn²⁺-efflux systems are represented; the P-type ATPase ZntA (brown), the CDF-family CzcD (orange), and a tripartate RND family transport system CzcABC (purple).

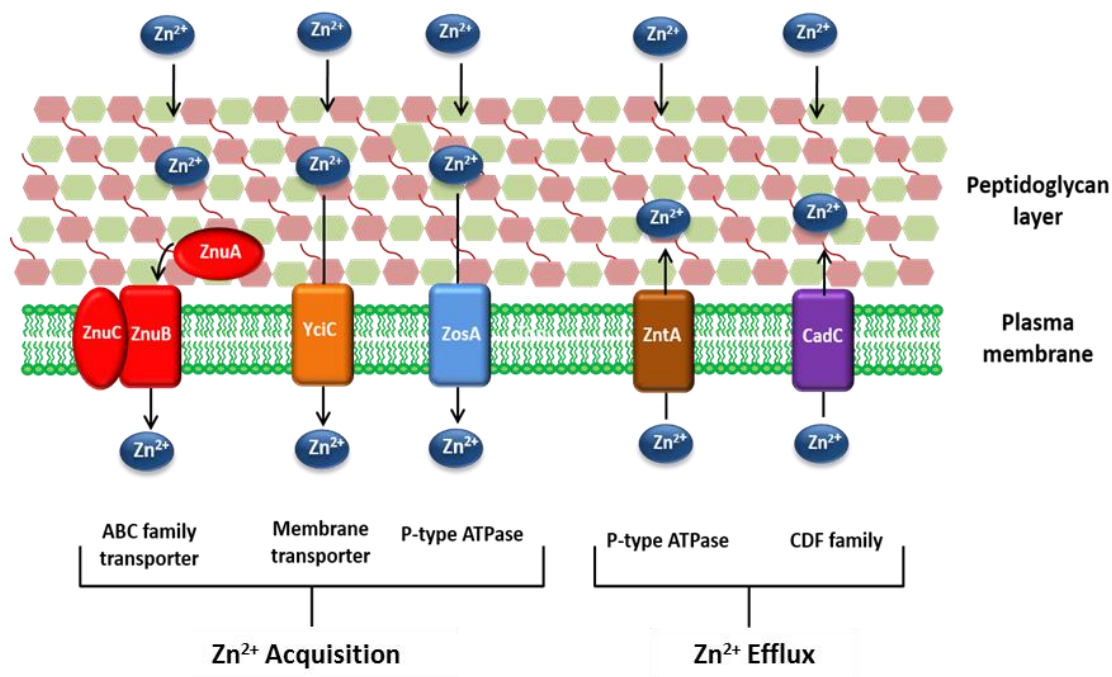


Figure 1.2: The mechanism of Zn²⁺ acquisition and efflux in Gram-positive bacteria

The Zn²⁺-acquisition and efflux system in Gram-positive bacteria are shown diagrammatically. The dark blue ellipsoids represent Zn²⁺ ions (Zn²⁺). Zn²⁺ is imported via a number of mechanisms, exemplified by (i) ZnuABC (red), an ABC transporter, (ii) a low affinity Zn²⁺ importer YciC (orange; found in *B. subtilis*) and (iii) ZosA (cyan; found in *B. subtilis*), a P-type ATPase family protein. Zn²⁺ ions can be effluxed from the bacterial cytoplasm by two dedicated exporters, (i) ZntA (brown), a P-type ATPase and (ii) the CadC (purple) CDF-family protein.

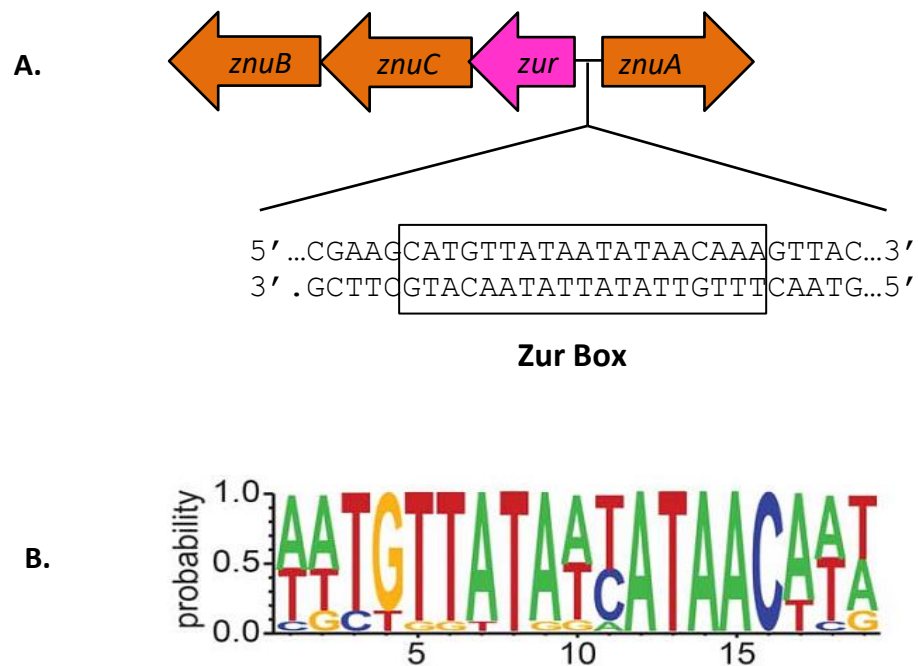


Figure 1.3: Schematic diagram of a putative Zur box in *A. baumannii*

Schematic representation of (A) the genomic region containing *znuA* and the *zur/znuCB* operon in *A. baumannii*; the sequence corresponding to a putative 19 bp Zur box is shown. (B) Consensus sequence of Zur binding (Zur Box) in *A. baumannii*; the sequence and relative probability of nucleotides occurring at any given position is shown (adapted from Hood *et al.*, 2012)

representation of the mechanisms used by Zn²⁺-uptake systems in *A. baumannii* is shown in Figure 1.4.

The transport of Zn²⁺ across the *A. baumannii* outer membrane is mediated by ZnuD (ZnuD1 and ZnuD2) (Figure 1.4). The expression of these two TonB-dependent receptors (TDBR) in *A. baumannii* under Zn²⁺-limiting conditions indicates that the transport of Zn²⁺ across the outer membrane of *A. baumannii* may be energised via the TonB-ExbB-ExbD system (Hood *et al.* 2012). This TonB-ExbB/D system couples energy from the proton motive force generated at the inner membrane to facilitate transport across the outer membrane (Figure 1.1) (Mortensen and Skaar 2013). Not only are the genes encoding ZnuD1 and ZnuD2, regulated by Zur (Mortensen *et al.* 2014), numerous other genes have been shown to be part of the Zur regulon including *znuABC*, *tonB*, *exbB*, *exbD*, *rpmE2*, as well as genes annotated as A1S_3411 (*zigA*) and A1S_3412 in strain ATCC 17978 (Mortensen *et al.* 2014; Nairn *et al.* 2016). A recent study showed that A1S_3411 designated as ZigA binds Zn²⁺ and exhibits Zn²⁺-stimulated GTPase activity and is required for full growth in Zn²⁺-limiting conditions (Nairn *et al.* 2016).

To avoid Zn²⁺ toxicity, strict regulation of intracellular levels of this metal is critical for bacterial cells. Zur is essential for *A. baumannii* growth in both low and high concentrations of zinc (Mortensen *et al.* 2014). In high levels, Zn²⁺ toxicity is prevented in part through Zur-mediated repression of acquisition systems. This is usually undertaken together with the application of heavy metal-efflux transporters. The mechanism of Zn²⁺ efflux in *A. baumannii* has not been fully elucidated, however, an RND efflux system has been proposed (Mortensen *et al.* 2014). The RND efflux pump in *A. baumannii* strain ATCC 17978 (A1S_3217-3219) has been suggested to export Zn²⁺, Co²⁺, and Cd²⁺ to maintain sub-toxic Zn²⁺ levels in the cells. Another putative Zn²⁺-efflux system (encoded by the Zur-independent genes annotated as A1S_1044-1045) has been found to have increased expression in an *A. baumannii* Δ *zur* mutant, and is predicted to be in direct response to increased intracellular levels of Zn²⁺ due to derepression of the Zn²⁺-uptake systems (Mortensen *et al.* 2014).

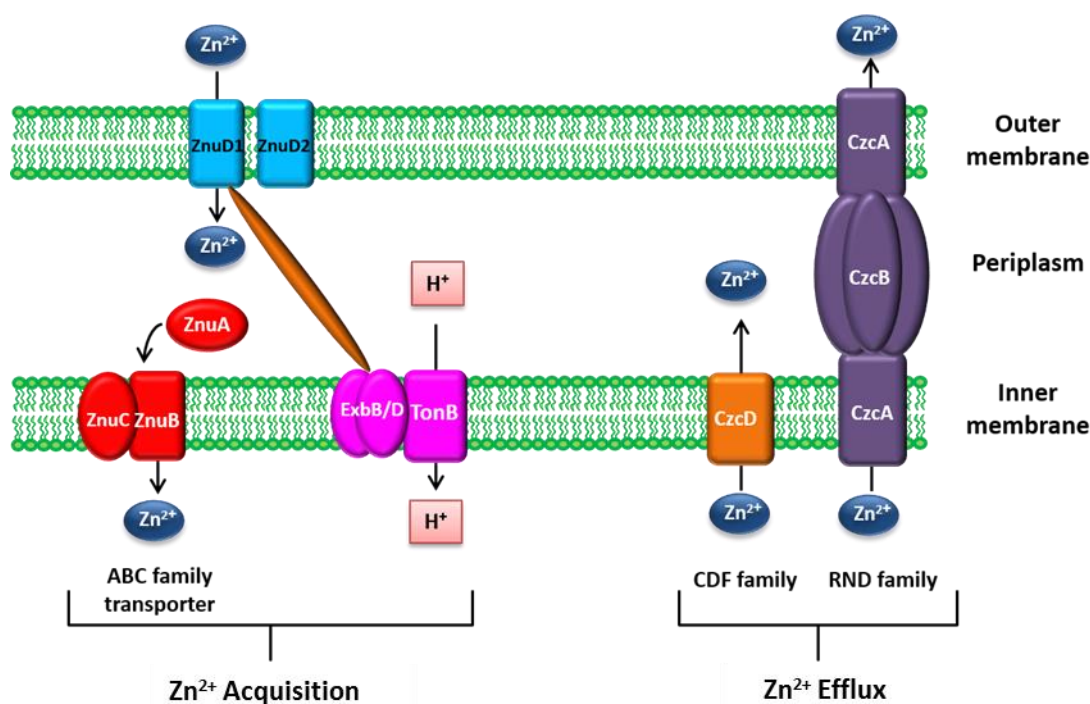


Figure 1.4: The mechanism of Zn²⁺ acquisition and efflux in *A. baumannii*

This panel depicts the Zn²⁺ acquisition and efflux systems described in *A. baumannii* ATCC 17978 to date, however Zn²⁺-acquisition systems are predicted to vary amongst *A. baumannii* strains. Zn²⁺ (dark blue ellipsoids) transport across the outer membrane occurs via two Zn²⁺-regulated TDBR, ZnuD1 and ZnuD2 (cyan). Transport is energised by a Zn²⁺-regulated TonB-ExbB-ExbD system (magenta) and requires the proton motive force (represented by hydrogen ions; H⁺ pink boxes). Inner membrane transport is mediated by the high-affinity ZnuABC Zn²⁺ transporter (red), where ZnuA represents the periplasmic Zn²⁺-binding protein, ZnuB the inner membrane Zn²⁺ transporter energised by ATP hydrolysis that is undertaken by ZnuC. Zn²⁺ efflux is mediated via two known systems in *A. baumannii* ATCC 17978; a RND-efflux transporter system represented by CzcABC (purple) and a putative transmembrane transporter designated CzcD (orange). Unlike in *E. coli*, no ZntA system has been described in *A. baumannii*.

1.8 Zinc plays a significant role in bacterial virulence and the response to oxidative stress

1.8.1 Zinc in bacterial virulence and pathogenesis

There is increasing evidence for the importance of Zn^{2+} in the pathogenesis and virulence of various bacteria including *E. coli* (Sabri *et al.* 2009), *S. pneumoniae* (Eijkelkamp *et al.* 2014a), *S. aureus* (Corbin *et al.* 2008), *L. monocytogenes* (Corbett *et al.* 2012), *P. mirabilis* (Nielubowicz *et al.* 2010), and *Enterococcus faecalis* (Abrantes *et al.* 2011).

Metal chelation has been demonstrated to be an effective strategy for inhibiting microbial growth inside abscessed tissue caused by *S. aureus* infections (Corbin *et al.* 2008). Other Zn^{2+} -chelation experiments have indicated that biofilm formation can be inhibited; Zn^{2+} depletion via chelation specifically prevented biofilm formation in *Staphylococcus epidermidis* and methicillin-resistant *S. aureus* (MRSA) (Conrady *et al.* 2008; Geoghegan *et al.* 2010). The surface protein Aap (accumulation-associated protein) has been implicated in this process, where the G5 domain (a self-association repeat sequence element) within Aap is predicted to mediate Zn^{2+} -dependent early and late stage biofilm formation in *Staphylococcus* spp. and is also used for intercellular adhesion (Conrady *et al.* 2008). It has similarly been shown that Zn^{2+} is required for SasG (a surface protein) mediated biofilm formation in *Staphylococcus* spp. (Geoghegan *et al.* 2010).

Zn^{2+} is important for the intracellular growth of *L. monocytogenes* (Corbett *et al.* 2012) and for motility of *E. coli* (Sabri *et al.* 2009), *P. mirabilis* (Nielubowicz *et al.* 2010) and *Myxococcus xanthus* (Kearns *et al.* 2002). Zn^{2+} availability can also affect the ability of bacteria to form biofilms through its roles in bacterial pilus assembly and curli production (Lim *et al.* 2011). A study conducted by Labrie *et al.* (2010) showed that the low concentrations of Zn^{2+} in the medium inhibited biofilm production in *Actinobacillus pleuropneumoniae*. In addition, the mutation of genes encoding the Zur-regulated L31 ribosomal protein YkgM and ZitA in *E. coli* greatly affected biofilm formation under fluidic conditions but no inhibition was observed in static conditions (Lim *et al.* 2011). In contrast, some studies have revealed that

the addition of Zn^{2+} to growth media inhibits the formation of biofilms (Hancock *et al.* 2010). For example, the addition of micromolar concentrations of Zn^{2+} was found to effectively block biofilm formation in *A. pleuropneumoniae*, *S. enterica* Serotype Typhimurium and *Haemophilus parasuis* in a dose-dependent manner (Hancock *et al.* 2010). These differences between bacterial species of the effect of Zn^{2+} on biofilm formation are possibly due to each species/strain having a different optimum cell concentration of Zn^{2+} required for cellular processes.

Perturbation of the ZnuABC transporter system can affect virulence. In *S. enterica* Serotype Typhimurium, it is showed that a *znuC* mutant exhibited reduced virulence compared to the WT strain when used to orally or intraperitoneally inoculate BALB/c mice. This indicates that the ZnuABC system plays a principal role during mouse infection (Ammendola *et al.* 2007). The presence of a functional Zn^{2+} -binding ATP-binding protein, ZnuC, allows *P. mirabilis* to grow to a higher density under Zn^{2+} limitation and ZnuC has been shown to be required for *P. mirabilis* motility (Nielubowicz *et al.* 2010). In *S. pneumoniae*, a reduction of Zn^{2+} uptake via deletion of both the Zn^{2+} -uptake gene *adcA* and a Zn^{2+} -binding lipoprotein, *adcAll*, prevented *S. pneumoniae* from establishing an infection in three mouse models; nasopharyngeal colonisation, pneumonia and sepsis (Bayle *et al.* 2011).

1.8.2 Zn^{2+} and oxidative stress

Reactive oxygen species (ROS), such as superoxide anion (O_2^-), hydrogen peroxide (H_2O_2) and hydroxyl radicals, are generated by the partial reduction of oxygen (Ray *et al.* 2012). Aerobically growing cells have to be able to cope with these ROS as they can damage essential cellular structures, DNA lipids or proteins. ROS can be generated during normal aerobic metabolism as well as a result of exogenous drugs, radiation exposure or an immunological response from the infected host (Leichert *et al.* 2003). The reactive by-products of oxygen (superoxide anion radical [O_2^-], hydrogen peroxide [H_2O_2], and the highly reactive hydroxyl radicals [$^{\cdot}OH$]) are persistently being produced in aerobically growing cells (Cabiscol *et al.* 2000). ROS can induce oxidative modifications to the amino acids cysteine,

methionine, histidine, and tryptophan (Hare *et al.* 2011). A review article by Jomova and Valko (2011) highlighted that redox active metal ions such as Fe^{2+} , Cu^{2+} , chromium (Cr^{2+}), Co^{2+} and Zn^{2+} undergo redox cycling reactions and are able to produce reactive radicals. Although these metal ions can be hazardous for living organisms, they also function as signal mediators in signalling pathways. Thus, disruption of metal ion homeostasis may also lead to oxidative stress and therefore increased formation of ROS (Jomova and Valko 2011). Zn^{2+} is a redox inert metal that does not participate in oxidation-reduction reactions (Jomova and Valko 2011) but functions as an antioxidant via protection of protein sulphhydryl groups against free radical attack or by inhibiting free radical formation by competing with redox-active metals such as Fe^{2+} (Bray and Bettger 1990; Smith *et al.* 2009).

In *P. aeruginosa*, a large number of antioxidant defence proteins are encoded on the genome that offer resistance against oxidative stress including superoxide dismutases (SODs), catalases (KatABC), the hydroperoxide-resistance protein and alkyl hydroperoxide reductase (AhpCF). In *E. coli*, the oxidative stress response is controlled by two major systems, OxyR and SoxR. The OxyR global regulator is activated by H_2O_2 and regulates the expression of many genes, meanwhile SoxR is activated by O_2^- , and is induced by compounds including paraquat (Hare *et al.* 2011). In *B. subtilis* expression of the Zn^{2+} -uptake protein, ZosA (formerly YkvW), is induced by H_2O_2 and repressed by the PerR metalloregulatory protein (Gaballa and Helmann 2002). ZosA has been shown to be important for resistance to both H_2O_2 and the thiol-oxidising agent, diamide, suggesting that an increase of intracellular Zn^{2+} may protect thiols from oxidation (Gaballa and Helmann 2002).

1.9 Ribosomal proteins

Ribosomal proteins are encoded in all genomes of cellular life forms and have remained highly conserved during evolution (Makarova *et al.* 2001). Ribosomes contain individual proteins with the same characteristic/function amongst all organisms and are called universal proteins, consisting of 34 members but also contain some proteins that are broadly specific for the each of the domains

namely, bacteria, archaea and eukaryotes (Korobeinikova *et al.* 2012). In bacteria, in addition to these universal proteins, there are 22 specific ribosomal proteins including eight proteins belonging to the small ribosomal subunit and 14 belonging to the large ribosomal subunit (Korobeinikova *et al.* 2012). Ribosomal proteins stabilise rRNA and have other additional roles in ribosomal function (Brodersen and Nissen 2005). During the process of translation in bacteria, 70S ribosomes are assembled on the mRNA using the 30S and 50S subunits. The 30S subunit usually contains 21 proteins and the 16S rRNA; and the 50S subunit consists of 36 proteins together with 23S and 5S rRNA (Owen *et al.* 2007).

Each ribosomal protein is usually encoded by a single, highly conserved gene. However, ribosomal genes can infrequently undergo duplication and several paralogous pairs of ribosomal protein genes have been identified. These duplicate ribosomal proteins are found among different bacteria as well as within single genomes and include L31 (RpmE), L32 (RpmF), L33 (RpmG), L36 (RpmJ), L28 (RpmB), S18 (RpsR), and S14 (RpsN). The two forms of each ribosomal protein differ by the presence or absence of a Zn²⁺-ribbon motif that usually consists of two pairs of conserved cysteine residues. The presence or absence of cysteine Zn²⁺ ligands in these proteins has led to their designation as C⁺ or C⁻ forms (Makarova *et al.* 2001).

1.9.1 L31 ribosomal proteins

The evolution of the C⁺ or C⁻ form of ribosomal proteins is thought to have occurred via ancient duplication of the ancestral C⁺ form of each gene, that was then followed by the evolution of C⁻ forms, followed by the loss of the C⁺ or C⁻ forms in different lineages (Makarova *et al.* 2001). However, some bacterial genomes maintain both C⁺ and C⁻ forms of certain ribosomal genes. In the *E. coli* genome, most ribosomal proteins are in the C⁻ form with the exception of L31 that is present in both the C⁺ and C⁻ form. In contrast, most *B. subtilis* genomes encode both the C⁺ and C⁻ forms of the genes encoding the ribosomal proteins S14, L31, and L33 (Makarova *et al.* 2001).

As stated above, bacterial L31 ribosomal genes are present in both the C⁺ and C⁻ forms. The C⁺ form of L31 usually contains the metal-binding Zn²⁺-ribbon

motif that consists of four conserved cysteines (*i.e.*, containing two CxxC motifs) but in some cases the cysteines are replaced by histidines. In the C⁻ form the metal-chelating residues are completely or partially replaced. The C⁺ form of L31 in *B. subtilis* called RpmE1, has been shown to play a role in Zn²⁺ homeostasis and can be a major source of Zn²⁺, especially in cells that are rapidly growing in Zn²⁺-limited conditions (Nanamiya *et al.* 2006). Furthermore, during growth in Zn²⁺-limited conditions the expression of *ytiA*, encoding the C⁻ form of the L31 protein called RpmE2, is up-regulated as *ytiA* is under the control of Zur (Nanamiya *et al.* 2006). Studies in *B. subtilis* showed that mutations in the Zn²⁺-binding (CxxC) motif of RpmE1, resulted in the loss of Zn²⁺ binding as well reduced levels of RpmE1, and is likely due to increased degradation of the protein (Nanamiya *et al.*, 2004). Additionally, expression of the C⁻ form of the L31 protein, is increased during exponential growth or by inactivation of Zur, and repressed by the addition of Zn²⁺ to the culture (Nanamiya *et al.* 2006). A study in *S. coelicolor* showed that the C⁺ form (RpmE1) in this bacterium is regulated by the sigma factor σ^R , as predicted from the promoter sequence. Expression of *rpmE1* was slightly increased during growth in Zn²⁺-limited conditions, suggesting that Zn²⁺ depletion may stimulate the σ^R regulatory system. The σ^R factor is involved in the stress response to thiol oxidation that involves the use of Zn²⁺ to protect cells (Shin *et al.* 2007).

1.9.2 L31 proteins and intracellular Zn²⁺ storage

Extensive studies conducted with *B. subtilis* have demonstrated that the Zn²⁺-binding L31 protein can be a crucial source of Zn²⁺ for the bacterial cell and a Zn²⁺-mobilisation model has been proposed (Figure 1.5). During normal/exponential growth of *B. subtilis* Zn²⁺ is freely available and the Zn²⁺-binding RpmE1 is constitutively produced. During this time the ribosome complex incorporates the Zn²⁺-containing RpmE1 and the expression of RpmE2 is repressed (Abrantes *et al.* 2011; Akanuma *et al.* 2006; Nanamiya *et al.* 2004). In the absence of Zn²⁺, at the end of exponential growth, or in Zn²⁺-limited conditions, Zur is unable to bind to the Zur box in the *rpmE2* promoter region and de-repression of expression ensues. The newly synthesised RpmE2 has a higher affinity for the ribosome than RpmE1 and thus RpmE2 is efficiently incorporated into the ribosome displacing RpmE1.

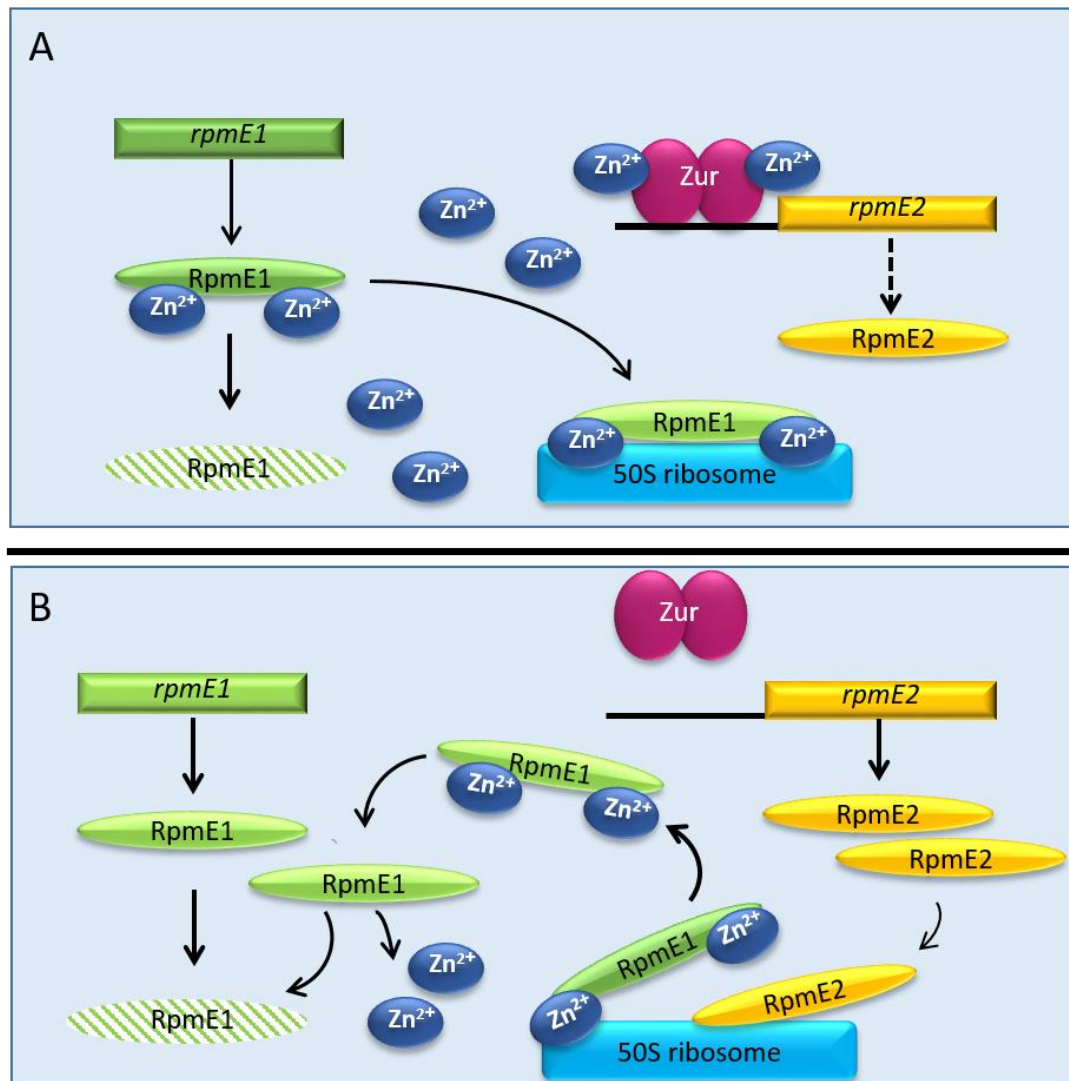


Figure 1.5: Mechanism of Zn²⁺ mobilisation from the RpmE1 L31 ribosomal protein

Diagrammatic representation of (A) Zn²⁺-sufficient (normal conditions) and (B) Zn²⁺-limited conditions. In the presence of Zn²⁺ (blue ellipsoid), the Zn²⁺-dependent Zur regulator (magenta) is Zn²⁺ loaded and represses the transcription of *rpmE2* (yellow). This results in ribosomes containing Zn²⁺-bound RpmE1 (green). In the absence of Zn²⁺, Zur is unable to bind to the region up-stream of *rpmE2*, allowing for transcription of *rpmE2* to occur. The newly synthesised RpmE2 has a higher affinity for the ribosome than RpmE1, and thus displaces the bound RpmE1. The released RpmE1 is then degraded by protease(s), releasing the bound Zn²⁺ making it bioavailable. Under these conditions, any newly synthesised RpmE1 cannot to bind Zn²⁺ and is thus unstable (stippled green). This regulatory system contributes to zinc homeostasis in the cell under zinc-limited conditions.

The RpmE1 protein is then degraded by an unknown protease(s) allowing for the release of Zn. Under these conditions any newly synthesised RpmE1 is unstable as there is no available Zn. It is believed that RpmE1 cannot be released from ribosomes in the absence of functional RpmE2, even if the cells encounter Zn²⁺-deficient conditions (Akanuma *et al.* 2006). According to this Zn²⁺-mobilisation model, the major function of the L31 RpmE1 protein is to store Zn²⁺ ions, rather than being an important functional component of the ribosome (Natori *et al.* 2007). Supporting this, there is evidence to suggest that L31 (unlike most ribosomal proteins) is not absolutely essential and is only loosely associated with the ribosome (Akanuma *et al.* 2006). Thus RpmE1 is likely to represent the major Zn²⁺-storage system within bacterial cells.

There has only been limited studies on the L31 proteins produced by *A. baumannii*. A study using an *A. baumannii* Δ zur strain showed that the non-Zn²⁺ binding L31, RpmE2, was up-regulated which indicated that this protein is under Zur regulation (Mortensen *et al.* 2014). However, to date, there has been no study that has investigated the role of the L31 proteins in *A. baumannii* Zn²⁺ storage.

1.9.3 Other ribosomal proteins with Zn²⁺-binding motifs

Several other ribosomal proteins have paralogs including the S14 ribosomal proteins in *B. subtilis*, RspN (C⁺) and YhzA (C⁻, a Zur-regulated paralog). The S14 protein is essential for the assembly of the ribosome, and the non-Zn²⁺ binding protein YhzA that is negatively regulated by Zur under Zn²⁺-sufficient conditions, may function as a substitute S14 protein (Gabriel and Helmann 2009). However, unlike the rapid replacement of RpmE1 with RpmE2, the replacement of the Zn²⁺-binding RspN in the ribosome with YhzA is slow. It has been postulated that YhzA provides a mechanism for providing the essential S14 for *de novo* ribosome synthesis under Zn²⁺-limited conditions, referred to as a “failsafe” model (Natori *et al.* 2007). Other ribosomal proteins such as L32 (RpmF) and L36 (RpmJ) in *B. subtilis* also have CxxC motifs and it is possible that they also bind Zn²⁺ (Gabriel and Helmann 2009), but there is no evidence of any non Zn²⁺-binding paralogs and thus cannot be substituted. It is presumed that the Zn²⁺ bound to these ribosomal

proteins is only available once the ribosome is degraded. In *S. coelicolor* the L33 ribosomal protein has both a C⁺ form (RpmG) and C⁻ forms (RpmG2 and RpmG3). RpmG2 has been shown to be controlled by Zur, however its role in intracellular Zn²⁺ storage is not yet clear (Shin *et al.* 2007). The *A. baumannii* L36 ribosomal protein (RpmJ, A1S_3060 in ATCC 17978) contains the Zn²⁺-binding motif CXXC, but no paralogs have been identified indicating it is unlikely that this ribosomal protein is involved in Zn²⁺ storage.

Previous studies and knowledge about L31 proteins indicate that these paralogous proteins are potential factors for maintaining Zn²⁺ homeostasis especially during growth in Zn²⁺-limited environments or for survival in host niches and therefore for bacterial virulence. However, little is known about the role of these proteins in *A. baumannii*. Thus, investigation of these proteins in *A. baumannii* is an important step to advance the understanding of its pathogenicity and to find a potential target for the development of antimicrobial for *A. baumannii* infection.

1.10 Scope of this thesis

A. baumannii is known as a major agent of hospital-associated infections and its role as a significant human pathogen has been well established. Various factors have been showed to enhance *A. baumannii* pathogenicity. Studies revealed that micronutrition, including metal ions and in particular Zn²⁺, is one of the crucial factors required by bacteria to be a successful pathogen. However, little is known about the role of Zn²⁺ in *A. baumannii* expression of virulence features which can assist its colonisation in host niches. Zn²⁺ is known as an essential element for bacteria for diverse biological processes. In the host the level of free Zn²⁺ is very limited therefore the ability to acquire and store Zn²⁺ enables bacteria to survive during the course of infection. Microorganisms utilise various mechanisms to prevent bioavailable Zn²⁺ level in its cytoplasm. The strategies utilised by bacterial cells in response to Zn²⁺ limitation or toxicity are via transcriptional regulation by metal-sensing metalloregulatory proteins and Zn²⁺ efflux and acquisition across cell membranes. In addition, bacteria utilise a mechanism to release Zn²⁺ from Zn²⁺-

bound proteins to achieve a free pool of Zn^{2+} in Zn^{2+} -deprived conditions. It has been shown that two paralogous L31 proteins, RpmE1 and RpmE2, are implicated in Zn^{2+} storage in bacteria such as *B. subtilis* (Akanuma *et al.* 2006).

The aim of this study was to examine the impact of the micronutrient Zn^{2+} on *A. baumannii* and in particular that the role of L31 proteins, RpmE1 and RpmE2, play in *A. baumannii* Zn^{2+} homeostasis and virulence characteristics. The effects of Zn^{2+} starvation were examined using transcriptomic and phenotypic assays. Comparative genomic analyses were carried out to assess the transcriptome of *A. baumannii* strain ATCC 17978 under defined Zn^{2+} -replete and Zn^{2+} -limiting conditions. The role of L31 proteins, RpmE1 and RpmE2 in *A. baumannii* was investigated by the deletion of *rpmE1* or *rpmE2* in *A. baumannii* ATCC 17978. Comprehensive analysis of the differences between these constructed mutants and the parent, by means of transcriptomics and phenotypic characterisations, aided in identification of molecular mechanisms that play a role in zinc homeostasis in *A. baumannii*. Overall, the wide range of experimental approaches and analyses utilised in this study generated a wealth of information on the *A. baumannii* virulence features. The results presented here have advanced the understanding about the importance of Zn^{2+} and L31 proteins that contribute to the *A. baumannii* virulence capacity.

CHAPTER 2
MATERIALS AND METHODS

2.1 Reagents, buffers, solutions and growth media

Stock solutions of media and buffers along with their constituents used in this study are described in Table 2.1, all of which were prepared according to the manufacturers' instructions. The chemicals used in the preparation of bacterial growth media were typically molecular grade and obtained from Sigma-Aldrich (Australia) unless otherwise specified. All growth media, buffers, and solutions were sterilised, when needed, by autoclaving at 121 °C for 15 minutes (min) or by passaging solutions through a 0.22 µm filter (Sartorius Stedim, Germany).

2.2 Bacterial strains and growth conditions

The bacterial strains and plasmids used in this study are listed in Table 2.2 and Table 2.3, respectively. Bacterial cultures were routinely grown in either Mueller Hinton (MH), Luria Bertani (LB) or M9 media at 37 °C unless otherwise stated. Tubes with broth cultures were incubated at a 45° angle with shaking (200 rpm) to achieve appropriate aeration.

For creating Zn²⁺-limited conditions two media were used, MH and M9 media. MH Zn²⁺-limited medium was prepared using MH broth as per the manufacturer's instructions. The MH broth was treated with 2.5% (v/v) Chelex 100[®] (Bio-Rad, Australia) and incubated overnight (ON) at 4 °C with shaking. After incubation, the Chelex 100[®] was removed from the medium, the pH adjusted to 7.3 and the media filtered sterilised. This MH chelex treatment medium was called MH[C] medium. Into MH[C] medium, 50 µM Mg²⁺, 50 µM Ca²⁺ and 5 µM Cu²⁺ were added and this was named MH[CR]. Before being used for bacterial growth, the MH[CR] medium was supplemented with 50 µM Fe²⁺, 5 µM Mn²⁺ and µM Zn²⁺ to create MH Zn²⁺-replete medium or MH[CRsup] medium. The MH[CR] medium, with the addition of 50 µM Fe²⁺ and 5 µM Mn²⁺ with no Zn²⁺ supplementation was named MH Zn²⁺-limited medium or MH[CRsup-Zn²⁺].

Table 2.1: Media, buffers, solutions and reagents

| Constituents | |
|----------------------------------------|---------------------------------------------------------------------------------------------------------------------------------------------------------------------|
| Media | |
| Luria-Bertani broth | 1% (w/v) NaCl, 1% (w/v) tryptone, 0.5% (w/v) yeast extract, pH 7.5 |
| LB agar | LB broth with 1% (w/v) agar |
| M9 salt stock solution (5X) | 64 g (Na ₂ PO ₄)7H ₂ O, 15 g KH ₂ PO ₄ , 2.5 g NaCl, 5.0 g NH ₄ Cl, dH ₂ O to 1000 ml |
| M9 minimal medium | 200 ml M9 salt (5X), 2 ml 1 M MgSO ₄ , 20 ml of 20% succinic acid, 100 µl of CaCl ₂ , sterile dH ₂ O up to 1000 ml |
| M9 agar | M9 medium with 1% (w/v) agar |
| M9 sucrose medium | M9 agar with 5% (v/v) sucrose |
| Mueller Hinton broth | MH broth was prepared as per the manufacturer's instructions |
| MH agar | MH agar was prepared as per the manufacturer's instructions |
| Dulbecco's Modified Eagle medium | DMEM was prepared as per the manufacturer's instructions |
| Reagents, buffers and solutions | |
| 80% glycerol solution | Per 100 ml: 80 ml of glycerol in dH ₂ O |
| GelRed solution | Per 100 ml: 30 µl of GelRed nucleic acid stain and 3.3 ml 3 M NaCl in dH ₂ O |
| Agarose gel | 1% (w/v) agarose in 0.5% TAE buffer |

Table 2.1: Cont.

| Constituents | |
|---------------------------------|-----------------------------------------------------------------------------------------------------------------------------|
| Reagents, buffers and solutions | |
| TAE buffer stock solution (50X) | 24.2% (w/v) Tris-base, 50 mM ethylenediaminetetra-acetic acid (EDTA) pH 8.0, 5.71% (v/v) glacial acetic acid |
| Phosphate buffered saline (PBS) | 136 mM NaCl, 2.7 mM KCl, 1.76 mM KH_2PO_4 , 8.1 mM $(\text{Na}_2\text{HPO}_4)_2\text{H}_2\text{O}$, pH 7.5 |
| Trypan blue solution | 4 g Trypan blue in 80 ml PBS |
| Crystal violet | 1 g Crystal violet in 1000 ml in dH_2O |

Table 2.2: Bacterial strains used in this study

| Strain | Genotype or description ^a | Reference/ source |
|------------------------------------------------------------------------------------------|--------------------------------------------------------------------------------------------------------------------------------|--------------------------------------------------------|
| <i>Acinetobacter baumannii</i> | | |
| <i>A. baumannii</i> ATCC 17978 ^b | Non-international clone; Meningitis isolate | CP000521 (Smith <i>et al.</i> 2007) ^c |
| <i>A. baumannii</i> ATCC 17978_ <i>rpmE1</i> ::Ery ^R ($\Delta rpmE1$) | <i>rpmE1</i> deletion in <i>A. baumannii</i> ATCC 17978; Ery ^R | This study |
| <i>A. baumannii</i> ATCC 17978_ <i>rpmE2</i> ::Ery ^R ($\Delta rpmE2$) | <i>rpmE2</i> deletion in <i>A. baumannii</i> ATCC 17978; Ery ^R | This study |
| <i>A. baumannii</i> $\Delta rpmE1$:pWH1266 | <i>A. baumannii</i> ATCC 17978 $\Delta rpmE1$ mutant containing pWH1266; Amp ^R and Ery ^R | This study |
| <i>A. baumannii</i> $\Delta rpmE2$:pWH1266 | <i>A. baumannii</i> ATCC 17978 $\Delta rpmE2$ mutant containing pWH1266; Amp ^R and Ery ^R | This study |
| <i>A. baumannii</i> $\Delta rpmE1$:pWH <i>rpmE1</i> | <i>A. baumannii</i> ATCC 17978 $\Delta rpmE1$ mutant containing pWH <i>rpmE1</i> ; Amp ^R and Ery ^R | This study |
| <i>A. baumannii</i> $\Delta rpmE2$:pWH <i>rpmE2</i> | <i>A. baumannii</i> ATCC 17978 $\Delta rpmE2$ mutant containing pWH <i>rpmE2</i> ; Amp ^R and Ery ^R | This study |

Table 2.2: Cont.

| Strain | Genotype or description ^a | Reference/ source |
|-------------------------------------------|---------------------------------------------------------------------------------------------------------------------------------------------------------------------------------------------------------------------------|----------------------|
| <i>Escherichia coli</i> strains | | |
| <i>E. coli</i> DH5 α | <i>fhuA2</i> Δ (<i>argF-lacZ</i>)U169 <i>phoA</i> <i>glnV44</i> Φ 80 Δ (<i>lacZ</i>)M15 <i>gyrA96 recA1 relA1 endA1 thi-1 hsdR17</i> | (Hanahan 1983) |
| <i>E. coli</i> TOP10 | <i>mcrA</i> , Δ (<i>mrr-hsdRMS-mcrBC</i>), Δ <i>lacX74</i> , <i>deoR</i> , <i>recA1</i> , <i>araD139</i> Δ (<i>ara-leu</i>)7697, <i>galk</i> , <i>rpsL</i> , <i>endA1</i> , <i>nupG</i> | Invitrogen |
| <i>E. coli</i> SM10- λ <i>pir</i> | TpR SmR <i>recA</i> , <i>thi</i> , <i>pro</i> , <i>hsdR-</i> <i>M+RP4</i> : 2-Tc:Mu: Km Tn7 λ <i>pir</i> | Invitrogen |

^a. Ery^R: resistance to erythromycin at 10 μ g/ml; Amp^R: resistance to ampicillin at 100 μ g/ml

^b. ATCC: American Type Culture Collection

^c. Department Bacteriologie-Virologie, Hospital de Bicetre, Le-Kremlin-Bicetre, France.

Table 2.3: Plasmids used in this study

| Strain | Genotype or description ^a | Reference/ source |
|-------------------------|------------------------------------------------------------------------------------------------------------------------------------------------------------------------------------------------------------|------------------------------|
| pBluescript-SKII+ | Amp ^R ; Expression vector | (Alting-Mees and Short 1989) |
| pBS_ <i>rpmE1</i> | Amp ^R ; pBluescript-SKII+ containing flanking regions (1.5 kb up-stream and down-stream) of <i>rpmE1</i> (A1S_2423) (<i>EcoRI</i> - <i>XbaI</i>) (6 kb) | This study |
| pBS_ <i>rpmE2</i> | Amp ^R ; pBluescript-SKII+ containing flanking regions (1.5 kb up-stream and down-stream) of <i>rpmE2</i> (A1S_0391) (<i>EcoRI</i> - <i>XbaI</i>) (6 kb) | This study |
| pBS_ <i>rpmE1</i> ::Ery | Amp ^R Ery ^R ; pBluescript-SKII+ containing flanking regions (1.5 kb up-stream and down-stream) of <i>rpmE1</i> (A1S_2423) with Ery cartridge (<i>EcoRI</i> - <i>XbaI</i>) (6.8 kb) | This study |
| pBS_ <i>rpmE2</i> ::Ery | Amp ^R Ery ^R ; pBluescript-SKII+ containing flanking regions (1.5 kb up-stream and down-stream) of <i>rpmE2</i> (A1S_0391) with Ery cartridge (<i>EcoRI</i> - <i>XbaI</i>) (6.8 kb) | This study |

Table 2.3: Cont.

| Strain | Genotype or description ^a | Reference/ source |
|-----------------------------|-------------------------------------------------------------------------------------------------------------------------------------------------------------------------------------------------|------------------------------------------|
| pEX18Tc | Tet ^R ; <i>sacB</i> -based suicide vector | (Hoang <i>et al.</i> 1998) |
| pEX18Tc_ <i>rpmE1</i> ::Ery | Tet ^R Ery ^R ; pEX18Tc containing flanking regions (1.5 kb up-stream and down-stream) of <i>rpmE1</i> (A1S_2423) with Ery cartridge (<i>KpnI</i> - <i>XbaI</i>) (9.8 kb) | This study |
| pEX18Tc_ <i>rpmE2</i> ::Ery | Tet ^R Ery ^R ; pEX18Tc containing flanking regions (1.5 kb up-stream and down-stream) of <i>rpmE2</i> (A1S_0391) with Ery cartridge (<i>KpnI</i> - <i>XbaI</i>) (9.8 kb) | This study |
| pVA819 | Cm ^R Ery ^R ; source for Ery cartridge | Invitrogen |
| pWH1266 | Amp ^R Tet ^R ; <i>Acinetobacter/E. coli</i> shuttle vector, generated by ligation of pBR322 to a cryptic <i>Acinetobacter</i> plasmid using <i>PvuII</i> (8.9 kb) | (Hunger <i>et al.</i> 1990) ^b |
| pWH <i>rpmE1</i> | Amp ^R Tet ^R ; pWH1266 containing <i>rpmE1</i> (A1S_2423) via <i>BamHI</i> sites (9.1 kb) | This study |

Table 2.3: Cont.

| Strain | Genotype or description ^a | Reference/ source |
|----------|-----------------------------------------------------------------------------------------------------------------------|----------------------|
| pWHrpmE2 | Amp ^R Tet ^R ; pWH1266 containing <i>rpmE2</i> (A1S_0391) via <i>Bam</i> HI sites (9.1 kb) | This study |

^a. Ery^R: resistance to erythromycin at 10 µg/ml; Amp^R: resistance to ampicillin at 100 µg/ml; Cm^R: resistance to chloramphenicol at 25 µg/ml; Tet^R: resistance to tetracycline at 12 µg/ml.

^b. Institut Für Mikrobiologie und Biochemie, Frederich-Alexander Universität Erlangen-Nürnberg, Germany.

M9 Zn²⁺-limited medium was prepared using M9 salt stock solution (Table 2.1). Briefly, 5X M9 salt stock solution was treated with 5% (v/v) Chelex 100[®] (Bio-Rad, Australia) and incubated ON at 4 °C with shaking, followed by filter sterilisation. After Chelex 100[®] treatment, the solution was diluted (1:5) and supplemented with 2 mM MgSO₄, 0.4% (w/v) succinic acid and 0.1 mM CaCl₂ on the day of use and was named M9[C] medium. To deplete the medium of any remaining Zn²⁺, *N,N,N',N'*-tetrakis-(2-pyridylmethyl) ethylenediamine (TPEN) was added to the M9[C] medium at room temperature (RT) for 30 min at a final concentration of 5 μM; this medium was named M9[CT] medium. To prepare the M9 Zn²⁺-limited medium, M9[CT] was supplemented with sterile solutions of FeSO₄ and MnSO₄ to give a final concentrations of 50 μM Fe²⁺ and 5 μM Mn²⁺, respectively, and was called M9[CTFM] medium. Sterile solutions of ZnSO₄ were added to this M9[CTFM] medium to give a final concentration of 50 μM Zn; this medium was called M9 Zn²⁺-replete medium or M9[CTFM+Zn²⁺].

For antibiotic selection on solid media, the media were allowed to cool to approximately 50 °C after autoclaving before the addition of the antibiotic. In experiments involving *E. coli* the following antibiotic concentrations were used when appropriate; 100 μg/ml ampicillin (Amp), 25 μg/ml chloramphenicol (Cm), 50 μg/ml erythromycin (Ery) or 12 μg/ml tetracycline (Tet). The following antibiotic concentrations were used in experiments with *A. baumannii*; 100 μg/ml Amp, 25 μg/ml Cm, 10 μg/ml Ery or 12 μg/ml Tet.

2.3 Bacterial phenotypic assays

2.3.1 Bacterial growth under Zn²⁺-limited and Zn²⁺-replete conditions

In this study, MH medium was initially used for creating Zn²⁺-limited culture (see Section 2.2). For growth assays, bacterial cultures were grown ON in 5 ml LB medium. The ON culture was pelleted at 8000 x *g* for 5 min and re-suspended in 5 ml PBS (repeated 3 times). After this washing process, the pellets were resuspended in MH[CRsup-Zn] medium (Section 2.2). Washed cells (200 μl) were diluted 1:50 into the appropriate media, MH[CRsup] or MH[CRsup-Zn] (Section 2.2), and incubated at

37 °C for 8 hours (hr) in a shaking incubator at 200 rpm. Growth was measured using the optical density (OD) of the culture at 600 nm (OD_{600}) using a spectrometer (Beckman®, USA) every hr.

A Zn^{2+} -limiting culture was also prepared using M9 medium (see Section 2.2). Bacterial growth was achieved using an ON bacterial culture grown in 5 ml LB medium. The ON cells were pelleted at 8000 x *g* for 5 min and re-suspended in 5 ml of M9[CTFM] medium (this wash was repeated 3 times). After this the pellets were re-suspended in 5 ml M9[CTFM] medium and used for growth assays as follows. Washed cells (200 μ l) were diluted 1:50 into the appropriate medium (M9[CTFM] or M9[CTFM+Zn]) and incubated at 37 °C for 8 hr in a shaking incubator at 200 rpm. Growth was measured using the OD_{600} using a spectrometer (Beckman®, USA) every hr.

2.3.2 Minimum inhibitory concentration

The minimal inhibitory concentration (MIC) of bacterial strains to various antimicrobial compounds in MH medium was investigated using two different methods. First, the MIC was determined using a micro-dilution assay in a 96 well trays as described previously by Wiegand et al. (2008). For MIC assays using *A. baumannii*, an ON culture was adjusted to $OD_{600} = 0.6$ and then diluted 1:1000 in MH broth. A 2-fold dilution series of each antimicrobial compound was prepared and added at a 1:1 (v/v) ratio to 100 μ l culture to give a final volume of 200 μ l. To prevent the bacteria from adhering to the bottom of each well, the trays were incubated at 37 °C with shaking at 200 rpm. To minimise evaporation, each tray was wrapped with aluminium foil. Bacterial growth was examined after 18 hr of incubation by measuring the absorbance at OD_{600} using a FLUOstar Omega spectrometer (BMG Labtech, Germany).

The second method to determine the MIC used an agar dilution plate previously described by Wiegand et al. (2008) but with the following modifications. The appropriate volume of a 2-fold dilution series of each antibiotic was added to molten MH agar. Once solidified, 2 μ l of ON bacteria culture grown in LB medium (adjusted to $OD_{600} = 0.01$) was spotted onto each MH plate containing antibiotic.

The plates were incubated at 37 °C for 18 hr and the growth of *A. baumannii* observed. Each MIC assay was performed in duplicate on a given day and repeated three times. A 2-fold or greater difference in the MIC between the test and control strains using either MIC assay was considered significant.

2.3.3 Disk diffusion method for antibiotic resistance

A disk diffusion method was used to investigate the antibiotic resistance profile of *A. baumannii* strains based on the Kirby-Bauer disk susceptibility test (CLSI 2014). Briefly, an ON *A. baumannii* culture grown in LB was diluted in phosphate buffered saline (PBS) to a fixed density (0.5 McFarland units) and 100 µl was spread evenly across the surface of a MH agar plate. Antibiotic discs (Oxoid®, Australia) were then applied to the surface of plate and the plate incubated at 37 °C for 18 hr. Susceptibility was determined by measuring the zone of inhibition.

For investigating the effect of Zn²⁺ limitation on *A. baumannii* antibiotic susceptibility, this disk diffusion method was performed using MH agar with/without the addition of 30 µM TPEN. In addition, prior to the assay, each ON culture was washed three times with PBS as described above and resuspended in PBS prior to addition to the agar plate.

2.3.4 Static biofilm assay

A static biofilm formation assay was performed as described previously (Eijkelkamp et al., 2011) with the following modifications. A single bacterial colony was used to inoculate LB medium that was incubated ON at 37 °C in a shaking incubator. Fifty µl of culture was subsequently diluted 1:100 into either fresh LB broth, or Zn²⁺-limited and Zn²⁺-replete M9 media in a 50 ml plastic tube. Cultures were incubated statically for 72 hr at 37 °C in the dark. Following incubation, the OD₆₀₀ of the culture containing the planktonic growing bacteria was measured and compared to the WT strain to determine growth characteristics. The residual liquid culture was then discarded and adherent cells washed once with PBS then stained by incubating in a solution containing 0.1% crystal violet for 30 min at 4 °C, followed by three washes in PBS. The dye was released from the bound cells by the addition

of 5 ml of an ethanol:acetone (4:1) solution and shaken at 200 rpm for 30 min at RT. Absorbance of the solution was measured at OD₅₉₅ on a FLUOstar Omega spectrometer (BMG Labtech, Germany). The biofilm data for each strain were calculated from the average of at least three independent experiments that each had two technical replicates.

2.3.5 Eukaryotic cell adherence assays

Adherence of *A. baumannii* strains to A549 cells (human type II pneumocytes) was undertaken as previously described (Eijkelkamp *et al.* 2011a; Giard *et al.* 1973). Briefly, Dulbecco's Modified Eagle medium (DMEM) (Invitrogen, Australia), supplemented with 10% foetal bovine serum (Bovogen, Australia), streptomycin 100 µg/ml and 2 mM L-glutamine was used to grow and maintain the A549 cell line. The cell monolayer was examined microscopically to ensure >95% coverage. After washing the A549 cell monolayers with PBS, approximately 1×10^7 colony forming units (CFU) of bacteria were added to each well. The exact number of bacteria used for the assay was based on the CFU determined by a viable count assay. The infected A549 cell monolayers were incubated at 37 °C for 4 hr. After removal of the culture medium, A549 cells in each well were washed three times with 1 ml of PBS. The A549 cells were then detached from the surface of each well by treatment with 0.25% trypsin in PBS. The washed A549 cells were lysed using 200 µl of 0.025% Triton X-100. Aliquots (20 µl) of a 10-fold dilution series of the lysed cell suspension were plated onto LB agar to determine the number of CFU of adherent bacteria per well. For each bacterial strain examined, three independent adherence assays were performed and each assay contained four technical replicates.

2.3.6 Motility assay

Motility, in the form of migration on semi-solid surfaces (swarming), was analysed on agarose (0.25% and 0.5%) containing 5 g/l tryptone and 2.5 g NaCl (Heindorf *et al.* 2014). Motility assays in Zn²⁺-limited medium were performed on semi-solid agarose as described above except that after autoclaving the solution

was cooled down to 56 °C and mixed with the metal ion/ Zn^{2+} chelator TPEN at a concentration of 5 μ M and 10 μ M. Material obtained from a single colony of ON growth on LB-agar was spotted onto the semi-solid agarose plates by puncturing the surface with a sterile toothpick (Heindorf *et al.* 2014). Once inoculated, plates were sealed with parafilm to prevent evaporation and incubated ON at 37 °C. After 18 hr each plate was analysed for bacterial growth and motility and the results documented. Motility was assessed by observing how far the bacteria move from the initial site of inoculation. At least three independent replicates were performed for each strain and condition.

2.3.7 Oxidative stress assay

Survival under conditions of oxidative stress was determined as previously described (Membrillo-Hernandez *et al.* 1997) with the following modifications. Briefly, bacteria were grown ON at 37 °C then diluted 1:50 in MH media supplemented with different concentrations (100, 300, and 500 μ M) of 1,1-dimethyl-4,4-bipyridinium (paraquat) (Sigma Aldrich, Australia) and incubated at 37 °C for 8 hr in a shaking incubator. The bacterial growth (OD_{600}) in media with/without paraquat was measured using a FLUOstar Omega spectrometer (BMG Labtech, Germany).

2.3.8 Statistical analyses

Statistical analyses of the data obtained for the eukaryotic cell adherence assays and the biofilm formation assays were performed using a two-tailed student *t*-test. P value of < 0.05 was considered significant.

2.4 Inductively coupled plasma-mass spectrometry analysis

Inductively coupled plasma mass spectrometry (ICP-MS) was performed on an Agilent 7500 ICP-MS by Flinders University Analytical Services to determine the level of intracellular cations in the bacteria. The samples were prepared as follows. Briefly, bacteria were grown in 10 ml Zn^{2+} -limited (M9[CTFM]) or replete

(M9[CTFM+Zn]) media for 10 hr, followed by centrifugation for 5 min at 4500 x *g*. The cell pellets were washed three times with 10 ml of 5 mM EDTA (pH 7.5) in PBS, followed by three washes in PBS alone. The pellets were re-suspended in 1 ml PBS in a 1.5 ml tube and centrifuged in a microcentrifuge for 5 min at maximum speed (11,000 x *g*). Cell pellets were dried by incubating at 95 °C for 18 hr after which they were dissolved by the addition of 1 ml 35% HNO₃ and incubated for a further 1 hr at 95 °C, following by vortexing for 1 min. High speed centrifugation was then performed at 11,000 x *g* for 30 min and the supernatant was retained. Aliquots of 200 µl were diluted 1:10 with 3.5% HNO₃ and the level of metal ions, specifically Fe²⁺, Zn²⁺, Cu²⁺, Mn²⁺, magnesium (Mg²⁺) and calcium (Ca²⁺) were analysed.

2.5 DNA techniques

2.5.1 Plasmid DNA isolation

Between 1 and 5 ml of ON culture was used for the isolation of plasmid DNA depending on the copy number of the plasmid of interest. The ISOLATE II Plasmid Mini Kit (Bioline, Australia) was used as per manufacturer's instructions and the resulting concentration of the isolated DNA determined as described in Section 2.5.3.

2.5.2 Genomic DNA isolation

Up to 5 ml of ON culture was used to isolate *Acinetobacter* genomic DNA using the Wizard[®] genomic DNA purification kit (Promega, USA) as per manufacturer's instructions using the protocol designed for DNA isolation from Gram-negative bacteria. Concentrations of purified genomic DNA were determined as described in Section 2.5.3.

2.5.3 Quantitation and quality assessment of DNA and RNA

The quality and concentration of isolated DNA and RNA was assessed using a Thermo Scientific NanoDrop™ 1000 spectrophotometer. For both OD₂₆₀/OD₂₈₀

(protein contamination) and OD_{260}/OD_{230} (salt and or detergent contamination), a ratio of absorbance of 1.8 or greater was deemed acceptable for sensitive downstream applications, such as sequencing, qRT-PCR or RNA sequencing. For all other applications the quantity and integrity of isolated DNA was investigated by agarose gel electrophoresis and compared to the Hyperladder™ I DNA standard (BioLine, Australia).

2.5.4 Polymerase chain reaction

Oligonucleotides were synthesised by either GeneWorks (Thebarton South, Australia) or Sigma Aldrich (Australia). A typical 50 µl polymerase chain reaction (PCR) contained 150 ng of template (either plasmid or genomic DNA), 0.2 mM of each dNTP, 200 ng of each primer (Table 2.4), DNA polymerase and 5X PCR buffer Velocity (BioLine, Australia). Standard PCRs were performed on a MultiGene Thermal Cycler (Labnet International, USA) with the following cycling conditions: an initial denaturation step for 2 min at 94 °C, followed by 35 cycles each consisting of a denaturation step for 90 seconds (sec) at 94 °C, an annealing step for 90 sec at 60 °C, and a 72 °C extension for 1 min per kb of expected product. Cycles were followed with a final extension at 72 °C for 5 min. The initial denaturation step was extended to 10 min when performing PCR using bacterial colony material (colony PCR) as template. Agarose gel electrophoresis (Section 2.5.5) was performed to visualise and assess the size, quantity and quality of PCR products.

Colony PCRs were used for screening of the transformed *E. coli* cells harbouring the DNA of interest. Briefly, an single isolated colony was transferred using a sterilised toothpick from a LB agar plate into 8 µl of Milli-Q H₂O. Colony PCR reactions were typically in a 20 µl volume, containing 8 µl of colony material diluted in Milli-Q dH₂O which was added to 0.2 mM of each dNTP, 200 ng of each primer complementary to the 3' and 5' ends of the region to be amplified, 5 units (U) of Econotaq (Lucigen, Australia) or Gotaq® (Promega, Australia) DNA polymerase and

Table 2.4: Oligonucleotides used in this study

| Name ^a | Forward primer (5'-3') ^b | Reverse primer (5'-3') | Reference / source |
|---------------------------------------|-------------------------------------|------------------------------|----------------------|
| Oligonucleotides for qRT-PCR analysis | | | |
| A1S_2501 | CAACACTGGTAAATGGCGTG | ACAACGTTTTTCATTTTCG CC | (Eijkelkamp 2011) |
| A1S_2565 | TGGCTCGATATTCAACGTCA | TAAACAGCAAACCACCAC CACCAA | (Eijkelkamp 2011) |
| A1S_1647 | GGACGCCATCGTCTCG | CGTCCCGGCTTTGTA | (Eijkelkamp 2011) |
| A1S_1266 | ATGCGTGCATCTGATATTGC | TAAACCTAAAGCCGCAC CTG | (Eijkelkamp 2011) |
| A1S_0895 | GCGCAAAGCTGGACTTAAAG | CGGTAAACTGTCGCAAG TCC | (Eijkelkamp 2011) |
| A1S_0145 | CTGTGTTGTGCTGCGAAATC | AAGGTCATCAGGCTGCA TTC | (Eijkelkamp 2011) |
| A1S_0146 | TACAGGCGGCTCAAGCTTAC | GTCATCCGTTAAGGCAC CAG | (Eijkelkamp 2011) |
| A1S_2382 | GGTCGCTCTGGCAACG | GGTCGCTCTGGCAACG | (Eijkelkamp 2011) |
| A1S_1509 | CCAAGGAAGGCGCTGT | TTGGGGAATGGCTTGC | (Eijkelkamp 2011) |

Table 2.4: Cont.

| Name ^a | Forward primer (5'-3') ^b | Reverse primer (5'-3') | Reference / source |
|-------------------|-------------------------------------|--------------------------|----------------------|
| A1S_3177 | GTTTTCCCTGGGCTGATTC | GATCGTGGTGCCATTAT CG | (Eijkelkamp 2011) |
| A1S_0391 | ACACGCCCTTCATTA CTTC | CATGACACCAATGCAGA CG | This study |
| A1S_2423 | CCAGCAAAACGTTGTTGA A | TGCAACTTGTCTTGCG GTA | This study |
| A1S_0452 | AGTCGTTGAAAAGCCAAAG C | TCGCCCTGTAAATCTTTT GG | This study |
| A1S_1217 | GGCTTGGGTACAGGCAGAT A | AGGTAAGGCCAACACA ATCG | This study |
| A1S_3217 | GGTTTACCGGTGCTGAGTG T | TGCTGGTCTTCTAGGCG AAT | This study |
| A1S_3060 | AAGCTTCTGTAAAGAAAAT TTGTGG | CTTGACGCTGCTTATGA CGA | This study |
| A1S_r01 | CAGCTCGTGTCGTGAGATG T | CGTAAGGGCCATATGAC TT | (Eijkelkamp 2011) |
| A1S_1320 | TATCTCTCGATTGGCGGAA G | TTCTTGCCCCAACACATC AT | (Eijkelkamp 2011) |
| A1S_3382 | GGTGCAACGCTGTTACAAG A | GCCAAGGTAAATCCGA CAA | (Eijkelkamp 2011) |

Table 2.4: Cont.

| Name ^a | Forward primer (5'-3') | Reverse primer (5'-3') | Reference / source |
|-------------------------------------------------------------------------------------------------------------------|------------------------------------------------|------------------------------------------------|--------------------|
| A1S_0092 | CAAACGCAACTCGACTTT GA | GCGTCTTTATAGCTGAC CGC | This study |
| A1S_3475 | AGGGTCTGAGCTGTTAGG CA | TGACAGCGTGATCTGGA GAC | This study |
| A1S_1045 | TAAGGGTATAACGATGGC CG | CAGCAATGTTGGCGATA GAA | This study |
| Oligonucleotides for mutagenesis/cloning of Zn ²⁺ -regulated genes from <i>A. baumannii</i> ATCC 17978 | | | |
| Upstream _rpmE2/EcoRI | GAGAG GAATTC GTGTAGT CAATGAGGTATCG | | This study |
| Upstream _rpmE2/ BamHI | | GAGAG GATCC CAATGA CCCTAAAAGGCTAC | This study |
| Downstream _rpmE2/ BamHI | GAGAG GATCC GAAGCCT AAGACTCATCTCCTC | | This study |
| Downstream _rpmE2/XbaI | | GAGAT CTAG AGCATCTC ACTAAAGGGGTGGTTC | This study |
| Upstream _rpmE1/EcoRI | GAGAG GAATTC GGCTATG GTCACATTGCGATTG | | This study |
| Upstream _rpmE1/ BamHI | | GAGAG GATCC CGTCGA TTACTCCTAATTGAAG | This study |

Table 2.4: Cont.

| Name ^a | Forward primer (5'-3') | Reverse primer (5'-3') | Reference / source |
|-----------------------------|---------------------------------------|--------------------------------------|--------------------|
| Downstream _rpmE1/ BamHI | GAGAGGATCCACTTCAAA ACGAAACAAAAACGG | | This study |
| Downstream _rpmE1/XbaI | | GAGATCTAGAGAAATC AAAGTCAGCATCAGG | This study |
| EryFor | GAGAGGATCCGAAGGAG TGATTACATGAACAA | | This study |
| EryRev | | GAGAGGATCCCTCATAG AATTATTCCTCCCG | This study |
| CheckUp_ rpmE1/For | GCTTTACGCTGGCATTG TTG | | This study |
| CheckDown_ rpmE1/Rev | | CTTAGGCCAGTTCGAT CAAG | This study |
| CheckUp_ rpmE2/For | GTTGTAGTCAATGAGGTA TCG | | This study |
| CheckDown_ rpmE2/Rev | | CTTAGGCCAGTTCGAT CAAG | This study |
| rpmE1_ BamHI | GAGAGGATCCGTGATCA ATTGCGATGACAGC | GAGAGGATCCGCATAA GCCCGTTTTTTGTTTC | This study |

Table 2.4: Cont.

| Name ^a | Forward primer (5'-3') | Reverse primer (5'-3') | Reference / source |
|--------------------|--------------------------------------------|---------------------------------------------|--------------------|
| <i>rpmE2_BamHI</i> | GAGAG GATCCC CTTTTAG GGTTACATTGA | GAGAG GATCCCC AATG GTTTAAGTGTATTG | This study |
| M13 | GTAAAACGACGGCCAG | CAGGAAACAGCTATGAC | |
| pEX18Tc | GAGACCTCTTCGCTATTA CGCCAG | GAGAGTTGTGTGGAATT GTGAGCG | This study |

^a. Name assigned to primer set, except where single primers are stated.

^b. Nucleotide sequence in bold font indicates introduced restriction endonuclease sites.

1X Econotaq (Lucigen, Australia) or Gotaq® (Promega, Australia) buffer, respectively. Standard cycling conditions for a colony PCR were as follows: 5 min initial denaturing step at 94 °C, followed by 25 cycles of a 30 sec denaturing step at 94 °C, 30 sec annealing step at 55 °C 1 min per kb extension step at 72 °C, followed by a final extension step at 72 °C for 10 min. PCR product were visualised by gel agarose electrophoresis (Section 2.5.5).

2.5.5 Agarose gel electrophoresis of DNA

DNA fragments obtained from PCR amplification (Section 2.5.4) were electrophoresed on an agarose gel following standard molecular biology methods. Agarose gels were made by dissolving agarose in 0.5X TAE buffer to give a final concentration of 1% agarose, which was used for the resolution of DNA fragments ranging from 0.2 to 10 kb. The Hyperladder I (BioLine, Australia) was used as a molecular weight standard. Agarose gels were electrophoresed in 0.5X TAE buffer at 100 volts until the loading dye (bromophenol blue) had migrated approximately two thirds down the length of the gel. Gels were stained in GelRed (Biotium, Australia) for approximately 20 min prior to visualisation and imaged using a DigiDoc™UV imager (Bio-Rad, Australia).

2.5.6 Extraction and purification of DNA from agarose gel

DNA fragments were electrophoresed and stained as described in Section 2.5.5, then visualised using UV trans illuminator 2000 (Bio-Rad, Australia). Fragments of interest were excised using a sterile scalpel blade and transferred to sterile 1.5 ml microfuge tubes. They were subsequently purified using the Bio-Line Isolate PCR and Gel kit (BioLine, Australia) according the manufacturer's instructions.

2.5.7 Purification of DNA fragments

PCR generated DNA fragments that had been excised from agarose gels (Section 2.5.6) were purified using the ISOLATE PCR and Gel Kit (BioLine, Australia)

as per manufacturer's instructions. DNA concentrations of purified fragments were determined as described in Section 2.5.3.

2.5.8 DNA sequencing

All Sanger sequencing reactions were performed by the Australian Genome Research Facility (AGRF, Australia) using capillary separation. Depending on the size of the template, up to 500 ng of template DNA was used per reaction, together with 3.2 pmol of the appropriate sequencing primer (Table 2.4).

2.6 RNA Techniques

2.6.1 RNA isolation

Cells were grown for mRNA analysis as described in the relevant Chapters. Typically, up to 10 ml of culture were grown to an $OD_{600} = \sim 0.5$ unless otherwise stated. Cells were pelleted by centrifugation ($8,000 \times g$ for 10 min at 4°C) and lysed in 1 ml TRIzol[®] reagent (Invitrogen[™], ThermoFisher, Australia) with 200 μl chloroform by mixing, followed by phase separation using centrifugation ($15,000 \times g$ for 20 min at 4°C). The aqueous phase was removed and transferred to a clean 1.5 ml microcentrifuge tube and the RNA extracted using the ISOLATE II RNA Mini Kit (BioLine, Australia) as per the manufacturer's instructions. RNase-free disposable plastic ware was used during all steps of the RNA isolation. Diethyl pyrocarbonate (DEPC)-treated Milli-Q water was used for elution and preparation of 70% ethanol solution. The isolated RNA was stored at -20°C for short term storage or at -70°C for long term storage.

2.6.2 Quantitative reverse transcription-PCR

Copy DNA (cDNA) was synthesised from isolated RNA using random hexamers (GeneWorks, Australia) and M-MLV reverse transcriptase (Promega, USA) according to the manufacturer's instructions. The oligonucleotides used in this study were designed using the Primer3 primer design software and are listed in Table 2.4.

Real-time quantitative PCR (qRT-PCR) reactions were performed on a Rotor-Gene RG-3000 (CorbettLifeScience™, Qiagen, Germany) using the DyNAmo SYBR®green qPCR kit (Finnzymes™, ThermoFisher, Australia). A typical qRT-PCR reaction was setup as follows; initial denaturation for 10 min at 95 °C, followed by 40 cycles each consisting of 10 sec at 95 °C, 15 sec at 55 °C and 20 sec at 72 °C. The reaction was completed with melting temperature analysis using 0.5 °C increments ranging from 72 °C to 95 °C. The results of the melt curves were used to examine both specific products as well as for the identification of non-specific amplicons. Transcriptional differences were calculated using the $\Delta\Delta C_t$ method (Livak and Schmittgen 2001). Amplification products generated from the GAPDH (A1S_2501) and 16sRNA genes (A1S_r01) were used for reference.

2.6.3 Next-generation RNA sequencing analysis

Samples for transcriptomic profiling using RNA-seq analysis were prepared by growing *A. baumannii* cells in Zn²⁺-limited and Zn²⁺-replete media to an OD₆₀₀ = 0.5. Cells were pelleted by centrifugation at 8,000 x g for 10 min and the RNA was then purified as described above (Section 2.6.1). The RNeasy MinElute Cleanup Kit (Qiagen, Australia) was used to further purify and concentrate the RNA as per manufacturer's instructions. RNA isolated from three separate RNA extractions were pooled. For RNA-seq, two RNA samples were prepared; 500 ng in 3 µl to assess the quality of the RNA and 1500 ng in 5 µl for the RNA-seq assay. The Ribo-Zero™ Magnetic Kit (Illumina, USA) was used for ribosomal RNA reduction to remove the 23S, 16S and 5S rRNA. RNA was size fractionated to ~300 bp, converted to cDNA and barcoded to allow identification after RNA sequencing. Sequencing was undertaken by the Adelaide Integrated Bioscience Laboratories (Adelaide, South Australia) using an Illumina HiSeq 2500 sequencing system.

2.7 DNA manipulations

2.7.1 Digestion and ligation

Restriction digestions were performed as per manufacturer's recommendations using restriction endonucleases from New England Biolabs. Single digestions were performed using the appropriate buffer for the restriction enzyme used. Double digestions were performed with a buffer that was most compatible with the two restriction enzymes used. Shrimp alkaline phosphatase (Promega, Australia) treatment was performed to minimise the amount of self-ligated products. Restriction enzymes and alkaline phosphatase used in the reactions were heat-inactivated as per manufacturer's recommendations. Ligation reactions were performed in a 25 μ l volume containing 2.5 μ l 10X ligation buffer (commercially supplied), 1 μ l of T4 DNA (10 units/ μ l, BioLine, Australia) and a 1:3 ratio of free ends for vector to insert DNA; volume was made up to 25 μ l with sterile Milli-Q H₂O. Ligation reactions were incubated ON at 4 °C or for 30 min at RT.

2.7.2 Conjugation

Conjugative DNA transfer was utilised to transfer plasmid into recipient bacterial cells. Briefly, 200 μ l of *E. coli* SM10 donor cells (Table 2.2) and the recipient cells were separately grown in 10 ml of LB medium in 50 ml tubes and incubated ON at 37 °C in a shaking incubator. Each culture was washed in LB medium then centrifuged at 8,000 x *g* for 5 min and the cell pellet re-suspended in 10 ml fresh LB medium. The re-suspended donor and recipient cells were mixed together at a 1:10 ratio and then centrifuged at 4,000 x *g* for 5 min. The supernatant was removed and the cell pellet containing both strains was re-suspended in 200 μ l of fresh LB medium and placed into the centre of a LB plate. Plates were incubated for 4 hr at 37 °C to allow for conjugation. Cells were recovered by scraping the surface of the agar plate and transferred into 50 ml tubes with 5 ml of fresh LB medium. One hundred μ l aliquots of each of 10-fold serial dilution of the cell suspension were plated onto LB medium with the appropriate antibiotics (to select for the recipient strain containing the transferred plasmid) and incubated ON at 37 °C.

2.7.3 Preparation of chemically competent *E. coli* cells

A single colony of *E. coli* DH5 α was used to inoculate 10 ml of LB broth and grown shaking ON at 37 °C. The following day this was diluted 1:100 into 20 ml of LB, grown shaking at 37 °C until early log-phase ($OD_{600} = 0.4$) and then placed on ice for 10 min. Cells were pelleted by centrifugation (8,000 $\times g$ for 5 min at 4 °C), carefully re-suspended in 10 ml of ice cold 100 mM MgCl₂ and incubated on ice for 5 min. Cells were pelleted by centrifugation (8,000 $\times g$ for 10 min at 4 °C) and re-suspended in 2 ml of ice cold 100 mM CaCl₂ before being a further incubation on ice for 1 hr. Glycerol was added up to 30% and 100 μ l aliquots of cells were snap-frozen and stored at -80 °C for future use.

2.7.4 Transformation of chemically competent *E. coli* cells

For each transformation experiment, a 100 μ l aliquot of frozen chemically competent *E. coli* cells (Section 2.7.3) was thawed on ice prior to use. Purified plasmid DNA \sim 250 ng/ μ l (Section 2.5.1) or a ligation reaction (Section 2.7.1) was added to the cells and gently mixed before being incubated on ice for 30 min. Cells were then heat-shocked at 42 °C for 30 sec and allowed to recover on ice for 30 min. LB broth (400 μ l) was added to the transformed cells and the transformation mix was incubated with shaking at 37 °C for 1-2 hr. Aliquots of transformed cells were plated onto selective LB agar (containing the appropriate antibiotic/s), and incubated ON at 37 °C; single colonies were re-streaked onto selective LB agar for further analysis.

2.7.5 Preparation of electrocompetent *A. baumannii* cells

Electrocompetent *A. baumannii* cells were prepared as follows. An ON culture from a single colony of *A. baumannii* strain ATCC 17978 was used to inoculate at 1:50 dilution into 20 ml of LB medium. The culture was incubated at 37 °C with shaking until early log-phase ($OD_{600} = 0.4$) and then placed on ice for 10 min. Cells were pelleted by centrifugation (8,000 $\times g$ for 10 min at 4 °C) and the pellet was washed three times using 10 ml sterile, pre-chilled 10% glycerol (v/v in Milli-Q

H₂O). Following another round of centrifugation at 8,000 x *g* for 10 min at 4 °C cells were re-suspended in 10 ml 10% glycerol and placed on ice for approximately 30 min. Cells were then pelleted by slow centrifugation (5,000 x *g* for 10 min at 4 °C) and the supernatant carefully removed by decanting. The cell pellet was resuspended in 10 ml of sterile Milli-Q water and centrifuged again before the supernatant was carefully removed. The final cell pellet was re-suspended in the residual liquid to generate approximately 200 µl of electrocompetent cells.

2.7.6 Transformation of electrocompetent *A. baumannii* cells

Transformation of electrocompetent *A. baumannii* cells was performed as previously described (Aranda *et al.* 2010). For each transformation, an aliquot of electrocompetent *A. baumannii* cells (prepared as described in Section 2.7.5) was carefully mixed with plasmid DNA (up to a volume of 25 µl and an approximate quantity of 500 ng) and incubated on ice for 5 min. The mixture was then transferred to a pre-chilled sterile electroporation cuvette (1 mm electrode gap, Bio-Rad, Australia) and electroporated at 2.0 kV, 200 Ω and 25 µF using a MicroPulser (Bio-Rad, Australia). Cells were allowed to recover by the addition of 1 ml of fresh LB medium and incubated in the shaking incubator at 37 °C for at least 1 hr. Aliquots of the transformation mix were plated onto LB agar containing the appropriate antibiotic selection and incubated ON 37 °C. Single colonies were re-streaked on selective LB agar for further analysis.

2.7.7 Construction of *A. baumannii* mutant strains by gene replacement

The construction of *A. baumannii* ATCC 17978 mutants was undertaken by gene replacement via homologous recombination. For construction of the mutagenesis cassettes, the up-stream and down-stream regions of the target gene were PCR amplified from genomic DNA isolated from *A. baumannii* ATCC 17978 using primer pairs specific for each target gene (Table 2.4). Primers for flanking region amplification incorporated restriction sites suitable for cloning into the pBluescript II SK+. An erythromycin cassette (Ery cartridge) was amplified using primers EryFor and EryRev using pVA819 DNA as the template (Table 2.3). The up-

stream and down-stream region PCR products were digested then ligated together as outlined above (Section 2.7.1). After ligation, PCR was conducted using this ligation product as the template with the primers Upstream/For and Downstream/Rev (Table 2.4) specific for the up-stream and down-stream regions surrounding the target gene. The PCR products then were purified (Section 2.5.6), digested with the appropriate restriction site enzymes, and cloned into pBluescript II SK+.

The Ery cartridge was cloned in between the flanking regions using methods previously described (Section 2.7.1). Colonies containing the desired construct were isolated on an LB plate with Ery²⁵ and identified by PCR. After confirmation of the insertion of the Ery cartridge, plasmids were purified (Section 2.7.1) and subsequently digested with the appropriate restriction site enzymes to excise the construct containing the flanking regions with Ery cartridge insertion. The product was subsequently cloned into a digested pEXT18Tc suicide vector with appropriate restriction enzymes. Following transformation into *E. coli* DH5 α (Section 2.7.4), transformant cells were grown on LB plates with Ery¹⁰ and Tet¹² ON 37 °C. Colonies were screened by PCR and visualised by gel electrophoresis (Section 2.5.4). Colonies indicating a correctly sized PCR pattern, were re-isolated on LB plates containing Tet¹² and the plasmid DNA isolated and purified (Section 2.5.1). Plasmid DNA was digested with appropriate restriction endonucleases (Section 2.7.1) to confirm the presence of pEXT18Tc and a ligated insert of up-stream and down-stream flanking regions of the gene of interest and the Ery cartridge. Agarose gel electrophoresis (Section 2.5.5) was carried out to examine and confirm the successful cloning of the region. Plasmids then were isolated and DNA sequencing analysis was undertaken (Section 2.5.8).

Electroporation of the *A. baumannii* strain ATCC 17978 was performed with approximately 500 μ g of the pEX18Tc plasmid containing the region of interest (see Section 2.5.1). Homologous recombination was selected for by growth on 5% M9-sucrose medium containing Ery¹⁰ for 48 hr. The replacement of the gene of interest with the Ery resistance cassette was confirmed by PCR analysis and sequencing using primers outside the flanking regions for each specific gene of interest (Table 2.4).

2.7.8 Generation of complementation strains

In order to generate *A. baumannii* complementation strains by reintroducing a WT copy of the deleted gene into the mutant strain, primers were designed to amplify the WT target gene as follows (Table 2.4). A forward primer, located upstream which included the -10 and -35 region of the promoter sequence of the target gene, and a reverse primer, located immediately downstream of the target gene, were synthesised to incorporate appropriate restriction sites for cloning into the vector pWH1266. Each set of primers was used to amplify the WT target gene using *A. baumannii* ATCC 17978 genomic DNA as template (*rpmE1-BamHI* and *rpmE2_BamHI* for *rpmE1* and *rpmE2* genes, respectively) (Table 2.3). The generated PCR product was then digested with the appropriate enzymes, ligated with similarly restricted pWH1266 shuttle vector DNA and the mixture transformed into competent *E. coli* DH5 α (Section 2.7.4). The screening for the plasmids harbouring the gene of interest was undertaken by plating the transformed cells onto a LB plate containing Amp²⁰⁰ and incubation ON at 37 °C. Isolated colonies were chosen, purified and plasmid DNA extracted (Section 2.5.1). Plasmid DNA was digested with appropriate restriction endonucleases (Section 2.7.1) and examined by agarose gel electrophoresis to confirm the successful cloning of the region. After this screening for the correct clone, the complementing plasmid was then introduced into the appropriate *A. baumannii* mutant strain via electroporation (Section 2.7.7). *A. baumannii* transformants containing the complementing plasmid were selected on Ery¹⁰ and Amp¹⁰⁰ containing plates and later confirmed by PCR.

2.8 Bioinformatics analyses

2.8.1 Alignments and *in silico* manipulations

Sequence alignments and manipulation of DNA sequences for plasmid construction and cloning were initially analysed using the Chromas Lite, then further analysed with SequencherTM 4.1.4 program. Alignments were visualised by CLC sequence viewer (CLC bio).

2.8.2 Genomic DNA analyses

Searches for matches to nucleotide sequences, amino acid sequences or protein domain searches were performed using Blastn from National Center for Biotechnology Information (NCBI), Blastp (NCBI) and the conserved domain database (NCBI), respectively (Marchler-Bauer *et al.* 2011).

2.8.3 RNA-seq analyses

The quality of the cDNA reads obtained from the RNA-seq experiment was checked using 'Fastqc' (<http://www.bioinformatics.babraham.ac.uk/projects/fastqc/>). Reads were subsequently mapped to the reference genome using the program 'Bowtie' (<http://bowtie-bio.sourceforge.net/index.shtml>). For the reads obtained, approximately 95% were mapped to the ATCC 17978 genome of which 78% mapped to the coding regions. In order to determine changes in gene expression the number of reads obtained for each open reading frame (ORF) was normalised using reads per kb of transcript per million reads mapped.

2.8.4 Clusters of Orthologous Groups analysis

The Clusters of Orthologous Groups (COG) grouping was created based on the COG protein database (<http://clovr.org/docs/clusters-of-orthologous-groups-cogs/>). The COG data are shown in percentages indicating the proportion of genes in any given COG set whose expression altered 2-fold (Log_2 of 1) either in the differing conditions tested or compared to the WT parent.

CHAPTER 3
INVESTIGATION OF *A. BAUMANNII* ATCC 17978
UNDER ZN^{2+} -LIMITED CONDITIONS

3.1 Introduction

Zn^{2+} is an essential cofactor required by numerous metalloenzymes and is important for structural and regulatory systems in bacterial cells (Jacobsen *et al.* 2011). As Zn^{2+} is a trace element, bacterial cells require only very small quantities, where the exact amount needed for optimal cell growth varies among bacterial species; *e.g.*, in *E. coli* the Zn^{2+} quota per cell is approximately 10^5 atoms of Zn. However, when the levels of Zn^{2+} were adjusted to cell volume, the total Zn^{2+} concentration was significantly similar between species with ranges between 0.1 to 0.5 mM (Outten and O'Halloran 2001). The majority of intracellular Zn^{2+} is bound to proteins and free Zn^{2+} is thought to be present at only very low levels (Eide 2006).

Due to Zn^{2+} limitation and the toxic effect of high levels of free Zn^{2+} ions, the intracellular Zn^{2+} concentration is carefully controlled (Hantke 2005). A balance between the requirement for metals and their toxicity is achieved via several mechanisms: storage mechanisms within the cell safely deposit loosely bound metals for later use; export systems can rid the cells of surplus metals; and both high- and low-affinity systems are utilised to import and export extracellular metals when required (Hantke 2005) (see Section 1.6). Zn^{2+} homeostasis is maintained by Zn^{2+} -uptake and efflux systems. For example, in *E. coli* a Zn^{2+} -deficient cell responds by increasing the expression of Zn^{2+} uptake and decreasing the expression of Zn^{2+} -efflux transporters. This results in a rapid cycle between periods of intracellular Zn^{2+} limitation and Zn^{2+} repletion (Hantke 2005). Under normal bacterial growth conditions, the expression of genes encoding the Zn^{2+} -uptake system is switched off as only small amount of Zn^{2+} is needed for bacterial growth. This repression protects the cell from metal toxicity in the presence of excess extracellular Zn^{2+} and reduces the energy cost to the cell (Porcheron *et al.* 2013). A change in conditions that can occur during *in vitro* growth or during the course of an infection may prompt the bacterial cell to change the expression levels of Zn^{2+} -associated genes. The ability of cells to precisely respond to changes in the immediate environment is largely due to the role of key regulatory mechanisms (Porcheron *et al.* 2013) (see Section 1.6).

The expression of the majority of the genes required for the control of intracellular levels of Zn^{2+} is regulated by the Zn^{2+} -uptake regulator, Zur, and the

Zn²⁺-efflux regulator, ZntR (Li *et al.* 2009); both respond to femtomolar changes in the concentration of Zn²⁺ ions. Under normal growth conditions, when sufficient levels of Zn²⁺ are present, Zur is bound to the Zur box and represses the expression of Zur-regulated genes including *znuA*, *znuB*, *znuC* (Nanamiya *et al.* 2004) (see Section 1.6). In contrast, when Zn²⁺ is not present in adequate concentrations, Zur is released from the Zur box and the Zn²⁺-uptake genes are expressed (Akanuma *et al.* 2006). It also has been shown that one form of the Zur-regulated L31 ribosomal protein can be used as a source of Zn²⁺ when extracellular Zn²⁺ is not available (Akanuma *et al.* 2006). This C⁺ form of L31 contains a metal-binding Zn²⁺-ribbon (CXXC motif) and is a paralogue of the C⁻ form that lacks this motif (Li *et al.* 2009) (see Section 1.9). These genes and their expression are examined in fine detail in the following chapters.

This study aimed to investigate the mechanisms for Zn²⁺ acquisition and the adaptation mechanisms used by *A. baumannii* to grow in a Zn²⁺-limited environment. Following development and optimisation of defined media, the effect of Zn²⁺ starvation on *A. baumannii* ATCC 17978 was investigated at both the phenotypic and transcriptomic levels.

3.2 Results and discussion

3.2.1 Optimisation of Zn²⁺-limited growth conditions

Zn²⁺ is an important micronutrient and the depletion of Zn²⁺ from culture media is likely to have an impact on cell viability. However, since bacteria have an impressive ability to acquire Zn²⁺, it is exceptionally difficult to achieve an environment totally Zn²⁺ deficient (Graham *et al.* 2009). Studies examining the response of bacteria to Zn²⁺ limitation have been conducted using specific Zn²⁺ chelators, such as TPEN (Graham *et al.*, 2009) or calprotectin (Hood *et al.*, 2012).

In this study, Zn²⁺-limited conditions were achieved in two different media, MH and M9 minimal medium (see Section 2.2). To ensure these conditions, glassware use for culturing bacteria underwent extensive acid washing and only newly purchased high purity chemicals and metal-free pipette tips were used.

Chemically-defined M9 minimal and MH medium were depleted of contaminating cations by chelation using Chelex 100[®]. Chelating ion exchange resin, such as Chelex 100[®] (Bio-Rad, Australia), has high preference for divalent ions, such as Cu, Fe²⁺, Mn²⁺, Zn²⁺ and other heavy metals over monovalent cations such as sodium and potassium. Therefore, to alleviate the removal of ions other than Zn²⁺ by Chelex 100[®] treatment, media were supplemented with specific metal ions following Zn²⁺ depletion for both MH and M9 media. Plastics such as, bottles, tubes and tubing used in media preparations were chosen based on their composition and relatively low levels of metal leaching (Graham *et al.* 2009).

Initially, MH medium was used for creating Zn²⁺-limiting conditions (see Section 2.2). As the treatment of MH medium with Chelex 100[®] can alter the pH of the medium, the pH was adjusted back to neutral after treatment. The growth of cells in MH[C] and MH[CR] media (see Section 2.2) were compared to growth in MH[CRsup] (a MH[CR] medium supplemented with defined concentrations of Zn²⁺ and Mn²⁺). The results of the growth assays showed that Chelex 100[®] treatment of MH medium (MH[C]) abrogated *A. baumannii* growth (Figure 3.1, light green) compared to the original medium (MH) (Figure 3.1, dark blue). Surprisingly the addition of defined amounts of Fe²⁺, Mn²⁺ and Zn²⁺ (MH[CRsup]) did not restore bacterial growth to the levels observed in untreated MH medium (Figure 3.1, magenta). This may be because the Chelex 100[®] treatment can also chelate other important trace metal ions in the medium. Growth of *A. baumannii* in MH[CR]) supplemented with Zn²⁺ and Mn²⁺ but lacking Fe²⁺ or supplemented with only Fe²⁺ and Mn²⁺ but lacking Zn²⁺ was not significantly different to growth observed in MH[CR]) supplemented with defined concentrations of these three metal ions (Fe²⁺, Mn²⁺ and Zn²⁺) or (MH[CRsup]). Interestingly, the growth of *A. baumannii* was slightly better when the MH[CR] media were supplemented with Fe²⁺ and Zn²⁺ but not Mn²⁺ (Figure 3.1, dark green), indicating that *A. baumannii* may be sensitive to Mn²⁺ toxicity. In addition, bacterial growth in MH[CRsup] and in MH[CRsup-Zn²⁺] media was also not significantly different, indicating that Chelex 100[®] treatment alone was not sufficient to remove Zn²⁺ from the media.

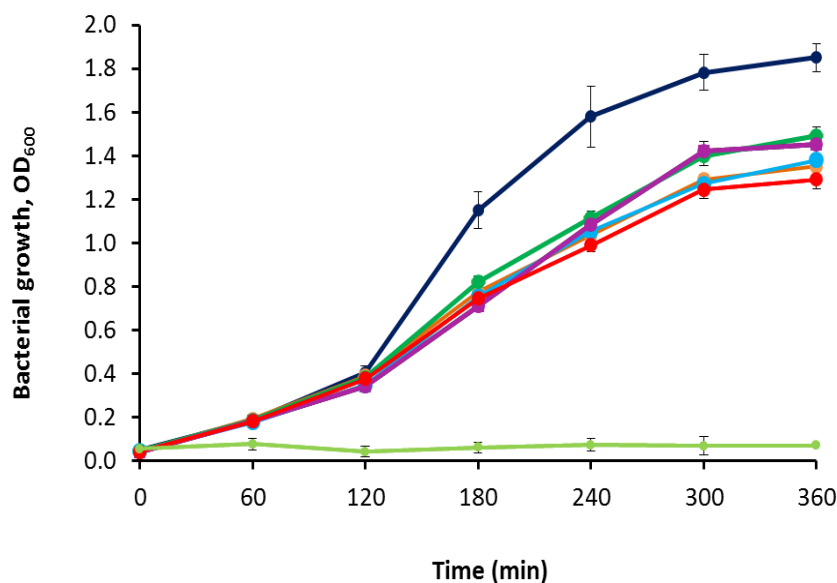


Figure 3.1: The effect of supplementation of MH media with the metal ions Fe²⁺, Mn²⁺ and Zn²⁺ on *A. baumannii* ATCC 17978 growth

The growth of *A. baumannii* in three different media supplemented with three different combinations of the metal ions Fe²⁺, Mn²⁺ and Zn²⁺ was assessed: MH (MH, dark blue); MH treated with Chelex 100[®] (MH[C]), light green); and MH-chelex with the addition of 50 μM Mg²⁺, 50 μM Ca²⁺ and 25 μM Cu²⁺ (MH[CR], red). Growth in MH[CR] medium supplemented with the following metal ions was also measured: (i) 50 μM Fe²⁺, 50 μM Zn²⁺ and 5 μM Mn²⁺ (MH[CRsup], magenta); (ii) 50 μM Zn²⁺ and 5 μM Mn²⁺ (cyan); (iii) 50 μM Fe²⁺ and 5 μM Mn²⁺ (MH[CRsup-Zn²⁺], orange); and (iv) 50 μM Fe²⁺ and 5 μM Zn²⁺ (dark green). Bacteria were grown ON in LB medium washed 3 times with PBS and then diluted 1:100 into each of the media. Absorbance readings, OD₆₀₀, were obtained every hr for 6 hr; the data represent the average of three separate experiments. Error bars show the standard deviation.

Therefore, to further removed Zn^{2+} , MH media was treated with the synthetic Zn^{2+} chelator TPEN. However, preparation of these media was time consuming and costly since it was employed several steps including Chelex 100[®] treatment, filter sterilisation and pH adjustment, which increased the possibility of introducing Zn^{2+} contamination, therefore an alternative medium (M9 medium) was utilised.

M9 medium was prepared as described in Section 2.2. The M9[C] medium was prepared with M95X salt treated with Chelex 100[®]. This Chelex 100[®] treatment did not alter the pH of the M9[C] medium (data not shown). In order to determine the optimal concentration required for Zn^{2+} removal, TPEN was added to M9[C] to a final concentration of either 5 μ M or 10 μ M. *A. baumannii* growth in media containing either concentration of TPEN was significantly affected; mid-log phase ($OD_{600} = 0.6$) was delayed by approximately 60 min compared to growth in untreated media (Figure 3.2). Moreover, the total biomass was reduced by more than 40% by the time cells reached stationary phase (> 420 min). Addition of 10 μ M TPEN did not result in a greater inhibition of the growth rate. Therefore, a 5 μ M concentration of TPEN was chosen for further experiments (M9[CT]). However, at the time of performing these experiments another study found that the critical concentration of TPEN required to deplete MH-chelex medium was 10 μ M (Hood *et al.* 2012). It is likely therefore that a higher concentration of TPEN was required for depletion of Zn^{2+} from MH medium as it is more nutrient rich and contains more metal ions compared to M9 medium (Hood *et al.* 2012).

3.2.2 Optimisation of metal ion concentration for growth assays

Preparation of M9 medium is described in Section 2.2. M9-chelex medium was prepared using M9 salts treated with Chelex 100[®] (M9[C]) followed by the addition of TPEN to a final concentration of 5 μ M (M9[CT]) (Section 3.2.1). Here, M9 Zn^{2+} -limited medium was prepared by the addition of combinations of different concentrations of Fe^{2+} and Mn^{2+} . Based on the preliminary experiments, the optimum final concentrations of Fe^{2+} and Mn^{2+} added to the M9[CT] medium were

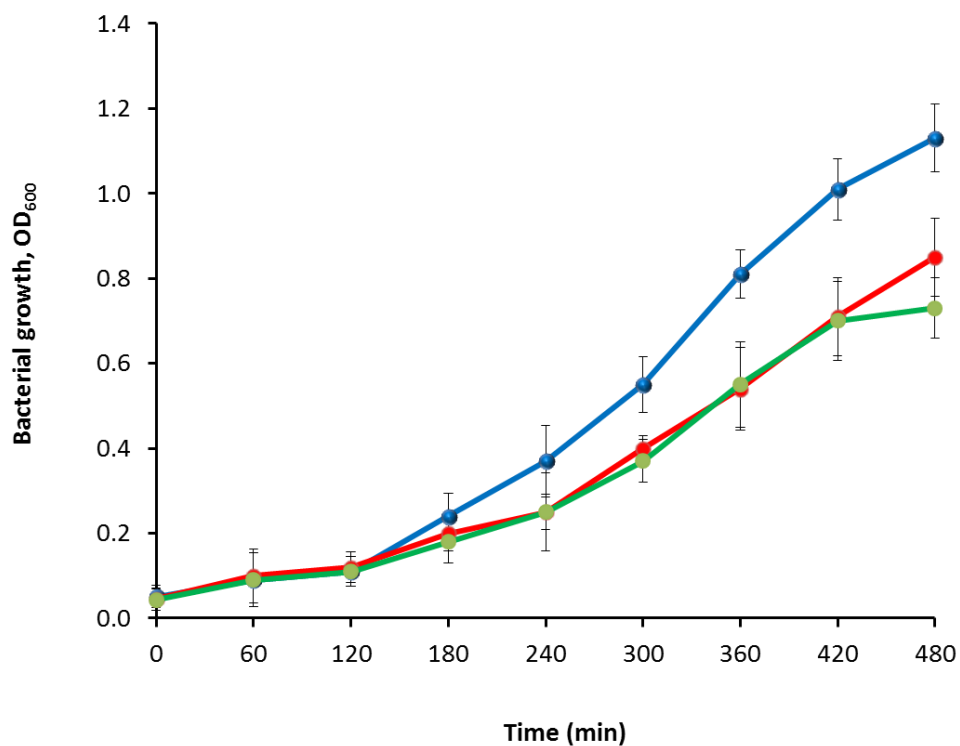


Figure 3.2: The effect of TPEN on *A. baumannii* ATCC 17978 growth

Comparison of growth in M9[C] (blue) or with the addition of the Zn²⁺-chelating agent TPEN (M9[CT]) at a final concentration of 5 μM (green) or 10 μM (red). The addition of either concentration of TPEN resulted in a similar level of bacterial growth, which was significantly reduced compared to growth in M9[C]. Absorbance readings, OD₆₀₀, were obtained every hr for 8 hr; the data represent the average of three separate experiments. Error bars show the standard deviation.

50 μM and 5 μM , respectively (data not shown). M9[CT] medium with the addition of 50 μM Fe^{2+} and 5 μM Mn^{2+} was defined as M9[CTFM]. To determine the amount of Zn^{2+} , two concentrations of Zn^{2+} , 50 μM and 100 μM , were added to M9[CTFM] medium (Figure 3.3). Figure 3.3 shows the assessment of growth of *A. baumannii* ATCC 17978 in M9[C] and M9[CTFM] media. The addition of 50 μM Zn^{2+} to M9[CTFM] medium recovered the growth of bacteria to levels similar to that seen in M9[C] medium.

This demonstrates that 50 μM Zn^{2+} is sufficient for bacterial growth and the addition up to 100 μM Zn^{2+} does not significantly affect bacterial growth. Attempts to use higher concentrations of Zn^{2+} led to precipitation in the medium. Therefore, a final concentration of 50 μM Zn^{2+} together with M9[CTFM] medium was chosen for the subsequent experiments. For the rest of this thesis, M9[CT] medium with the addition of 50 μM Fe^{2+} and 5 μM Mn^{2+} (M9[CTFM]) is called **Zn^{2+} -limited medium**, while M9[CT] with the addition of 50 μM Fe^{2+} , 5 μM Mn^{2+} and 50 μM Zn^{2+} (M9[CTFM+ Zn^{2+}]) is called **Zn^{2+} -replete medium**.

3.2.3 The effect of Zn^{2+} limitation on the bacterial phenotype

Zn^{2+} is known to play an important role in various biological processes in bacteria including biofilm formation, motility, antibiotic resistance and required for full virulence (see Section 1.3). To investigate the influence of Zn^{2+} levels on such phenotypes in *A. baumannii*, phenotypic characterisation assays were undertaken under both Zn^{2+} -limited and Zn^{2+} -replete conditions.

3.2.3.1 The effect of Zn^{2+} limitation on *A. baumannii* motility

Zn^{2+} plays a role in motility in a variety of bacteria (Kearns *et al.* 2002; Nielubowicz *et al.* 2010; Sabri *et al.* 2009) as sub-optimal levels of Zn^{2+} can affect the ability of the bacterial cell to migrate across a surface. For example, the inactivation of Zn^{2+} transport systems in *E. coli* has a direct effect on motility (Sabri *et al.* 2009), in *P. mirabilis* Zn^{2+} acquisition is required for normal swimming/swarming motility (Nielubowicz *et al.* 2010) and in *M. xanthus* a Zn^{2+} -metalloprotease involved with the extracellular matrix is needed for motility (Kearns *et al.* 2002).

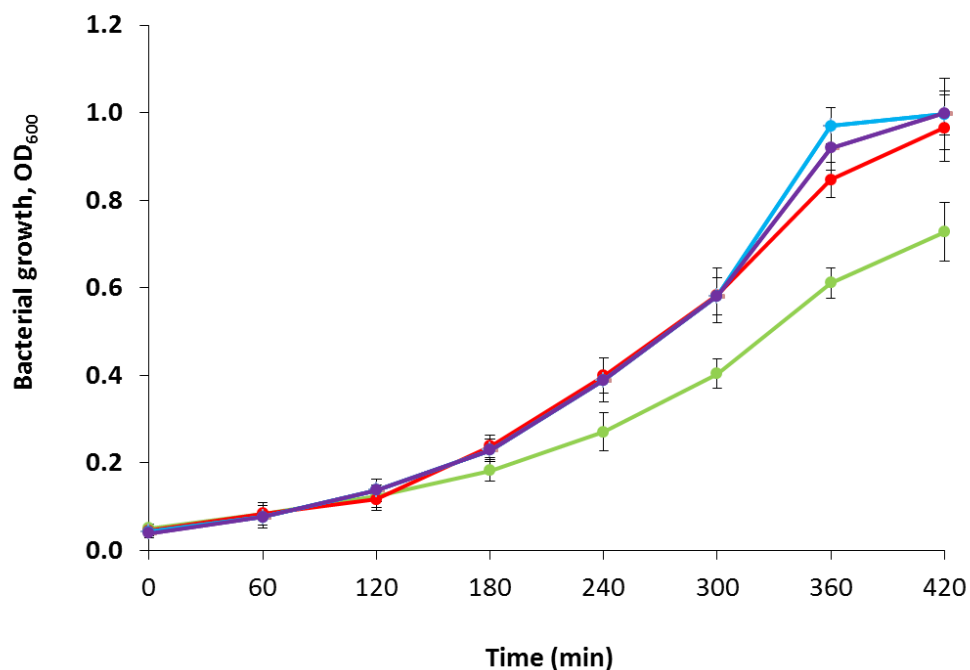


Figure 3.3: The effect of supplementation of Zn²⁺ on *A. baumannii* ATCC 17978 growth in various M9 media

Growth of *A. baumannii* ATCC 17978 was assessed in M9 medium without treatment (M9[C] medium, red) and M9[C] medium with the addition of TPEN, Fe²⁺, and Mn²⁺ to final concentration of 5 μM, 50 μM, and 5 μM, respectively (M9[CTFM], green). The addition of 50 μM Zn²⁺ to M9[CTFM] medium restored the growth of bacteria to levels similar to that seen in M9[C] medium (purple). The addition of 100 μM Zn²⁺ to M9[CTFM] also returned growth to levels similar to that seen in M9[C] medium supplemented with 50 μM Zn²⁺ (blue). Absorbance readings, OD₆₀₀, were obtained every hr for 7 hr; the data represent the average of three separate experiments. Error bars show the standard deviation.

To investigate the effect of Zn^{2+} limitation on the motility of *A. baumannii* ATCC 17978, bacteria were inoculated onto 0.25% and 0.5% agarose agar supplemented with 5 μ M TPEN, incubated ON at 37 °C, and assessed for motility (Section 2.3.6). The results revealed that there was no difference in the motility observed on Zn^{2+} -limited compared to Zn^{2+} -replete agar. A previous study in *A. baumannii* showed that limitation of Fe^{2+} in the medium led to an inhibition of bacterial surface motility (Eijkelkamp *et al.* 2011a). A reduction in motility of *A. baumannii* has also been reported following inactivation of *sodA* that encodes the Mn^{2+} -superoxide dismutase (Heindorf *et al.* 2014). Although metal ions such as Zn^{2+} , Fe^{2+} and Mn^{2+} have all been reported to contribute to bacterial motility, it appears that the limitation of Zn^{2+} alone was not adequate to significantly inhibit the motility of *A. baumannii* ATCC 17978.

3.2.3.2 The effect of Zn^{2+} limitation on biofilm formation in *A. baumannii*

Biofilm formation is important for the survival of bacteria in hostile environments as bacteria within biofilms are usually more resistant to antibiotics and disinfectants than when in a planktonic form (Wu *et al.* 2013). It has been shown that Zn^{2+} availability affects the ability of *E. coli* to form biofilms through its roles in bacterial pilus assembly and curli production (Lim *et al.* 2011). To investigate the role of Zn^{2+} on the ability of *A. baumannii* ATCC 17978 to form a biofilm, bacteria were grown in Zn^{2+} -limited and Zn^{2+} -replete media in plastic tubes (Section 2.3.4). Cultures were incubated at 37 °C for 72 hr in dark static conditions. Following incubation, the planktonic growth was carefully transferred into another tube and the OD_{600} was measured to determine the effect of Zn^{2+} limitation on planktonic bacterial growth. Biofilms attached to each plastic tube were stained with 0.01% crystal violet and the OD_{595} was measured. The results showed that there was a significant difference in biofilm levels ($p < 0.05$) between bacteria grown in Zn^{2+} -limited and Zn^{2+} -replete media (Figure 3.4). Biofilm production in Zn^{2+} -limited conditions was reduced by 20% compared to the biofilm formed under Zn^{2+} -replete conditions.

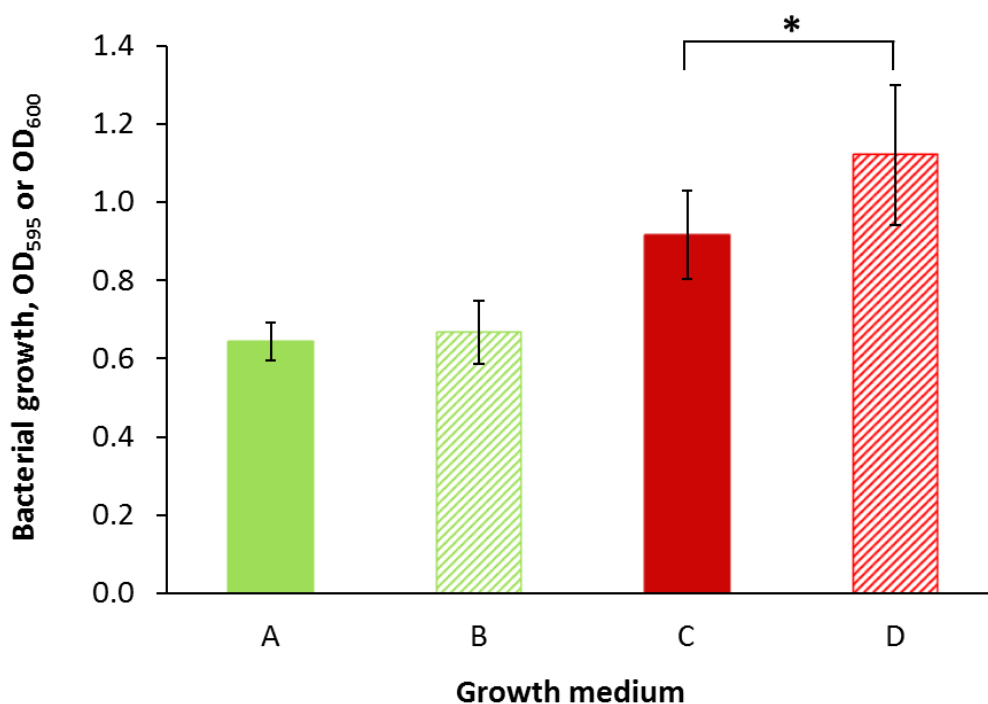


Figure 3.4: Comparison of biofilm production by *A. baumannii* ATCC 17978 in Zn²⁺-limited and Zn²⁺-replete media

The level of growth of *A. baumannii* ATCC 17978 under planktonic (green) or biofilm conditions (red) was measured at OD₅₉₅ in M9 medium with 5 μ M TPEN (solid bar) and M9 medium with 5 μ M TPEN plus 50 μ M Zn²⁺ (stippled bar). There was a significant difference between the production of biofilm in Zn²⁺-limited (C) compared to Zn²⁺-replete media (D) (*) $p < 0.05$, and no significant difference between planktonic growth in Zn²⁺-limited (A) and Zn²⁺-replete media (B). The data represent the average of three separate experiments. Error bars show the standard deviation.

The finding that Zn^{2+} limitation impacts on the ability of *A. baumannii* to form a biofilm is similar to findings in other species. In *A. pleuropneumoniae*, Labrie et al. (2010) showed that low concentrations of Zn^{2+} inhibited biofilm production and resulted in the up-regulation of *znuA*. Zn^{2+} depletion via chelation specifically prevented biofilm formation in MRSA (Conrady et al. 2008). In addition, the mutation of genes encoding *ykgM* and *zitA* in *E. coli* greatly affected biofilm formation under fluidic conditions but no inhibition was observed in static conditions (Lim et al. 2011). However, some studies have revealed that the addition of Zn^{2+} to growth media can also inhibit the formation of biofilms (Hancock et al. 2010). In *A. pleuropneumoniae*, *S. enterica* Serotype Typhimurium and *H. parasuis* it has been shown that the addition of micromolar concentrations of Zn^{2+} effectively blocked biofilm formation in a dose-dependent manner (Wu et al. 2013). These disparities on the effect of Zn^{2+} on biofilm formation are possibly due to each bacterial species/strain having a different optimum concentration of Zn^{2+} required for cellular processes, as high concentrations of Zn^{2+} are toxic to bacteria and therefore in some instances could hinder biofilm formation.

3.2.3.3 The effect of Zn^{2+} limitation on *A. baumannii* antibiotic resistance

A. baumannii exhibits an outstanding display of mechanisms used for antibiotic resistance (Peleg et al. 2008), including β -lactamases (Valentine et al. 2008). The most common β -lactam resistance mechanism among Gram-negative bacteria is via the production of β -lactamase (Sowmiya et al. 2012), a highly efficient enzyme that inactivates β -lactam antibiotics by catalysing hydrolysis of the four-membered β -lactam ring (Tamilselvi and Mugesh 2008). These β -lactamases are classified into two major categories: serine β -lactamases and MBLs. The MBLs require one or two Zn^{2+} ions in their active sites to catalyse the hydrolysis of all classes of β -lactam antibiotics, including penicillins, cephalosporins, and carbapenems (Tamilselvi and Mugesh 2008) (see Section 1.2.2). To investigate the effect of Zn^{2+} limitation on the ability of *A. baumannii* to resist β -lactam antibiotics, ATCC 17978 was grown on MH-agar with, and without, the addition of 30 μ M of TPEN (Section 2.3.3). Disk diffusion assays were then conducted on the two types of media using β -lactam antibiotics known to be hydrolysed by metalloenzymes,

Table 3.1: Antibiotic susceptibility of *A. baumannii* ATCC 17978 grown on MH agar with and without the addition of 30 μ M TPEN

| Antibiotic disk | Diameter of inhibition zones without TPEN ^a | Diameter of inhibition zones with TPEN ^b |
|---------------------------------------------|--------------------------------------------------------|-----------------------------------------------------|
| Penicillin G (10 μ g) | 6 | 6 |
| Cefotaxime (30 μ g) | 9 | 20* |
| Ceftriaxone (30 μ g) | 17 | 25* |
| Amp (10 μ g) | 12 | 19* |
| Amoxicillin/clavulanic acid (20/10 μ g) | 8 | 17* |
| Gentamicin (10 μ g) | 17 | 12* |
| Nalidixic acid (30 μ g) | 19 | 19 |
| Cm (30 μ g) | 6 | 27* |

^a. Diameter of clear zone surrounding the antibiotic disk is measured in mm.

^b. Susceptibility test using MH agar with the addition of 30 μ M TPEN.

* Significant difference was observed between the inhibition zone of the bacteria grown in MH agar with and without the addition of TPEN, ($p < 0.05$).

including penicillin G, cefotaxime and ceftriaxone as well as other β -lactam antibiotics including amoxicillin/clavulanic acid, and Amp. Additionally, resistance to non β -lactam antibiotics including nalidixic acid, Cm, and gentamicin was also assessed.

The results showed that Zn^{2+} chelation by TPEN affected the ability of *A. baumannii* to resist many of the antibiotics. *A. baumannii* ATCC 17978 was significantly more susceptible to Cm, Amp, amoxicillin clavulanic acid, cefotaxime, and ceftriaxone in MH medium limited of Zn^{2+} compared to untreated MH (Table 3.1). No differences were observed for the susceptibility against nalidixic acid and gentamicin. Bioinformatics analyses showed that ATCC 17978 produces Class C and D serine β -lactamases. It is known that serine β -lactamases are not Zn^{2+} -dependant enzymes. Therefore, the increase in susceptibility to the third generation cephalosporins, such as cefotaxime and ceftriaxone, indicates that Zn^{2+} limitation indirectly influences the resistance mediated by these β -lactamases. The effect of Zn^{2+} limitation on susceptibility to Cm needs further investigation. It is known that Cm is a bacteriostatic antibiotic that functions by inhibiting protein synthesis. The results obtained here indicate that limitation of Zn^{2+} affected the 50S L31 ribosomal protein. This may have a downstream effect by altering the affinity of Cm to the 23S rRNA of the 50S ribosomal subunit (Beringer 2008). Surprisingly, the addition of TPEN reduced the sensitivity to gentamicin which indicates that Zn^{2+} -limitation plays role in antibiotic susceptibility in ATCC 17978. This result also requires further investigation by analysing the effect of Zn^{2+} -limitation on other aminoglycoside antibiotics. Zn^{2+} starvation may indirectly affect ribosomal proteins by inducing conformational changes in the rRNA changing the susceptibility to gentamicin (Wilson 2014). The mechanism of action used by aminoglycoside antibiotics is by these drugs binding to the 30S ribosomal sub-unit. It has been reported that bacteria can employ several different mechanisms of aminoglycoside resistance including, reducing cell permeability, modifying the ribosomal target binding site, and producing aminoglycoside modifying enzymes (Garneau-Tsodikova and Labby 2016).

3.2.4 Quantitative-reverse-transcriptase PCR measurements of selected *A. baumannii* genes under Zn²⁺-limited conditions

To determine the effect of Zn²⁺ limitation on gene expression, preliminary qRT-PCR was performed (see Section 2.6.2). For RNA extraction and analysis, *A. baumannii* cells were grown in Zn²⁺-limited and Zn²⁺-replete conditions until early log phase growth was reached (~ 4 hr at 37 °C with shaking 200 rpm), and cells were harvested for RNA extraction as described in Section 2.6.1. The level of transcription from four genes known to be influenced by Zn²⁺ and/or involved in Zn²⁺ homeostasis was analysed. This included A1S_0145 (*zur*) and the divergently transcribed A1S_0146 (*znuA*) (see Table 2.4). Oligonucleotides were designed for the reference genes A1S_r01 (*16S rRNA*) and A1S_2501 (*GAPDH*) to act as internal controls as they were predicted to be unaffected by the availability of Zn²⁺ (see Section 2.6.2). Additionally, the Fe²⁺-responsive genes A1S_0895 (*fur*) and A1S_1647, previously shown to be highly expressed under Fe²⁺-limited conditions (Eijkelkamp *et al.* 2011a), were included as controls to demonstrate that this Zn²⁺-depletion method was specific for Zn.

The qRT-PCR results (Figure 3.5) showed that when *A. baumannii* ATCC 17978 cells were grown in Zn²⁺-limited medium compared to cells grown in Zn²⁺-replete medium, transcriptional levels for *zur* and *znuA* increased more than 4-fold and 13-fold, respectively. As expected, RNA expression of *fur* and the siderophore biosynthesis gene, A1S_1647, were unaffected by Zn²⁺-limitation, confirming that the Zn²⁺-limited medium used had sufficient Fe²⁺.

3.2.5 Global RNA expression changes in *A. baumannii* during growth in Zn²⁺-limited conditions

To understand the global gene expression responses of *A. baumannii* to Zn²⁺ deficiency, next-generation sequencing transcriptome profiling (RNA-seq) analysis was conducted on *A. baumannii* ATCC 17978 cells grown under both Zn²⁺-replete and Zn²⁺-limited conditions. Growth of the *A. baumannii* strains for RNA extraction and transcriptomic analyses was undertaken as described below. The *A. baumannii*

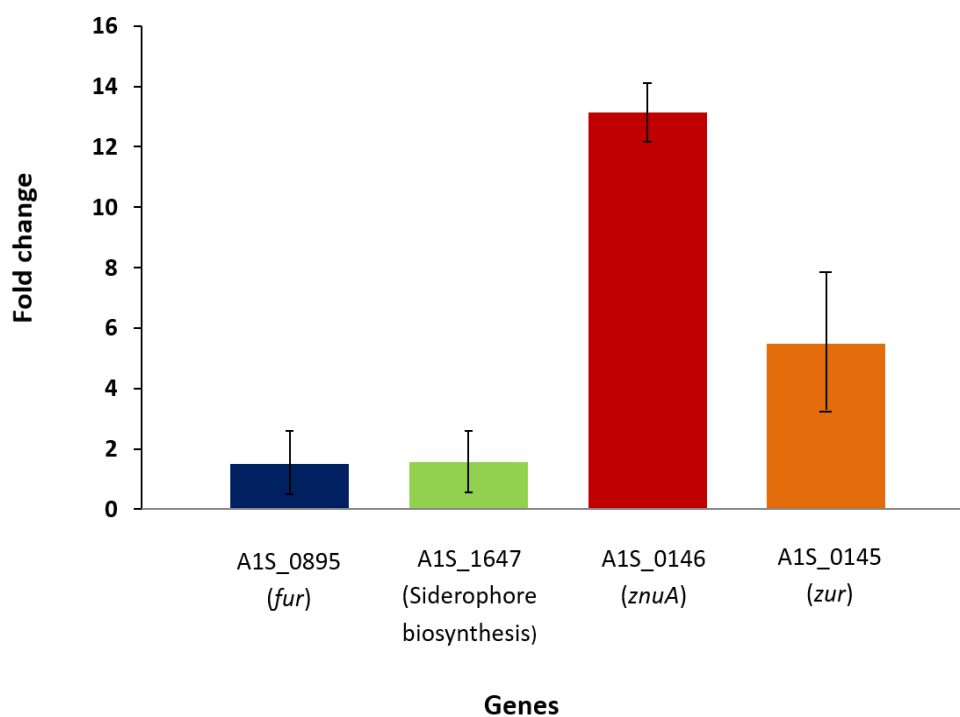


Figure 3.5: qRT-PCR expression analysis of selected *A. baumannii* ATCC 17978 genes during growth in Zn²⁺-limited and Zn²⁺-replete conditions

Transcriptomic analysis showing the fold changes in expression of *fur*, *zur*, *znuA*, and the siderophore biosynthesis gene (A1S_1647) when bacteria were grown in Zn²⁺-limited or Zn²⁺-replete media for ~4 hr at 37 °C with shaking. Data are presented as expression fold changes and represent the average of three separate experiments. Error bars show the standard deviation.

ATCC 17978 cells were each grown in Zn²⁺-limited and Zn²⁺-replete medium, prepared as described previously (see Section 2.2). For RNA extraction, ON cultures of each *A. baumannii* strain (grown in LB medium) were pelleted by centrifugation and washed three times with Zn²⁺-limited medium. The resuspended cells were then diluted 1:50 in either Zn²⁺-replete or Zn²⁺-limited medium and incubated with shaking at 37 °C. RNA was extracted (see Section 2.6.1) from cells in early log phase (after approximately 4 hr until OD₆₀₀ = 0.5). The total RNA used for the RNA-seq reactions was composed of RNA extracted and pooled from three biological replicates. Other aliquots from the same RNA samples were used for qRT-PCR to confirm the RNA-seq data. RNA-seq analysis was undertaken as described in Section 2.6.3.

The RNA-seq analysis in this thesis was based on the annotation of *A. baumannii* ATCC 17978, GenBank accession number: CP000521.1 (Smith *et al.* 2007). Unfortunately, this initial annotation has since been found to contain a number of errors in the allocation of the start sites of the ORFs as well as missing some ORFs altogether. Recently a new annotation of ATCC 17978 was released (GenBank accession number: CP012004) (Weber *et al.* 2013) correcting the issues with the older sequence and the associated annotation. Regrettably, at the time of undertaking the work and writing of this thesis the new sequence was unavailable, therefore, the annotation of the older sequence was used for the work presented unless otherwise stated. As a number of genes are of central importance in this thesis, their expression based on RNA-seq was also mapped to the new CP012004 sequence. The expression of A1S_0143, A1S_0144, A1S_0145 and A1S_0146 obtained from RNA-seq based on the old annotated ATCC 17978 sequence were 2-fold, 2-fold, 2-fold and 6-fold up-regulated, respectively (Appendix 1). The expression obtained from the reanalysis based on the CP012004 sequence revealed that similar expression levels for A1S_0143 (ACX60_17365), A1S_0144 (ACX60_17360), A1S_0145 (ACX60_17355) and A1S_0146 (ACX60_17350) of 2-fold, 2-fold, 2-fold and 7-fold up-regulated, respectively (Appendix 11) could be seen. The expression of the Zur-regulated gene L31 ribosomal protein (A1S_0391) was 400-fold up-regulated (Appendix 1) compared to 360 fold up-regulated (ACX60_16160), in the new annotated sequence (Appendix 11).

RNA-seq data (Figure 3.6) generated from the RNA extracted from cells grown in Zn^{2+} -limited culture revealed that the expression of 60 genes had increased by more than 2-fold; the most up-regulated gene was *rpmE2* (427-fold up-regulated). Significantly, more genes had reduced expression in Zn^{2+} -limited conditions; 279 genes had expression levels at least 2-fold lower than the levels exhibited in Zn^{2+} -replete conditions. To validate these results qRT-PCR analysis of a subset of differentially-expressed genes (A1S_0092, A1S_0391, A1S_0145, A1S_0146, A1S_3217, and A1S_0452) was performed using the oligonucleotides listed in Table 2.4. These six genes were selected based on their level of expression and ranged from the most to the least expressed. A good correlation between the data obtained from the qRT-PCR and the RNA-seq analyses was observed (Figure 3.7). Overall the qRT-PCR data showed higher fold changes than those determined by RNA-seq, e.g., A1S_0391 was expressed at 9.3-fold in qRT-PCR compared to 8.7-fold in RNA-seq (Table 3.2). However, a tendency for RNA-seq analyses to underestimate fold changes relative to expression changes determined using qRT-PCR has been previously observed (Brooks *et al.* 2011; Hazard *et al.* 2008). Additionally, the RNA-seq data obtained in this study may also have been affected by the relatively poor annotation of the *A. baumannii* ATCC 17978 genomic sequence. Annotation issues can lead to sequence data being mapped to multiple ORFs identified with increased expression in Zn^{2+} -limited conditions encoded proteins in the 'hypothetical' and/or 'unknown function' categories indicating a potential role for Zn^{2+} in the homeostasis of these genes.

3.2.5.1 Functional categories of genes identified as differentially expressed

Genes identified as differentially expressed in the RNA-seq data were assigned to COG functional categories (Figure 3.8). The distribution of genes into COGs revealed that about 27% of genes identified as down-regulated under Zn^{2+} -limited conditions played a role in lipid metabolism, with most encoding Zn^{2+} -dependent enzymes. The effect of Zn^{2+} -depletion on the genes in this group will be discussed in detail in Section 3.2.5.7. It was also shown that more than 25% of the genes identified with decreased expression under Zn^{2+} -limited conditions encode

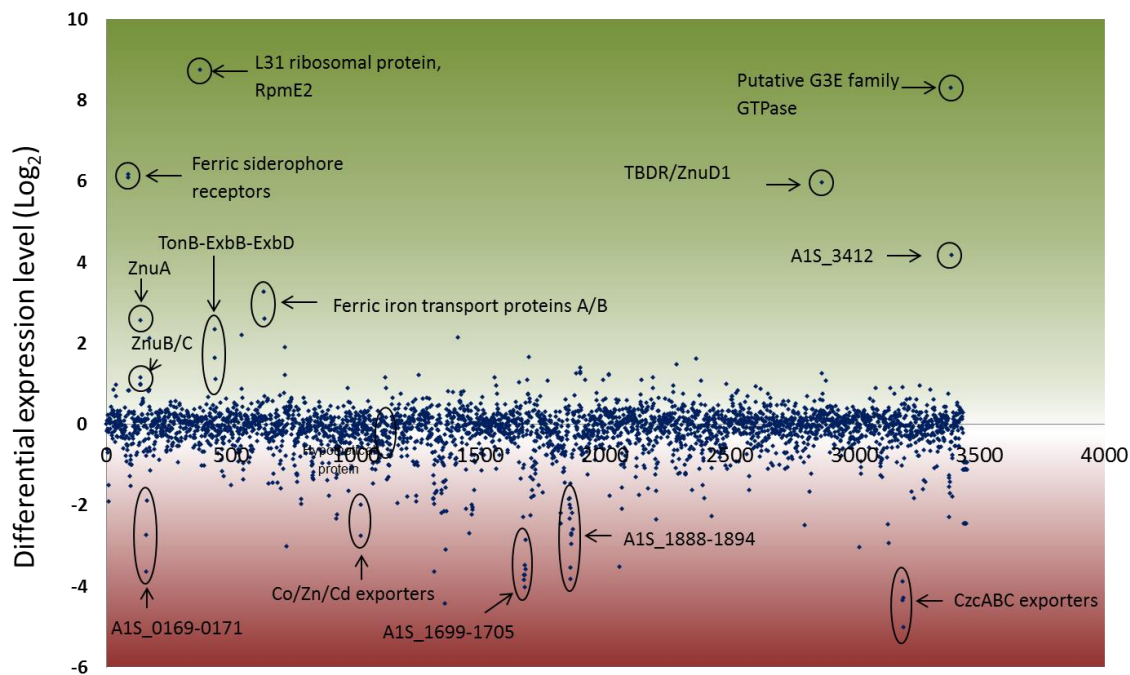


Figure 3.6: Overview of the transcriptional responses to Zn^{2+} limitation in *A. baumannii* ATCC 17978

Comparison of the global RNA expression of *A. baumannii* ATCC 17978 grown in Zn^{2+} -limited and Zn^{2+} -replete conditions. The expression levels of all 3500 genes in the ATCC 17978 genome were measured by RNA-seq and are represented on the X-axis in order of ascending locus-tag number (Smith *et al.* 2007). Differential expression levels in bacterial cells grown in Zn^{2+} -replete and Zn^{2+} -limited conditions are displayed in Log_2 -values on the Y-axis. Genes exhibiting increased or decreased expression under Zn^{2+} -limited conditions are displayed in the green and red sections, respectively. The circled dots indicate selected genes that are highly differentially expressed during growth in Zn^{2+} -limited conditions.

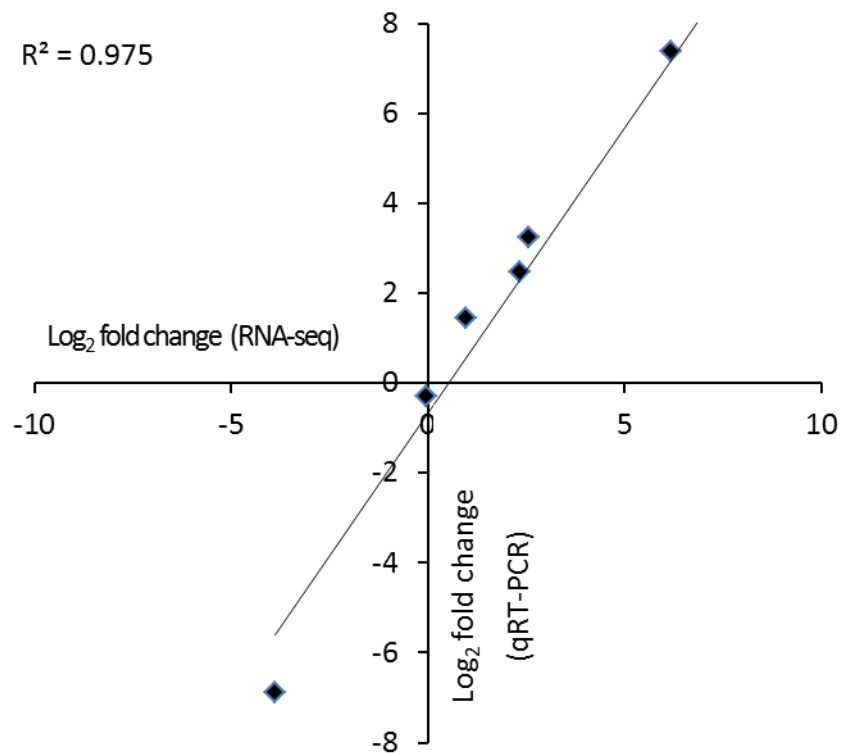


Figure 3.7: Correlation of Log₂-based fold changes for six genes showing altered expression in *A. baumannii* ATCC 17978 grown in Zn²⁺-limited conditions

The Y axis represents the Log₂-fold change of gene expression determined by qRT-PCR and the X axis represents the Log₂-fold change of gene expression determined by RNA-seq data. Derived from the RNA-seq and qRT-PCR data, a correlation coefficient (R^2) of 0.975 was determined.

Table 3.2: Validation of transcriptomic data generated from *A. baumannii* ATCC 17978 grown in Zn²⁺-limited conditions

| Locus-tag | qRT-PCR (Log ₂) | RNA-seq (Log ₂) |
|-----------|-----------------------------|-----------------------------|
| A1S_0092 | 7.370 | 6.173 |
| A1S_0145 | 1.445 | 0.979 |
| A1S_3217 | -6.008 | -3.892 |
| A1S_0452 | 2.470 | 2.349 |
| A1S_0391 | 9.375 | 8.742 |
| A1S_0146 | 3.255 | 2.59 |

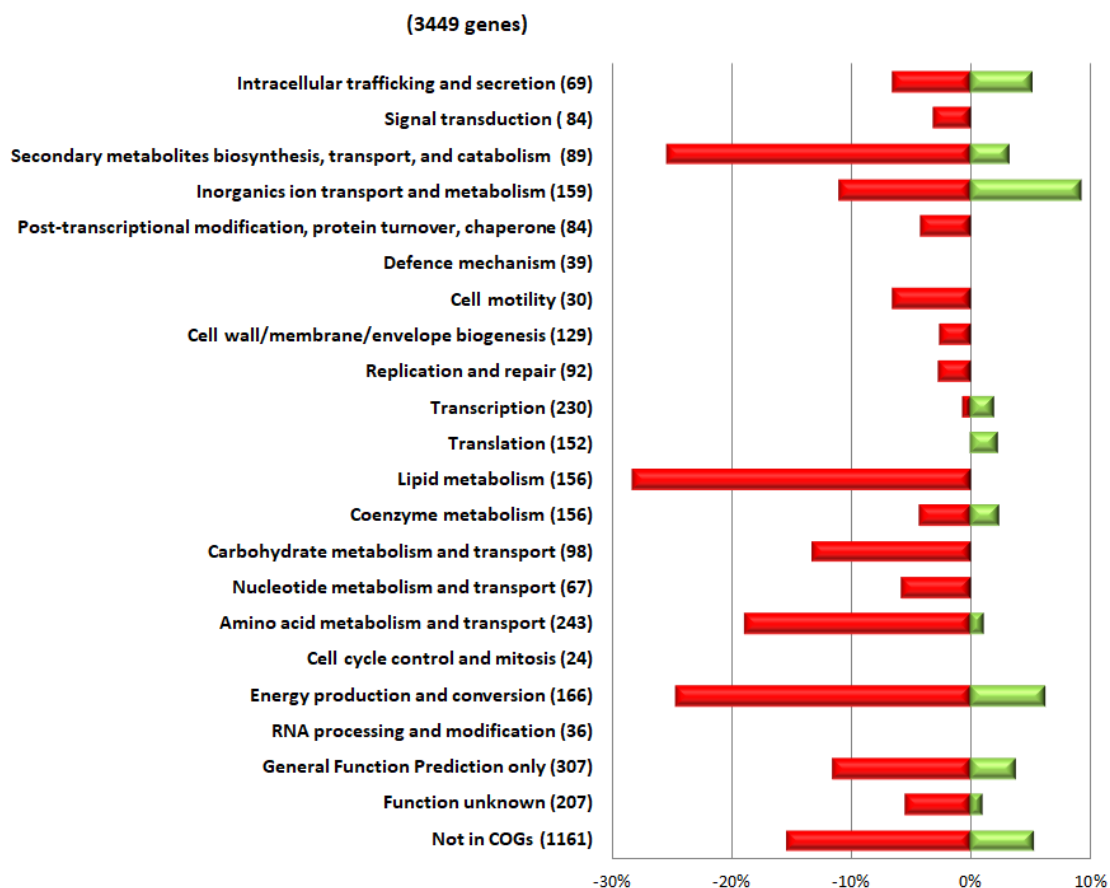


Figure 3.8: Transcriptional changes in *A. baumannii* ATCC 17978 during growth in Zn^{2+} -limited conditions relative to Zn^{2+} -replete conditions, displayed by COG function

The percentage of differentially expressed genes (≥ 2 -fold as determined using RNA-seq) belonging to each COG category is shown. The figure depicts the COG and the percentage of down-regulated (red) and up-regulated (green) genes in *A. baumannii* ATCC 17978. The total number of differentially expressed genes per COG is shown in parentheses.

proteins involved in secondary metabolites biosynthesis, transport, and catabolism, and energy production and conversion. Genes potentially involved in energy production and conversion included dihydrolipoamide dehydrogenase (DLDH) (represented by ORFs A1S_1701-1703) showing a decrease in expression between ~12- to 17-fold (Figure 3.6; A1S_1699-1705 cluster). The down-regulation of genes involved in energy production may due to a general slowing or reduction of cell metabolism (Figure 3.8). Many amino acid metabolism and transport genes also had decreased expression in Zn²⁺-limited conditions. The wide effect of Zn²⁺-limitation on genes belonging to a range of COGs shows the pleiotropic effect of Zn²⁺ removal; many of the changes in expression may not necessarily be a directly due to Zn²⁺ removal but more likely due to indirect effects. However, the expression of genes encoding proteins involved in the biosynthesis of capsule, A1S_0049-A1S_0066 (Eijkelkamp *et al.* 2014b), were not affected by Zn²⁺-limitation.

Various genes involved in amino acid metabolism and transport showed highly reduced expression (Figure 3.8). A group of genes involved in inorganic ion transport and metabolism was found to be differentially expressed in Zn²⁺-limited conditions (both increased and decreased). This may reflect a need by the cell to modulate the intracellular Zn²⁺ concentration (Lim *et al.* 2013). Among the up-regulated genes in inorganic ion transport and metabolism were *znuABC* and genes encoding the putative Fe²⁺-transport protein A/B (A1S_0652/A1S_0653) (Figure 3.6). Additionally, within this category was the gene encoding the ferric siderophore receptor (A1S_0092), which was very highly over-expressed (> 60-fold) (Figure 3.6). Changes also included genes with highly reduced expression, such as genes encoding the CzcABC exporter (A1S_3217-3219) and an outer membrane Cu receptor (A1S_0170) (Figure 3.6). Based on these data it is revealed that *A. baumannii* showed a strong transcriptional response to Zn²⁺ starvation, predominantly via increased expression of Zn²⁺-acquisition mechanisms and other ion transporters and receptors. However, many genes differentially expressed in response to Zn²⁺-limited conditions were involved in processes other than Zn²⁺ acquisition, such as carbohydrate metabolism, lipid metabolism, secondary metabolites biosynthesis, transport and catabolism, and energy production and conversion.

3.2.5.2 Categorisation of genes differentially expressed in response to Zn²⁺ limitation in *A. baumannii*

The expression of many genes was affected by growth under Zn²⁺-limited conditions. Table 3.3 shows the functions of genes that had expression modulated by at least 2-fold during growth in Zn²⁺-limited conditions. The genes responsible for metal homeostasis had increased expression levels ranging from 3-fold to more than 300-fold. Many of the genes involved in metal homeostasis, also involved in Zn²⁺ homeostasis, are highlighted in green, including A1S_0144, A1S_0146, A1S_0391, A1S_0452, A1S_0454, A1S_2892, and A1S_3411 and are known to be regulated by *zur*. However, other up-regulated genes are involved in Fe²⁺ homeostasis, including genes encoding a siderophore receptor (A1S_0092), Fe²⁺-transport proteins (A1S_0652 and A1S_0653), ferredoxin (A1S_1719) and acinetobactin (A1S_2389). This increased expression of several Fe²⁺-transport proteins and receptors may be due to the interaction between Zn²⁺ and Fe²⁺ ions. Alternatively these genes have been wrongly assigned a function in Fe²⁺ transport or homeostasis. Additionally, a number of genes involved in metabolic processes also showed increased expression, indicating that there is a general response to Zn²⁺ depletion within the cell.

Zn²⁺ limitation also resulted in the decreased expression of transcriptional regulators, secreted proteins and virulence factors, signal peptides, ribosomal proteins, and various genes in metabolic processes. A number of hypothetical proteins were also affected by growth in Zn²⁺-limited conditions, which may indicate a role for Zn²⁺ in the expression of these genes or that Zn²⁺ limitations leads to a downstream effect that influences their expression. However, it has also been suggested that the reduced expression of various genes in cells grown in Zn²⁺-limited conditions is not solely because of the absence of Zn²⁺ but is due the decrease in specific growth rate seen when under Zn²⁺ starvation conditions (De Nicola *et al.* 2007).

Table 3.3: *A. baumannii* ATCC 17978 genes with altered expression in response to Zn²⁺-limitation as determined by RNA-seq

| Locus tag | Predicted/known function of protein ^a | Fold change ^b |
|-------------------------------------------------------|------------------------------------------------------|--------------------------|
| Up-regulated genes | | |
| Genes encoding proteins involved in metal homeostasis | | |
| A1S_0092 | Ferric siderophore receptor protein | 72.1 |
| A1S_0144 | High affinity Zn ²⁺ transport protein | 2.2 |
| A1S_0146 | High affinity Zn ²⁺ transport protein | 5.9 |
| A1S_0391 | RpmE; 50S ribosomal protein L31 | 427.9 |
| A1S_0452 | Periplasmic protein TonB | 5.0 |
| A1S_0453 | Biopolymer transport protein (ExbB) | 3.1 |
| A1S_0454 | Biopolymer transport protein (ExbD) | 2.2 |
| A1S_0652 | Fe-transport protein A | 9.6 |
| A1S_0653 | Fe-transport protein B | 6.1 |
| A1S_1719 | 4Fe-4S ferredoxin | 3.1 |
| A1S_2389 | Ferric acinetobactin transport system | 3.1 |
| A1S_2892 | TonB-dependent receptor protein | 62.5 |
| A1S_3411 | G3E family GTPase | 314.8 |
| Genes encoding proteins with various functions | | |
| A1S_0737 | Homocysteine S-methyltransferase | 3.7 |
| A1S_0738 | Flavoprotein oxidoreductase | 2.3 |
| A1S_1681 | Methyltransferase | 2.1 |
| A1S_1712 | DMT family permease | 2.1 |
| A1S_1908 | Phospho-2-dehydro-3-deoxyheptonate aldolase | 2.4 |
| A1S_1924 | Cytochrome d terminal oxidase polypeptide subunit I | 2.5 |
| A1S_1925 | Cytochrome d terminal oxidase polypeptide subunit II | 2.4 |
| A1S_1944 | Alpha/beta hydrolase | 2.1 |
| A1S_2016 | Phage-related lysozyme | 2.1 |

Table 3.3: Cont.

| Locus tag | Predicted/known function of protein | Fold change |
|-------------------------------------------------------|-------------------------------------------|-------------|
| Genes encoding proteins with various functions | | |
| A1S_2169 | Cytochrome o ubiquinol oxidase subunit IV | 2.1 |
| A1S_2217 | Protein CsuA | 2.2 |
| A1S_2310 | TrnR | 2.8 |
| A1S_2909 | tRNA-Leu | 2.1 |
| Genes encoding hypothetical proteins | | |
| A1S_0093 | Hypothetical protein | 67.6 |
| A1S_0180 | Hypothetical protein | 4.3 |
| A1S_0561 | Hypothetical protein | 4.6 |
| A1S_1143 | Hypothetical protein | 2.2 |
| A1S_1276 | Hypothetical protein | 2.3 |
| A1S_1435 | Hypothetical protein | 4.4 |
| A1S_1583 | Hypothetical protein | 2.2 |
| A1S_1794 | Hypothetical protein | 2.1 |
| A1S_1926 | Hypothetical protein | 2.6 |
| A1S_2038 | Hypothetical protein | 2.3 |
| A1S_2039 | Hypothetical protein | 2.4 |
| A1S_2408 | Hypothetical protein | 2.1 |
| A1S_2893 | Hypothetical protein | 2.4 |
| A1S_3412 | Hypothetical protein | 1.8 |
| Down-regulated genes | | |
| Genes encoding proteins involved in metal homeostasis | | |
| A1S_0009 | Putative RND type efflux pump | -3.8 |
| A1S_0010 | RND type efflux pump | -2.8 |
| A1S_0170 | Outer membrane Cu receptor | -6.7 |

Table 3.3: Cont.

| Locus tag | Predicted/known function of protein | Fold change |
|-------------------------------------------------------|-----------------------------------------------------------|-------------|
| Genes encoding proteins involved in metal homeostasis | | |
| A1S_0708 | Cu-resistance protein B precursor | -2.7 |
| A1S_1044 | Co/Zn/Cd efflux system | -4.0 |
| A1S_1045 | Co/Zn/Cd efflux system | -6.8 |
| A1S_1266 | Hypothetical Mn ²⁺ transporter/MntH | -3.8 |
| A1S_3214 | Cation efflux system protein | -2.0 |
| A1S_3217 | RND efflux transporter CzcA | -14.8 |
| A1S_3218 | RND efflux transporter CzcB | -20.4 |
| A1S_3219 | RND efflux transporter CzcC | -32.4 |
| Genes encoding transporters | | |
| A1S_0010 | RND type efflux pump | -2.8 |
| A1S_1004 | Citrate transporter | -2.2 |
| A1S_1094 | D-serine/D-alanine/glycine transporter | -2.8 |
| A1S_1467 | Glutamate symport transmembrane protein | -4.3 |
| A1S_1491 | Glutamate/aspartate transporter | -4.7 |
| A1S_1492 | Glutamate/aspartate transporter | -4.1 |
| A1S_1493 | Glutamate/aspartate transporter | -4.3 |
| A1S_1724 | Dicarboxylic acid transport protein | -4.8 |
| A1S_1730 | Short-chain fatty acid transporter | -3.5 |
| A1S_1887 | 4-hydroxybenzoate transporter | -14.1 |
| A1S_1888 | 4-hydroxybenzoate transporter | -6.7 |
| A1S_3135 | Putative APC family S-methylmethionine transporter (MmuP) | -2.5 |
| A1S_3404 | Amino acid APC transporter | -4.9 |
| A1S_1730 | Short-chain fatty acid transporter | -3.5 |

Table 3.3: Cont.

| Locus tag | Predicted/known function of protein | Fold change |
|--------------------------------------------------------|--------------------------------------------------|-------------|
| Genes encoding transcriptional regulators | | |
| A1S_0399 | Putative transcriptional regulator (LysR family) | -2.0 |
| A1S_0732 | Transcriptional regulator (AraC family) | -2.1 |
| A1S_0848 | Transcriptional regulator | -2.0 |
| A1S_1687 | Transcriptional regulator | -2.5 |
| A1S_1697 | Transcriptional regulator | -4.9 |
| A1S_1738 | Transcriptional regulator | -3.4 |
| A1S_1746 | Putative transcriptional regulator | -2.1 |
| A1S_1775 | Transcriptional activator | -3.2 |
| A1S_2082 | Transcriptional regulator | -11.4 |
| A1S_2101 | Putative transcriptional regulator | -2.1 |
| A1S_2451 | Transcriptional regulator (AsnC family) | -4.8 |
| A1S_3264 | Transcriptional regulator | -3.5 |
| Genes encoding secreted proteins and virulence factors | | |
| A1S_1193 | OmpA/MotB protein | -3.8 |
| A1S_1383 | Surface antigen | -21.6 |
| A1S_1386 | Catalase | -2.6 |
| A1S_3159 | Lipase chaperone | -5.6 |
| A1S_3160 | Lipase | -7.7 |
| A1S_3220 | VGR-like protein | -19.6 |
| Genes encoding proteins with a signal peptide | | |
| A1S_0786 | Putative signal peptide | -2.3 |
| A1S_0787 | Putative signal peptide | -2.4 |
| A1S_1158 | Putative signal peptide | -2.5 |
| A1S_1745 | Putative signal peptide | -2.3 |
| A1S_2183 | Putative signal peptide | -2.1 |
| A1S_3253 | Putative signal peptide | -3.2 |

Table 3.3: Cont.

| Locus tag | Predicted/known function of protein | Fold change |
|-----------------------------------|-------------------------------------------|-------------|
| Genes encoding ribosomal proteins | | |
| A1S_r02 | Ribosomal RNA | -2.2 |
| A1S_r05 | Ribosomal RNA | -2.2 |
| A1S_r08 | Ribosomal RNA | -2.2 |
| A1S_r11 | Ribosomal RNA | -2.2 |
| A1S_r14 | Ribosomal RNA | -2.2 |
| A1S_2423 | Ribosomal L31 | -3.5 |
| A1S_r03 | Ribosomal RNA | -5.4 |
| A1S_r04 | Ribosomal RNA | -5.4 |
| A1S_r07 | Ribosomal RNA | -5.5 |
| A1S_r10 | Ribosomal RNA | -5.4 |
| A1S_r13 | Ribosomal RNA | -5.4 |
| Genes encoding various functions | | |
| A1S_0101 | Pseudogene | -2.4 |
| A1S_0104 | Putative acetyl-CoA synthetase | -2.9 |
| A1S_0106 | Putative enoyl-CoA hydratase | -2.0 |
| A1S_0408 | Putative glutathione S-transferase | -2.0 |
| A1S_0482 | Acetate kinase (propionate kinase) | -2.2 |
| A1S_0490 | Putative hydrolase | -2.4 |
| A1S_0566 | Pyridine nucleotide transhydrogenase | -2.6 |
| A1S_0567 | Pyridine nucleotide transhydrogenase | -2.2 |
| A1S_0690 | FilA | -2.7 |
| A1S_0691 | FilB | -2.3 |
| A1S_0691 | FilC | -2.3 |
| A1S_0721 | Glutaryl-CoA dehydrogenase | -3.0 |
| A1S_0803 | Trehalose-6-phosphate synthase | -3.6 |
| A1S_0850 | Betaine/choline/glycine transport protein | -2.5 |

Table 3.3: Cont.

| Locus tag | Predicted/known function of protein | Fold change |
|----------------------------------|----------------------------------------------------|-------------|
| Genes encoding various functions | | |
| A1S_0852 | Dioxygenase alpha subunit | -2.4 |
| A1S_0853 | Succinate-semialdehyde dehydrogenase | -2.3 |
| A1S_0855 | Dioxygenase beta subunit | -2.6 |
| A1S_0910 | Gamma-glutamyltranspeptidase precursor | -2.6 |
| A1S_0949 | Putative dioxygenase | -2.4 |
| A1S_0951 | Ferredoxin reductase | -4.7 |
| A1S_1008 | Isocitrate lyase | -2.1 |
| A1S_1091 | Succinylornithine transaminase | -2.1 |
| A1S_1104 | Chlorogenate esterase | -2.2 |
| A1S_1261 | Putative 3-hydroxyacyl-CoA dehydrogenase | -2.0 |
| A1S_1274 | Alcohol dehydrogenase GroES-like protein | -2.0 |
| A1S_1336 | Phenylacetate-CoA oxygenase subunit PaaA | -3.6 |
| A1S_1337 | Phenylacetate-CoA oxygenase subunit PaaB | -3.6 |
| A1S_1339 | Phenylacetate-CoA oxygenase PaaJ subunit | -2.8 |
| A1S_1340 | Phenylacetate-CoA oxygenase/reductase PaaK subunit | -3.9 |
| A1S_1341 | Enoyl-CoA hydratase/carnithine racemase | -12.5 |
| A1S_1342 | Enoyl-CoA hydratase | -3.3 |
| A1S_1349 | Thioesterase domain-containing protein | -3.1 |
| A1S_1368 | Pyruvate ferredoxin/ferredoxin oxidoreductase | -4.6 |
| A1S_1369 | Putative oxidoreductase protein | -3.3 |
| A1S_1370 | Oxidoreductase | -3.1 |
| A1S_1376 | Acyl-CoA dehydrogenase | -2.7 |
| A1S_1378 | Putative long chain fatty-acid CoA ligase | -2.7 |
| A1S_1379 | Putative SAM-dependent methyltransferase | -2.0 |
| A1S_1380 | Putative protein (DcaP-like) | -4.4 |

Table 3.3: Cont.

| Locus tag | Predicted/known function of protein | Fold change |
|----------------------------------|----------------------------------------------------|-------------|
| Genes encoding various functions | | |
| A1S_1384 | CinA-like protein | -8.6 |
| A1S_1387 | Oxidoreductase | -4.4 |
| A1S_1424 | Malonate decarboxylase beta subunit | -2.0 |
| A1S_1466 | Glutaminase-asparaginase | -2.2 |
| A1S_1500 | tRNA-Met | -3.1 |
| A1S_1529 | Leucine-responsive regulatory protein | -2.2 |
| A1S_1588 | Phage terminase-like protein large subunit | -2.1 |
| A1S_1698 | Lipoate synthase | -2.0 |
| A1S_1699 | Acetoin:26-dichlorophenolindophenol oxidoreductase | -13.2 |
| A1S_1700 | Acetoin:26-dichlorophenolindophenol oxidoreductase | -14.4 |
| A1S_1701 | Dihydrolipoamide acetyltransferase | -16.2 |
| A1S_1702 | Dihydrolipoamide dehydrogenase | -11.1 |
| A1S_1703 | Dihydrolipoamide dehydrogenase | -13.1 |
| A1S_1704 | Acetoin dehydrogenase | -12.0 |
| A1S_1705 | (RR)-butanediol dehydrogenase | -7.3 |
| A1S_1724 | Dicarboxylic acid transport protein | -4.8 |
| A1S_1726 | Aspartate ammonia-lyase (aspartase) | -2.5 |
| A1S_1731 | Acetoacetyl-CoA transferase beta subunit | -2.1 |
| A1S_1732 | Acetoacetyl-CoA transferase subunit α | -3.1 |
| A1S_1736 | Putative membrane protein | -2.6 |
| A1S_1737 | 3-hydroxybutyrate dehydrogenase | -2.0 |
| A1S_1758 | Short-chain dehydrogenase/reductase SDR | -2.9 |
| A1S_1846 | 3-oxoacid CoA-transferase subunit A | -5.5 |
| A1S_1847 | 3-oxoadipate CoA-transferase subunit B | -4.6 |
| A1S_1857 | Vanillate O-demethylase oxidoreductase | -2.3 |
| A1S_1858 | Short-chain dehydrogenase/reductase SDR | -2.1 |

Table 3.3: Cont.

| Locus tag | Predicted/known function of protein | Fold change |
|----------------------------------|-------------------------------------------------------|-------------|
| Genes encoding various functions | | |
| A1S_1860 | (2Fe-2S) protein | -2.2 |
| A1S_1880 | Pyrroloquinoline-quinone quiA | -3.6 |
| A1S_1881 | Porin | -3.5 |
| A1S_1882 | 3-dehydroshikimate dehydratase | -5.0 |
| A1S_1883 | 3-dehydroquinate dehydratase | -4.0 |
| A1S_1884 | Protocatechuate 3,4-dioxygenase alpha chain (3,4-PCD) | -2.8 |
| A1S_1885 | Protocatechuate 3,4-dioxygenase subunit beta | -4.2 |
| A1S_1886 | Gamma-carboxymuconolactone decarboxylase (CMD) | -11.6 |
| A1S_1889 | 3-oxoadipate enol-lactonase | -6.5 |
| A1S_1890 | 3-carboxy-cis,cis-muconate cycloisomerase | -7.8 |
| A1S_1893 | 3-oxoadipate CoA-transferase subunit B | -4.6 |
| A1S_1894 | 3-oxoadipate CoA-transferase subunit A | -6.1 |
| A1S_1954 | Serine proteinase | -2.4 |
| A1S_2091 | Putative exported protein | -3.0 |
| A1S_2148 | Putative acetyl-CoA synthetase | -2.5 |
| A1S_2149 | Putative acyl CoA dehydrogenase | -2.1 |
| A1S_2196 | Membrane-associated dicarboxylate transport protein | -3.0 |
| A1S_2224 | Threonine efflux protein | -2.4 |
| A1S_2229 | Putative acyl-CoA dehydrogenase-related protein | -2.1 |
| A1S_2318 | Putative membrane protein | -2.3 |
| A1S_2325 | Putative outer membrane protein | -2.3 |
| A1S_2344 | tRNA-Asn | -2.0 |
| A1S_2345 | tRNA-Asn | -2.3 |
| A1S_2346 | tRNA-Asn | -2.4 |
| A1S_2373 | Acinetobactin biosynthesis protein | -3.1 |

Table 3.3: Cont.

| Locus tag | Predicted/known function of protein | Fold change |
|----------------------------------|---------------------------------------------------|-------------|
| Genes encoding various functions | | |
| A1S_2415 | tRNA-Val | -2.9 |
| A1S_2452 | NAD-dependent aldehyde dehydrogenase | -2.1 |
| A1S_2513 | tRNA-Asn | -2.2 |
| A1S_2527 | Putative thioesterase protein | -2.0 |
| A1S_2601 | Putative outer membrane protein A | -2.4 |
| A1S_2678 | tRNA-Leu | -2.1 |
| A1S_2724 | Putative hemagglutinin | -2.0 |
| A1S_2744 | SAM-dependent methyltransferase | -2.1 |
| A1S_2755 | Putative acyltransferase | -2.1 |
| A1S_2823 | Hypothetical protein | -5.7 |
| A1S_2850 | Putative acyl-CoA transferase | -2.3 |
| A1S_3049 | Putative integral membrane protein | -2.4 |
| A1S_3129 | Succinylarginine dihydrolase | -2.4 |
| A1S_3130 | Succinylglutamic semialdehyde dehydrogenase | -2.1 |
| A1S_3300 | ActP; acetate permease | -3.0 |
| A1S_3301 | Putative membrane protein | -2.6 |
| A1S_3309 | Acetyl-CoA synthetase | -2.7 |
| A1S_3402 | Arginase/agmatinase/formimionoglutamate hydrolase | -2.5 |
| A1S_3403 | Imidazolonepropionase | -2.9 |
| A1S_3404 | Proline transport protein (APC family) | -4.9 |
| A1S_3405 | Histidine ammonia-lyase | -2.4 |
| A1S_3406 | Urocanate hydratase | -3.3 |
| A1S_3407 | Urocanase | -2.7 |
| A1S_3418 | 4-hydroxyphenylpyruvate dioxygenase | -3.5 |
| A1S_3458 | Putative Na ⁺ -dependent transporter | -2.2 |

Table 3.3: Cont.

| Locus tag | Predicted/known function of protein | Fold change |
|--------------------------------------|-------------------------------------|-------------|
| Genes encoding protein hypotheticals | | |
| A1S_0171 | Hypothetical protein | -3.7 |
| A1S_0184 | Hypothetical protein | -2.2 |
| A1S_0517 | Hypothetical protein | -2.9 |
| A1S_0779 | Hypothetical protein | -2.0 |
| A1S_0785 | Hypothetical protein | -2.3 |
| A1S_0788 | Hypothetical protein | -2.7 |
| A1S_0804 | Hypothetical protein | -3.9 |
| A1S_0918 | Hypothetical protein | -3.4 |
| A1S_0946 | Hypothetical protein | -2.5 |
| A1S_0996 | Hypothetical protein | -3.1 |
| A1S_1151 | Hypothetical protein | -2.6 |
| A1S_1156 | Hypothetical protein | -2.0 |
| A1S_1233 | Hypothetical protein | -3.5 |
| A1S_1268 | Hypothetical protein | -3.4 |
| A1S_1338 | Hypothetical protein | -2.0 |
| A1S_1345 | Hypothetical protein | -3.2 |
| A1S_1385 | Hypothetical protein | -3.0 |
| A1S_1696 | Hypothetical protein | -2.1 |
| A1S_1862 | Hypothetical protein | -2.7 |
| A1S_2041 | Hypothetical protein | -3.4 |
| A1S_2602 | Hypothetical protein | -3.1 |
| A1S_2843 | Hypothetical protein | -3.2 |
| A1S_3051 | Hypothetical protein | -2.1 |
| A1S_3343 | Hypothetical protein | -2.1 |

^{a.} The predicted function of the protein based on the data from KEGG: Kyoto Encyclopaedia of Genes and Genomes.

^{b.} Negative values mean the expression was down-regulated.

^{c.} Green box indicates genes known to be Zur-regulated.

3.2.5.3 Restriction of Zn²⁺ affects the transcription of a number of transporter genes

The global transcriptomic analyses revealed that expression of a number of transporters were affected by growth under Zn²⁺-limited conditions (see Table 3.3) corresponding well with Zn²⁺-transport systems predicted to be affected by Zn²⁺ depletion using bioinformatics analyses (Hood *et al.* 2012). The RNA-seq data described here revealed that several genes predicted to have Zur-binding sites showed increased expression in Zn²⁺-limited conditions, including A1S_0145, A1S_0146, A1S_0391, A1S_0452, A1S_2892, A1S_3411, and A1S_3412 (Table 3.3). Transporters known to be Zur-regulated, such as *znuABC* (A1S_0144-0146), showed increased expression of 2- to 6-fold under Zn²⁺ limitation. However, some transporter genes that have a Zur box up-stream of the ORF (Hood *et al.* 2012) were not differentially regulated during Zn²⁺ limitation. These included A1S_0410, A1S_1679, A1S_3103, and A1S_3225. The data also revealed that the *mntH* gene (A1S_1266), encoding a putative Mn²⁺ and Fe²⁺ transporter in the NRAMP family, showed a 3-fold decrease in expression in response to Zn²⁺-depletion. Reduced expression of *mntH* has also been reported in *P. fluorescens* when grown in Zn²⁺-limited medium (Lim *et al.* 2012).

The genes encoding the aspartate/glutamate transport proteins (A1S_1490-1493), belonging to the ABC family of transporters, also showed 4- to 5-fold reduced expression. The proteins that make up the aspartate/glutamate transporter are encoded by four genes clustered on the *A. baumannii* genome (as are the homologues in other *Acinetobacter* spp.) and share approximately 45% amino acid identity with aspartate/glutamate transporters in other bacterial species. It has been reported that this transporter is essential for optimal micro aerobic growth on dicarboxylic amino acids in *C. jejuni*, and is a surface exposed antigen that has a major role in adherence and host colonisation (Muller *et al.* 2007). It has been suggested that Zn²⁺ binding contributes to the function of this transporter however, this has not yet been clearly defined (Leon-Kempis *et al.* 2006).

In addition, growth in Zn²⁺-limited medium resulted in a 14- to 30-fold reduced expression of genes encoding the RND superfamily efflux system, *czcABC*

(A1S_3217-3219) which is predicted to be involved in the efflux of metals. The reduced expression of this efflux pump may indicate that the cells are attempting to prevent Zn^{2+} from leaving the intracellular compartment. A similar finding has been shown in *P. protegens* in response to Zn^{2+} -limited conditions (Lim *et al.* 2013). Although the role of the *czcABC* cluster in *A. baumannii* has not been defined, the orthologous system in *Alcaligenes eutrophus* has been shown to be involved in the efflux of metals such as Zn^{2+} , Cd^{2+} and Co^{2+} (Nies 1995). In *P. aeruginosa* the expression of *czcABC* is regulated by the CzcR–CzcS two-component system that was found to also be down-regulated in response to Zn^{2+} limitation (Hassan *et al.* 1999; Perron *et al.* 2004). This two component system has not been identified in *A. baumannii* ATCC 17978 but the heavy metal response regulator A1S_2937 and A1S_2938 share 55% and 32% amino acid identity, respectively, with the *P. aeruginosa* CzcR–CzcS system. However, the transcriptomic data obtained for *A. baumannii* did not detect a significant change in expression for A1S_2937 and A1S_2938 during growth in Zn^{2+} -limited medium.

The *czcD* (A1S_3214) gene adjacent to the *czcABC* cluster described above showed 2-fold reduced expression in Zn^{2+} -limited conditions. The *czcD* gene encodes a predicted protein within the CDF family that transports metal ions from the host cell (Lim *et al.* 2013). The CzcD transporter has been implicated in resistance to excess Co^{2+} , Zn^{2+} and Cd^{2+} in some bacterial genera (Anton *et al.* 1999). Similar to the changes in expression observed in *A. baumannii*, *czcD* in *S. aureus* (Kuroda *et al.* 1999) and *S. pneumoniae* (Jacobsen *et al.* 2011; Shafeeq *et al.* 2011), as well as the ortholog *zitB* in *E. coli* (Grass *et al.* 2001), are all differentially expressed in response to changes in Zn^{2+} concentration. The *A. baumannii* CzcD protein has ~39% amino acid identity to *zitB*, which is involved in the efflux of Zn^{2+} across the cytoplasmic membrane, thus reducing the accumulation of Zn^{2+} in the cytoplasm rendering bacteria more resistant to Zn^{2+} toxicity. Thus, in *A. baumannii*, *czcD* (A1S_3214) may also contribute to Zn^{2+} homeostasis.

Interestingly, the expression of a predicted heavy metal transport protein (A1S_1217), belonging to the P-type ATPase family, was unchanged during growth in low Zn^{2+} conditions. Transporters of the P-type ATPase family are involved in cation translocation across the membrane (Lutsenko and Kaplan 1995).

Bioinformatic analysis predicted that A1S_1217 transports Zn^{2+} and/or Cd^{2+} and is homologous to the *E. coli* Zn^{2+} P-type ATPase (ZntA) (Rensing *et al.* 1997; Wang *et al.* 2012). ZntA is a well-characterised transporter in *E. coli*; however, it has yet to be described in *A. baumannii*. Based on the observation that there was no change in A1S_1217 expression under Zn^{2+} -limited conditions, it is possible that this is a redundant Zn^{2+} transporter that is active only when the activity of CzcABC is insufficient to maintain optimal intracellular Zn^{2+} levels. Additionally, RNA-seq data identified a putative Zn^{2+} -efflux system (A1S_1044-1045), the expression of which was reduced > 4-fold under Zn^{2+} -limited conditions. Although annotated as two ORFs, A1S_1044 and A1S_1045 in *A. baumannii* ATCC 17978, these represent a single gene based in the CP012004 annotated sequence (ACX60_13160), the product of which shares high amino acid identity to the Co/Zn/Cd efflux protein CzcD. The down-regulation this CzcD homologue indicates that *A. baumannii* shuts off the efflux systems during growth in Zn^{2+} -limited conditions to prevent the export of Zn^{2+} and therefore maintain the intracellular Zn^{2+} level.

3.2.5.4 Zn^{2+} limitation increases the expression of TonB-dependent receptor genes

A TBDR potentially specific for Zn^{2+} uptake, called ZnuD, was identified in *N. meningitidis* (Pawlik *et al.* 2012) and in *Cyanobacterium anabaena* spp. strain PCC 7120 (Napolitano *et al.* 2012). *A. baumannii* strain ATCC 17978 encodes two predicted TBDRs, A1S_2892 on the chromosome while A1S_3475 is carried on a native plasmid (Hood *et al.* 2012). A1S_2892 and A1S_3475 are 41-42% identical to the *N. meningitidis* ZnuD, respectively. ZnuD is Zur-regulated and has been shown to be involved in both Zn^{2+} and heme transport in *N. meningitidis* (Stork *et al.*, 2010). In our study, the ZnuD homologue A1S_2892 increased in expression by >62-fold under Zn^{2+} limitation (Table 3.3), suggesting that this receptor may facilitate Zn^{2+} uptake in *A. baumannii* ATCC 17978. Furthermore, the expression of the TonB-ExbB-ExbD (A1S_0452-0454) complex also increased (2- to 5-fold) in response to Zn^{2+} -limited conditions (Table 3.3).

Transcriptomic analysis of *A. baumannii* under Zn^{2+} -limited conditions also revealed reduced expression of A1S_0170, a putative outer membrane Cu receptor that shares 50% amino acid identity with OprC (PA3790) in *P. aeruginosa*. OprC is a

TonB-dependent Cu receptor that in other bacteria plays a role in Cu utilisation (Lim *et al.* 2012; Yoneyama and Nakae 1996). Expression of *oprC* in *A. baumannii* ATCC 17978 was reduced by approximately 7-fold during growth under Zn^{2+} -limited conditions. However, bioinformatics analysis revealed there is no *zur* box up-stream of *oprC* indicating that this gene is unlikely to be directly regulated by Zur.

3.2.5.5 The effect of Zn^{2+} limitation on known Zn^{2+} -dependent proteins

Recently, an *A. baumannii* gene cluster (A1S_3411-3412) was identified that is likely to be regulated by *zur* as these genes displayed increased expression in a Δzur mutant strain (Mortensen *et al.* 2014) and have a Zur-binding site immediately up-stream. In concordance with this result, we found in our study that Zn^{2+} limitation increased the transcription of A1S_3411 by >300-fold and A1S_3412 by 18-fold (Table 3.3). Bioinformatic analysis indicated that A1S_3412 has no known function and was annotated as a hypothetical protein, while A1S_3411 encoded a protein predicted to belong to the G3E family of GTPases and also belongs to the COG0523 family, a large and diverse subfamily of proteins with poorly defined functions (Haas *et al.* 2009).

Members of the COG0523 family are involved in many functions, including participating in cobalamin biosynthesis, serving as a nitrile hydratase activator and have been suggested as a metallochaperone (Lim *et al.* 2013). It has also been proposed that some function as Zn^{2+} -specific chaperones (Haas *et al.* 2009). The region of highest similarity between proteins belonging to COG0523 and other members of the G3E family is the GTPase domain, defined by the canonical Walker A and B motifs (Haas *et al.* 2009). ORF A1S_3411 also contains the GTPase domain motifs GCXCC and EXXG and all members of COG0523 have a conserved, putative, metal-binding CXCC motif. However, the neighbouring gene, A1S_3412, also encoding a hypothetical protein, contains neither the GTPase domain nor the CxCC motif but showed increased expression under Zn^{2+} -limited conditions (this study) as well as in the Δzur mutant strain (Mortensen *et al.* 2014). The differential expression of this gene may be because this gene is co-transcribed with A1S_3411. The increased expression of A1S_3411 under Zn^{2+} -limited conditions and in response to inactivation of *zur* (Mortensen *et al.* 2014) suggests a dominant role in

the response of *A. baumannii* to Zn²⁺ limitation. This is supported by the presence in other bacterial genomes of predicted Zur-binding sites associated with genes encoding COG0523 proteins (Schröder et al., 2010). Interestingly, some COG0523 members in species such as *B. subtilis* (Gabriel et al., 2008) and *Corynebacterium glutamicum* (Schröder et al., 2010) were also controlled by the availability of Zn. It has been hypothesised that Zur-dependent expression of COG0523 proteins and Zn²⁺-dependent proteins may represent a mechanism for hierarchal Zn²⁺ distribution and sparing in environments with an inadequate Zn²⁺ supply (Haas et al. 2009).

A very recent study examining A1S_3411 (ZigA), which exhibits Zn²⁺-stimulated GTPase activity, showed that this protein plays a role as a zinc metallochaperone and functioned in zinc sparing in *A. baumannii* (Nairn et al. 2016). It also showed that GTPase activity of the protein increased in the presence of Zn²⁺. In addition, ZigA is encoded adjacent to the Hut system and binds Zn²⁺ and required for the degradation of histidines by HutH allowing Zn²⁺ to be release from the histidine-Zn²⁺ pool and led to increase the free Zn²⁺ intracellular in Zn²⁺-limiting conditions (see Section 1.6) (Nairn et al. 2016).

3.2.5.6 The effect of Zn²⁺ limitation on the transcription of ribosomal proteins

This study of Zn²⁺ limitation in *A. baumannii* ATCC 17978 revealed that Zn²⁺ starvation affected the expression of a number of ribosomal proteins. It has been previously discussed that L31 plays a role in intracellular Zn²⁺ levels in *B. subtilis* and *E. coli* (see Section 1.8). It has also been reported that expression of the *A. baumannii* ribosomal L31 protein is regulated by Zur (Mortensen et al. 2014). However, the functional significance of this gene and its role(s) in Zn²⁺ homeostasis have not been fully defined. There are two paralogs of the ribosomal protein L31 in *A. baumannii* ATCC 17978, A1S_2423 is classed as a C⁺ form and A1S_0391 is classed as a C⁻ form. Similar to what was observed in the Δ zur mutant of *A. baumannii* ATCC 17978 (Mortensen et al. 2014), expression of the C⁻ form (A1S_0391) increased under Zn²⁺-limited conditions (>400-fold), while expression of the C⁺ form (A1S_2423) did not change (Table 3.3); these results were also confirmed by qRT-PCR (see Table 3.2). The existence of two paralogous L31 ribosomal proteins

enables the cells to mobilise Zn^{2+} from the C^+ form, which provides a mechanism to acquire Zn^{2+} during periods of Zn^{2+} starvation. It has been previously discussed (Section 1.9.2) that in Zn^{2+} -limited conditions, the newly synthesised RpmE1 which does not bind to Zn^{2+} will be degraded by a yet unknown protease(s). In the RNA-seq data obtained in this project, the expression of proteases such as the Clp complex which encodes the proteolytic subunit of the Clp protease (A1S_0476-A1S_0476) did not show any changes (data not shown). This may indicate that this protease is not involved in the degradation of RpmE1. To further investigate the role of this ribosomal protein in Zn^{2+} homeostasis, A1S_0391 and A1S_2423 were inactivated to see the effect of the deletion of the C^- form and to inactivate the C^+ form (see Chapter 4 and 5).

Zn^{2+} limitation also caused reduced expression (2- to 5-fold) of other ribosomal genes A1S_r02-r05, A1S_r07-r08 and A1S_r10-r14 (Table 3.3). Repression of ribosomal gene expression under Zn^{2+} -limited conditions was also observed in the study conducted by Higgins *et al* (2003) which highlighted the general starvation response to Zn^{2+} limitation. However, it has been suggested in another study that reduced expression of ribosomal proteins in cells grown in Zn^{2+} -limited medium is due to a decrease in specific growth rate rather than a direct effect of Zn^{2+} depletion (De Nicola *et al.* 2007).

3.2.5.7 The effect of Zn^{2+} -limitation on bacterial metabolism

Genes in the A1S_1697-1705 locus involved in acetoin (also known as 2,3-butanediol) catabolism, showed significantly reduced expression under Zn^{2+} -limited conditions (Figure 3.9). Acetoin acts as an external carbon storage and is synthesised and excreted during exponential growth, but can cause over acidification of the bacterial environment. The ability to degrade acetoin is important for bacteria to be able to utilise this harnessed energy (Huang *et al.* 1999). In *A. baumannii* ATCC 17978 grown in Zn^{2+} -limited conditions there was decreased expression of the gene encoding acetoin-26-dichlorophenolindophenol oxidoreductase (A1S_1699-1700) (15-fold); this enzyme is likely to be involved in acetoin degradation. In *Acinetobacter calcoaceus* the degradation of acetoin occurs

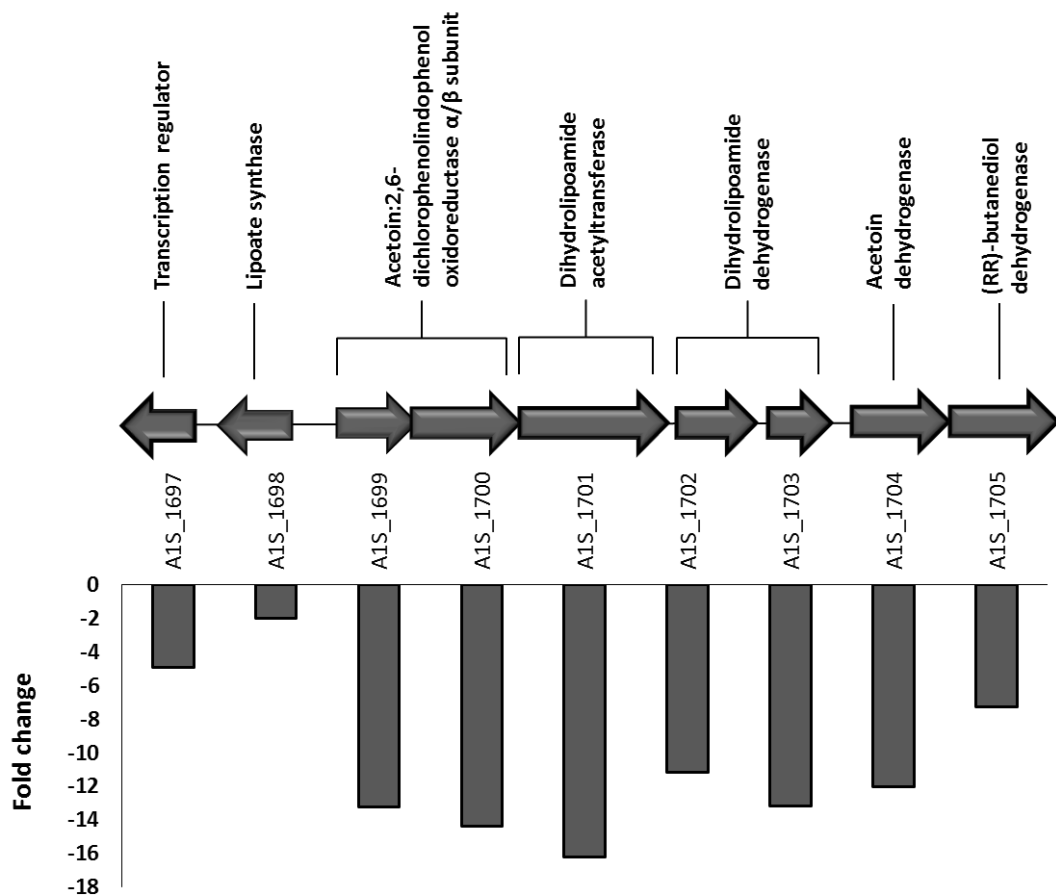


Figure 3.9: RNA expression of genes within the A1S_1697-1705 cluster in *A. baumannii* ATCC 17978 under Zn^{2+} -limited conditions

Arrows represent ORFs and their direction of transcription. Square brackets indicate ORFs which encode separate functional regions of the enzyme described. The graph shows the fold change (Y axis) in RNA expression for each ORF (bars), as determined by RNA-seq analysis.

via the 2,3-butanediol cycle but this pathway has not been fully elucidated (Xiao and Xu 2007).

According to de Berardinis and coworkers (2008) there are two different routes for acetoin dissimilation via the 2,3-butanediol cycle involving 2,3-butanediol dehydrogenase or acetoin dehydrogenase. The low expression of acetoin catabolic genes in bacteria may lead to a reduced ability to survive in environments where other carbon and energy sources are required or in acidic environments where catabolism of acetoin would result in de-acidification. An acetoin reductase from *Clostridium beijerinckii* (Cb-ACR) has been characterised, this enzyme belongs to the threonine dehydrogenase and related Zn²⁺-dependent dehydrogenases class/group (COG1063). Metal analysis of purified Cb-ACR confirmed the presence of two Zn²⁺ atoms (Raedts *et al.* 2014). Thus, given the Zn²⁺ capacity of this protein, it is perhaps unsurprising that when Zn²⁺ availability is low the expression of this gene is reduced.

Dihydrolipoamide dehydrogenase (DLDH), encoded by A1S 1702-1703, was reduced in expression, 11- and 13-fold, respectively (Figure 3.9). These two genes have been annotated as two separate ORFs in *A. baumannii* ATCC 17978 (A1S 1702-1703) but based on the CP012004 sequence, these genes represent one ORF, (ACX60_09395). Inactivation of this DLDH enzyme in bacteria leads to an inability to import sugars, including galactose and the α -galactoside sugars (Hakansson and Smith 2007). In addition to the known functional domains and motifs in this highly conserved enzyme, analysis of the nucleotide sequence also revealed the presence of an N-terminal lipoyl domain. Previous studies have shown that DLDH-negative *S. pneumoniae* are avirulent in a murine model of sepsis and lung infection, indicating that DLDH activity is necessary for the survival of pneumococci within the host (Smith *et al.* 2002). However, the role of this system in *A. baumannii* virulence has not yet been explored.

The gene cluster A1S_1880-1894, had significantly reduced expression in Zn²⁺-limited conditions (2- to 8-fold) (Figure 3.10). Included in this region is a gene encoding pyrroloquinoline-quinone (PQQ, A1S_1880) that is 3.5-fold down regulated and is a cofactor required for several dehydrogenases including glucose dehydrogenase. Many bacteria can synthesise this enzyme, however, *E. coli* and

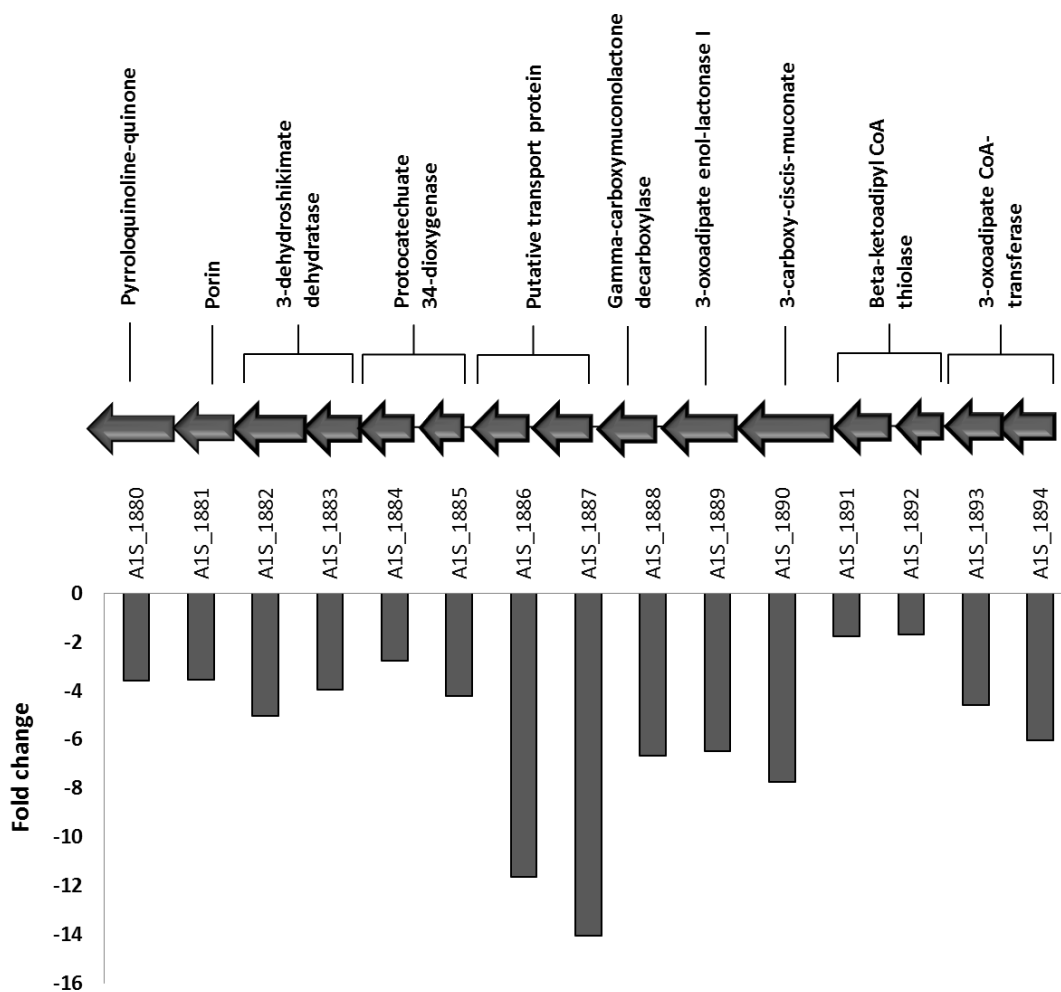


Figure 3.10: RNA expression of genes within the A1S_1880-1894 cluster in *A. baumannii* ATCC 17978 under Zn²⁺-limited conditions

Arrows represent ORFs and their direction of transcription. Square brackets indicate ORFs which encode separate functional regions of the protein described. The graph shows the fold change (Y axis) in RNA expression for each ORF (bars), as determined by RNA-seq analysis.

S. enterica Serotype Typhimurium were thought to be unable to synthesise PQQ (Matsushita *et al.* 1997). There have been no studies examining PQQ in *A. baumannii*, but it is believed that in most bacteria PQQ plays a role in protecting against oxidative stress (Misra *et al.* 2004). Although *E. coli* does not contain a gene encoding PQQ, *E. coli* cells given a recombinant PQQ synthase gene showed higher tolerance to oxidative stress and higher catalase and super-oxide dismutase activities (Misra *et al.* 2004). The genes A1S_1881-1887 within this cluster all encode proteins belonging to the CoA-transferase family; the systematic name of this enzyme class is succinyl-CoA:3-oxoadipate CoA-transferases. These enzymes participate in benzoate degradation via hydroxylation (Cersini *et al.* 1998) and contain a Zn²⁺-binding motif. The availability of Zn²⁺ is therefore crucial to maintaining the function of this enzyme as it has been shown that the deletion of the Zn²⁺-binding motif completely abolishes enzymatic activity (Bilder *et al.* 2006).

The expression of the remaining genes (A1S_1888-1894) within the A1S_1880 to A1S_1894 cluster, were also affected by Zn²⁺ limitation (expression reduced 2- to 8-fold). Bioinformatic analysis of these genes indicated they encoded enzymes involved in the biosynthesis of aromatic amino acids, including 3-dehydroshikimate dehydratase, protocatechuic acid decarboxylase, and catechol 1,2-dioxygenase. These enzymes enable the bacteria to use such aromatic compounds as carbon sources (Weber *et al.* 2012). Mutations in genes coding for the biosynthesis of aromatic amino acids (*aro* mutants) have been shown to reduce the virulence of a number of bacteria including *Salmonella* sp. and *M. tuberculosis* (Parish and Stoker 2002; Sebkova *et al.* 2008). Such *aro* mutants have an inability to produce aromatic metabolites, mainly aromatic amino acids such as phenylalanine, tyrosine, and tryptophan. Since aromatic amino acids are not freely available inside most hosts, *aro* mutants are usually incapable of replication within the host (Sebkova *et al.* 2008). The *aroA* and *aroD* genes in *S. enterica* Serotype Typhimurium have also been inactivated to produce avirulent strains for vaccine trials (Sebkova *et al.* 2008). Whether the homologous genes in *A. baumannii* are essential for the virulence of this bacterium has not been examined to date.

3.3 Conclusions

Zn²⁺ is a trace element which is crucial for a range of metabolic processes within bacterial cells. In this study, Zn²⁺-limited growth media was developed and optimised via treatment with Chelex 100[®] and by the addition of TPEN, Fe²⁺ and Mn²⁺. The treatment of M9 medium with Chelex 100[®] alone did not result in complete removal of Zn²⁺ and the addition of TPEN was required to eliminate the remaining Zn. Phenotypic investigation revealed that Zn²⁺ limitation affected the ability of *A. baumannii* to form a biofilm and susceptibility to β -lactam and aminoglycosides antibiotics.

Initial qRT-PCR experiments revealed an increase in the expression of Zn²⁺-related genes, including *zur* and *znuABC* when cells were grown under Zn²⁺-limited conditions, but there was no effect on the expression of the Fe²⁺-siderophore biosynthesis gene. This indicated that the treatment of the media with Chelex 100[®] and TPEN did not affect the intracellular Fe²⁺ concentration. This was also shown when qRT-PCR was used to measure the expression of *fur* which was not altered.

The global effect of Zn²⁺ limitation on the transcriptome of *A. baumannii* ATCC 17978 was then examined. In total, 60 genes showed significantly (≥ 2 -fold) increased expression and 279 genes significantly reduced expression. The global regulatory gene, *zur*, increased in expression during growth in Zn²⁺-limited medium. As *zur* is autoregulatory, the absence of Zn²⁺ bound to the Zur protein caused subsequent derepression of *zur*, leading to an increase in expression. Other genes controlled by Zur were also derepressed during growth in Zn²⁺-limited medium, including *znuABC*, the *tonB-exbB-exbD* complex (A1S_0452-0454), the TBDR (A1S_2892) and the G3E family GTPase (A1S_3411). Additionally, numerous genes were shown to be significantly differentially expressed in response to Zn²⁺ limitation that did not have a Zur-binding site suggesting that not all expression changes were due to direct regulation by Zur. Zn²⁺ starvation also significantly affected the expression (mostly reduced) of enzymes-containing a Zn²⁺-binding motif.

As seen from the RNA-seq data, the transcriptional responses to growth under Zn²⁺-limited conditions were strikingly pleiotropic. Genes identified as differentially expressed encoded a large range of cellular functions that would

seemingly be unrelated to Zn²⁺ availability. However, a number of genes affected by Zn²⁺ limitation encoded proteins that require Zn²⁺ as a catalytic or structural component. In *A. baumannii* ATCC 17978, Zn²⁺ limitation affected the expression of genes involved in various metabolic processes including carbohydrate storage and lipid metabolism. Future studies should examine if inactivation of selected genes identified in this study affects the virulence capacity of this organism. In the following chapters the effect of inactivation of the L31 ribosomal proteins in *A. baumannii* will be examined in detail.

CHAPTER 4
THE ROLE OF RPME1 AND RPME2
IN *A. BAUMANNII* ATCC 17978
IN Zn^{2+} HOMEOSTASIS AND VIRULENCE

4.1 Introduction

The effect of Zn^{2+} limitation on the phenotype and transcriptomic profile of *A. baumannii* ATCC 17978 has been examined in the previous chapter (Chapter 3) and revealed that Zn^{2+} plays an important role in bacterial growth, in the formation of biofilms and in resistance to antibiotics. Transcriptome analysis of *A. baumannii* grown under Zn^{2+} -limited conditions by RNA-seq also revealed global transcriptional changes. One of the genes identified as highly expressed (400-fold) under Zn^{2+} -limited conditions was the Zur-regulated L31 gene, *rpmE2*. In Section 1.9.1, it was discussed that one strategy utilised by bacteria in response to Zn^{2+} starvation is via a Zn^{2+} -sparing mechanism, which enables the cells to increase the expression of non- Zn^{2+} -requiring proteins to replace essential Zn^{2+} -dependent enzymes and proteins. The Zur-regulated L31 protein has been showed to play a critical role in Zn^{2+} sparing in *B. subtilis* (Akanuma *et al.* 2006; Gabriel and Helmann 2009), *E. coli* (Hensley *et al.* 2012) and *S. coelicolor* (Shin *et al.* 2007). The L31 ribosomal proteins are encoded by two paralogous genes, one contains the Zn^{2+} -binding motif (RpmE1, C^+ form) and the other does not (RpmE2, C^- form) (Panina *et al.* 2003) (see Section 1.9). The expression of the C^- form (RpmE2) is derepressed in Zn^{2+} -limited conditions. Under such conditions, RpmE2 displaces the C^+ form (RpmE1) bound to the 50S ribosomal complex, facilitating the Zn^{2+} ions bound to RpmE1 to be liberated and used by the cell (see Figure 1.5). The ability of the bacteria to alternate between the two forms of L31 effectively increases the availability of Zn^{2+} ions during growth in Zn^{2+} -limited conditions, allowing for Zn^{2+} to be available for use in metabolically critical cell functions (Akanuma *et al.* 2006) (see Section 1.9.2).

The two L31 proteins in *A. baumannii* ATCC 17978 vary significantly in their amino acid sequence in that RpmE1 (A1S_3424) contains the CXXC and CXC Zn^{2+} -binding motifs while these motifs are absent in RpmE2 (A1S_0391) (Figure 4.1). A previous study on an *A. baumannii* *zur* mutant revealed that the expression of *rpmE2* increased 350-fold when *zur* was inactivated (Mortensen *et al.* 2014). However, the exact role that the L31 paralogs RpmE2 and RpmE1 play in

```

RpmE1      MRADIHPKYEKLVATCSCGNV-----IETRS---ALG--KE   31
RpmE2      MRKDIHPAYQQVLEFHD TNADVFLIGSTIQTKQTKEYQGQVYP  43
          **  ****  *:::  :  ::*          *:*:.   *

RpmE1      TIYLDVCSACHPFYTGKQKNVDTGGRIDKFKQRFAGMSRSIKR  74
RpmE2      YVTLDISSASHPFYTGQEVQRASNEGRVASFNKRFRARFNKRS-- 84
          :  **:.**.******:  :...  **:  .*::***  :.*.

```

Figure 4.1: Amino acid sequence alignment of RpmE1 and RpmE2 from *A. baumannii* ATCC 17978

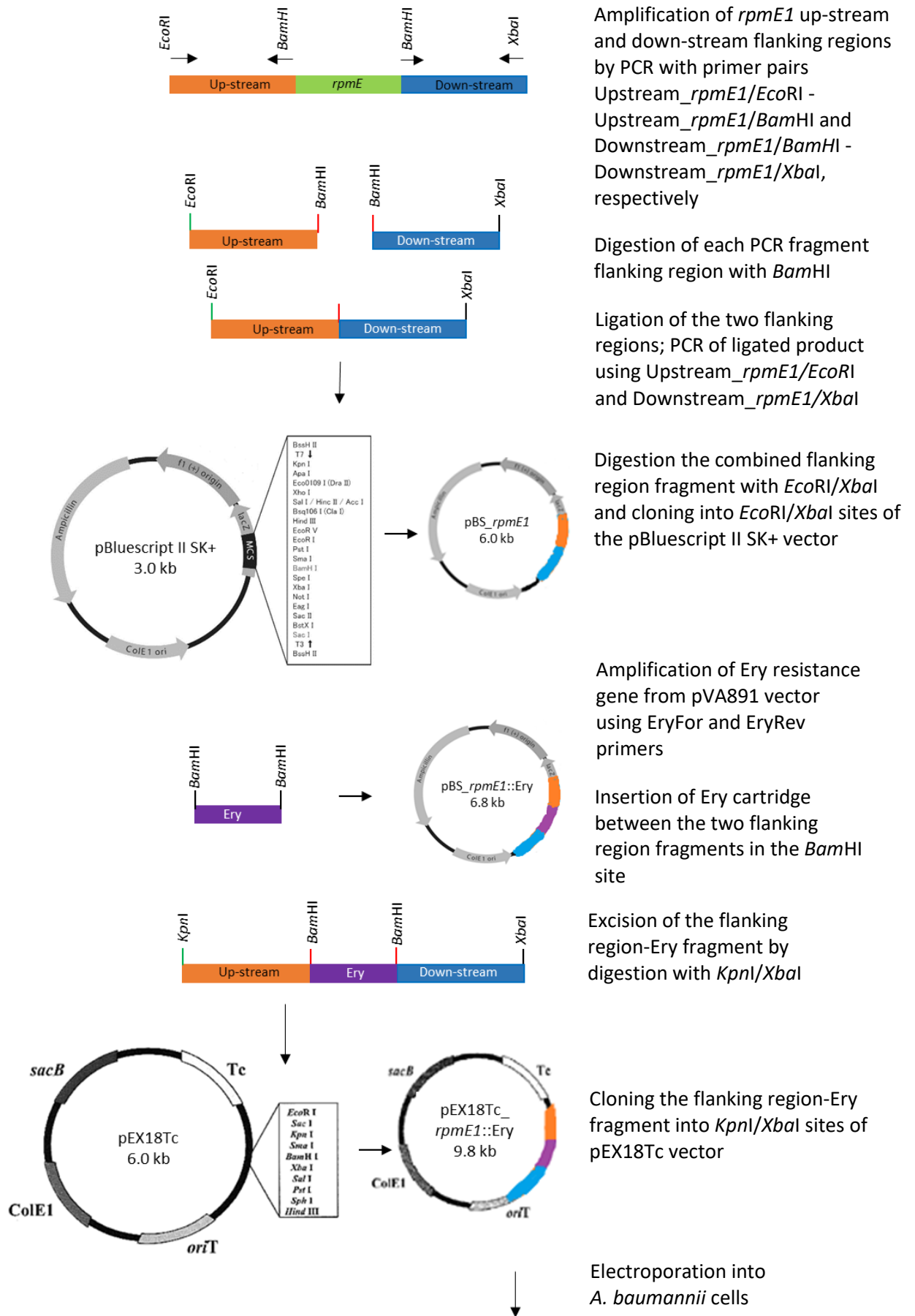
The alignment was performed using Clustal Omega (<http://www.ebi.ac.uk/Tools/msa/clustalo/>). Stars indicate identical amino acids; a colon indicates highly similar amino acids and a period indicates similar amino acids. The two motifs (CXC and CXXC) in RpmE1 associated with Zn²⁺ binding are highlighted in green. RpmE1 (A1S_2423) and RpmE2 (A1S_0391) were obtained from GenBank (accession number ABO12841.1 and ABO10850.1, respectively).

A. baumannii ATCC 17978 Zn²⁺ homeostasis has not been fully elucidated. Thus, to comprehensively assess the role of the L31 paralogous proteins in Zn²⁺ homeostasis and to examine the effect that their inactivation has on the phenotype of *A. baumannii*, *rpmE1* and *rpmE2* deletion mutants were constructed. The effect of each mutation on the levels of intracellular Zn²⁺, and on the ability of *A. baumannii* to grow under Zn²⁺-limited conditions was investigated. Further, to examine the effect of each mutation on selected phenotypes, mutants were examined for their motility characteristics, the ability to form a biofilm, the capacity to adhere to eukaryotic cells and the ability to survive oxidative stress.

4.2 Results and Discussion

4.2.1 Construction of *A. baumannii* ATCC 17978 *rpmE1* and *rpmE2* mutants and complemented derivatives

Construction of a $\Delta rpmE1$ *A. baumannii* ATCC 17978 mutant. Construction of *A. baumannii* ATCC 17978 mutants was undertaken by gene replacement via homologous recombination (Section 2.7.7). Plasmid pVA891 containing an Ery resistance gene (Table 2.4) was chosen as the source of the resistance cartridge. Primers were designed to amplify the Ery cartridge with the addition of *Bam*HI restriction endonuclease sites (Table 2.4). The outline of the mutant construction is shown in Figure 4.2. The up-stream and down-stream regions (approximately 1.5 Kb each) of the target gene, A1S_2423 (*rpmE1*), were amplified from genomic DNA of *A. baumannii* ATCC 17978 (Section 2.5.4) using primer pairs Upstream_*rpmE1/Eco*RI + Upstream_*rpmE1/Bam*HI and Downstream_*rpmE1/Bam*HI + Downstream_*rpmE1/Xba*I, respectively (Table 2.4). The PCR products from this first step were digested with *Bam*HI restriction endonuclease and equivalent amounts of each product were ligated ON at 4 °C (Section 2.7.1). To generate a single fragment containing the two flanking regions, PCR was conducted using the ligation product as the template with the primers Upstream_*rpmE1/Eco*RI and Downstream_*rpmE1/Xba*I (Table 2.4). Amplification of the two ligated regions was confirmed by gel electrophoresis (size of the two flanking regions should be 3 Kb).



Amplification of *rpmE1* up-stream and down-stream flanking regions by PCR with primer pairs Upstream_ *rpmE1*/*EcoRI* - Upstream_ *rpmE1*/*BamHI* and Downstream_ *rpmE1*/*BamHI* - Downstream_ *rpmE1*/*XbaI*, respectively

Digestion of each PCR fragment flanking region with *BamHI*

Ligation of the two flanking regions; PCR of ligated product using Upstream_ *rpmE1*/*EcoRI* and Downstream_ *rpmE1*/*XbaI*

Digestion the combined flanking region fragment with *EcoRI/XbaI* and cloning into *EcoRI/XbaI* sites of the pBluescript II SK+ vector

Amplification of Ery resistance gene from pVA891 vector using EryFor and EryRev primers

Insertion of Ery cartridge between the two flanking region fragments in the *BamHI* site

Excision of the flanking region-Ery fragment by digestion with *KpnI/XbaI*

Cloning the flanking region-Ery fragment into *KpnI/XbaI* sites of pEX18Tc vector

Electroporation into *A. baumannii* cells

Continued on the next page

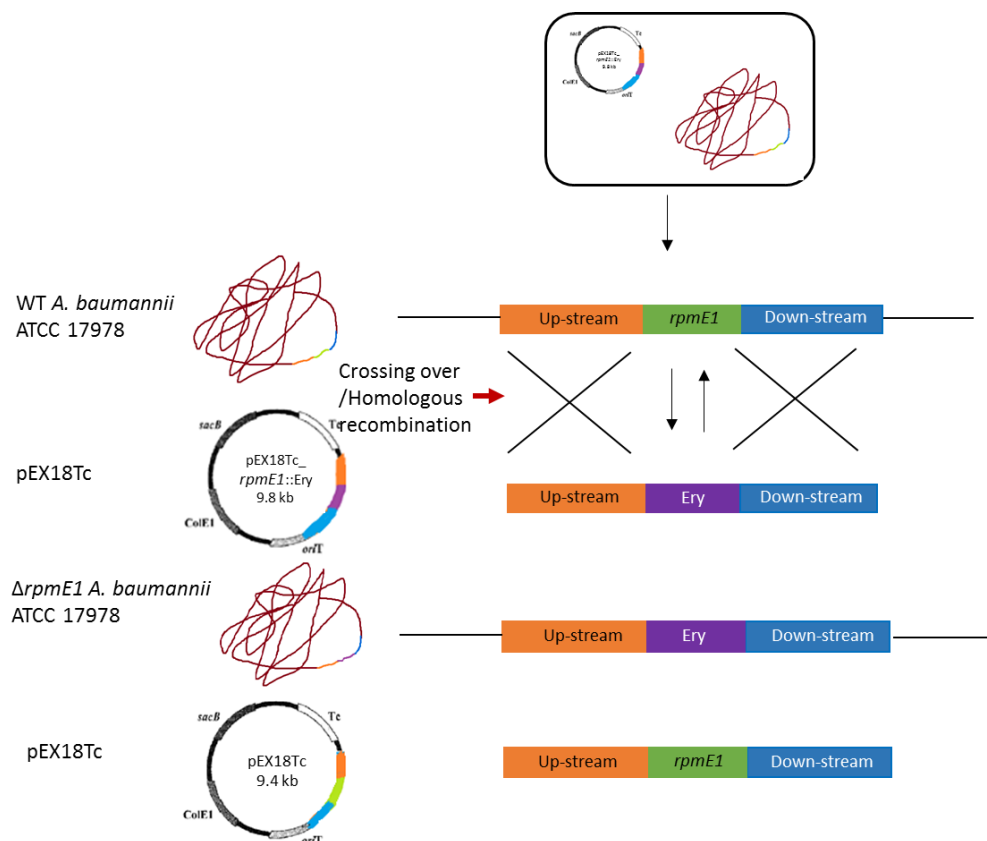


Figure 4.2: Strategy via homologous recombination for generation of the *rpmE* mutants

This schematic shows the construction of the $\Delta rpmE1$ mutant as an example of how the $\Delta rpmE1$ and $\Delta rpmE2$ derivatives were constructed, via gene replacement using an Ery cartridge. DNA fragments containing the down- (blue) and up-stream (orange) sequences were obtained by PCR using *A. baumannii* ATCC 17978 DNA as a template. To facilitate cloning, restriction sites were incorporated into the primers used to generate each PCR fragment. Each fragment was digested with the appropriate enzyme, ligated, and the ligation PCR-amplified to generate two flanking region fragments. The combined flanking region fragment was cloned into the pBlueScript II SK+. This was then followed by cloning the Ery cartridge (purple) via *Bam*HI sites. The entire region was cloned into the suicide vector pEX18Tc and introduced into *A. baumannii* ATCC 17978 via electroporation. Replacement of the gene was achieved via homologous recombination between the *A. baumannii* sequence on the plasmid and the *A. baumannii* chromosome, resulting in deletion of *rpmE1* (green) and incorporation of the Ery cartridge. A similar procedure was used to obtain the *A. baumannii* $\Delta rpmE2$ derivative.

DNA sequencing of the PCR fragment containing the two flanking regions was undertaken to ensure that there was no error during amplification (Section 2.5.7). Sequence analysis by Sequencher™ 4.1.4 program (Gene Code Corp.) revealed that the fragment sequence was 100% homologous to the reference sequence of *A. baumannii* ATCC 17978 in the NCBI database (GenBank accession number: ABO12841.1).

The *rpmE1* flanking regions generated via PCR were digested with *EcoRI* and *XbaI* restriction endonucleases, cloned into pBluescript II SK+ and subsequently transformed into *E. coli* DH5 α (Section 2.7.4). Colonies were screened by PCR for insertion of this PCR product to produce pBS_*rpmE1* (6.0 kb) (Table 2.3) and DNA was isolated. The next step was the insertion of an Ery cartridge between these two flanking regions. The Ery cartridge was amplified using primers EryFor and EryRev (Table 2.4) using pVA819 DNA (Invitrogen) as the template (Section 2.7.8); the products were purified and digested with *BamHI* (Section 2.7.1). The Ery cartridge was ligated into *BamHI* digested pBS_*rpmE1* and transformed into *E. coli* DH5 α cells (Section 2.7.5). Transformants containing the flanking regions with the Ery cartridge inserted were screened by plating onto LB agar supplemented with Ery²⁵ and further by colony PCR using M13 primers (Section 2.5.4, Table 2.4). The Ery-resistant colonies containing pBS_*rpmE1*::Ery (6.8 kb) (Table 2.3) were isolated and then plated onto LB agar supplemented with Ery²⁵.

After successful generation of the pBS_*rpmE1*::Ery plasmid (Table 2.3), the fragment was excised with *KpnI* and *XbaI* and cloned into the pEX18Tc suicide vector which was digested with the same enzymes. The ligation mixture was transformed into *E. coli* DH5 α cells (Section 2.7.5) and plated onto LB agar supplemented with Ery¹⁰ and Tet¹². Colonies were screened by PCR using pEXTc18 primers (Table 2.4) and those containing pEX18Tc incorporating the Ery cartridge inserted between the two flanking regions (pEX18Tc_*rpmE1*::Ery, 9.8 kb) (Table 2.3) were isolated. The pEX18Tc_*rpmE1*::Ery plasmid was then introduced into *A. baumannii* ATCC 17978 via electroporation (Section 2.7.6). To identify where the double crossover event had taken place, the transformants were grown on M9 agar containing 5% sucrose with Ery¹⁰. To aid in selection against the integrated pEX18TC plasmid, which carries the *sacB* suicide gene from *Bacillus subtilis*, bacterial cells

were grown in the presence of 5% sucrose to provide a direct selection for loss of the plasmid. The loss of the mutagenesis plasmid was confirmed by checking for growth of each transformant on a Tet¹² LB plate (Section 2.7.7). Since pEX18Tc vector confers Tet resistance (see Table 2.3), a lack of growth on Tet¹² LB confirmed the loss of the plasmid from *A. baumannii* ATCC 17978.

To confirm the double homologous recombination event had occurred, and the Ery cartridge was in the correct location within the *A. baumannii* ATCC 17978 chromosome, locus specific primers were designed 50 bp external to the flanking regions used for the homologous recombination (Table 2.4). PCR was undertaken using the primers EryFor and CheckDown_*rpmE1*/Rev and EryRev and CheckUp_*rpmE1*/For (Table 2.4). Figure 4.3 shows the combination of oligonucleotides used for PCR confirmation of the $\Delta rpmE1$ construct and the expected size of the PCR product. Agarose gel electrophoresis of PCR products confirmed the presence of the Ery cartridge in the correct position within the *A. baumannii* chromosome (Figure 4.4).

Construction of a *rpmE2* *A. baumannii* ATCC 17978 mutant. The same procedures used for construction of the $\Delta rpmE1$ mutant were used for the construction of the $\Delta rpmE2$ *A. baumannii* ATCC 17978 strain. For the construction of the mutagenesis cassettes of the target gene A1S_0391 (*rpmE2*), the up-stream and down-stream regions (approx. 1.5 kb each) were PCR amplified from genomic DNA isolated from *A. baumannii* ATCC 17978 using primer pairs Upstream_*rpmE2*/*EcoRI* + Upstream_*rpmE2*/*BamHI* and Downstream_*rpmE2*/*BamHI* + Upstream_*rpmE2*/*XbaI* (Table 2.4), respectively. The reference sequence for *rpmE2* was obtained from the NCBI database (Gen accession number: ABO10850.1). The confirmation of the correct position of the Ery cartridge in the mutant strain was confirmed by PCR using primers EryFor + CheckDown_*rpmE2*/Rev and EryRev + CheckUp_*rpmE2*/For (Table 2.4) and visualised by gel electrophoresis (Figure 4.5).

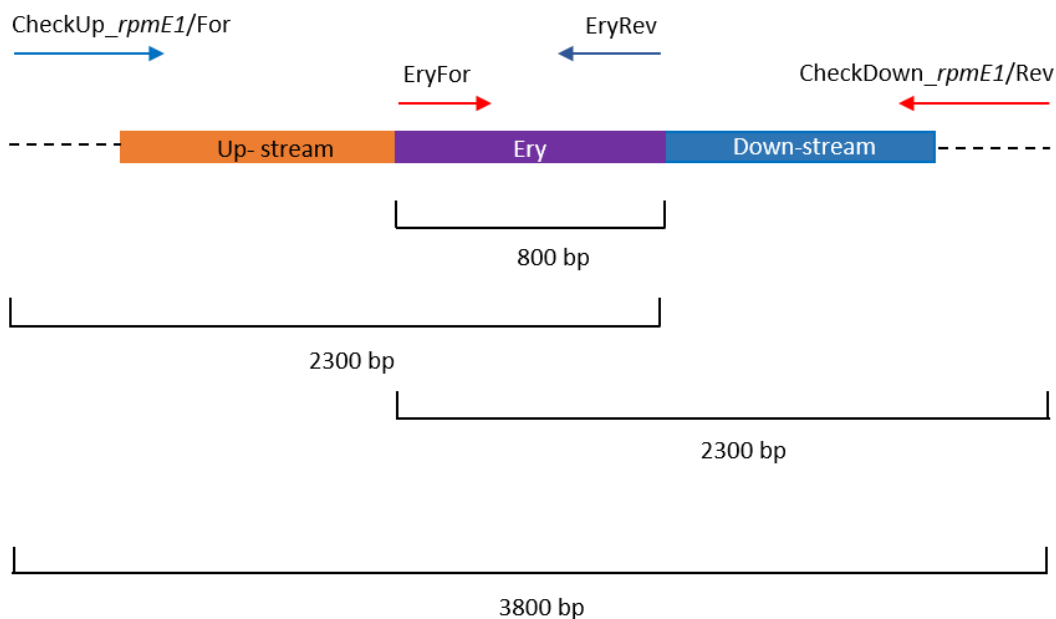


Figure 4.3: Schematic showing the position of oligonucleotides used for PCR confirmation of the *rpmE1* mutation

To confirm successful integration of the Ery cartridge and deletion of *rpmE1* in each mutant PCR analysis was performed. PCR reactions amplifying the region spanning the whole region were conducted using oligonucleotides (CheckUp_*rpmE1*/For and CheckDown_*rpmE1*/Rev) external to the regions used for the mutagenesis construct (orange and blue regions). Successful integration of the Ery cartridge was confirmed by a PCR using the CheckUp_*rpmE1*/For and EryRev primers (blue arrows), as well as a PCR using the EryRev and CheckDown_*rpmE1*/Rev (red arrows). The entire region was also sequenced to ensure sequence fidelity of the region flanking the Ery cassette.

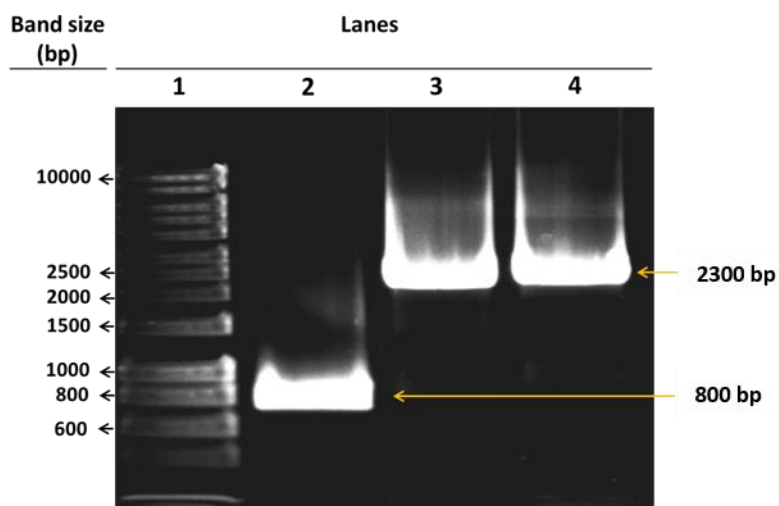


Figure 4.4: PCR products generated to confirm successful deletion of *rpmE1* and insertion of the Ery cartridge in *A. baumannii* ATCC 17978

An 1% agarose gel was used to confirm the size of generated PCR products. Lane 1, HyperLadder™ I molecular weight markers (Bio-Line, Australia); lane 2, PCR product obtained using EryFor/EryRev primers that shows a band of the correct size (800 bp) for the Ery cartridge; lane 3, PCR product obtained using CheckUp_*rpmE1*/For and EryRev primers showing a band of the correct size (2.3 kb) for the up-stream flanking region plus the Ery cartridge; lane 4, PCR product obtained using CheckDown_*rpmE1*/Rev and EryFor primers and that shows a band of the correct size (2.3 kb) for the down-stream flanking region plus the Ery cartridge. Arrows indicate the relative position and size of PCR products.

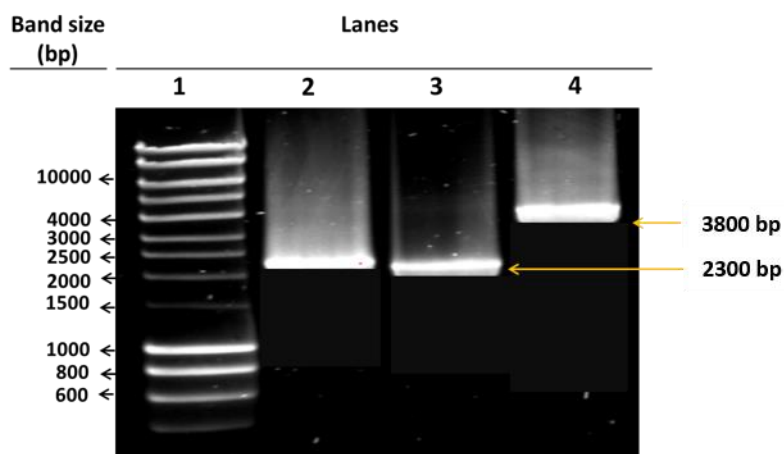


Figure 4.5: PCR products generated to confirm successful deletion of *rpmE2* and insertion of Ery cartridge in *A. baumannii* ATCC 17978

An 1% agarose gel was used to confirm the size of generated PCR products. Lane 1, HyperLadder™ I molecular weight markers (Bio-Line, Australia); lane 2, PCR product obtained using CheckUp_*rpmE2*/For and EryRev primers that show a band of the correct size (2.3 kb) for the up-stream flanking region plus Ery cartridge; lane 3, PCR product obtained using CheckDown_*rpmE2*/Rev and EryFor primers showing a band of the correct size (2.3 kb) for the down-stream flanking region plus Ery cartridge; lane 4 PCR product obtained using CheckUp_*rpmE2*/For and CheckDown_*rpmE2*/Rev that show a band of the correct size (2.3 kb) for the up-stream and down-stream flanking region plus the Ery cartridge. Arrows indicate the relative position and size of PCR products.

Construction of complemented derivatives of the $\Delta rpmE$ *A. baumannii* ATCC 17978 mutants. For complementation studies, WT copies of *rpmE1* and *rpmE2* were amplified from ATCC 17978 DNA using primers pairs *rpmE1_BamHI* and *rpmE2_BamHI* (Table 2.4), respectively, and separately cloned into the shuttle vector pWH1266 using *BamHI* restriction sites and transformed into *E. coli* DH5 α (Section 2.7.8). Transformed cells were plated onto LB agar containing Amp¹⁰⁰ and incubated ON at 37 °C. Colonies were isolated and plasmid DNA was extracted (Section 2.5.1) for screening. Plasmid DNA was digested with *BamHI* and the digested product (Section 2.7.1) examined by agarose gel electrophoresis to confirm successful cloning of the region. The resulting pWH*rpmE1* or pWH*rpmE2* plasmids were then introduced into the appropriate *A. baumannii* mutant strain via electroporation (Section 2.7.7). *A. baumannii* transformants containing the complementing plasmid ($\Delta rpmE1$:pWH*rpmE1* or $\Delta rpmE2$:pWH*rpmE2*) were selected on Ery¹⁰ and Amp²⁰⁰ agar plates and later confirmed by PCR (Section 2.5.4).

4.2.2 Growth of *A. baumannii* $\Delta rpmE1$ and $\Delta rpmE2$ mutants in LB broth

To determine the growth rate of each mutant strain, growth in LB medium of the WT ATCC 17978 and each $\Delta rpmE1$ and $\Delta rpmE2$ mutant was measured. In brief, 200 μ l of ON culture was used to inoculate 10 ml of fresh LB medium and the culture incubated with shaking 200 rpm at 37 °C (Section 2.2). At standard time points, 1 ml was removed from each culture and the OD₆₀₀ determined using a spectrophotometer. The results revealed that the $\Delta rpmE1$ and $\Delta rpmE2$ strains both exhibited a delay in entering the exponential phase of growth compared to the WT strain (Figure 4.6). However, the final OD₆₀₀ of all the cultures was similar indicating that the inactivation of *rpmE1* or *rpmE2* had only a minor effect on growth in LB medium.

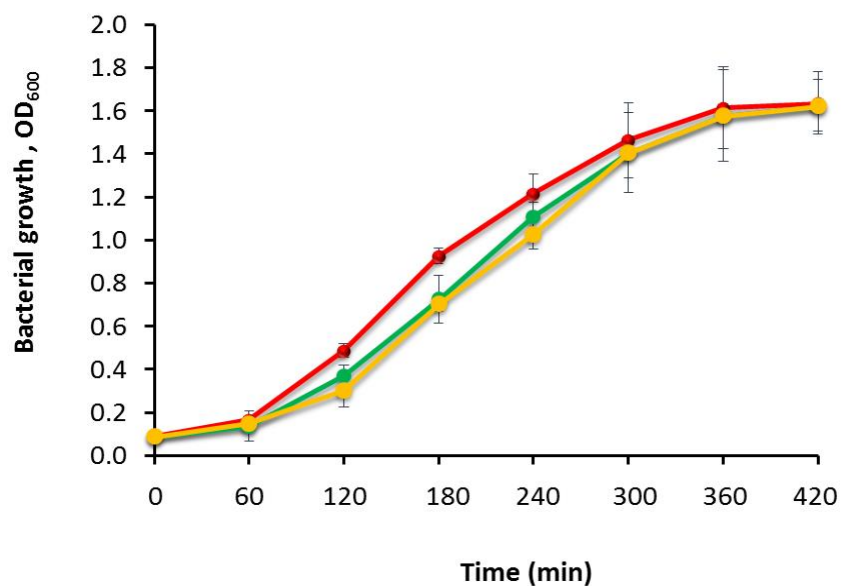


Figure 4.6: The effect of *rpmE1* and *rpmE2* inactivation on *A. baumannii* growth in LB medium

Growth of *A. baumannii* ATCC 17978 WT (red), $\Delta rpmE1$ (green) and $\Delta rpmE2$ (yellow) strains in LB medium at 37 °C. Absorbance was measured every hr at OD₆₀₀ for 7 hr; the data represent the average of three separate experiments. A clear lag in entering the exponential phase of growth is observed for both the $\Delta rpmE1$ and the $\Delta rpmE2$ cells after which they display a growth rate similar to the WT. Error bars indicate the standard deviation over the three experiments.

4.2.3 Growth of *A. baumannii* $\Delta rpmE1$ or $\Delta rpmE2$ mutants under Zn^{2+} -limited conditions

The effect of inactivation of *rpmE1* or *rpmE2* on cell growth was investigated in both Zn^{2+} -replete and Zn^{2+} -limited media as described in Section 2.3.1. Both mutants displayed a lag in both media compared to the ATCC 17978 WT strain grown in the same conditions. In the Zn^{2+} -limited medium, cultures of $\Delta rpmE1$ or $\Delta rpmE2$ did not reach the same OD as the WT ATCC 17978 even after 12 hr of growth (Figures 4.7 and 4.8). This reduction in growth of the $\Delta rpmE$ mutants has been observed previously; a study undertaken in *B. subtilis* revealed that the deletion of *rpmE1* reduced bacterial growth after 6 hr by approximately 10% (Akanuma *et al.* 2006). However, mutation of *ytiA* encoding the C⁻ form of the L31 protein in *B. subtilis* did not alter the growth of the bacteria in CSM medium which closely resembles M9 medium (Akanuma *et al.* 2006) but is not strictly a Zn^{2+} -limited medium and therefore any growth defect may have been masked. Our study in *A. baumannii* suggests that, even though inactivation of *rpmE1* or *rpmE2* only slightly affected the bacterial growth in Zn^{2+} -limited medium, both proteins are required to achieve WT levels of growth.

The growth defect observed in both mutants indicates that production of a single RpmE protein (either RpmE1 or RpmE2) in *A. baumannii* cannot fully compensate for the loss of the other. This has been also observed in *S. coelicolor*, however the lag in growth occurred only after $\Delta rpmE1$ had reached mid to late log phase (Owen *et al.* 2007). In this study, the *A. baumannii rpmE1* and *rpmE2* mutants displayed a lag at the start of the incubation whereas in the *S. coelicolor* study the lag was during the log phase of growth indicating there may have been trace amounts of Zn^{2+} available.

4.2.4 The effect of *rpmE1* and *rpmE2* inactivation on the expression of genes involved in Zn^{2+} homeostasis

To assess whether the inactivation of *rpmE1* or *rpmE2* affects the expression of *rpmE2* or *rpmE1*, respectively, as well as known Zn^{2+} -dependent genes involved in Zn^{2+} homeostasis (*zur* and *znuA*), qRT-PCR analysis was performed using primers

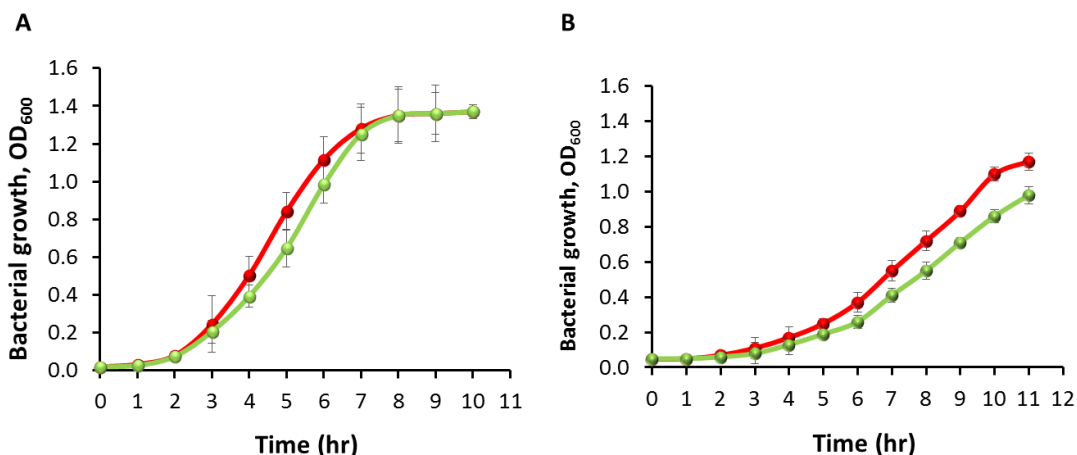


Figure 4.7: The effect of *rpmE1* inactivation on growth of *A. baumannii* in Zn²⁺-replete and Zn²⁺-limited media

Growth of the *A. baumannii* ATCC 17978 WT (red) and $\Delta rpmE1$ strains (green) were assessed under (A) Zn²⁺-replete and (B) Zn²⁺-limited conditions. Absorbance was measured every hr at OD₆₀₀ for 11 hr; the data represent the average of three separate experiments. Error bars show the standard deviation. (A) During growth in Zn²⁺-replete conditions a difference in the growth rate of the $\Delta rpmE1$ mutant can be observed however the final OD was similar to that of the WT culture. (B) During growth in Zn²⁺-limited conditions, a difference in the growth rate and the final OD of the $\Delta rpmE1$ culture compared to the WT culture can be seen. Comparisons of the growth rate for each strain grown in Zn²⁺-replete and Zn²⁺-limited media revealed that both the WT and $\Delta rpmE1$ strains had a reduction in growth when grown in Zn²⁺-limited medium compared to Zn²⁺-replete medium but the reduction in growth rate was greater in the mutant strain.

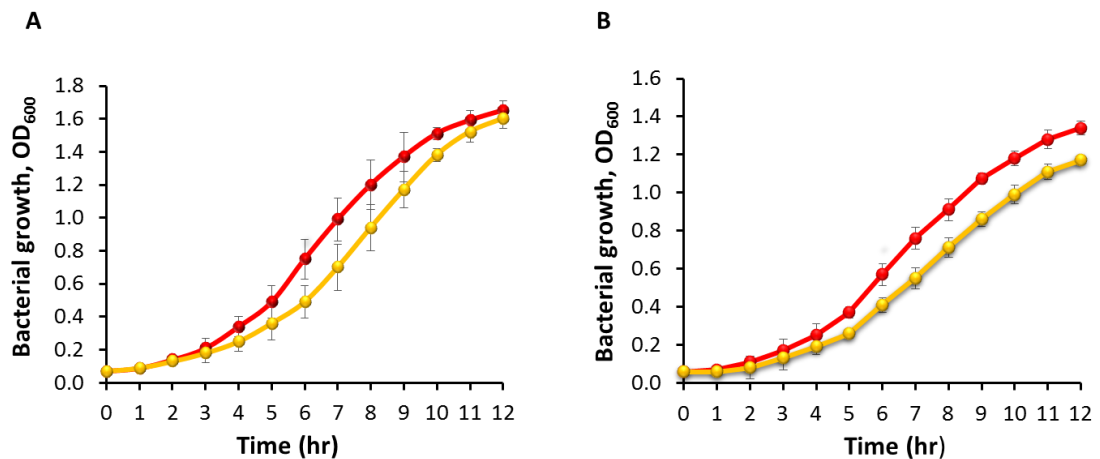


Figure 4.8: The effect of *rpmE2* inactivation on growth of *A. baumannii* in Zn²⁺-replete and Zn²⁺-limited media

Growth of the *A. baumannii* ATCC 17978 WT (red) and $\Delta rpmE2$ strains (yellow) were assessed under (A) Zn²⁺-replete and (B) Zn²⁺-limited conditions. Absorbance was measured every hr at OD₆₀₀ for 11 hr; the data represent the average of three separate experiments. Error bars show the standard deviation. (A) During growth in Zn²⁺-replete conditions a difference in the growth rate of the $\Delta rpmE2$ mutant can be observed, however the final OD was similar to that of the WT culture. (B) During growth in Zn²⁺-limited conditions, a difference in the growth rate and the final OD of the $\Delta rpmE2$ culture compared to the WT culture can be seen. Comparison of the growth rate between Zn²⁺-replete and Zn²⁺-limited conditions revealed that both of the strains showed a reduction in the growth rate in Zn²⁺-limited medium compared to Zn²⁺-replete medium, but the reduction in growth rate was greater in the mutant strain.

designed to amplify regions within each gene (Table 2.4). RNA was extracted (see Section 2.6.1) from the WT *A. baumannii* ATCC 17978, $\Delta rpmE1$ and $\Delta rpmE2$ strains grown in Zn^{2+} -limited or Zn^{2+} -replete liquid media for approximately 4 hr at 37 °C with shaking. Analysis of *A. baumannii* ATCC 17978 grown in Zn^{2+} -limited conditions revealed that there was an increase in transcription of various genes, including *zur*, *znuABC*, *tonB-exbB-exbD*, *rpmE2*, a TBDR gene (A1S_2892) and a gene encoding a GTPase (G3E family) (A1S_3411) (see Table 3.3) indicating that these genes were Zn^{2+} regulated. On the other hand, the expression of *rpmE1* was down-regulated by 3.5-fold (Table 3.3). It previously has been suggested that RpmE1 is continually produced under Zn^{2+} -limited growth conditions (Akanuma *et al.* 2006), however production is lower. In contrast, the expression of the Zur-regulated *rpmE2* increased by more than 400-fold during growth in Zn^{2+} -limited conditions (Table 3.3), clearly demonstrating that the expression of this gene is dependent on Zn^{2+} availability.

qRT-PCR was undertaken of the $\Delta rpmE1$ and $\Delta rpmE2$ strains and expression levels of various genes were compared to the WT ATCC 17978 strain grown in the same condition. In the $\Delta rpmE1$ strain, expression of *zur* was down-regulated when bacteria were grown in Zn^{2+} -replete or Zn^{2+} -limited conditions (Table 4.1). Correlating with the decreased expression of *zur* in $\Delta rpmE1$, the expression of *rpmE2* and *znuA* was up-regulated by more than 900- and 6.7-fold, respectively (Table 4.1). Meanwhile, the expression of these genes in Zn^{2+} -limited conditions was up-regulated by 1.6-fold (*znuA*) and down-regulated by 24.8-fold (*zur*). The expression of *rpmE2* (0.9-fold) in $\Delta rpmE1$ grown in Zn^{2+} -limited medium was comparable to the levels seen in the WT strain (Section 3.2.4). Since the loss of *rpmE1* caused a reduction in *zur* transcription, the Zur-regulated genes, *rpmE2* and *znuA*, were derepressed and therefore their expression increased regardless of Zn^{2+} -availability. This suggests that the loss of *rpmE1* leads to the bacterial cells mimicking the cellular response as if in Zn^{2+} -starvation conditions.

On the other hand, transcript analysis of *rpmE1*, *zur* and *znuA* expression in the $\Delta rpmE2$ strain grown in Zn^{2+} -replete conditions revealed that there was an up-regulation of *rpmE1* (2.2-fold), a small increase in the expression of *znuA* (1.6-fold), and no significant change in *zur* expression (0.8-fold) (Table 4.1). Meanwhile the

Table 4.1: Expression of zinc-associated genes in the $\Delta rpmE1$ and $\Delta rpmE2$ ATCC 17978 strains grown in Zn^{2+} -replete and Zn^{2+} -limited conditions determined by qRT-PCR

| Gene | Zn-replete conditions | | Gene | Zn-limited conditions | |
|--------------|--------------------------|----------------|--------------|--------------------------|----------------|
| | $\Delta rpmE1$ | $\Delta rpmE2$ | | $\Delta rpmE1$ | $\Delta rpmE2$ |
| | Fold change ^a | | | Fold change ^b | |
| <i>rpmE1</i> | NA ^c | 2.2 | <i>rpmE1</i> | NA | 3.4 |
| <i>rpmE2</i> | 900 | NA | <i>rpmE2</i> | 0.9 | NA |
| <i>zur</i> | -12.9 ^d | 0.8 | <i>zur</i> | -24.8 ^d | 1.1 |
| <i>znuA</i> | 6.7 | 1.6 | <i>znuA</i> | 1.6 | 2.3 |

^a. The fold change of the expression of the genes in the mutant strains relative to the expression in the WT ATCC 17978 strain when grown in zinc-replete medium.

^b. The fold change of the expression of the genes in the mutant strains relative to the expression in the WT ATCC 17978 strain when grown in zinc-limited medium.

^c. NA = The expression was very low and cannot be assessed.

^d. Negative value indicates that gene expression was down-regulated.

expression of these genes in Zn^{2+} -limited conditions was increased by 3.4-, 1.1-, and 2.3-fold for *rpmE1*, *zur* and *znuA*, respectively (Table 4.1). The increase in expression compared to WT in the same condition may indicate that the loss of *rpmE2* influences Zn^{2+} homeostasis even when sufficient Zn^{2+} is present. The increase of expression of *rpmE1* (3.4-fold) in Zn^{2+} -limited conditions may indicate an attempt by the mutant to compensate for the loss of a functional RpmE2 protein.

4.2.5 The role of *rpmE1* and *rpmE2* in intracellular Zn^{2+} levels in *A. baumannii* ATCC 17978

To examine if the deletion of *rpmE1* or *rpmE2* affects the levels of intracellular Zn^{2+} , the concentration of this cation and others were measured using ICP-MS (Section 2.4). The measurement revealed that although there is a slight decrease in Zn^{2+} in the $\Delta rpmE1$ and $\Delta rpmE2$ strains compared to the WT ATCC 17978 when grown in Zn^{2+} -replete conditions, this is not statistically significant (Figure 4.9). This result indicates that during growth in Zn^{2+} -replete conditions, the loss of either *rpmE1* or *rpmE2* does not lead to a significant reduction in intracellular Zn^{2+} , as cells were able to obtain Zn^{2+} from the environment.

On the other hand, the intracellular Zn^{2+} levels within the $\Delta rpmE1$ and $\Delta rpmE2$ strains grown in Zn^{2+} -limited conditions were reduced by approximately 25% compared to the WT ATCC 17978 strain (Figure 4.9). The lower Zn^{2+} level in $\Delta rpmE1$ can be explained by the loss of Zn^{2+} storage via Zn^{2+} ions normally bound to the RpmE1 ribosomal protein. In *B. subtilis* the intracellular Zn^{2+} levels in a $\Delta rpmE1$ were also shown to be lower than levels in the WT strain; it was demonstrated that the RpmE1 protein contained one Zn^{2+} ion per protein molecule (Nanamiya *et al.* 2004). An analogous result was seen when comparing the WT strain to the *A. baumannii* $\Delta rpmE2$. This result is similar to the intracellular Zn^{2+} levels observed when the L31 gene, *ykgM*, was inactivated in *E. coli* (Lim *et al.* 2011). It has also been demonstrated in *B. subtilis* that during Zn^{2+} shortage, *rpmE2* is derepressed by *zur* and the RpmE2 protein preferentially binds to the ribosome, displacing RpmE1 and allowing the freed Zn^{2+} to be recycled within the cell (Akanuma *et al.* 2006).

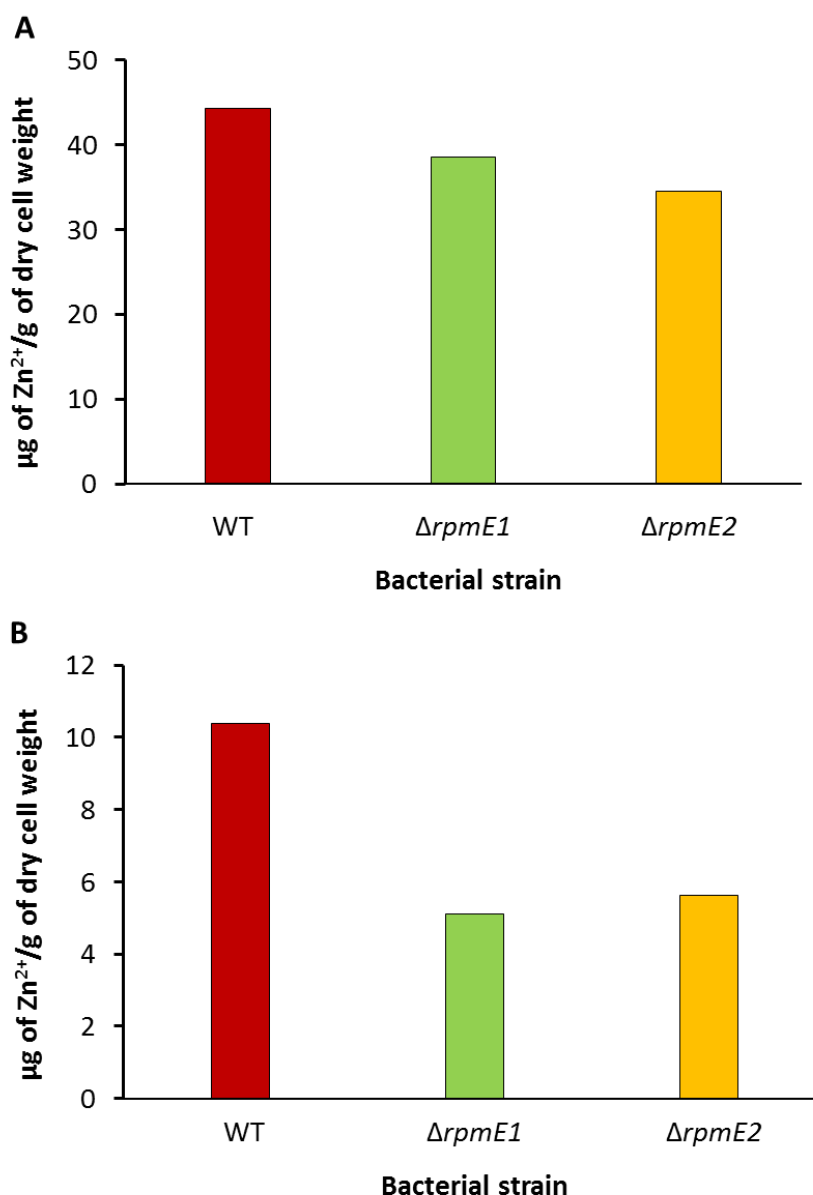


Figure 4.9: Level of intracellular Zn²⁺ in ATCC 17978, $\Delta rpmE1$ and $\Delta rpmE2$ cells grown in Zn²⁺-replete and Zn²⁺-limited conditions

Intracellular levels of metal ions (μg/g of dry cell weight) in cells grown in Zn²⁺-replete and in Zn²⁺-limited conditions. The levels of intracellular Zn²⁺ in the three strains grown in (A) Zn²⁺-replete conditions and (B) Zn²⁺-limited conditions are presented as μg/g of dry cell weight. The level of Zn²⁺ in $\Delta rpmE1$ and $\Delta rpmE2$ cells was significantly different to that in the WT ATCC 17978 cells. The data represent two independent experiments.

Based on this knowledge, the lower levels of intracellular Zn^{2+} present in the $\Delta rpmE2$ strain may be due to a disturbance of the Zn^{2+} recycling process, as the Zn^{2+} bound to RmpE1 cannot be utilised unless the ribosome complex is degraded. Over time this would lead to a reduction in Zn^{2+} levels within the cells.

The levels of other metal ions, such as Mn^{2+} , Fe^{2+} and Mg^{2+} were also measured using ICP-MS. The Mn^{2+} levels were significantly higher in $\Delta rpmE1$ and $\Delta rpmE2$ strains when grown in Zn^{2+} -limited conditions compared to Zn^{2+} -replete conditions (Figure 4.10). This observed increase may indicate that there is an interplay between Zn^{2+} and Mn^{2+} uptake, and in Zn^{2+} -limited conditions the mutants increase Mn^{2+} acquisition. It has been previously shown in *S. pneumonia* that the addition of Zn^{2+} to the medium reduced the total concentration of intracellular Mn^{2+} but there was no decrease in levels of other metal ions cells (Jacobsen *et al.* 2011). In contrast, this study found the levels of Fe^{2+} and Mg^{2+} ions remained essentially the same in both conditions across all three strains indicating that the intracellular levels of these ions are unaffected by the presence or absence of Zn^{2+} (Figure 4.10).

4.2.6 Impact of the inactivation of *rpmE1* or *rpmE2* on the virulence characteristics of *A. baumannii* ATCC 17978

The above experiments revealed that deletion of *rpmE1* or *rpmE2* had various effects on *A. baumannii* ATCC 17978, including affecting growth rates, the levels of intracellular Zn^{2+} and the expression of various genes. Studies in other bacteria have shown that changes in Zn^{2+} homeostasis also affect a range of bacterial virulence characteristics. To investigate the impact of the inactivation of *rpmE1* and *rpmE2* in *A. baumannii* ATCC 17978 on virulence, the constructed mutants were examined using a number of phenotypic assays to assess antibiotic sensitivity, biofilm formation, motility, the ability to adhere to eukaryotic cells and survival under oxidative stress.

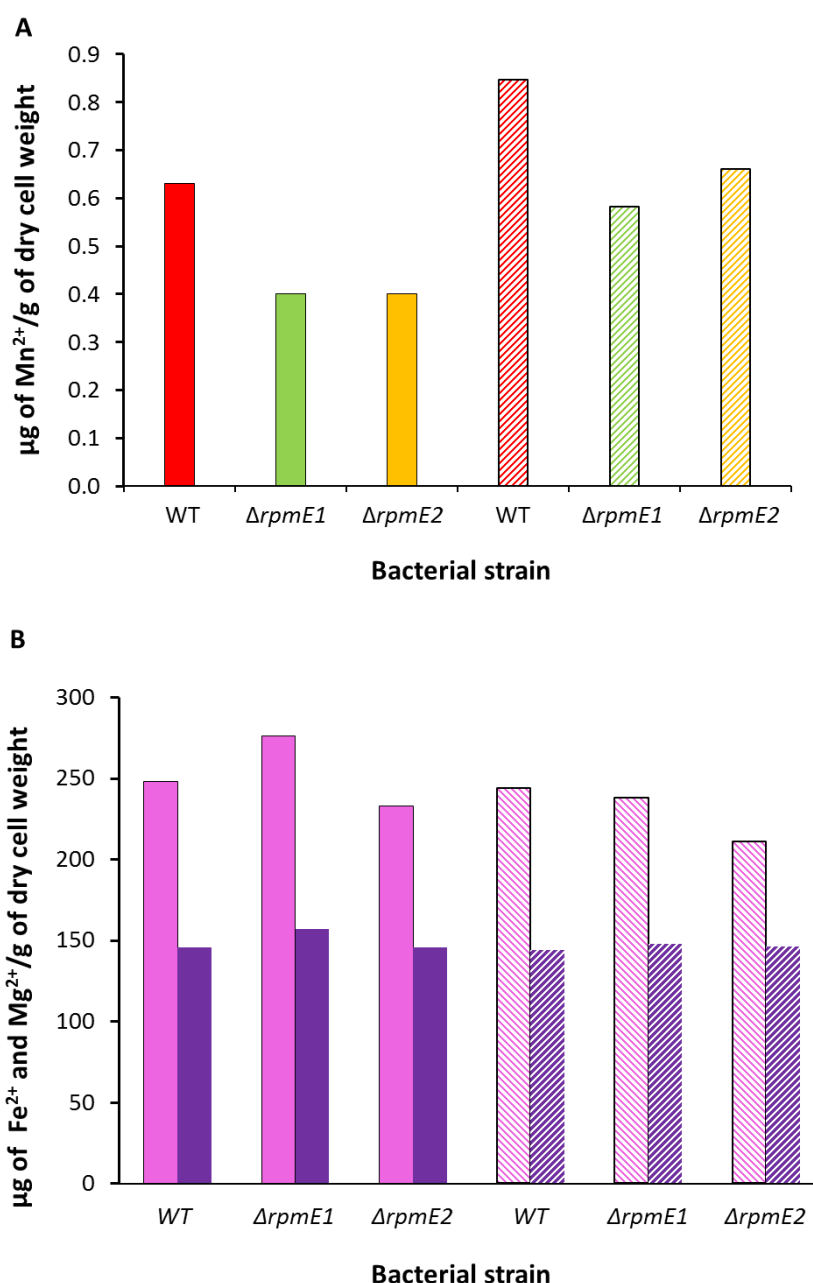


Figure 4.10: Level of intracellular Mn^{2+} , Fe^{2+} and Mg^{2+} in ATCC 17978, $\Delta rpmE1$ and $\Delta rpmE2$ cells grown in Zn^{2+} -replete and Zn^{2+} -limited conditions

Intracellular levels of metal ions ($\mu\text{g/g}$ of dry cell weight) in cells grown in Zn^{2+} -replete and Zn^{2+} -limited conditions. (A) Levels of Mn^{2+} in the three strains, WT (red), $\Delta rpmE1$ (green) and $\Delta rpmE2$ (yellow) grown in Zn^{2+} -replete (solid bars) and Zn^{2+} -limited (stippled bars) media. (B) Levels of Fe^{2+} (magenta) and Mg^{2+} (purple) in the three strains grown in Zn^{2+} -replete (solid bars) and Zn^{2+} -limited (stippled bars) media. Error bars represent the standard deviation.

4.2.6.1 The effect of *rpmE1* or *rpmE2* inactivation on bacterial susceptibility to antibiotics

A. baumannii uses a variety of resistance mechanisms to combat antimicrobial action, including expression of β -lactamases (see section 1.2.2). In a previous experiment it was shown that the removal of available Zn^{2+} from MH agar (via the addition of TPEN) increased the susceptibility of *A. baumannii* ATCC 17978 to the β -lactam-antibiotics cefotaxime and ceftriaxone, amoxicillin, clavulanic acid and ampicillin (Section 3.2.3.3). Limitation of Zn^{2+} also significantly reduced susceptibility to aminoglycoside antibiotics, including gentamicin, kanamycin, amikacin and streptomycin (see Table 3.1).

To investigate if the inactivation of *rpmE1* or *rpmE2* had an effect on susceptibility to these antibiotics, the three strains were grown on MH agar with/without the addition of the Zn^{2+} -chelator TPEN. Disk diffusion assays were used to test resistance to the β -lactam antibiotics (penicillin G, cefotaxime and ceftriaxone, amoxicillin clavulanic acid and ampicillin) and non β -lactam antibiotics (nalidixic acid, chloramphenicol, gentamicin, streptomycin, kanamycin and amikacin).

Comparison of the WT ATCC 17978 strain with the $\Delta rpmE1$ and $\Delta rpmE2$ strains grown on MH medium revealed no difference in penicillin resistance (Table 4.2). Interestingly, the $\Delta rpmE1$ and $\Delta rpmE2$ strains were more sensitive to amoxicillin-clavulanic acid than the WT strain. Meanwhile, on MH medium pre-treated with TPEN, the $\Delta rpmE1$, $\Delta rpmE2$ and WT strains, all increased in susceptibility to all β -lactam antibiotics tested, except for penicillin G. The susceptibility to these tested β -lactam antibiotics increased with higher concentrations of TPEN (data not shown). The resistance profile observed for both mutants indicates that $\Delta rpmE1$ and $\Delta rpmE2$ strains respond similarly to antibiotic stress. As ATCC 17978 contains type C and D serine β -lactamases, the absence of Zn^{2+} in the medium appears to indirectly affect the activity of the β -lactamase enzyme.

Table 4.2: Susceptibility of WT *A. baumannii* ATCC 17978, $\Delta rpmE1$ and $\Delta rpmE2$ strains to various antibiotics

| Antibiotic disk | Diameter of inhibition zones without TPEN ^a | | | Diameter of inhibition zones with TPEN ^b | | |
|----------------------------------------|--------------------------------------------------------|----------------|----------------|-----------------------------------------------------|----------------|----------------|
| | WT | $\Delta rpmE1$ | $\Delta rpmE2$ | WT | $\Delta rpmE1$ | $\Delta rpmE2$ |
| Penicillin G (10 µg) | 6 | 6 | 6 | 6 | 6 | 6 |
| Cefotaxime (30 µg) | 8 | 6 | 6 | 18* | 17* | 17* |
| Ceftriaxone (30 µg) | 17 | 15.5 | 15.5 | 24* | 25* | 25* |
| Amp (10 µg) | 12 | 8* | 8* | 19* | 16* | 14* |
| Amoxicillin/clavulanic acid (20/10 µg) | 8 | 14* | 13* | 16.5* | 20* | 20* |
| Gentamicin (10 µg) | 21.5 | 22 | 21 | 14.5* | 14* | 15* |
| Nalidixic acid (30 µg) | 19 | 16 | 17 | 19 | 17 | 17 |

^a. Diameter of clear zone surrounding the antibiotic disk is measured in mm.

^b. Susceptibility test using MH agar with the addition of 30 µM TPEN.

* Significant difference was observed between the inhibition zone of the bacteria grown in medium with and without the addition of TPEN ($p < 0.05$).

The addition of TPEN to growth media was shown to increase the resistance of ATCC 17978 to aminoglycoside antibiotics (see Table 3.1, Chapter 3). To assess this for the $\Delta rpmE1$ and $\Delta rpmE2$ strains, a disk diffusion assay of kanamycin, gentamicin, amikacin and streptomycin was undertaken. The results show that there was no significant difference in resistance to aminoglycosides between the WT and either of the $\Delta rpmE$ mutants (Table 4.3).

Susceptibility testing on MH medium that was pre-treated with 30 μ M TPEN revealed that all three strains became more resistant to gentamicin, streptomycin and kanamycin, whereas no difference in susceptibility was observed for amikacin. There is no clear explanation as to why this increase in *A. baumannii* resistance to aminoglycosides under Zn^{2+} -limited conditions occurred. Resistance to aminoglycosides can be attributed to changes in permeability, modification of the target ribosome, and modification of aminoglycoside modifying enzymes (Garneau-Tsodikova and Labby *et al*, 2016). Resistance can also be conferred by mutations and/or deletions of ribosomal proteins, which are usually present as single gene copies (Wilson, 2014). This study suggested that the increased antibiotic resistance displayed by all strains in the absence of available Zn^{2+} may be induced by the indirect effect of the conformational changes in the rRNA.

4.2.6.2 The effect of *rpmE1* or *rpmE2* inactivation in *A. baumannii* ATCC 17978 on bacterial motility

Bacterial motility is an essential virulence trait which allows *A. baumannii* to spread across solid surfaces and affects bacterial survival. It has been suggested that the motility phenotype is determined by various factors. In the previous chapter (Section 3.2.3.1), it was revealed that limitation of Zn^{2+} alone was not adequate to significantly inhibit the motility of *A. baumannii* ATCC 17978 grown on semisolid agar. However, it has been demonstrated that inactivation of L31 protein YkgM and *zitA* in *E. coli* affected biofilm formation; *ykgM* deletion led to the inhibition of curli (surface fibres connected with adhesion) biosynthesis (Lim *et al.* 2011). Since motility and biofilm are very close traits, the effect of the inactivation of the L31 genes on the ability to be motile in *A. baumannii* ATCC 17978 was examined; this was achieved by inoculate semisolid medium containing 0.5% agarose, 5 g/l

Table 4.3: Susceptibility of WT *A. baumannii* ATCC 17978 and $\Delta rpmE1$ and $\Delta rpmE2$ strains to aminoglycoside antibiotics

| Antibiotic disk | Diameter of inhibition zones without TPEN ^a | | | Diameter of inhibition zones with TPEN ^b | | |
|-------------------------|--------------------------------------------------------|----------------|----------------|-----------------------------------------------------|----------------|----------------|
| | WT | $\Delta rpmE1$ | $\Delta rpmE2$ | WT | $\Delta rpmE1$ | $\Delta rpmE2$ |
| Gentamicin (10 µg) | 19 | 20 | 20.5 | 12* | 12.5* | 12* |
| Streptomycin (10 µg) | 14 | 14 | 13.5 | 6* | 6* | 6* |
| Kanamycin (30 µg) | 20 | 22 | 23 | 15.5* | 17* | 19* |
| Amikacin (50 µg) | 19 | 21.5 | 23 | 15.5* | 19* | 18* |

^a. Diameter of clear zone surrounding the antibiotic disk is measured in mm.

^b. Susceptibility test using MH agar with the addition of 30 µM TPEN.

* Significant difference was observed between the inhibition zone of the bacteria grown in medium with and without the addition of TPEN, ($p < 0.05$).

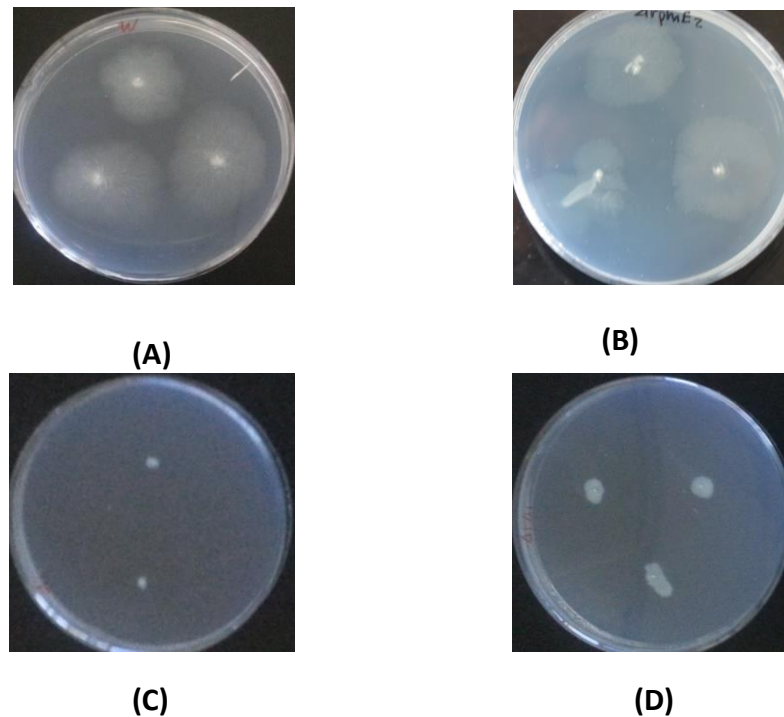


Figure 4.11: Assessment of motility of *A. baumannii* ATCC 17978 WT, $\Delta rpmE1$ and $\Delta rpmE2$ strains carrying the pWH1266 shuttle vector, and $\Delta rpmE1$ carrying pWHrpmE1

Motility assays were performed by spotting an *A. baumannii* colony onto semisolid (0.5%) agar. (A) WT ATCC 17978 showing swarming motility, (B) $\Delta rpmE2$ harbouring pWH1266 showing swarming motility, (C) $\Delta rpmE1$ harbouring pWH1266 demonstrates no halo of growth around the colony, (D) $\Delta rpmE1$ harbouring pWHrpmE1 displays a partial restoration of the motility phenotype.

tryptone and 2.5 g/l NaCl (Heindorf *et al.* 2014) with the mutants and corresponding complemented mutant strains (Section 2.3.6). Plates were incubated ON at 37 °C and each strain was assessed for motility.

The results revealed that deletion of *rpmE2* had no influence on motility (Figure 4.11B). In contrast, deletion of *rpmE1* significantly reduced the motility of *A. baumannii* (Figure 4.11C). Complementation of the *rpmE1* mutant with a WT copy of *rpmE1* on the shuttle plasmid pWH1266 resulted in only limited restoration of the motility phenotype (Figure 4.11D). Despite complementation failing to fully restore motility to WT levels, the reduction of motility in the $\Delta rpmE1$ mutant indicates that a functional *rpmE* may be required for full motility in *A. baumannii* ATCC 17978.

4.2.6.3 The effect of *rpmE1* or *rpmE2* inactivation on the ability to form biofilms

In order to investigate the effect of *rpmE1* and *rpmE2* inactivation on biofilm formation, the ability of the $\Delta rpmE1$ and $\Delta rpmE2$ strains and their respective complemented counterparts, to form a biofilm was assessed. The bacterial cells were grown in Zn²⁺-replete or Zn²⁺-limited M9 medium in plastic tubes under static conditions for 72 hr in the dark at 37 °C (Section 2.3.4). Following incubation, the liquid culture containing planktonic growth was decanted and the density measured by OD₆₀₀ to determine the effect Zn²⁺ limitation has on overall bacterial growth. The residual biofilm growth was stained with crystal violet and measured by OD₅₉₅ (Section 2.3.4). The results showed that there was a significant reduction (25%, $p < 0.05$) in the amount of biofilm formed by both of the $\Delta rpmE$ strains compared to the WT when the cells were grown in Zn²⁺-limited media (Figure 4.12). Even though overall, the total growth of the mutant strains was less than that of the WT strain, measurements of the planktonic portion of each culture at the end of the experiment (72 hr) revealed that there was no significant difference between the ability of the mutant strains and the WT strain ATCC 17978 to grow planktonically.

Together, the results indicate that the deletion of either *rpmE1* or *rpmE2* affected biofilm growth in *A. baumannii*. Unfortunately, attempts to restore the WT phenotype by providing each mutant with a WT copy of the inactivated gene on the plasmid pWH1266 were unsuccessful; this may have been due to the lack of

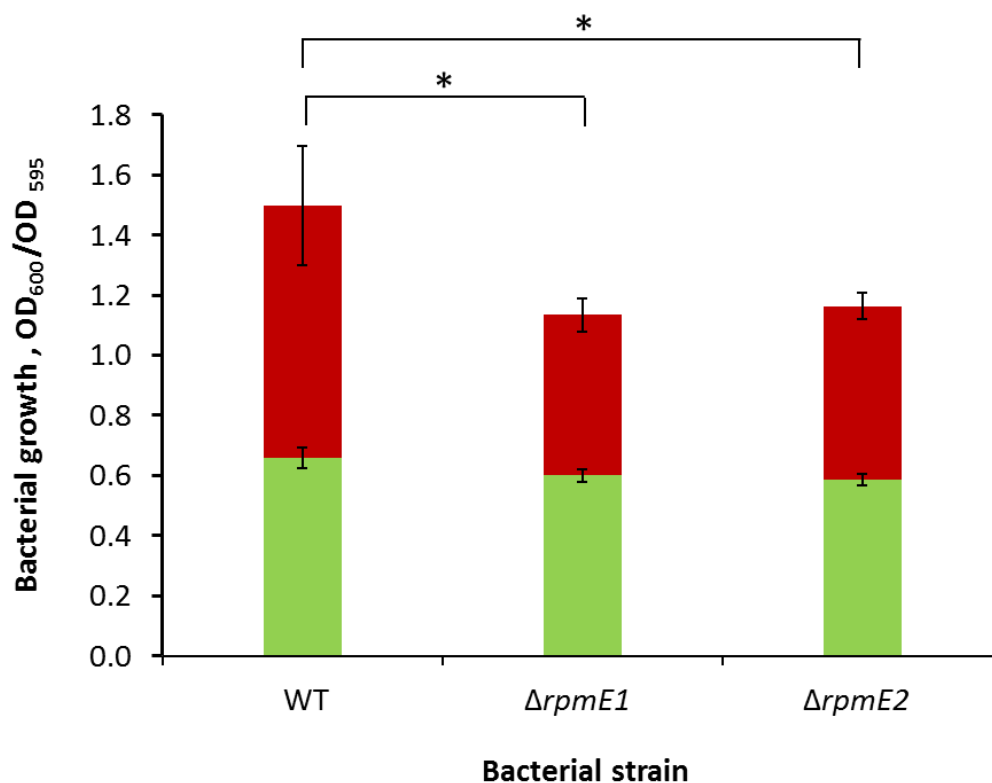


Figure 4.12: Biofilm production by *A. baumannii* ATCC 17978, $\Delta rpmE1$ and $\Delta rpmE2$ strains grown under Zn^{2+} -limited conditions

The levels of bacterial growth of ATCC 17978 WT and the two *rpmE* mutants under planktonic (green) and biofilm (red) conditions were assessed. Bacteria cells were grown in Zn^{2+} -limited culture medium in plastic tubes and incubated in static dark conditions at 37 °C for 72 hr. The amount of planktonic growth and biofilm attached to the plastic tube were measured at OD₆₀₀ and OD₅₉₅, respectively. A significant reduction was seen in the amount of biofilm produced by the $\Delta rpmE1$ and $\Delta rpmE2$ mutants compared to the WT strain (* $p < 0.05$) but no significant difference was observed in the amount of planktonic growth between the three strains. Error bars show the standard deviation.

antibiotic selective pressure over the 72 hr growth period leading to instability and loss of the plasmid. A study examining biofilm formation by enteropathogenic *E. coli* showed that inactivation of *ykgM* did not affect the ability to form a biofilm when grown under static conditions. The difference here may be because the experiment used polystyrene 96-well microtiter plates and a shorter incubation period (24 hr) (Lim *et al.* 2011). However, there was a reduction in biofilm growth when the *E. coli ykgM* mutant was grown under fluidic conditions (Lim *et al.* 2011), indicating that a functional *rpmE2* may be required for normal biofilm formation.

4.2.6.4 The effect of *rpmE1* or *rpmE2* inactivation on cellular adherence to eukaryotic cells

The effect that the deletion of *rpmE1* or *rpmE2* had on the ability of *A. baumannii* ATCC 17978 to adhere, invade and replicate intracellularly in the human pneumocyte cell line type 2 A549 (Section 2.3.5) was investigated. This cell line has been commonly used to study interactions of *A. baumannii* with eukaryotic cells; it mimics adherence to the human lung and as such represents a potential model for pneumonial infection caused by *A. baumannii* (Gaddy *et al.* 2009; Giannouli *et al.* 2013; Smani *et al.* 2012). A549 cells were incubated separately with all three strains. The results revealed that there was no significant difference in the ability of any of the strains to adhere to A549 cells (Figure 4.13).

4.2.6.5 The effect of *rpmE1* or *rpmE2* inactivation on the ability of *A. baumannii* to survive oxidative stress

Bacteria are permanently in contact with ROS that can damage essential bacterial cellular structures as well as damage DNA, lipids and proteins (Paget *et al.* 1998) (see Section 1.8.2). These ROS molecules are detected using a number of different protein-based regulatory and sensory systems that stimulate the expression of proteins involved in the oxidative stress response. Many bacterial enzymes and regulatory proteins possess a Zn²⁺-containing redox centre, C-X-X-C, providing an ability to sense the redox status of the cell (see Section 1.8.2). A previous study in *N. gonorrhoeae* (Wu *et al.* 2006) indicated that RpmE1 is negatively regulated by PerR and responds to oxidative stress. Additionally, deletion

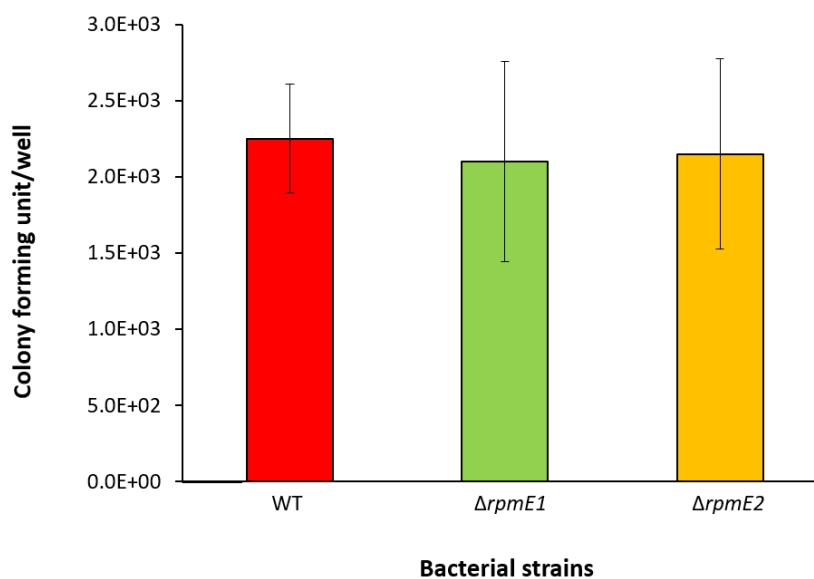


Figure 4.13: Cellular adherence of *A. baumannii* ATCC 17978, $\Delta rpmE1$ and $\Delta rpmE2$ strains to the pneumocyte cell line type 2 A549

The ability of WT, $\Delta rpmE1$ and $\Delta rpmE2$ *A. baumannii* ATCC 17978 cells to adhere to eukaryotic cells was examined by incubating the bacterial strains with the pneumocyte cell line A549 (Section 2.3.5). No significant difference was observed in the number of cells adhering to A549 cell line between the three strains. Error bars show the standard deviation.

of *perR* led to increased resistance to oxidative stress, indicating that the increased expression of genes normally repressed by *perR* provided protection against oxidative stress (Wu *et al.* 2006).

To investigate the role of RpmE1 and RpmE2 in *A. baumannii* ATCC 17978 in survival under oxidative stress, both $\Delta rpmE$ mutants and the corresponding complementing strains, were separately grown in MH media with/without the addition of 300 μ M paraquat (Section 2.3.7). Paraquat is a nonselective herbicide which induces oxidative stress by generating radical oxygen species as a result of its interaction with NADPH-cytochrome C reductase (Fukushima *et al.* 2002) (see Section 1.8.2). The paraquat stress assay revealed that this compound did not inhibit growth of the WT *A. baumannii* strain, but did of both the $\Delta rpmE1$ and $\Delta rpmE2$ mutants (Figure 4.14). The inhibition of growth of the $\Delta rpmE2$ cells caused a delay in the log phase and then the growth was slowly restored similar to that seen in the WT strain. On the other hand, the growth of $\Delta rpmE1$ was significantly impaired. Complementation of the $\Delta rpmE1$ and $\Delta rpmE2$ mutants with a WT copy of the appropriate gene partially restored the growth to WT levels after a 4 hr exposure to paraquat.

To determine the impact that deleting RpmE1 and RpmE2 has on genes involved in the oxidative stress response, qRT-PCR was conducted of four genes selected as they encode known stress response proteins; Fumarase C (*fumC*, A1S_1986), Catalase B (*katB*, A1S_3382), Alkyl hydro peroxide reductase subunit C (*ahpC*, A1S_1205) and Superoxide dismutase (*sodA*, A1S_2343). Briefly, bacteria were grown ON at 37 °C then diluted 1:50 in MH medium and incubated at 37 °C in a shaking incubator until the OD₆₀₀ reached 0.5. In this phase, cultures of *A. baumannii* ATCC 17978, $\Delta rpmE1$, and $\Delta rpmE2$ cells were exposed to paraquat at a final concentration of 500 μ M and incubated for further 45 min. The 500 μ M level of paraquat was chosen based on an experiment which showed that the addition of a final concentration of 500 μ M paraquat to the log phase of bacterial growth did not result in growth inhibition for all the strains (data not shown). Therefore, to give the cells a shock exposure in a short time period a higher paraquat concentration was chosen (500 μ M). Total cellular RNA was subsequently extracted, reverse

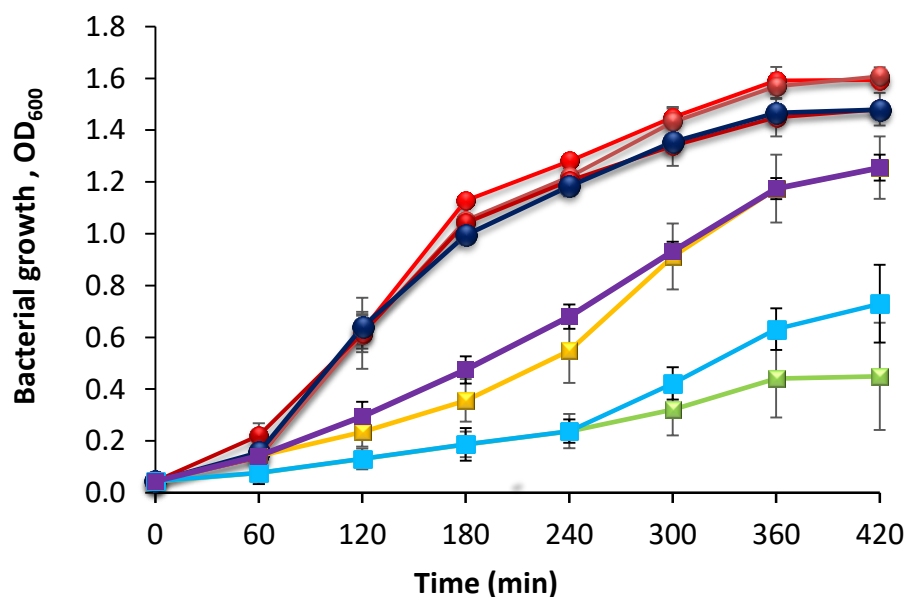


Figure 4.14: Effect of oxidative stress on the growth of *A. baumannii* ATCC 17978 $\Delta rpmE1$ and $\Delta rpmE2$ strains

The *A. baumannii* ATCC 17978 WT, $\Delta rpmE1$, and $\Delta rpmE2$ strains were grown in MH media without (WT, red; $\Delta rpmE1$, orange; and $\Delta rpmE2$, brown) and with the addition of 300 μM paraquat (WT, dark blue; $\Delta rpmE1$, light green; and $\Delta rpmE2$, yellow) to induce oxidative stress. The $\Delta rpmE1$ and $\Delta rpmE2$ containing complementing plasmids, $\Delta rpmE1$:pWHrpmE1 (cyan) and $\Delta rpmE2$:pWHrpmE2 (purple), respectively, were also grown in MH media with the addition of paraquat 300 μM . Absorbance was measured every hr at OD₆₀₀ for 7 hr; the data represent the average of three separate experiments. Error bars show the standard deviation.

transcribed (Section 2.6) and the transcriptional levels of the various genes examined by qRT-PCR using primers listed in Table 2.4.

Figure 4.15 shows the expression of the four selected stress response genes, where the fold changes generated in the mutant strains were compared to the expression level seen in the WT. The results revealed that the expression of *katB* and *ahpC* in both mutants increased under all conditions relative to WT. In particular, *katB* expression increased more than 4-fold in $\Delta rpmE1$ when exposed to paraquat, and a 2-fold increase in the $\Delta rpmE2$ derivative. On the other hand, the expression of *fumC* and *sodA* was lower in both mutant strains whether under paraquat stress or not. This reduction in gene expression in the absence of paraquat indicated that these two genes are repressed in the $\Delta rpmE$ mutants. Furthermore, the expression of *sodA* in the $\Delta rpmE1$ and $\Delta rpmE2$ strains were even lower under paraquat treatment. This may be due to a failure of the cells to respond to oxidative stress leading to a further repression of *sodA*. The increase in expression of *katB* and *ahpC* was possibly to compensate the decrease in expression of *fumC* and *sodA*.

Both of the $\Delta rpmE$ mutants were more sensitive to paraquat than the WT strain and displayed differential expression of genes associated with oxidative stress after paraquat exposure. Together, these data indicate that *rpmE1* and *rpmE2* are either directly or indirectly involved in the oxidative stress response in *A. baumannii*.

4.3 Conclusions

This study has shown that compared to *A. baumannii* ATCC 17978, the constructed *rpmE1* and $\Delta rpmE2$ mutants are slower in entering the exponential phase of growth and exhibit reduced growth in Zn^{2+} -limited media, clearly demonstrating that both RpmE1 and RpmE2 are important for normal growth of this strain. Although the reduced growth phenotype could be recovered by the addition of Zn^{2+} , the delay in entering the exponential phase of growth was not recoverable, suggesting that the deletion of *rpmE1* and *rpmE2* affected processes other than Zn^{2+} availability. The qRT-PCR experiments revealed that the expression of Zur was decreased in the $\Delta rpmE1$ mutant compared to the WT strain, indicating

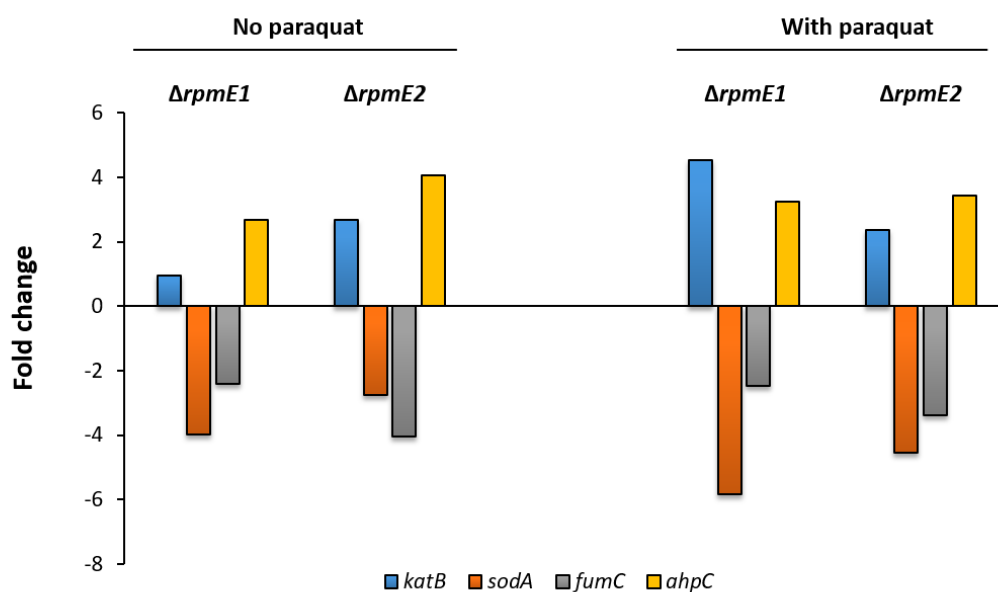


Figure 4.15: qRT-PCR expression analyses of selected stress-response genes during growth with/without paraquat

Transcriptomic analyses using qRT-PCR showing the fold change in expression of the *A. baumannii* oxidative stress-associated genes *katB*, *sodA*, *fumC*, and *ahpC* when $\Delta rpmE1$ and $\Delta rpmE2$ cells were grown in the presence/absence of 500 μ M paraquat. The fold change is relative to the expression in WT ATCC 17978. Data are presented as expression fold change and represent the average of two separate experiments.

that deletion of *rpmE1* affected expression of this regulator by an unknown mechanism. Moreover, when the $\Delta rpmE2$ mutant was grown in Zn^{2+} -limited conditions, the expression of *rpmE1* increased, suggesting that this may have been a compensating mechanism for the loss of *rpmE2*.

The intracellular Zn^{2+} levels determined for the $\Delta rpmE1$ and $\Delta rpmE2$ mutants, as measured by ICP-MS, were similar to levels in the WT ATCC 17978 strain when all cells were grown in Zn^{2+} -replete medium indicating that the mutants could still maintain normal intracellular levels of Zn^{2+} in the absence of either L31 protein. However, during growth in Zn^{2+} -limited medium the level of intracellular Zn^{2+} was reduced in both mutant strains, indicating that both RpmE1 and RpmE2 are required to maintain intracellular Zn^{2+} levels during Zn^{2+} -starvation conditions. Other phenotypic assays revealed that both the $\Delta rpmE1$ and $\Delta rpmE2$ strains showed a reduction in biofilm formation but only the $\Delta rpmE1$ displayed reduced motility during growth on semi-solid media. Together, these data indicate that *rpmE1* and *rpmE2* are both required for the formation of WT levels of biofilm but only *rpmE1* is essential for full motility. Antibiotic susceptibility testing revealed that similar to the WT strain, both the $\Delta rpmE1$ and $\Delta rpmE2$ derivatives had reduced susceptibility to aminoglycoside antibiotics. In contrast, susceptibility to β -lactam antibiotics was affected during growth in Zn^{2+} -limited medium and that this was dependent on the degree of Zn^{2+} depletion. Oxidative stress survival assays and analysis of the transcriptomic response to oxidative stress indicated that inactivation of either L31 protein affected cell survival and the expression of stress-response genes. These data indicate that *rpmE1* and *rpmE2* are either directly or indirectly involved in the *A. baumannii* response to oxidative stress.

Together, the phenotype and gene expression analyses of the mutant strains shows that RpmE1 and RpmE2 play a role in intracellular Zn^{2+} homeostasis as well as other processes that appear to be not directly related to Zn^{2+} homeostasis. Future studies should examine if deletion of either *rpmE1* or *rpmE2* affects the virulence of *A. baumannii* *in vivo*. In order to understand the overall effect of *rpmE1* and *rpmE2* inactivation in *A. baumannii*, global transcriptomic analyses were undertaken and are discussed in the following chapter.

CHAPTER 5
TRANSCRIPTIONAL EFFECTS AFFORDED
BY DELETION OF THE L31 GENES
IN *A. BAUMANNII* ATCC 17978

5.1 Introduction

In the previous chapter it was shown that the deletion of either gene encoding a L31 ribosomal protein, *rpmE1* or *rpmE2*, resulted in a bacterial growth defect in Zn^{2+} -limited media (see Section 4.2.3). For the $\Delta rpmE1$ strain this was likely due to reduced Zn^{2+} storage, as RpmE1 contains the CXXC Zn^{2+} -binding motif and is predicted to contain 0.82 atoms of Zn^{2+} per protein molecule (Nanamiya et al., 2004); therefore, the amount of Zn^{2+} stored by each $\Delta rpmE1$ cell is reduced. In contrast, though the loss of RpmE2 would not be predicted to alter the amount of Zn^{2+} stored, the growth of the $\Delta rpmE2$ strain in Zn^{2+} -limited conditions was inhibited. It is hypothesised that RpmE2 has a significant role in Zn^{2+} mobilisation due to its ability to displace RpmE1 in the ribosome (Akanuma et al. 2006). Therefore, the reduced ability of the *A. baumannii* $\Delta rpmE2$ mutant to grow in Zn^{2+} -limited conditions is likely due to an inability to liberate Zn^{2+} from RpmE1 as there is no RpmE2 protein to displace it from the ribosome. Supporting this hypothesis, a study in *B. subtilis* found that the alternative use of the two types of L31 RpmE proteins in the ribosome led to the release of Zn^{2+} molecules in Zn^{2+} -limited conditions (Akanuma et al. 2006).

To identify the role of these L31 RpmE1 and RpmE2 proteins in Zn^{2+} homeostasis and their influence on the expression of other *A. baumannii* genes, the two constructed L31 $\Delta rpmE$ mutants were investigated at a global transcriptional level. Transcriptomic changes during growth in Zn^{2+} -replete and Zn^{2+} -limited conditions were examined by comparing the response of the $\Delta rpmE1$ and $\Delta rpmE2$ mutants to that of the *A. baumannii* ATCC 17978 WT strain. In this chapter a number of comparisons have been made between these two L31 mutants and their growth under either Zn^{2+} -limited or Zn^{2+} -replete conditions. Due to the number of possible comparisons and numerous changes in the transcriptome only the most significantly affected genes are discussed.

5.2 Results and Discussion

5.2.1 Growth of *A. baumannii* in both Zn²⁺-replete and Zn²⁺-limited conditions for RNA-sequencing analysis

Growth of the *A. baumannii* strains for RNA extraction and transcriptomic analyses was undertaken as described below. The *A. baumannii* ATCC 17978 WT, $\Delta rpmE1$, and $\Delta rpmE2$ strains were each grown in Zn²⁺-limited and Zn²⁺-replete media, prepared as described previously (see Section 2.2). For RNA extraction, ON cultures of each *A. baumannii* strain (grown in LB medium) were pelleted by centrifugation and washed three times with Zn²⁺-limited medium. The resuspended cells were then diluted 1:50 in either Zn²⁺-replete or Zn²⁺-limited media and incubated with shaking at 37 °C. RNA was extracted (see Section 2.6.1) from cells in early log phase (after approximately 4 hr until OD₆₀₀ = 0.5). The total RNA used for each RNA-seq reaction was composed of RNA extracted and pooled from three biological replicates. Other aliquots from the same RNA samples were used for qRT-PCR to confirm the RNA-seq data.

5.2.2 Global transcriptomic analyses of the ATCC 17978 $\Delta rpmE1$ and $\Delta rpmE2$ mutants

To understand the global gene expression changes in *A. baumannii* ATCC 17978 in response to deletion of each of the L31 genes, RNA-seq analysis was performed using cells grown in the two different conditions described above. Firstly, for investigating the role of each of the L31 genes, the RNA-seq data of the $\Delta rpmE1$ and $\Delta rpmE2$ cells grown in Zn²⁺-replete conditions were compared with the data generated for the WT strain ATCC 17978 grown under the same conditions. This comparison was predicted to reveal the effect that the deletion of *rpmE1* or *rpmE2* has on the global gene expression of *A. baumannii* ATCC 17978. Secondly, to investigate the transcriptomic response of the $\Delta rpmE1$ and $\Delta rpmE2$ mutants under Zn²⁺ limitation, RNA-seq data from these two strains grown in Zn²⁺-limited conditions were compared to the WT ATCC 17978 strain grown under the same

conditions. This comparison was predicted to reveal the transcriptomic effect that deletion of *rpmE1* or *rpmE2* has on *A. baumannii* growth during Zn²⁺ limitation.

The RNA-seq analysis in this thesis was based on the annotation of the *A. baumannii* ATCC 17978, GenBank accession number: CP000521.1 (Smith *et al.* 2007). As has been previously discussed (see Section 3.2.5), this initial annotation has since been found to contain a number of errors in the allocation of the start sites of the ORFs as well as missing some ORFs. Recently a new annotation of ATCC 17978 GenBank accession number: CP012004 (Weber *et al.* 2013) was released. At the time of undertaking the work and writing of this thesis the new sequence was unavailable, therefore, the ORF annotation of the older sequence was used for the work presented unless otherwise stated.

It was found that low expression levels of the two deleted genes, *rpmE1* or *rpmE2*, could be seen in their respective deletion strains, $\Delta rpmE1$ and $\Delta rpmE2$. This is most likely due to background noise in the RNA-seq data, as the counts are very low and similar in both conditions, and can be disregarded as both *rpmE1* and *rpmE2* are inactive in the $\Delta rpmE1$ and $\Delta rpmE2$ strains, respectively. For example, in the case of the RNA-seq analysis obtained from the $\Delta rpmE2$ mutant cells, the reads/rpkm of *rpmE2* was 72.09 compared to 11.91, in Zn²⁺-replete and Zn²⁺-limited conditions, respectively (data not shown). A similar trend can be seen in the $\Delta rpmE1$ mutant. In this comparison, although the reads/rpkm of *rpmE1* were higher (~300) in both conditions, RT-PCR analysis confirmed that the *rpmE1* expression in the $\Delta rpmE1$ derivative is almost undetected (Table 4.1).

The RNA-seq data for the $\Delta rpmE1$ mutant, based on the old annotation sequence (CP000521.1) revealed that *rpmE1* (A1S_2423) was 19-fold down-regulated (Log₂ of -4.3) (Appendix 4) compared to when in the WT strain grown in Zn²⁺-replete conditions. It was expected that expression would be much lower than this. In addition, the expression of *rpmE1* in the RNA-seq data did not correspond to the data obtained from qRT-PCR of the $\Delta rpmE1$ mutant (Section 4.2.4). Therefore, to investigate this discrepancy, the expression of *rpmE1* was mapped to the newly annotated CP012004 sequence, which showed that expression of *rpmE1* (ACX60_05445) in $\Delta rpmE1$ was 830-fold lower (Log₂ of -9.7) than the WT when

grown in Zn²⁺-replete conditions (Appendix 14) indicating almost no expression of this gene. Expression of other Zn²⁺-regulated genes in Zn²⁺-replete conditions were also mapped to the new annotated sequence including A1S_0143 (ACX60_17365), A1S_0144 (ACX60_17360), A1S_0145 (ACX60_17355), and A1S_0146 (ACX60_17350). The Log₂ expression levels were -1.5, -1.9, -3.6 and 2.1 for A1S_0143, A1S_144, A1S_0145 and A1S_0146, respectively (Appendices 4 and 5). The Log₂ expression in the CP012004 sequence was -1.4, -2, -3.5, and 2.4 (Appendices 13 and 14) for ACX60_17365, ACX60_17360, ACX60_17355 and ACX60_17350, respectively. These data suggest that the expression of these genes closely correlate between the old and new ATCC 17978 sequences.

Similar comparison of RNA-seq data from the *ΔrpmE2* mutant to that of the WT showed that the expression of *rpmE2* was reduced by 8-fold (Log₂ of -3) in Zn²⁺-replete conditions (Appendix 8) and by 2000-fold (Log₂ of -11.3) in Zn²⁺-limited medium (Appendix 10). The expression levels under these two conditions were also mapped to the CP012004 sequence which revealed that in *ΔrpmE2*, *rpmE2* (ACX60_16160) expression in Zn²⁺-replete and Zn²⁺-limited media compared to the WT were 9.4-fold (Log₂ of -3.2, Appendix 16) and 3000-fold (Log₂ of -11.6, data not shown) down-regulated, respectively. These data demonstrated that there was almost no *rpmE2* expression in Zn²⁺-limited conditions.

5.2.3 Effect of the deletion of *rpmE1* or *rpmE2* on the *A. baumannii* ATCC 17978 transcriptome during growth in Zn²⁺-replete conditions

To investigate the effect of the inactivation of *rpmE1* or *rpmE2* on the *A. baumannii* ATCC 17978 transcriptome, the RNA-seq data generated from *ΔrpmE1* and *ΔrpmE2* grown in Zn²⁺-replete conditions was compared to data generated from the WT strain grown under the same conditions.

5.2.3.1 Effect of the inactivation of *rpmE1* on gene expression in *A. baumannii* ATCC 17978 grown under Zn²⁺-replete conditions

To examine the effect of the deletion of *rpmE1*, the RNA-seq data generated from the *rpmE1* mutant grown in Zn²⁺-replete conditions were compared to data

generated from the WT strain grown under the same conditions. The comparison revealed that there were 31 genes with ≥ 2 -fold ($\text{Log}_2 \geq 1$) increased expression in the $\Delta rpmE1$ strain (Appendix 3). The highest-expressed gene (149-fold) in the $\Delta rpmE1$ strain encoded a protein belonging to the G3E GTPase family (A1S_3411) (Figure 5.1). Under these Zn^{2+} -replete conditions, more genes in the $\Delta rpmE1$ strain showed decreased expression than increased expression; in total 350 genes had ≥ 2 -fold reduced expression when compared to expression in ATCC 17978. The RNA-seq data were subsequently validated by qRT-PCR analysis of a subset of differentially-expressed genes; A1S_0092, A1S_1045, A1S_0391, A1S_0146, A1S_2423, A1S_3217, and A1S_0452, using oligonucleotides specific for each gene (see Table 2.4). These genes were selected based on their level of expression, ranging from the least to the most differentially expressed. Overall, the qRT-PCR data showed slightly higher-fold changes for each gene examined than the results obtained from the RNA-seq expression data, such as the expression of *rpmE2* (A1S_0391) (Log_2 of -8 and -7 in qRT-PCR or RNA-seq, respectively) and *znuA* (A1S_0146) (Log_2 of 2.75 or 2.08 in qRT-PCR and RNA-seq, respectively) (Table 5.1). Nevertheless, a high correlation R value of 0.95 between data from the qRT-PCR and the RNA-seq analyses was observed (Figure 5.2).

Many of the differentially expressed genes in the 'hypothetical proteins' and 'unknown function' categories showed decreased expression, indicating that the absence of the L31 protein encoded by *rpmE1* may have potential pleiotropic effects on genes not directly related to either ribosomal structure or Zn^{2+} homeostasis. The deletion of *rpmE1* also resulted in reduced expression of genes located in loci A1S_1292-1310, A1S_1699-1705 and A1S_1880-1894 (Figure 5.1).

Interestingly, the data show that the deletion of *rpmE1* resulted in an 11-fold reduction in expression of the global transcription regulator Zur (Figure 5.1). As a result, a number of Zur-regulated genes showed increased expression, including; *rpmE2* (A1S_0391), *znuA* (A1S_0146), *tonB-exbB-exbD* (A1S_0452-0453), TBDR (A1S_2892), and a gene encoding a putative G3E family GTPase (A1S_3411) (Figure 5.1). These results are supported by a recent RNA-seq analysis of an *A. baumannii* ATCC 17978 Δzur mutant (Mortensen *et al.* 2014) that identified that the same

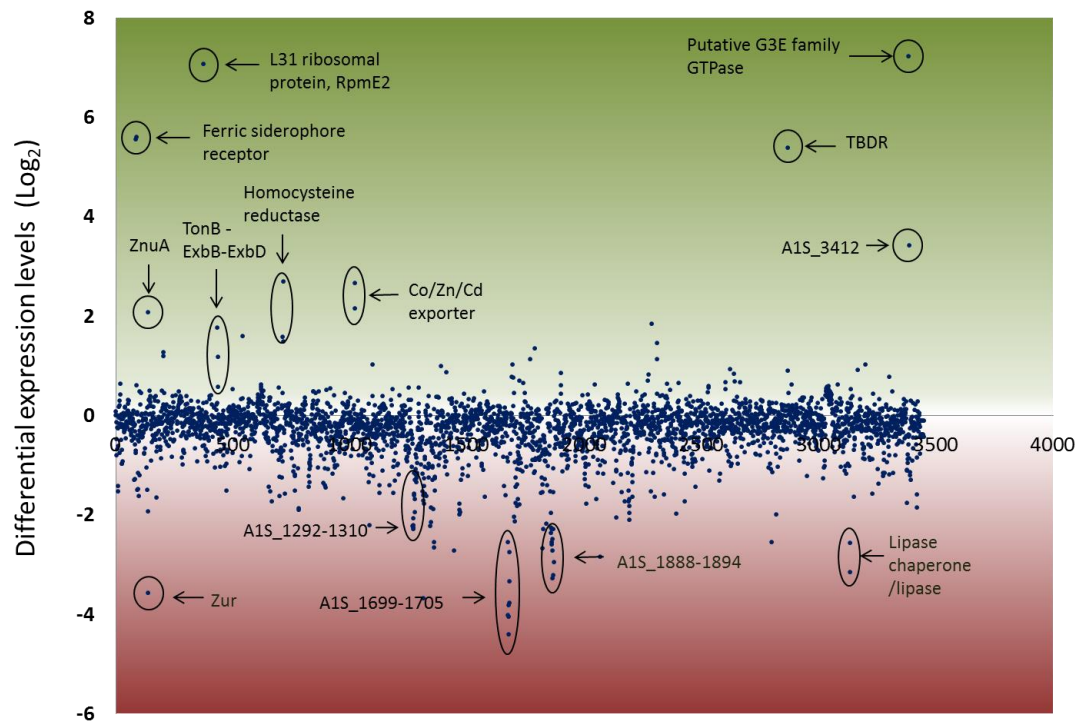


Figure 5.1: Transcriptional changes in the ATCC 17978 $\Delta rpmE1$ mutant in response to growth in Zn^{2+} -replete conditions

Comparison of the global RNA expression of *A. baumannii* ATCC 17978 $\Delta rpmE1$ and WT strains grown in Zn^{2+} -replete conditions. The expression levels of all 3500 genes in the ATCC 17978 genome were measured by RNA-seq and are represented on the X-axis in order of ascending locus-tag (Smith *et al.* 2007). Differential gene expression levels in the ATCC 17978 $\Delta rpmE1$ cells are displayed in Log₂-values on the Y-axis. Genes with increased and decreased expression are displayed in the green and red sections, respectively. The circled dots indicate selected genes that are differentially expressed by the $\Delta rpmE1$ mutant during growth in Zn^{2+} -replete conditions.

Table 5.1: Validation of the transcriptomic data generated from the ATCC 17978 *ΔrpmE1* grown in Zn²⁺-replete conditions by comparison of expression levels determined by RNA-seq and qRT-PCR analysis

| Locus tag | RNA-seq (Log ₂) | RT-PCR (Log ₂) |
|-----------|-----------------------------|----------------------------|
| A1S_0452 | 3.39 | 1.81 |
| A1S_0146 | 2.08 | 2.75 |
| A1S_0145 | -3.50 | -2.20 |
| A1S_0092 | 5.50 | 5.80 |
| A1S_3217 | -1.50 | -1.13 |
| A1S_1217 | -0.18 | -0.33 |
| A1S_0391 | -7.06 | -8.00 |

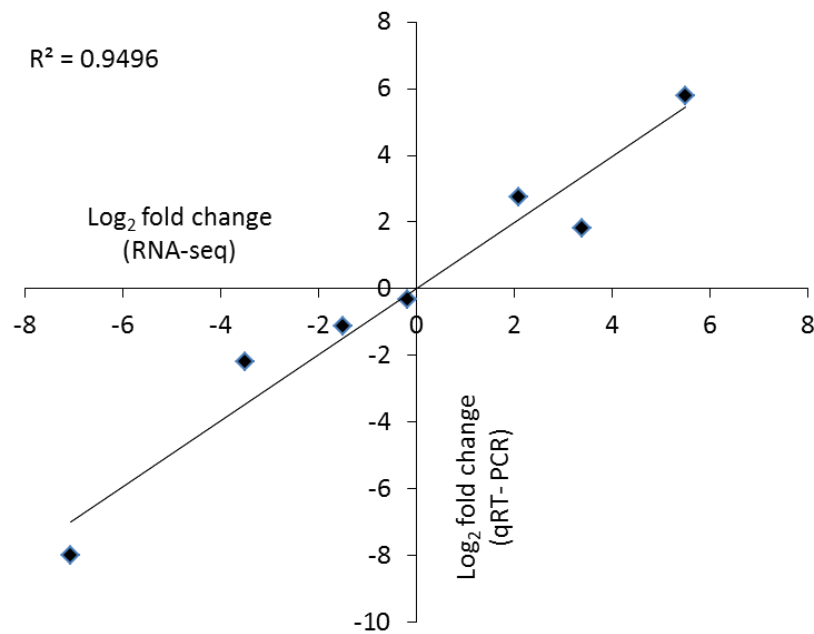


Figure 5.2: Correlation of the Log₂-based fold changes for six genes showing altered expressed in the *ΔrpmE1* grown in Zn²⁺-replete conditions

The Y axis represents the Log₂-fold change of gene expression determined by qRT-PCR and the X axis represents the Log₂-fold change of gene expression determined by RNA-seq data. Derived from the RNA-seq and qRT-PCR data, a correlation coefficient (R^2) of 0.9496 was determined.

genes as listed above were increased in expression in their Δzur mutant compared to the WT strain. Interestingly, in the same study, they found that genes which are not known to have a *zur*-binding site also showed increased expression, including the ferric-siderophore receptor (A1S_0092) (Mortensen *et al.* 2014).

5.2.3.1.1 Identification of COG functional categories

Differentially expressed genes were grouped into COG functional categories (Figure 5.3). These COG groupings revealed that 20% and 15% of genes with reduced expression encoded proteins involved in secondary (secondary metabolites biosynthesis, transport, and catabolism) and lipid metabolism, respectively. A number of genes involved in secondary metabolites biosynthesis, including genes involved in phenylacetic acid degradation (*paaA/B/J/K*), showed a decrease in expression of between 4- to 12-fold (see Appendix 4). Various genes related to lipid metabolism also showed decreased expression in the $\Delta rpmE1$ strain, including A1S_1704 encoding an acetoin dehydrogenase (10-fold reduced), as well as A1S_1846 and A1S_1847 (6- and 3-fold decreased, respectively) (see Appendix 4), that encode the 3-oxoacid CoA-transferase subunits A and B. Approximately 13% of genes encoding proteins involved in carbohydrate metabolism and transport showed decreased expression. The majority of genes involved in motility were not affected by deletion of *rpmE1*, with the exception of the *csuABABCDE* (A1S_2214-221) locus (\leq 3-fold decrease) involved in Csu pilus assembly. In addition, approximately 5% of the genes within the inorganic ion transport and metabolism COG group showed decreased expression.

The profiling of RNA expression changes and classification into COG groupings can be problematic since many of the *A. baumannii* genes are not represented in any categories, therefore other methods of profiling changes, *e.g.*, at the metabolic level, may be necessary to fully evaluate the effects of the deletion of *rpmE1* on *A. baumannii*. Nevertheless, even when grown in Zn^{2+} -replete conditions, the RNA-seq data clearly show that deletion of *rpmE1* has wide ranging effects on gene expression in *A. baumannii*.

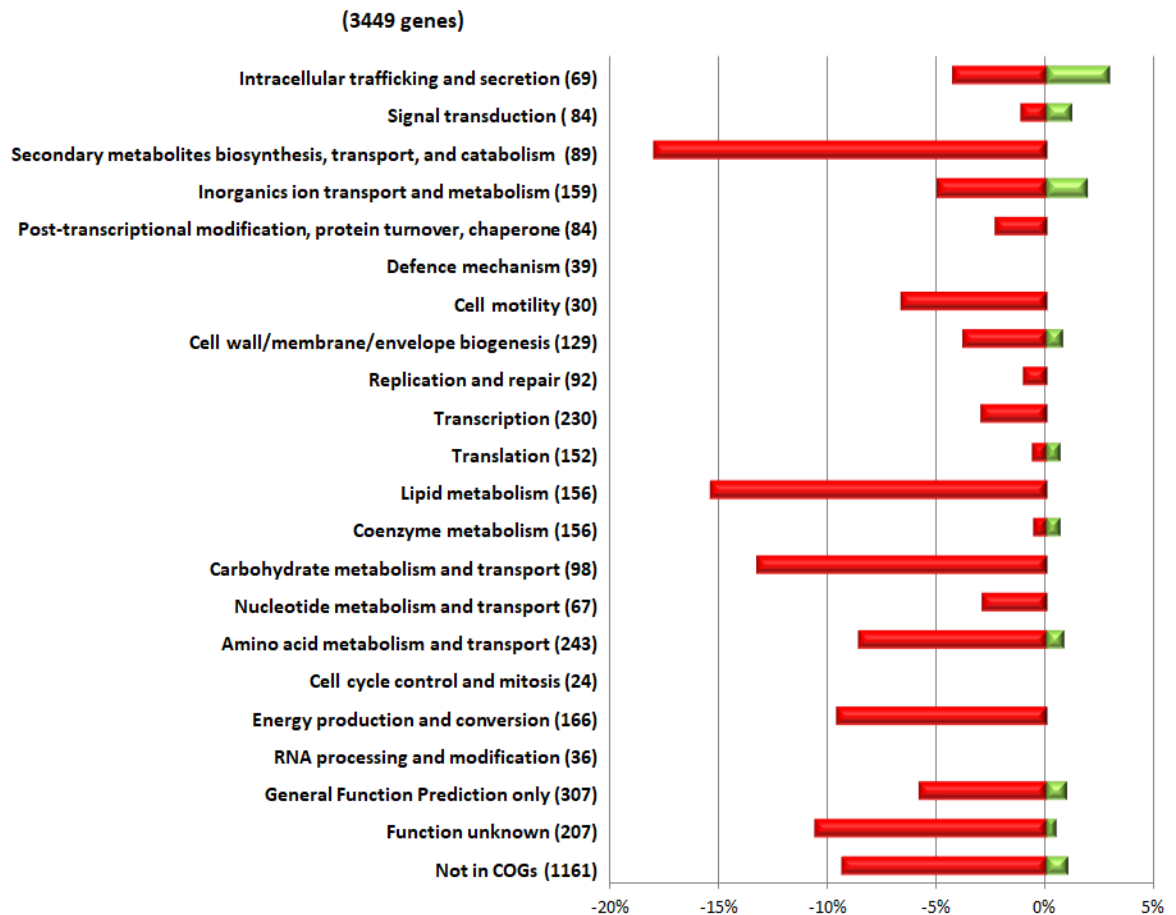


Figure 5.3: Transcriptional changes in the ATCC 17978 $\Delta rpmE1$ mutant relative to WT when both are grown in Zn^{2+} -replete conditions, displayed by COG function

The percentage of differentially expressed genes (≥ 2 -fold as determined using RNA-seq) belonging to each COG category is shown. The percentage of genes in the $\Delta rpmE1$ mutant with decreased expression relative to the WT strain, both grown under Zn^{2+} -replete conditions, is shown in red and genes with increased expression are shown in green. The total number of differentially expressed genes per COG function is shown in parentheses.

5.2.3.1.2 *The effect of rpmE1 deletion on the expression of Zn²⁺ homeostasis genes during growth in Zn²⁺-replete conditions*

The RNA-seq data generated from the $\Delta rpmE1$ mutant grown in Zn²⁺-replete medium (Figure 5.1) revealed that the transcription of *zur* (A1S_0145) was 11-fold to lower (Log₂ of -3.6) than in the WT ATCC 17978 strain. It is known that Zur binds DNA in a Zn²⁺-dependent manner and represses transcription of target genes when the intracellular levels of Zn²⁺ is sufficient (Sein-Echaluce *et al.* 2015). However, the reduced expression of *zur* in the $\Delta rpmE1$ mutant resulted in the expression of Zur-regulated genes in conditions when Zn²⁺ availability was not limited. In this unregulated state, the high affinity Zn²⁺-uptake gene, *znuA*, showed a 4-fold increase in expression. The expression levels of other Zur-regulated genes including *rpmE2*, *tonB-ExbB-ExbD*, and the gene encoding the TDBR (A1S_2829), were increased in the $\Delta rpmE1$ mutant to levels similar to those observed in the WT strain grown in Zn²⁺-limited conditions (see Section 3.2.5). However, a protein that shares high amino acid identity to CzcD, a Zn/Co/Cd efflux protein encoded on two ORFs, A1S_1044 and A1S_1045 (based on the new annotated sequenced CP012004, these genes represent one gene ACX60_13160), showed increased expression in the $\Delta rpmE1$ mutant under Zn²⁺-replete conditions and is not under *zur* control. These ORFs were not identified as differentially expressed in the WT strain in the Zn²⁺-limited conditions. Thus, the increased expression of *czcD* is likely to be in response to the higher levels of free Zn²⁺ either within the cell or within the Zn²⁺-replete medium. The increased expression of this Zn/Co/Cd efflux transporter was also seen in the *A. baumannii zur* mutant (Mortensen *et al.* 2014).

The reduced expression of *zur* in the $\Delta rpmE1$ mutant under Zn²⁺-replete conditions would not be expected to affect the expression of the RND efflux transporter system (A1S_3217-3219) as it does not contain a Zur-binding site. This is supported by transcriptomic analysis of an *A. baumannii* Δzur mutant which showed there was no change in expression of the RND efflux protein (Mortensen *et al.* 2014). However, this RND system may be involved in Zn²⁺ homeostasis as approximately a 20-fold decrease in expression in the WT ATCC 17978 strain when grown under Zn²⁺ limitation (see Section 3.2.5) was observed. The unchanged

expression of the RND efflux system in the $\Delta rpmE1$ mutant grown under Zn^{2+} -replete conditions indicates that these genes respond to Zn^{2+} levels despite being independent of the *zur* regulatory system.

Surprisingly, there was a large increase (46-fold) in the expression of A1S_0092-0093 in the $\Delta rpmE1$ mutant (see Appendix 4). These genes encode a ferric siderophore receptor and a putative membrane protein, respectively, and similarly lack a Zur-binding motif up-stream of the transcriptional start; interestingly A1S_0092 was up-regulated in the *zur* mutant by 33-fold (Mortensen *et al.* 2014). This led to the hypothesis that these genes are regulated by Zn^{2+} levels or they may be indirectly regulated by *zur*. It is clear that these genes respond to Zn^{2+} levels as their expression was up-regulated by 72-fold when the WT ATCC 17978 strain was grown under Zn^{2+} -limited conditions (see Section 3.2.5). It is possible that these genes play a role in Zn^{2+} homeostasis, rather than Fe^{2+} homeostasis, as a previous study by Eijkelkamp *et al.* (2011a) showed that the expression of these genes did not change when *A. baumannii* ATCC 17978 was grown in Fe^{2+} -limited medium. The expression of the Zn^{2+} -uptake genes *znuBC* (A1S_0144 and A1S_0143) were down-regulated which is likely due to the fact that these genes are transcriptionally coupled (*i.e.* expression driven by the same promoter) with *zur*.

In summary, the deletion of *rpmE1* in *A. baumannii* ATCC 17978 resulted in the reduced expression of *zur*. However, there is no clear mechanism that can explain this effect. One hypothesis is that the absence of the Zn^{2+} -binding RpmE1 protein indirectly affects *zur* expression due to an alteration in the intracellular levels of bound Zn.

5.2.3.1.3 The effect of the inactivation of *rpmE1* on the expression of the type VI secretion system

The inactivation of *rpmE1* in *A. baumannii* ATCC 17978 also resulted in a decrease in the expression of genes within the T6SS locus (A1S_1292-1310), ranging between 1.9- to 4.8-fold (Figure 5.4). T6SS are present in a wide range of Gram-negative bacterial species as described in Section 1.3.6 and act as a bacterial

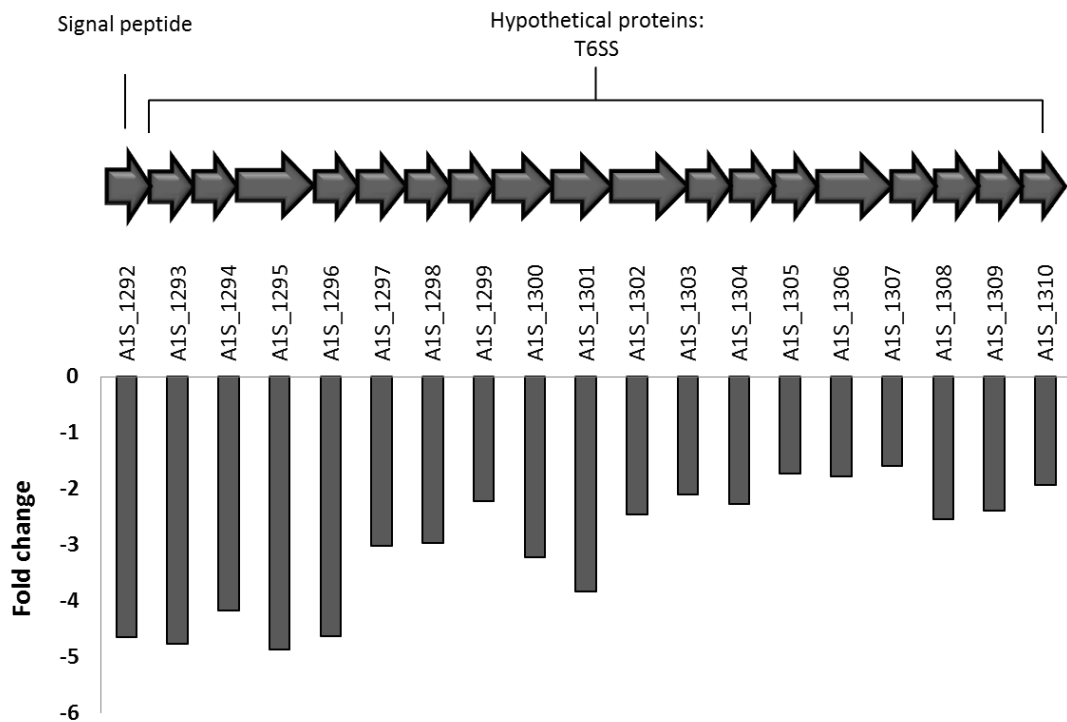


Figure 5.4: RNA expression of genes within the A1S_1292-1310 cluster encoding the T6SS in *A. baumannii* ATCC 17978 $\Delta rpmE1$ compared to WT under Zn^{2+} -replete conditions

Arrows represent ORFs and their direction of transcription. Square brackets indicate ORFs which encode separate functional regions of the protein described. The graph shows the fold change (Y axis) in RNA expression for each ORF (bars), as determined by RNA-seq analysis.

macromolecular machine that transports effector proteins into eukaryotic host cells or other bacteria (Ruiz *et al.* 2015). The T6SSs have also been identified for their roles in bacterial competition and pathogenicity in a number of pathogens (see Section 1.3.6). The role of the T6SS system in *Acinetobacter* spp. has been shown to be limited to intra- and inter-species competition; this T6SS is involved in inter-bacterial competition of *Acinetobacter nosocomialis* M2 (Carruthers *et al.* 2013).

5.2.3.1.4 The effect of inactivation of *rpmE1* on the expression of genes involved in bacterial carbohydrate metabolism

Transcriptomic analysis of the $\Delta rpmE1$ mutant grown in Zn^{2+} -replete conditions revealed reduced expression (5- to 21-fold) of the A1S_1699-1705 locus, predicted to be involved in acetoin degradation. As previously mentioned (see Section 3.2.5.7), acetoin is an important physiological metabolite excreted by many microorganisms and an important external carbon storage material for bacterial cells during growth (Huang *et al.* 1999).

The deletion of *rpmE1* resulted in 16-fold reduced expression of the acetoin-2-6-dichlorophenolindophenol oxidoreductase α/β subunit (ORFs A1S_1699-1700) and decreased expression of genes encoding the acetoin degradation enzymes, acetoin dehydrogenases (A1S_1704-1705) (Figure 5.5). The reduced expression of this locus was also observed when ATCC 17978 was grown in Zn^{2+} -limited medium (see Section 3.2.5.7). The reduced expression of these acetoin degradation genes in the $\Delta rpmE1$ mutant during growth in Zn^{2+} -replete conditions indicates that the availability of intracellular Zn^{2+} may mimic that within cells grown under Zn^{2+} -limited conditions (see Section 4.2.4). The lower levels of expression from the acetoin catabolic genes may lead to a reduced ability to survive in a hostile environment particularly when the bacterial cell needs to use other carbon and energy sources.

Similarly, the expression of the dihydrolipoamide acetyltransferase gene (A1S_1701) within this locus in the $\Delta rpmE1$ mutant showed a 21-fold reduction in expression. In the WT ATCC 17978 strain grown in Zn^{2+} -limited medium, this locus also showed reduced expression (see Section 3.2.5.7). In addition, there was a 13- to 14-fold reduced expression of the dihydrolipoamide dehydrogenase (DLDH) gene. However, there is no clear link between *rpmE1* inactivation and a change in

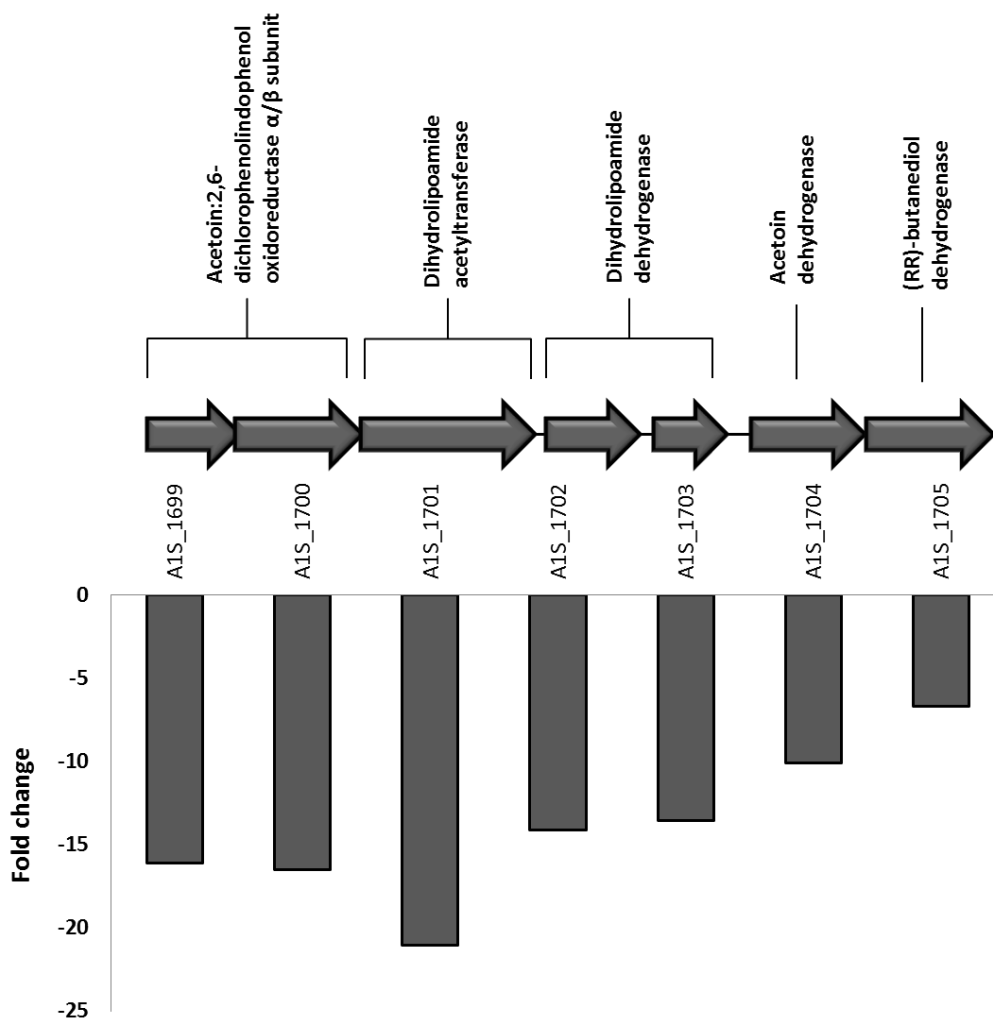


Figure 5.5: RNA expression of genes within the A1S_1699-1705 cluster in *A. baumannii* ATCC 17978 $\Delta rpmE1$ mutant compared to the WT under Zn^{2+} -replete conditions

Arrows represent ORFs and their direction of transcription. Square brackets indicate ORFs which encode separate functional regions of the protein(s) described. The graph shows the fold change (Y axis) in RNA expression for each ORF (bars) as determined by RNA-seq analysis.

expression of the DLDH enzyme as it does not appear to bind Zn^{2+} unlike the Zn^{2+} -dependent dehydrogenases described above. It is proposed that the Zn^{2+} and Fe^{2+} metal chelator EDTA does not involve in the inactivation of this enzyme (Yan *et al.* 2013).

A gene locus comprised of A1S_1880-1894 was identified as having significantly reduced expression in the $\Delta rpmE1$ mutant (Figure 5.6). This locus includes genes involved in carbohydrate metabolism, specifically for the use of aromatic amino acids as carbon sources (Weber *et al.* 2012). These genes were also identified as having a reduced expression in the WT cells when grown in Zn^{2+} -limited medium (see Section 3.2.6.3). This may indicate that the ability of the *rpmE1* mutant to use aromatic amino acids as a carbon source is reduced which may have an effect on bacterial growth even if the cells are grown in Zn^{2+} -replete culture. In other species, including *Salmonella* spp. and *M. tuberculosis*, mutations in aromatic amino acid biosynthetic genes have been used to successfully attenuate strains (Parish and Stoker 2002; Sebkova *et al.* 2008). The reduced virulence of such mutants was due to their inability to produce aromatic metabolites including phenylalanine, tyrosine, and tryptophan. Since these amino acids are not freely available inside a host, aromatic acid bacterial mutants are usually incapable of replication within the host (Sebkova *et al.* 2008).

Taken together, the decreased expression of these carbohydrate metabolism gene loci suggests that the inactivation of *rpmE1* effectively mimics Zn^{2+} -limited conditions inside the bacterial cell, even in a Zn^{2+} -replete environment.

5.2.3.1.5 The effect of inactivation of *rpmE1* on the expression of genes involved in lipid metabolism

The genes encoding the LipA lipase (A1S_3160) and lipase foldase (A1S_3159) showed 8- and 5-fold decreased expression, respectively, in the $\Delta rpmE1$ mutant (Figure 5.1). Lipases are esterase enzymes that catalyse the hydrolysis of acyl ester-bond containing substrates, allowing the release of fatty acids from the alcohol backbone (Pandey *et al.* 1999). In some bacteria, lipases require a specific chaperone-like protein, called a lipase-specific foldase or Lif-protein, which assists in

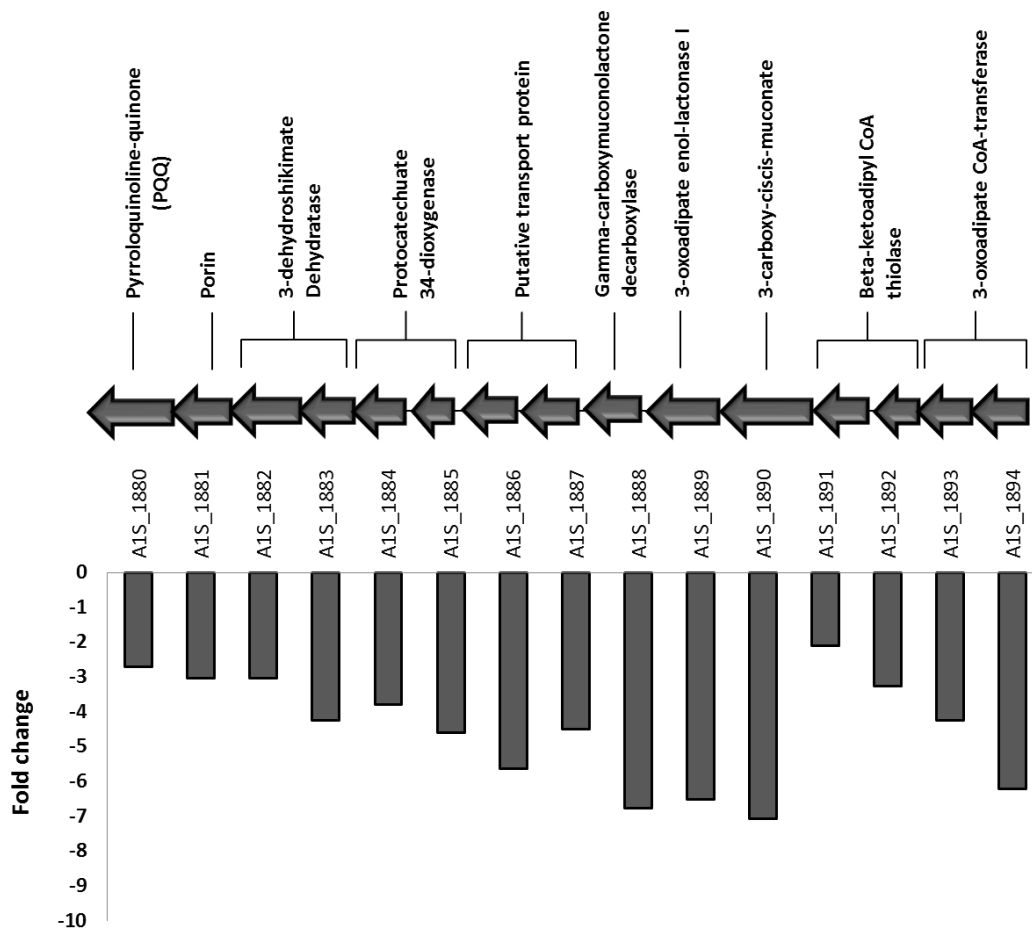


Figure 5.6: RNA expression of genes within the A1S_1880-1894 cluster in *A. baumannii* ATCC 17978 $\Delta rpmE1$ mutant compared to the WT under Zn^{2+} -replete conditions

Arrows represent ORFs and their direction of transcription. Square brackets indicate ORFs which encode separate functional regions of the protein(s) described. The graph shows the fold change (Y axis) in RNA expression for each ORF (bars), as determined by RNA-seq analysis.

the correct folding of the enzyme within the periplasm (Jaeger *et al.* 1994). The *A. baumannii* Lif-protein (A1S_3159) shows a high degree of amino acid sequence identity with Lif-proteins in other *Acinetobacter* species and its gene is located immediately up-stream of that for the lipase (A1S_3160). The ability to produce lipase is a potential virulence factor in bacteria as secreted lipases may play a role in supporting growth and colonisation during an infection. Lipases can cleave sebum-derived triacylglycerols (Stehra *et al.* 2003), providing nutrition and enhancing the ability of the bacteria to spread. In particular, it has been postulated that lipases may contribute to the pathogenesis of *Staphylococcal* species during a skin infection. *In vitro* studies have shown that purified lipase can affect some functions in human immune cells, such as the chemotaxis of neutrophils and granulocytes (Stehra *et al.* 2003).

In *P. aeruginosa*, a two-component regulatory system has been identified that controls the transcription of an operon that encodes a lipase that is secreted via a type II pathway (Rosenau and Jaeger 2000). However, the molecular mechanisms regulating lipase gene expression in most bacteria are unknown. What is understood is that the release of an enzymatically active lipase into the extracellular medium by a Gram-negative bacterium would require the concerted action of various bacterial cellular processes, culminating in the translocation of the lipase through both the inner and the outer membranes (Rosenau and Jaeger 2000).

It has been shown in other bacteria that lipases require metals either for, or to enhance, activity and (thermo) stability (Salameh and Wiegel 2007). Moreover, it has been revealed from the crystal structure of the lipase from *Geobacillus stearothermophilus* that the Zn²⁺-binding domain stabilised the structure of the enzyme (Carrasco-Lopez *et al.* 2009; Salameh and Wiegel 2007). The function and structural characteristics of lipases in *A. baumannii* ATCC 17978 have not been elucidated, however, the reduced expression of the genes encoding LipA and the lipase foldase in the $\Delta rpmE1$ mutant indicates that the encoded proteins are either directly or indirectly affected by the absence of the Zn²⁺-binding RpmE1 protein.

5.2.3.2 The effect of inactivation of *rpmE2* on the transcriptome of *A. baumannii* ATCC 17978 under Zn²⁺-replete conditions

To understand the transcriptional effects of deletion of the other L31 gene, *rpmE2* in *A. baumannii* ATCC 17978, RNA-seq data generated from the $\Delta rpmE2$ strain grown in Zn²⁺-replete conditions was compared to data generated from the WT strain grown under the same conditions. The comparison revealed that only 26 genes showed significantly increased expression (> 2-fold) (Appendix 7), with the most over-expressed (5-fold) gene (A1S_0737) encoding a 5-methyltetrahydropteroyltriglutamate-homocysteine S-methyltransferase. The majority of the differentially-expressed genes showed reduced expression (192 genes, > 2-fold) (Appendix 8).

The RNA-seq results were validated by qRT-PCR analysis using the same subset of differentially-expressed genes and gene-specific oligonucleotides described previously. The correlation between the RNA-seq and qRT-PCR data was performed by comparing gene expression in the $\Delta rpmE2$ mutant grown under Zn²⁺-limited and Zn²⁺-replete conditions (Table 5.2). This comparison was chosen instead of comparing the expression of the mutant and the WT in Zn²⁺-replete conditions (as was performed for the $\Delta rpmE1$ mutant) as many of the genes used for the correlation studies were not differentially expressed between the $\Delta rpmE2$ mutant and the WT under Zn²⁺-replete conditions. A high correlation (0.95) between data from the qRT-PCR and the RNA-seq analyses was observed (Figure 5.7).

Unlike the transcriptional changes observed in the $\Delta rpmE1$ mutant, the deletion of *rpmE2* caused increased expression (between 2- to 3-fold) of a set of genes encoding ribosomal proteins, including A1S_3068 that encodes the S14 (RspN) ribosomal protein (Figure 5.8). As previously discussed (see Section 1.6), *B. subtilis* has an S14 protein as well as a paralogous protein, YhzA, that is Zur-regulated. The S14 protein is essential for the assembly of the ribosome, and YhzA has been suggested to play role in ribosome synthesis to support S14 function in the absence of available zinc (Gabriel and Helmann 2009). However, in ATCC 17978, there is no paralog for S14. Nevertheless, it is suggested that the increased expression of the S14 protein in $\Delta rpmE2$ ATCC 17978 during growth under Zn²⁺-

Table 5.2: Validation of transcriptomic data generated from the ATCC 17978 *ΔrpmE2* mutant grown in Zn²⁺-limited and Zn²⁺-replete conditions by comparison of expression levels determined by RNA-seq and qRT-PCR analysis

| Locus tag | RNA-seq (Log ₂) | qRT-PCR (Log ₂) |
|-----------|-----------------------------|-----------------------------|
| A1S_0452 | 2.572 | 1.675 |
| A1S_0146 | 2.279 | 3.580 |
| A1S_0145 | 0.773 | 1.560 |
| A1S_0092 | 5.645 | 5.660 |
| A1S_3217 | -4.869 | -5.940 |
| A1S_1217 | -0.174 | 0.380 |

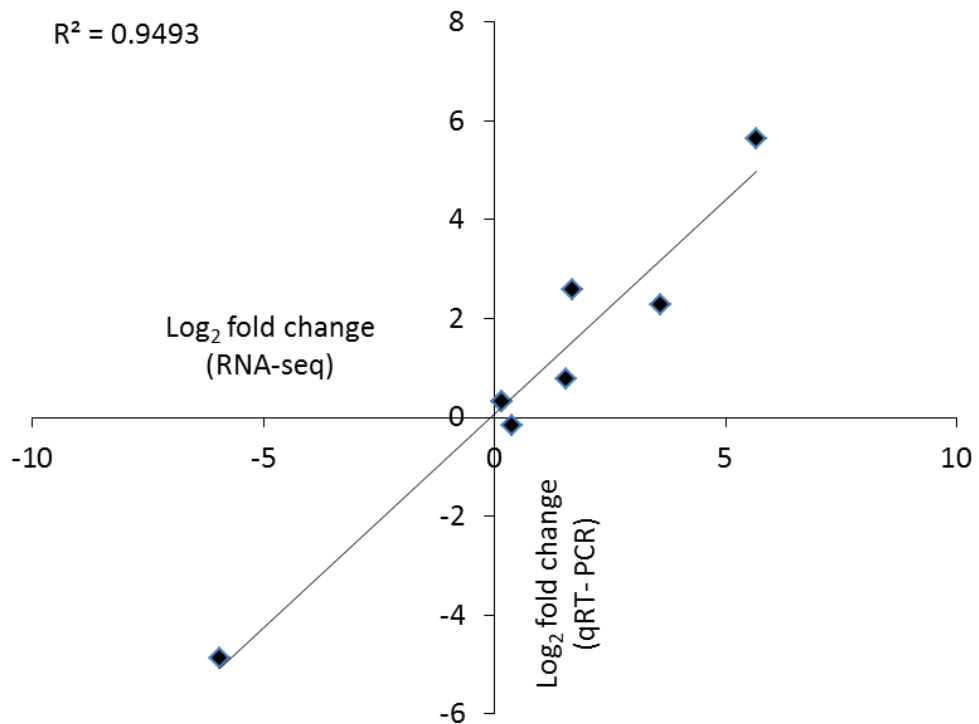


Figure 5.7: Correlation of Log₂-based fold changes for six genes showing altered expression in the *A. baumannii* ATCC 17978 Δ *rpmE2* mutant grown in Zn²⁺-limited and Zn²⁺-replete conditions

The Y axis represents the Log₂-fold change of gene expression determined by qRT-PCR and the X axis represents the Log₂-fold change of gene expression determined by RNA-seq data. Derived from the RNA-seq and qRT-PCR data, a correlation coefficient (R^2) of 0.9493 was determined.

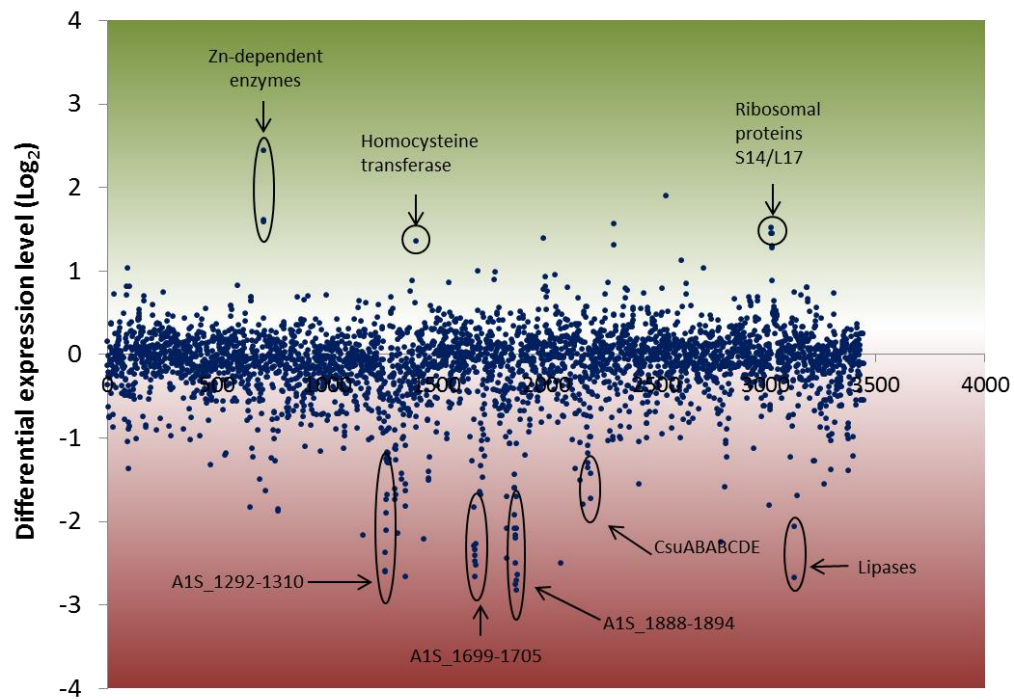


Figure 5.8: Transcriptional changes in the ATCC 17978 $\Delta rpmE2$ mutant in response to growth in Zn^{2+} -replete conditions

Comparison of the global RNA expression of the *A. baumannii* ATCC 17978 $\Delta rpmE2$ and WT strains grown in Zn^{2+} -replete conditions. The expression levels of all 3500 genes in the ATCC 17978 genome were measured by RNA-seq and are represented on the X-axis in order of ascending locus-tag number (Smith *et al.* 2007). Differential gene expression levels in the ATCC 17978 $\Delta rpmE2$ cells are displayed in Log_2 -values on the Y-axis. Genes with increased and decreased expression are displayed in the green and red sections, respectively. The circled dots indicate selected genes that were differentially expressed by the $\Delta rpmE2$ during growth in Zn^{2+} -replete conditions.

replete conditions may be one of the mechanisms to compensate for the loss of RpmE2 in this mutant. This is supported by the increased expression of other ribosomal proteins in the $\Delta rpmE2$ mutant. Interestingly, there was no change in the expression of *rpmE1* yet this would appear to be the easiest way to compensate for the loss of RpmE2. Other genes that increased in expression in the $\Delta rpmE2$ mutant included the enzymes homocysteine transferase (A1S_0737) and flavoprotein reductase (A1S_0738) which increased by 5.5- and 3-fold, respectively (Figure 5.8). These enzymes are involved in methionine metabolism and require Zn^{2+} as a cofactor.

In contrast, other gene loci showed a decrease in expression in the $\Delta rpmE2$ mutant grown in Zn^{2+} -replete conditions, including genes encoding LipA (A1S_3160) and the lipase foldase (A1S_3159), 8- and 4-fold decreased expression, respectively (Figure 5.8). In addition, the expression of genes encoding A1S_1292-1310, A1S_1699-1705, A1S_1880-1894, and CsuABABCDE (Figure 5.8) were also significantly reduced. Genes in these loci will be discussed in detail in the following sections.

5.2.3.2.1 COG functional categories

The RNA-seq data generated from the $\Delta rpmE2$ mutant grown in Zn^{2+} -replete conditions were used to categorise the differentially-expressed gene products into COGs (Figure 5.9). Analysis of genes displaying reduced expression revealed that more than 12% of the genes identified in the $\Delta rpmE2$ mutant encoded proteins involved in lipid metabolism, 8% of genes are involved in secondary metabolites biosynthesis, transport, and catabolism, and 8% of genes are involved in energy production and conversion (Figure 5.9), including those in the gene locus A1S_1699-1705 (4.8- to 5.5-fold down-regulated). The gene with the most reduced expression (6-fold) in the $\Delta rpmE2$ mutant was A1S_1894, located with the A1S_1880-1894 locus. Approximately 4% of the genes identified with reduced expression were within the cell motility COG and were specific to the Csu pili (A1S_2214-2219) (Figure 5.9). However, the down-regulation of Csu pili in this mutant strain did not result an observable effect in the motility assay (see Section 4.2.6.2). Although most of the differentially expressed genes identified in the $\Delta rpmE2$ mutant showed

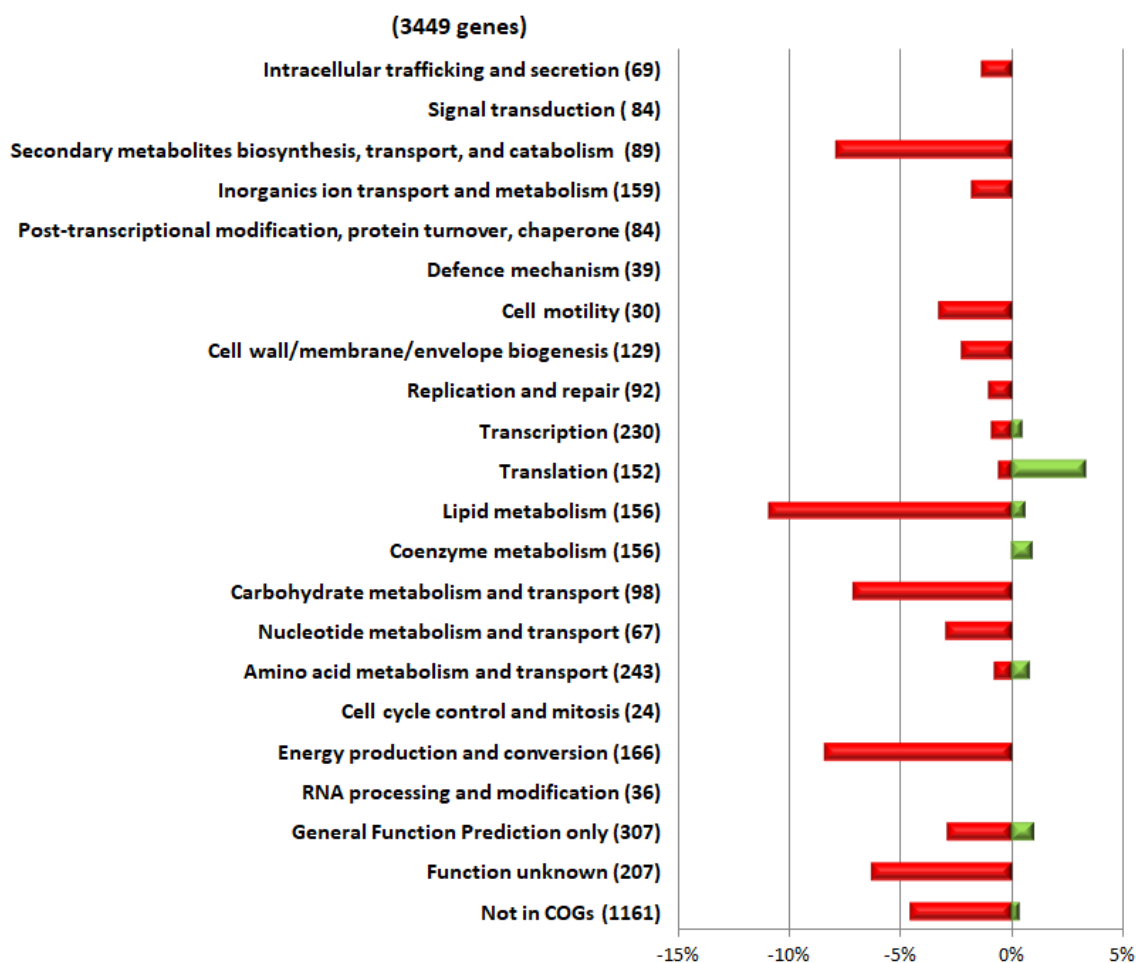


Figure 5.9: Transcriptional changes in the ATCC 17978 $\Delta rpmE2$ mutant relative to WT when both are grown in Zn^{2+} -replete conditions, displayed by COG function

The percentage of differentially expressed genes (≥ 2 -fold as determined using RNA-seq) belonging to each COG category is shown. Genes that exhibited a reduction in expression in the $\Delta rpmE2$ mutant relative to the WT when grown under Zn^{2+} -replete conditions are shown in red and genes with increased expression are shown in green. The total number of differentially expressed genes per COG is shown in parentheses.

down-regulation, two ribosomal genes (A1S_3055 and A1S_3060) encoding 50S ribosomal protein L17 (Figure 5.8) and the 50S ribosomal protein L36 (RpmJ), respectively, had increased expression. The increase in expression of these ribosomal proteins suggests that the cell may be trying to compensate for the loss of RpmE2 in order to maintain functional ribosomes.

Based on the data, inactivation of the *rpmE2* gene in ATCC 17978 resulted in the differential expression of a significant number of genes during growth in Zn²⁺-replete medium with most showing a decrease in expression. Similar to that observed with the $\Delta rpmE1$ mutant grown in Zn²⁺-replete medium, the $\Delta rpmE2$ mutant had reduced expression of the gene loci A1S_1292-1310, A1S_1699-1705, and A1S_1880-1894 encoding a T6SS, lipid and carbohydrate metabolism enzymes, respectively. However, the products of many of the genes identified could not be assigned to any COG functional grouping. Nevertheless, the RNA-seq data showed that the deletion of *rpmE2* influenced a number of processes in *A. baumannii*. Additionally, further comparison of the RNA-seq data revealed that deletion of either *rpmE* gene resulted in expression changes to a common set of genes (see below).

5.2.3.2.2 The effect of deletion of *rpmE2* on the heat shock protein HtpG

One gene, A1S_2823, encoding the heat shock protein HtpG, was identified as having a 4-fold decrease in expression in the $\Delta rpmE2$ mutant but there were no changes in its expression in the $\Delta rpmE1$ mutant. HtpG is an ATP-dependent molecular chaperone that is required for the activation and stabilisation of proteins, many of which are involved in important cellular pathways (Nakamoto *et al.* 2014). HtpG is reported to be important for survival in high temperatures and when under oxidative stresses in cyanotic bacteria (Nakamoto *et al.* 2014). Moreover, the eukaryotic homologue of HtpG is thought to be involved in phagocytosis and/or in bactericidal activity against bacteria in host cells (Yan *et al.* 2004). Its potential role in oxidative stress survival may explain the reduced ability of the *A. baumannii* ATCC 17978 $\Delta rpmE2$ strain to resist paraquat treatment (see Section 4.2.6.5). Interestingly, a proteomic study in *E. coli* reported an interaction between HtpG and 15 proteins including five ribosomal proteins (L2, L29, L33, S6 and S7) (Butland *et al.*

2005). In a separate study, HtpG was shown to be associated with the L2 50S ribosomal protein whereby L2 activates the ATPase function of HtpG (Motojima-Miyazaki *et al.* 2010). However, the function of this protein in *A. baumannii* is not clearly understood.

5.2.3.3 Comparison of ATCC 17978 *rpmE1* and *rpmE2* inactivated strains under Zn^{2+} -replete conditions

As previously discussed (Section 1.9), *rpmE2* has a Zur-binding site upstream. When intracellular levels of Zn^{2+} are low the RpmE2 protein can mobilise Zn^{2+} bound to RmpE1, by displacing RmpE1 from the ribosome complex leading to Zn^{2+} liberation (Section 1.9.2). The RNA-seq data revealed that the deletion of *rpmE2* from *A. baumannii* ATCC 17978 resulted in more differentially-expressed genes showing decreased rather than increased expression. These include A1S_1292-1310 (Figure 5.10), A1S_1699-1705 (Figure 5.11) and A1S_1880-1894 (Figure 5.12). The A1S_1292-1310 locus was down-regulated in both the $\Delta rpmE1$ and $\Delta rpmE2$ mutants; ranging from 2.4- to 6-fold in the $\Delta rpmE2$ mutant (Figure 5.10) and 1.9- to 4.8-fold in the $\Delta rpmE1$ mutant (Figure 5.4). The down-regulation of the A1S_1880-1894 locus, encoding proteins required for the use of aromatic amino acids as carbon sources, was also similar in both $\Delta rpmE1$ and $\Delta rpmE2$ mutants ranging from 2- to 7-fold and 2- to 8-fold, respectively) (Figures 5.6 and 5.12). In contrast, the down-regulation of genes within the A1S_1699-1705 locus differed between the two mutants; the expression from this locus in the $\Delta rpmE1$ mutant was highly affected with down-regulated by 6.8- to 21-fold whereas in the $\Delta rpmE2$ mutant expression was down-regulated by only 5- to 6-fold.

Together, the common gene expression changes found in the $\Delta rpmE1$ and $\Delta rpmE2$ mutants show an association between these ribosomal proteins beyond sharing the same function as a part of the ribosomal complex.

5.2.3.4 Shared and unique genes with altered expression in $\Delta rpmE1$ and $\Delta rpmE2$ mutants in Zn^{2+} -replete conditions

In order to obtain a clearer picture of the unique and common sets of genes between the two mutants with respect to transcription levels, differential

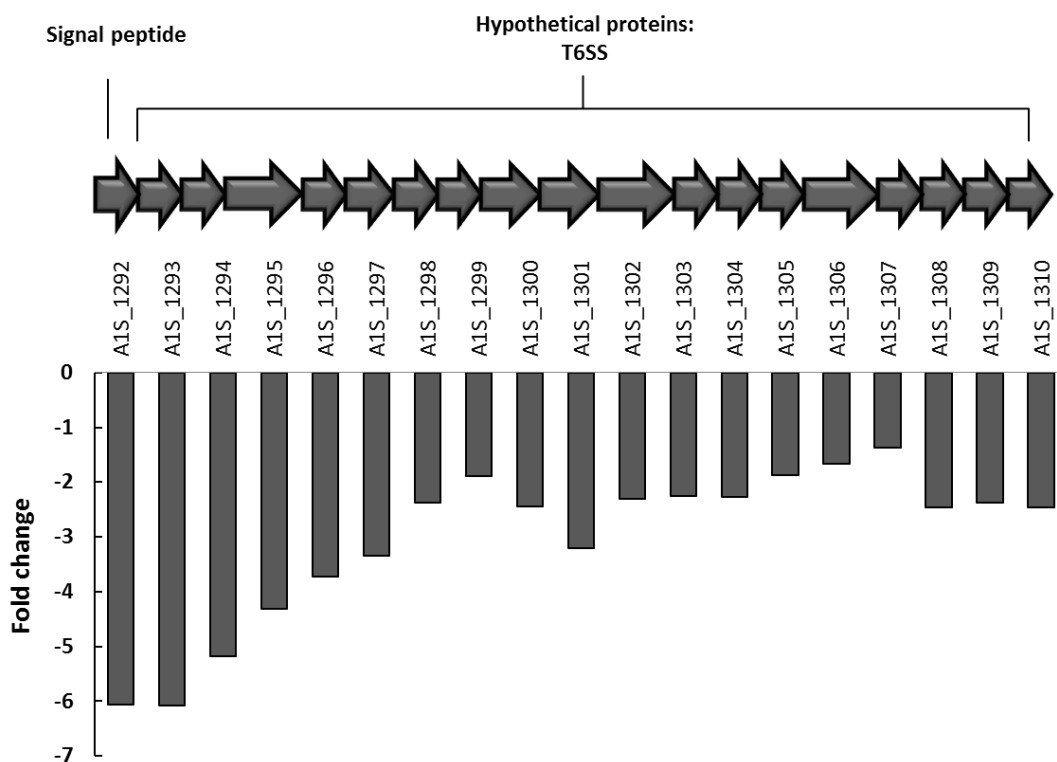


Figure 5.10: RNA expression of genes within the T6SS A1S_1292-1310 cluster in *A. baumannii* ATCC 17978 $\Delta rpmE2$ compared to WT under Zn^{2+} -replete conditions

Arrows represent ORFs and their direction of transcription. Square brackets indicate ORFs which encode separate functional regions of the protein(s) described. The graph shows the fold change (Y axis) in RNA expression for each ORF (bars), as determined by RNA-seq analysis.

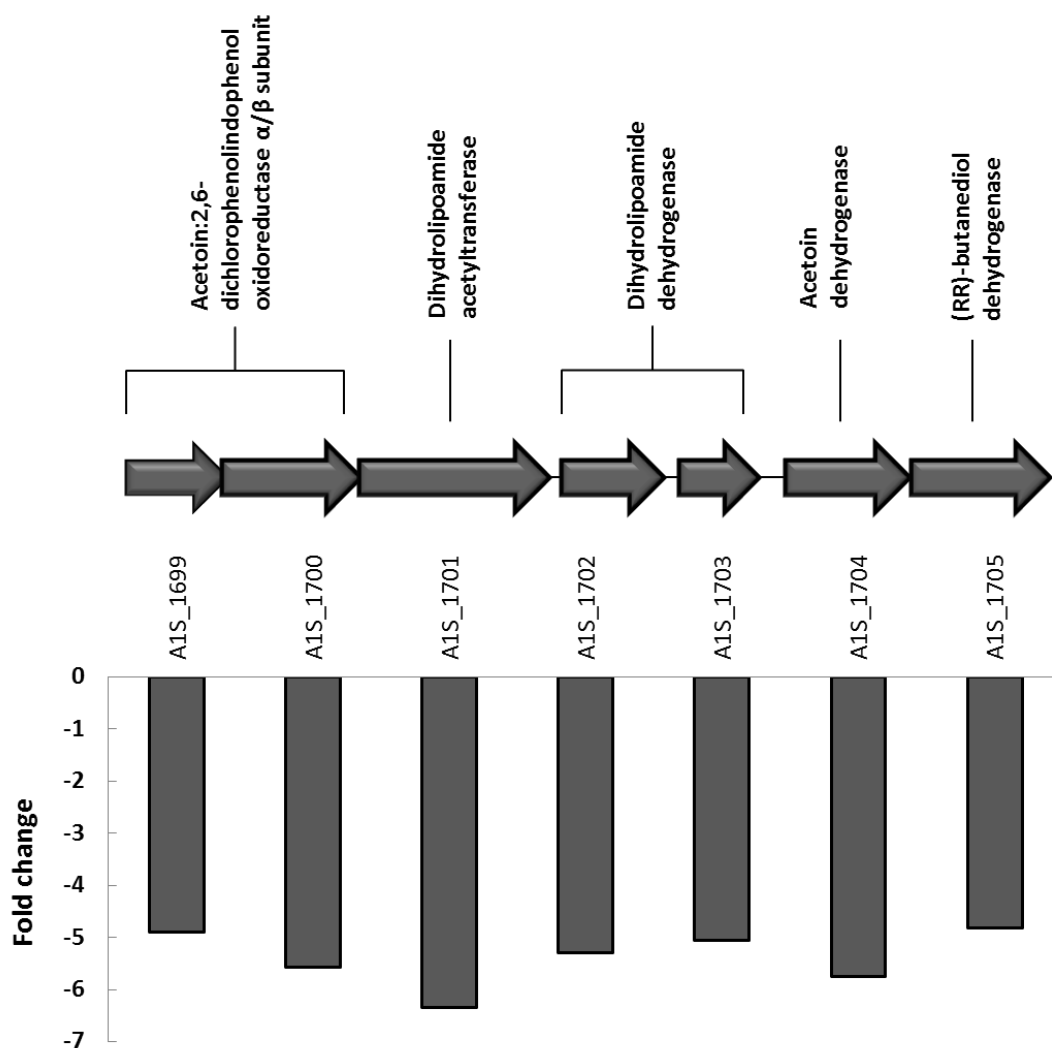


Figure 5.11: RNA expression of genes within the A1S_1699-1705 cluster in $\Delta rpmE2$ 17978 *A. baumannii* ATCC 17978 compared to WT under Zn^{2+} -replete conditions

Arrows represent ORFs and their direction of transcription. Square brackets indicate ORFs which encode separate functional regions of the protein(s) described. The graph shows the fold change (Y axis) in RNA expression for each ORF (bars), as determined by RNA-seq analysis.

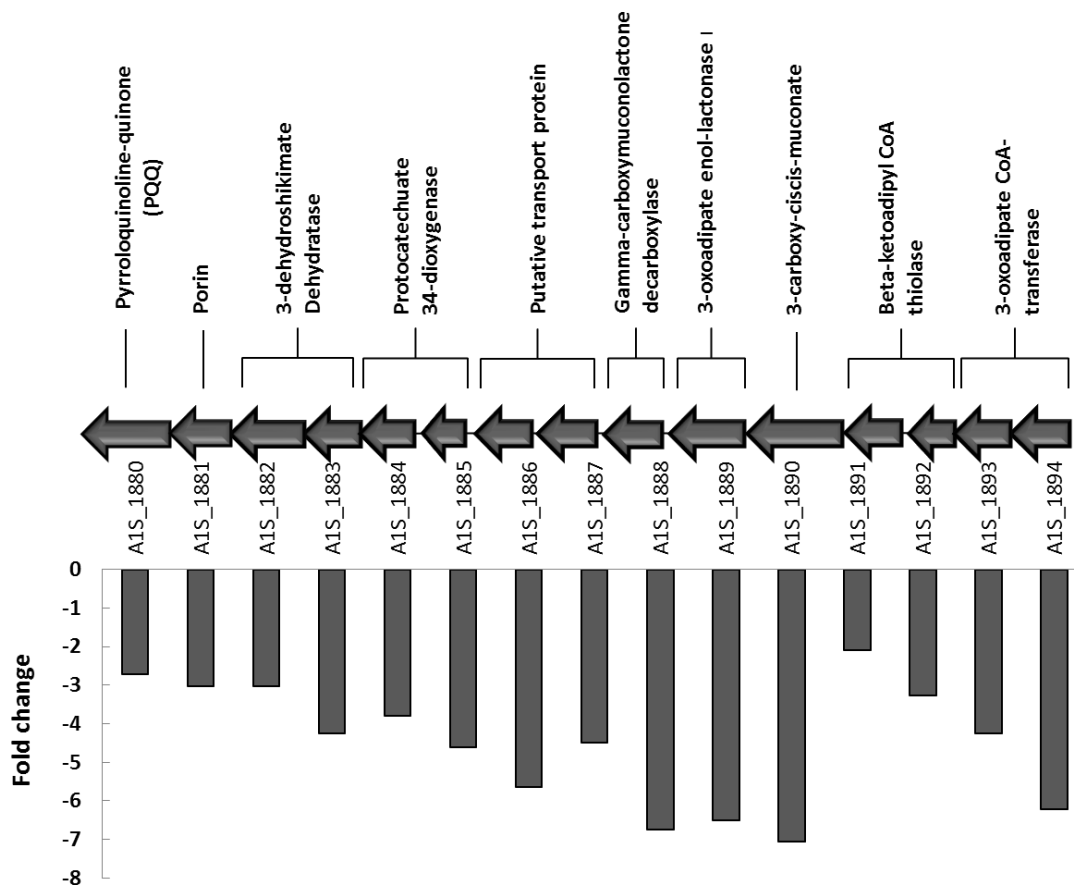


Figure 5.12: RNA expression of genes within the A1S_1880-1894 cluster in *A. baumannii* ATCC 17978 $\Delta rpmE2$ compared to WT under Zn²⁺-replete conditions

Arrows represent ORFs and their direction of transcription. Square brackets indicate ORFs which encode separate functional regions of the enzyme described. The graph shows the fold change (Y axis) in RNA expression for each ORF (bars), as determined by RNA-seq analysis.

expression analyses were performed by comparing RNA-seq data sets. Venn diagrams were constructed of genes that showed alterations in expression of ≥ 2 -fold when the $\Delta rpmE1$ and $\Delta rpmE2$ strains were grown in Zn^{2+} -replete medium. This section will provide a summary of the shared and unique genes previously discussed in Sections 5.2.3.1 and 5.2.3.2 and also will briefly discuss other genes which have not been considered before.

The Venn diagrams, Figures 5.13 and 5.14, show genes that were up-regulated and down-regulated when either *rpmE1* or *rpmE2* were inactivated and grown in Zn^{2+} -replete conditions. These include genes encoding the homocysteine methyltransferase (A1S_0737), flavoprotein oxidoreductase (A1S_0738), methylenetetrahydrofolate reductase (A1S_2335) and S-adenosyl-L-homocysteine (SAH) hydrolase (A1S_2334) (Figure 5.13). Methylenetetrahydrofolate reductase is a transferase that participates in methionine metabolism and requires two cofactors, orthophosphate and Zn^{2+} , to transfer one-carbon groups. SAH hydrolase is involved in the metabolic pathway of sulphur-containing amino acids and a variety of biological methylation (Sganga *et al.* 1992); its expression is affected by the deletion of either of the L31 proteins. Genes that exhibited an increase in expression in the $\Delta rpmE1$ mutant only (Figure 5.13) were largely those regulated by Zur. These included genes encoding TonB ExbB/D, a G3E-family protein, ZnuA, RpmE2, and the TonB receptor protein. In addition, A1S_0092, which encodes a ferric siderophore receptor protein that lacked a Zur-binding site, showed increased expression in the $\Delta rpmE1$ mutant. A number of ribosomal proteins (A1S_3055-3059) showed an increase in expression only in the $\Delta rpmE2$ mutant.

The second Venn diagram (Figure 5.14) depicts genes which were down-regulated in one or both mutants compared to WT when grown in Zn^{2+} -replete conditions. This revealed that 114 genes were down-regulated in both mutants; 21 genes were only down-regulated in the $\Delta rpmE2$ strain and 139 only in the $\Delta rpmE1$ strain. As previously discussed, down-regulated genes in both *rpmE* mutants included those in gene loci A1S_1292-1304, A1S_1883-1894 and A1S_2215-2218, indicating that the loss of either L31 protein from *A. baumannii* affected the expression of these genes. On the other hand, gene expression changes unique to the $\Delta rpmE1$ mutant included the down-regulation of *znuB*, *znuC* and *zur*.

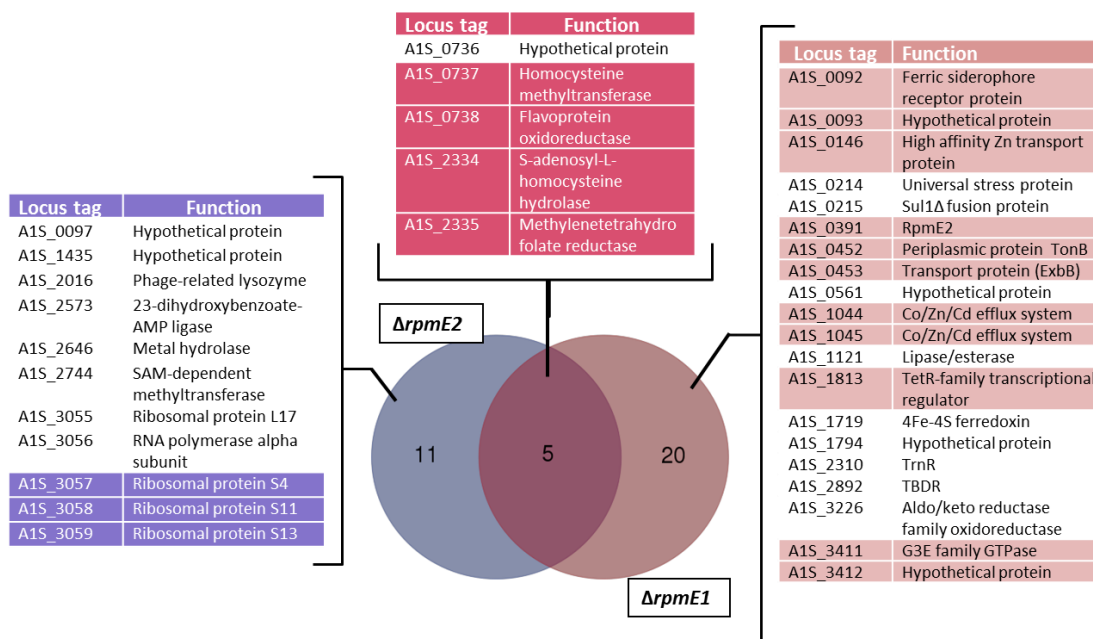


Figure 5.13: Comparison of up-regulated genes in the $\Delta rpmE1$ and $\Delta rpmE2$ mutants compared to WT when grown in Zn^{2+} -replete conditions

The Venn diagram shows shared (rose) and unique genes which are over-expressed (≥ 2 -fold) in the $\Delta rpmE1$ (pink) and $\Delta rpmE2$ mutants (blue) during growth in Zn^{2+} -replete medium. This analysis identified 11 unique genes over-expressed in the $\Delta rpmE2$ strain and 20 unique genes over-expressed in the $\Delta rpmE1$ strain plus 5 genes that are over-expressed in both strains. The *A. baumannii* ATCC 17978 gene locus tag and predicted protein function for each gene is given in the accompanying tables. The highlighted genes have been discussed in this chapter.

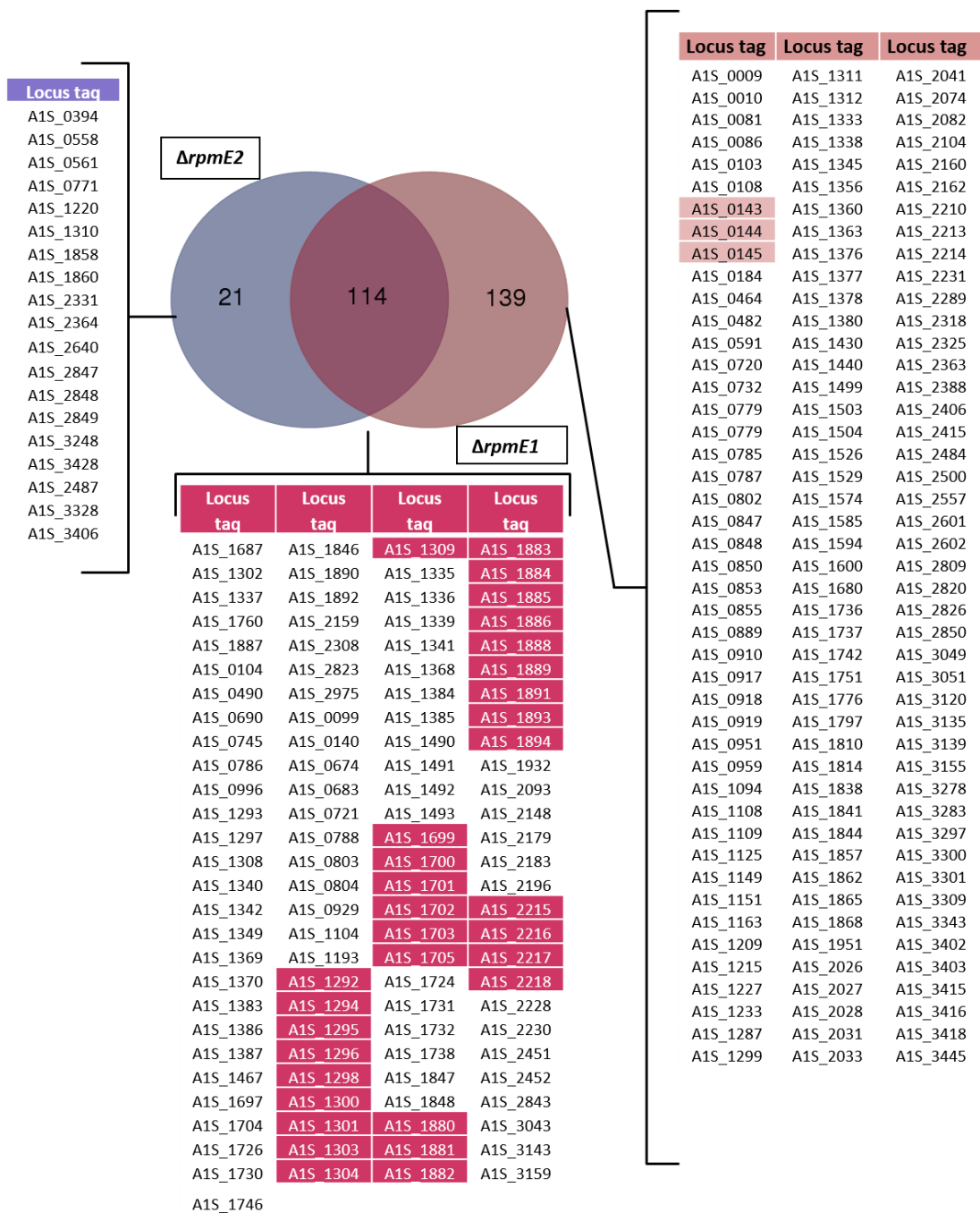


Figure 5.14: Comparison of down-regulated genes in the $\Delta rpmE1$ and $\Delta rpmE2$ mutants compared to WT when grown in Zn^{2+} -replete conditions

The Venn diagram shows shared (rose) and unique genes which show decreased expression (≥ 2 -fold) in the $\Delta rpmE1$ (pink) and $\Delta rpmE2$ mutants (blue) during growth in Zn^{2+} -replete medium. This analysis identified 21 unique genes with decreased expression in the $\Delta rpmE2$ strain and 139 unique genes with decreased expression in the $\Delta rpmE1$ strain plus 114 genes with decreased expression in both strains. The mutants grown under Zn^{2+} -limited conditions were compared to the profile of the *A. baumannii* ATCC 17978 WT strain grown under the same conditions. *A. baumannii* ATCC 17978 gene locus tag and predicted protein function for each gene is given in the accompanying tables. The highlighted genes have been discussed in this chapter.

5.2.4 The effect of Zn²⁺ limitation on the transcriptomes of the *ΔrpmE1* and *ΔrpmE2* mutants

The ability to alternate between the use of the two different L31 proteins in the ribosomal complex has been shown to be a survival mechanism for bacterial cells in conditions where Zn²⁺ is limited (Shin *et al.* 2007). To determine the effect of the deletion of *rpmE1* or *rpmE2* in *A. baumannii* during growth in Zn²⁺-limited conditions transcriptomic analyses were conducted. To do this, the gene expression profiles of the two mutants grown under zinc-limited conditions were compared to the profile of the *A. baumannii* ATCC 17978 WT strain grown under the same conditions.

5.2.4.1 The effect of inactivation of *rpmE1* on gene expression in *A. baumannii* ATCC 17978 grown under Zn²⁺-limited conditions

A comparison was undertaken between the RNA-seq data generated from the *A. baumannii* WT strain ATCC 17978 and the *ΔrpmE1* mutant when both were grown under Zn²⁺-limited conditions (Figure 5.15). The evaluation showed that the majority of differentially-expressed genes in the *ΔrpmE1* mutant were down-regulated (57 genes) with only 26 genes up-regulated ≥ 2 -fold. Genes which were down-regulated included *zur* (16.7-fold), as well as *znuB* (9.2-fold) and *znuC* (5.7-fold). This is in contrast to the 11-fold reduction in *zur* transcript levels when the *ΔrpmE1* mutant was grown in Zn²⁺-replete medium (Section 5.2.3.2). Together, this suggests that the decreased expression of *zur* is independent of Zn²⁺ availability and that the loss of the Zn²⁺-binding RpmE1 protein from the cell is responsible for the changes in *zur* expression (see Section 4.2.4). A number of genes showed increased expression in the *ΔrpmE1* mutant when grown under Zn²⁺-limited conditions that were unchanged when grown in Zn²⁺-replete medium. These included genes encoding ferredoxin (A1S_0945, 7.8-fold) and a transcriptional regulator (A1S_2082, 11-fold) (Figure 5.15).

During growth of the *ΔrpmE1* mutant in Zn²⁺-limited medium, the T6SS (A1S_1292-1310) locus (see Appendix 6) was significantly down-regulated (2.8- to 7.5-fold). These T6SS genes also were down-regulated (2- to 4.8-fold) when this mutant was

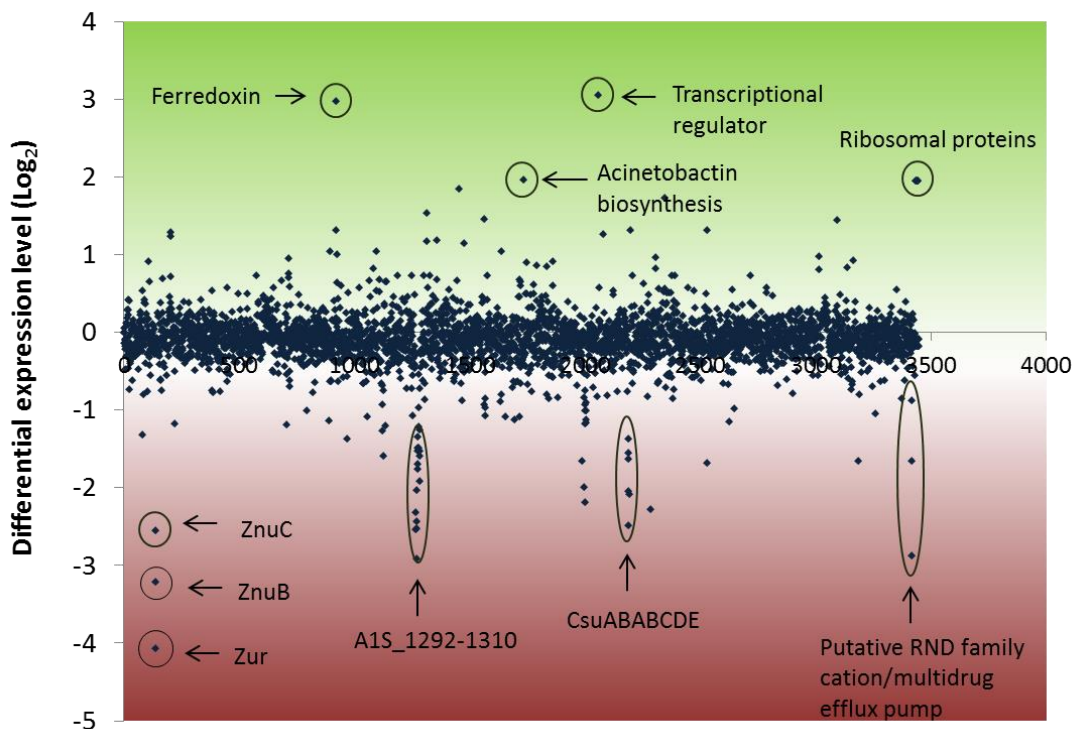


Figure 5.15: Transcriptional changes in the ATCC 17978 $\Delta rpmE1$ mutant in response to growth in Zn^{2+} -limited conditions

Global RNA expression of $\Delta rpmE1$ and WT *A. baumannii* ATCC 17978 strains grown in Zn^{2+} -limited conditions. The expression of all 3500 genes in the genome were measured by RNA-seq and are represented on the X-axis in order of ascending locus-tag number (Smith *et al.* 2007). Differential expression levels between $\Delta rpmE1$ and WT *A. baumannii* ATCC 17978 grown in Zn^{2+} -limited conditions are displayed in Log_2 values on the Y-axis. Genes with increased and decreased expression are displayed in the green and red sections, respectively. The circled dots indicate selected genes differentially expressed during growth in Zn^{2+} -limited conditions.

grown in Zn²⁺-replete conditions (see Section 3.2.8.2) clearly displaying that the changes in expression were not due to the level of Zn²⁺ availability, and indicating that a functional RpmE1 is required for normal expression of this system. Moreover, the Csu pili genes, *csuABABCDE* locus, were also down-regulated in both Zn²⁺-replete (2.5- to 4.2-fold) and Zn²⁺-limited conditions (2.8- to 4.3-fold). This also indicates that Csu pili expression requires a functional RpmE1 protein and is independent of Zn²⁺-availability. Interestingly, the ORFs A1S_3445-3447 which hypothetically function as a multidrug transporter were down-regulated (7-, 3- and 1.8-fold, respectively) in the $\Delta rpmE1$ mutant when compared to expression in the ATCC 17978 WT strain but only when grown in Zn²⁺-limited conditions (Figure 5.15).

5.2.4.2 The effect of inactivation of *rpmE2* on gene expression in *A. baumannii* ATCC 17978 when grown under Zn²⁺-limited conditions

The RNA-seq data generated from the *A. baumannii* WT strain ATCC 17978 grown in Zn²⁺-limited medium were compared to that generated from the $\Delta rpmE2$ mutant, also grown in the same conditions (Figure 5.16). Under Zn²⁺-limited conditions, 90 genes were identified as differentially expressed in the $\Delta rpmE2$ mutant and the majority of these (60 genes) were \geq 2-fold down-regulated. The most highly expressed genes in the $\Delta rpmE2$ mutant encoded ribosomal proteins; 15 ribosomal proteins (A1S_r01 to A1S_r15) showed an increased level of transcription (40- to 50-fold) (see Appendix 9).

The RNA-seq data generated from the $\Delta rpmE2$ mutant grown under Zn²⁺-limited conditions (Figure 5.16) revealed decreased expression of the T6SS genes (2.4- to 4.9- fold). Decreased expression of this system was also observed when the $\Delta rpmE2$ mutant was grown in Zn²⁺-replete conditions (2.4- to 6-fold, Section 5.2.2.2), clearly indicating that altered expression is due to loss of *rpmE2* and not due to Zn²⁺ availability. In addition, the Csu pili genes also showed decreased expression in Zn²⁺-limited medium (1.7- to 4-fold) similar to Zn²⁺-replete medium (1.6- to 2.5-fold) indicating that the changes in expression of the *csu* gene locus in the $\Delta rpmE2$ mutant was in response to *rpmE2* deletion and Zn²⁺ limitation.

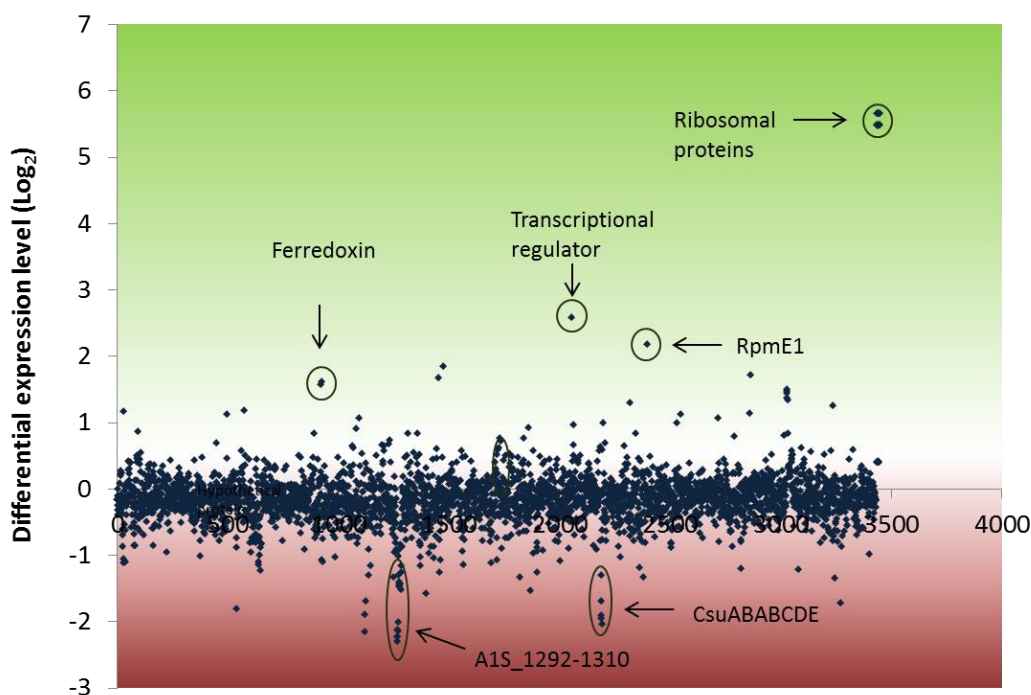


Figure 5.16: Transcriptional changes in the ATCC 17978 $\Delta rpmE2$ mutant in response to growth in Zn^{2+} -limited conditions

Global RNA expression of $\Delta rpmE2$ and WT *A. baumannii* ATCC 17978 grown in Zn^{2+} -limited conditions. The expression of all 3500 genes in the genome were measured by RNA-seq and are represented on the X-axis in order of ascending locus-tag number (Smith *et al.* 2007). Differential expression levels between $\Delta rpmE2$ and WT *A. baumannii* ATCC 17978 grown in Zn^{2+} -limited conditions are displayed in Log_2 values on the Y-axis. Genes with increased and decreased expression are displayed in the green and red sections, respectively. The circled dots indicate selected genes differentially expressed during growth in Zn^{2+} -limited conditions.

5.2.4.3 Shared and unique gene expression changes between the *rpmE1* and *rpmE2* mutants grown in Zn²⁺-limited conditions

The genes that were differentially expressed (≥ 2 fold) in the $\Delta rpmE1$ or $\Delta rpmE2$ mutants compared to WT grown in Zn²⁺-limited medium were identified and are displayed pictorially in Venn diagrams (Figures 5.17 and 5.18). Within the down-regulated group (Figure 5.17) 24 were identified in both mutant strains, 32 are unique to the $\Delta rpmE1$ mutant strain, and 36 are unique to the $\Delta rpmE2$ mutant strain. The 24 shared genes belonged primarily to two gene loci A1S_1292-1310 and *csuABABCDE*. The genes that were unique to the $\Delta rpmE1$ strain included *zur*, *znuB*, *znuC*, A1S_3445 and A1S_3446 (putative RND family cation efflux system). The genes that were unique to the $\Delta rpmE2$ strain included include various genes involved in transport and metabolic processes.

Figure 5.18 shows the up-regulated genes in both mutant strains, six genes were up-regulated in both strains, 20 genes are unique to the $\Delta rpmE1$ strain and 24 are unique to the $\Delta rpmE2$ strain. Among the six common genes, they were five genes encoding ferredoxin reductases and a gene encoding a transcriptional regulator (A1S_2082). The unique genes in the $\Delta rpmE2$ strain largely encoded ribosomal proteins and two encoded proteins with putative signal peptides.

5.3 Conclusions

The paralogous L31 ribosomal proteins RpmE1 and RpmE2 have been shown to play a role in Zn²⁺ homeostasis in bacteria such as *E. coli* and *B. subtilis*, where the RpmE1 protein acts as a source of Zn²⁺ in conditions where Zn²⁺ is limited (Lim *et al.* 2011; Nanamiya *et al.* 2006). It has been demonstrated that the alternate use of these two L31 proteins in Zn²⁺-limited conditions allows for the displacement of RpmE1 from the 50S ribosomal subunit by RpmE2, allowing for the breakdown of RpmE1 and the release of Zn²⁺ molecules (Akanuma *et al.* 2006). The transcriptional changes displayed by the mutation of *rpmE1* and *rpmE2* in *A. baumannii* strains grown under Zn²⁺-limited and Zn²⁺-replete conditions were investigated at the global transcriptional level using RNA-seq analysis.

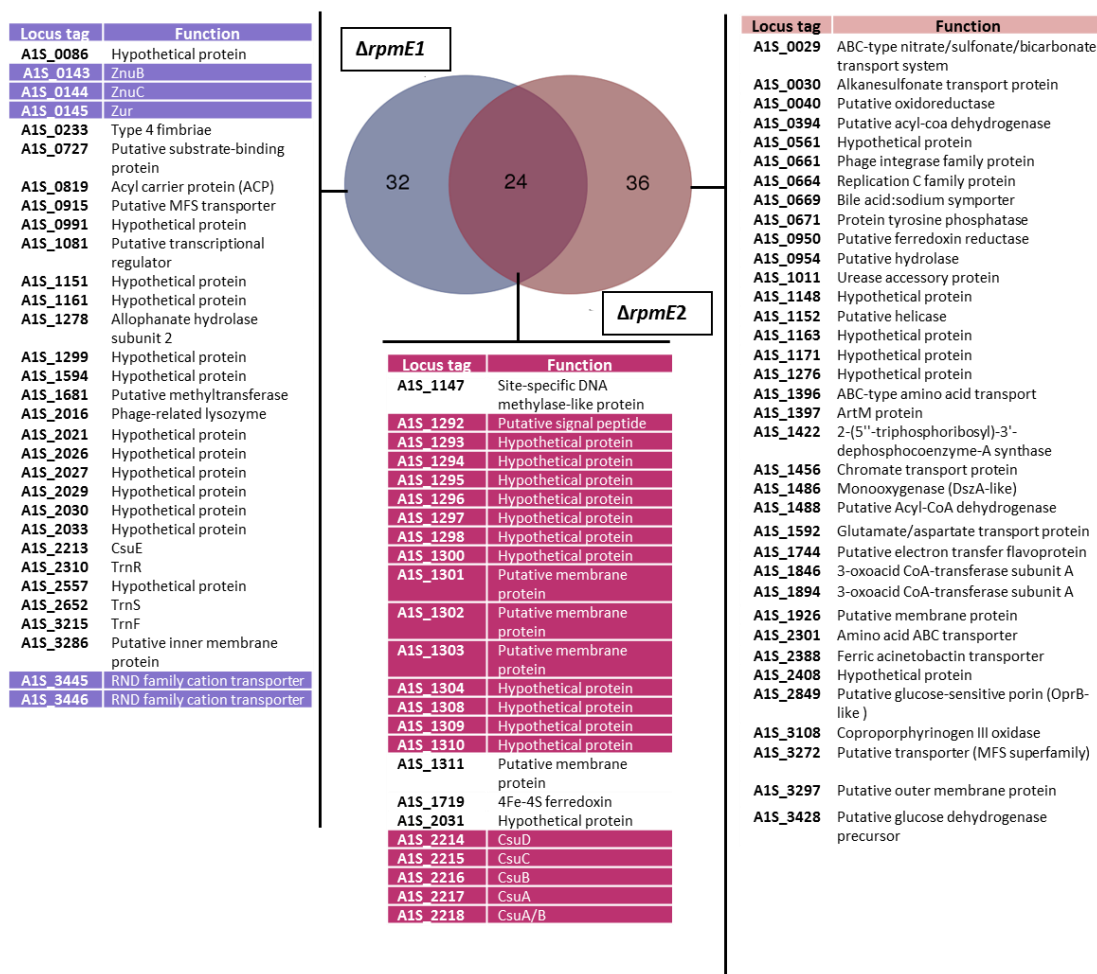


Figure 5.17: Comparison of genes down-regulated in $\Delta rpmE1$ and $\Delta rpmE2$ mutants compared to WT when grown in Zn^{2+} -limited conditions

The Venn diagram shows the shared (rose) and unique genes which are down-regulated (≥ 2 fold) in $\Delta rpmE1$ (blue) and $\Delta rpmE2$ (pink) cells when grown in Zn^{2+} -limited medium. This analysis identified 36 unique genes down-regulated in the $\Delta rpmE2$ strain, and 32 unique genes down-regulated in the $\Delta rpmE1$ strain plus 24 genes down-regulated in both strains. The *A. baumannii* ATCC 17978 gene locus tag and predicted protein function for each gene is given in the accompanying tables. The highlighted genes have been discussed in this chapter.

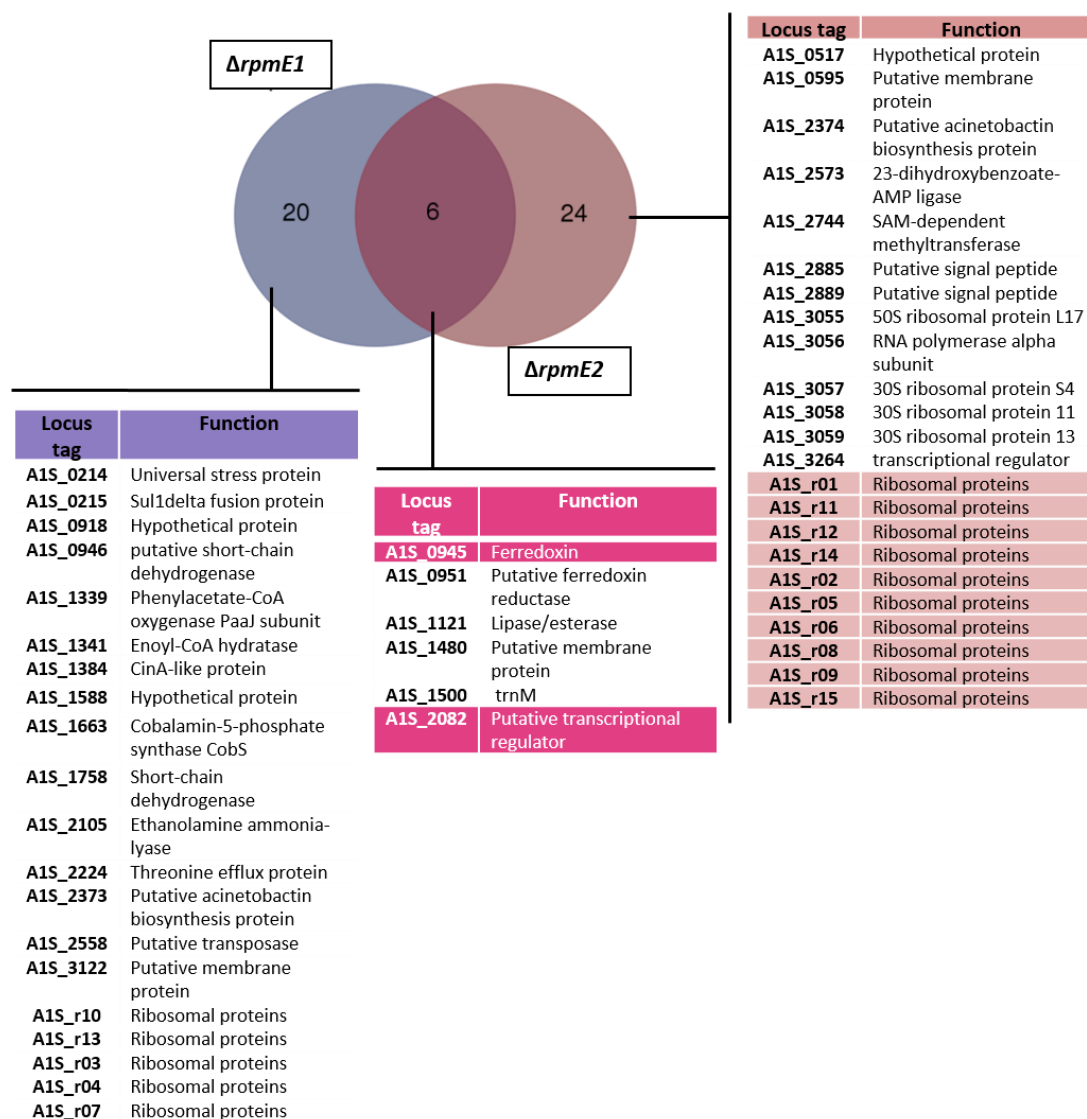


Figure 5.18: Comparison of genes up-regulated in $\Delta rpmE1$ and $\Delta rpmE2$ mutants compared to WT when grown in Zn^{2+} -limited conditions

The Venn diagram shows the shared (rose) and unique genes which are up-regulated (≥ 2 fold) in $\Delta rpmE1$ (blue) and $\Delta rpmE2$ (pink) cells when grown in Zn^{2+} -limited medium. This analysis identified 24 unique genes up-regulated in the $\Delta rpmE2$ strain and 20 unique genes up-regulated in the $\Delta rpmE1$ strain plus 6 genes up-regulated in both strains. The *A. baumannii* ATCC 17978 gene locus tag and predicted protein function for each gene is given in the accompanying tables. The highlighted genes have been discussed in this chapter.

The RNA-seq analysis revealed that there was a large number of shared genes differentially expressed in both mutants. This included genes involved in a T6SS (A1S_1292-1310), lipid metabolism (A1S_1699-1705), carbohydrate metabolism (A1S_1880-1894) and the *csuABABCDE* cluster (A1S_2213-2218). All of these showed decreased expression in both Zn²⁺-replete and Zn²⁺-limited conditions. The lower expression observed for these loci in both mutants indicates that although *rpmE1* and *rpmE2* both encode an L31 ribosomal protein, the lack of one L31 protein cannot be fully compensated for by the paralogous protein. Furthermore, the expression of these genes is not solely dependent on Zn²⁺ availability, as expression in both mutant strains was lower in Zn²⁺-limited conditions.

The unique effect of the deletion of *rpmE1* when grown in Zn²⁺-replete conditions was the down-regulation of the Zur global transcription repressor involved in Zn²⁺ homeostasis. Zur negatively regulates genes that have a Zur-binding site which include *rpmE2*, A1S_0146, A1S_0452, A1S_0453, A1S_2829, A1S_0391, A1S_3411, and A1S_3412. The derepression of Zur-regulated genes in the $\Delta rpmE1$ mutant was found to be independent of Zn²⁺ availability as *zur* expression is reduced in this mutant in Zn²⁺-replete conditions. There is no clear explanation as to why the expression of *zur* was reduced in the $\Delta rpmE1$ mutant even in Zn²⁺-replete conditions, but it is possible that *rpmE1* indirectly affects *zur* transcription via an unknown mechanism. Genes which do not have *zur*-binding sites but are responsive to Zn²⁺ limitation, such as a hypothetical Fe²⁺-receptor gene (A1S_0092) and a putative membrane protein (A1S_0093), also had increased expression in the $\Delta rpmE1$ mutant, indicating that these genes may play a role in Zn²⁺ acquisition rather than iron. In contrast, in the $\Delta rpmE2$ mutant grown in Zn²⁺-replete conditions, mostly ribosomal proteins (A1S_r01 to A1S_r15) showed increased expression between 40- to 50-fold possibly to compensate for the loss of RmpE2. Interestingly, the deletion of *rpmE2* led to a reduction in expression of HtpG that has previously reported to be associated with the 50S ribosomal protein L2 (Motojima-Miyazaki *et al.* 2010).

In Zn²⁺-limited conditions, the *rpmE1* and *rpmE2* mutants displayed some common differentially-expressed genes, including a transcriptional regulator

(A1S_2082) encoding a putative TetR-family regulatory protein. Since this gene was only differentially expressed during growth in Zn^{2+} -limited medium it indicated that its expression is altered in response to Zn^{2+} availability. In Zn^{2+} -limited conditions, the $\Delta rpmE1$ mutant showed uniquely reduced expression of genes including those involved in Zn^{2+} homeostasis *zur* (16.7-fold), *znuB* (9.2-fold) and *znuC* (5.7-fold). In addition, the expression of a number of genes in the $\Delta rpmE1$ mutant changed in response to reduced Zn^{2+} availability but did not appear to be *zur* regulated, such as the gene encoding ferredoxin (A1S_0945, 7.8-fold). It is possible that the deletion of *rpmE1* induces a state in the *A. baumannii* cell that mimics Zn^{2+} stress even when Zn^{2+} is freely available. The group of genes that were uniquely differentially expressed in both mutants regardless of Zn^{2+} availability was the gene loci encoding a type VI secretion system (A1S_1292-1310).

From the RNA-seq data, the transcriptional changes in response to the deletion of the two L31 ribosomal proteins showed the mutations led to pleiotropic effects. The data also show that *rpmE1* and *rpmE2* play significant roles in *A. baumannii* ATCC 17978, not only in response to Zn^{2+} limitation, but also in various metabolic processes and may also play a role in pathogenesis and virulence. In the previous chapter (Section 4.2.6) examination of some bacterial virulence characteristics showed that the deletion of this L31 protein affected biofilm formation, motility and antibiotic resistance. Further studies, however, should be conducted to examine the other genes identified in this study and what role they may have on the virulence capacity of this organism.

CHAPTER 6
DISCUSSION

6.1 Introduction

A. baumannii has emerged as one of the leading causes of hospital-acquired infections worldwide with high mortality rates (see Section 1.2.1). The pathogenicity of this organism is partly due to its MDR nature, its ability to persist in the environment and its virulence factors (see Section 1.3). A number of studies have revealed that maintaining biologically required level of transitional metal ions, in particular Zn^{2+} , is crucial for bacterial virulence capability (see Section 1.8.1). However, in spite of the apparent abundance of this metal in all cell types, the intracellular pool of loosely bound Zn^{2+} ions available for biological exchanges is in the picomolar range, as nearly all Zn^{2+} is tightly bound to proteins (Cerasi *et al.* 2013). Studies on Zn^{2+} homeostasis have shown that microorganisms have a remarkable capability to modify their intracellular Zn^{2+} content in response to variations in the environmental availability of this metal using diverse strategies (see Section 1.6 and 1.7). Understanding these mechanisms in particular, how bacteria regulate and achieve Zn^{2+} homeostasis, will hopefully lead to the identification of new targets for the next generation of antimicrobial agents.

The aim of the work presented in this thesis was to examine the role that Zn^{2+} storage plays in the lifestyle of *A. baumannii*. Many bacterial species, including *A. baumannii*, have two *rpmE* genes encoding ribosomal protein L31, where one is designated C^+ (*rpmE1*) capable of binding and storing Zn^{2+} and the other C^- (*rpmE2*) which is incapable of binding and storing Zn^{2+} (see Section 1.9). In order to undertake this work an extensively used *A. baumannii* strain ATCC 17978, that has been well characterised, fully sequenced and is amenable to genetic manipulation, was chosen (Eijkelkamp *et al.* 2011a; Hood *et al.* 2012; Mortensen *et al.* 2014). The initial work focused on designing growth media that was Zn^{2+} limited without affecting the availability of other cations (Section 3.2.1 and 3.2.2). Subsequently, the effect of growth in Zn^{2+} -limited and Zn^{2+} -replete conditions was examined using a number of phenotypic assays (Section 3.2.3). The effect on intracellular Zn^{2+} levels (Section 3.2.3) and on *A. baumannii* global expression was also undertaken (Section 3.2.5). To examine the individual roles of each *rpmE* paralogue, both of these genes were independently deleted by homologous recombination and as such likely

inactivated the major intracellular Zn^{2+} storage system (Section 4.2.1). A number of phenotypic assays and intracellular Zn^{2+} level measurements were undertaken to investigate the role of these protein in selected *A. baumannii* characteristics (Section 4.2). Transcriptomic analysis was conducted using RNA-seq to determine the transcriptional response for the parent and both mutants in Zn^{2+} -limited and Zn^{2+} -replete conditions (Section 5.2).

6.2 Development of Zn^{2+} -limited media

Study of bacterial Zn^{2+} acquisition and homeostasis is important in understanding bacterial pathogenicity, as this trace element is an essential factor for bacteria not only to grow but also a requirement for full bacterial virulence (see Section 1.8.1). However, a comprehensive understanding of the importance of Zn^{2+} has been difficult to achieve as obtaining Zn^{2+} -limited conditions without affecting the concentration of other cations is extremely difficult. Several techniques have been used to investigate the role of Zn^{2+} in bacteria; nonetheless no method has been shown to completely remove Zn^{2+} from the medium due to the high risk of Zn^{2+} contamination from the environment. This contamination can come from a variety of sources, such as glassware, pipette tips, tubes, plates and other cations added to the growth medium (Graham *et al.* 2009). Beside these external factors, the creation of Zn^{2+} -limiting conditions is also greatly influenced by the growth media used. Several studies investigating Zn^{2+} limitation in bacteria has utilised various different media; from minimal medium such as M9 (Lim *et al.* 2013) and GGM (Graham *et al.* 2009), to rich media such as LB (Ellison *et al.* 2013; Hood *et al.* 2012). In addition, different metal chelators, such as EDTA, EGTA (Patzer and Hantke 1998), chelex, calprotectin (Hood *et al.* 2012), and TPEN (Ammendola *et al.* 2007; Ellison *et al.* 2013; Hood *et al.* 2012; Pederick *et al.* 2015) have also been employed to remove Zn^{2+} from the media.

There are also various definitions of Zn^{2+} -replete and Zn^{2+} -limited conditions used in published studies. One study defined Zn^{2+} -replete and Zn^{2+} -limited conditions as a minimal medium with/without the addition of Zn^{2+} , respectively (Gaballa and Helmann 1998; Gunasekera *et al.* 2009). Another study treated the

minimal medium with a metal chelator chelex followed by the addition of Zn^{2+} in a defined concentration to create Zn^{2+} -replete conditions or without the addition of Zn^{2+} for Zn^{2+} -limited conditions (Graham *et al.* 2009). A study by Pederick *et al.* (2015) treated M9 medium with chelex and TPEN for defining Zn^{2+} -limiting conditions. Thus, although there are numerous studies examining the role of Zn^{2+} it is difficult to make comparisons between these studies as the definition of Zn^{2+} -limited and Zn^{2+} -replete conditions varies.

In this study, Zn^{2+} -limited growth media was developed and optimised via treatment of M9 medium with Chelex 100[®] and the addition of TPEN, Fe^{2+} and Mn^{2+} (See Section 2.2 and 3.2.2). TPEN was used because treatment with Chelex 100[®] alone did not result in complete removal of Zn^{2+} . Initially, this study used MH medium treated with Chelex 100[®] and the re-introduction of defined concentrations of Mg^{2+} , Ca^{2+} , Cu^{2+} , Mn^{2+} , and Fe^{2+} with/without Zn^{2+} (see Section 2.2 and 3.2.1). It was shown that Chelex 100[®] treatment significantly affected bacterial growth as almost no growth observed when cells were grown in MH chelex (MH[C]) (Figure 3.1). This indicated that Chelex 100[®] treatment potentially removed a great number of metal ions from the medium. Infact, chelex is not a specific metal chelator as it chelates various divalent ions, such as Cd^{2+} , Cu^{2+} , Fe^{2+} , Mn^{2+} , Zn^{2+} and other heavy metals over monovalent cations such as sodium and potassium. However, growth was significantly better when cells were grown in MH[C] supplemented with Mg and Ca (MH[CR]) (see Figure 3.1). Further, cells grown in (MH[CR]) medium exhibited growth as similar as seen in MH[CR] with the addition of Cu^{2+} , Fe^{2+} , Mn^{2+} , and Zn^{2+} (MH[CRsup]) (see Figure 3.1). These results indicated that the addition of Mg^{2+} and Ca^{2+} were sufficient for the cells to grow and the addition of other metals, such as Cu^{2+} , Fe^{2+} , and Mn^{2+} did not significantly increase the growth rate. It also indicated that the addition of Mg^{2+} and Ca^{2+} potentially introduced metal contaminations. Thus, to avoid metal contaminations introduced by the compound used, a specific Zn^{2+} -metal chelator TPEN was utilised to specifically removed Zn^{2+} from media without affecting other metal ions. To further removed Zn^{2+} , the MH medium was treated with the synthetic Zn^{2+} chelator, TPEN (data not shown). However, since the preparation of MH Zn^{2+} -limiting medium was time consuming and costly, as this employed several procedures (see Section 3.2.1) which also may

increase contamination with Zn^{2+} , an alternative minimal medium, M9, was chosen to create a Zn^{2+} -limited condition.

Preparation of the M9 media for creating Zn^{2+} -limited conditions is described in Section 2.2. For this, two metal chelators were used, Chelex 100[®] and TPEN. Chelex 100[®] was used to treat M9 5X salt and TPEN was added in the M9 medium which was prepared with Chelex 100[®] treated-M9 5X salt (see Section 2.2). The aim of the treating M9 5X salt with chelex was to remove Zn^{2+} contamination but minimise the effect of Chelex 100[®] to the medium. It was observed that this treatment did not alter the pH of the M9 media (data not shown). Figures 3.2 and 3.3 show that the addition of TPEN affected bacterial growth in M9[CTFM] medium (Zn^{2+} -limited medium), but growth was restored by the addition of 50 μ M of Zn^{2+} , creating (M9[CTFM+Zn] or Zn^{2+} -replete medium) (Figure 3.3). Additionally, qRT-PCR confirmed that this Zn^{2+} -limited medium was in fact Zn^{2+} limited. It revealed that the expression of *znuA* and *zur* is up-regulated (Figure 3.4). In addition the expression of the Fe^{2+} -uptake regulator (*fur*) and siderophore biosynthesis genes which have been shown to be highly up-regulated in Fe^{2+} -limiting conditions were not affected indicating that the addition of Fe^{2+} in the medium after Chelex 100[®] and TPEN treatment was sufficient. Comparisons of the RNA-seq data obtained from Zn^{2+} -limited medium to studies undertaken in *E. coli* using TPEN (Sigdel *et al.* 2006) revealed virtually no changes to genes regulated by Fur indicating that in this study the concentration of TPEN used to remove Zn^{2+} does not appear to influence Fe^{2+} levels.

As has been discussed above, the utilisation of Chelex 100[®] and TPEN to obtain Zn^{2+} -limiting conditions have been used in several studies. A study of *P. aeruginosa* which used M9 medium treated with Chelex 100[®] and TPEN, failed to show any effect that the addition of TPEN 10 μ M had on bacterial growth (Pederick *et al.* 2015). Yet, the used of a higher concentration (60 μ M) of TPEN, resulted in a reduction in bacterial growth, indicating that when applied at higher concentrations TPEN affected other metal ions or that *P. aeruginosa* has the ability to scavenge Zn^{2+} even if present at extremely low levels (Pederick *et al.* 2015). These types of studies highlight the difficulty in obtaining reliable Zn^{2+} -limited conditions. Therefore, the different preparation style of M9 or other Zn^{2+} -limiting media is likely

to influence the end result and the analysis of the respective study. For example, here in this study, RNA-seq data in *A. baumannii* grown in Zn²⁺-limited medium showed a high number of genes differentially expressed (≥ 300 genes ≥ 2 -fold) (Appendices 1 and 2). This is in comparison to other microarray analyses, including *E. coli* grown in Zn²⁺-limited medium which only showed 9 genes were differentially up-regulated (Graham *et al.* 2009), while a separate study identified only 101 differentially regulated gene (Sigdel *et al.* 2006). Although over 300 genes showed alterations in the expression profile in Zn²⁺-limited conditions, comparison to the study by Hood *et al.* in 2012, which used calprotectin to limit the amount of Zn²⁺ revealed only 14 loci in which transposon insertions led to sensitivity to calprotectin (Hood *et al.* 2012). Comparison between this study and the calprotectin study identified only one gene in common, the high affinity Zn²⁺-uptake protein (A1S_0143). The remaining 13 loci found to be sensitive to calprotectin (Hood *et al.* 2012) do not appear to be differentially expressed under the Zn²⁺-limited conditions used here.

As such, although there is some agreement between studies there are major differences, which are likely to be due to a number of factors including; differences in the media, the technique for removing Zn²⁺, and the bacterial species. Based on the data above, it can be concluded that the Zn²⁺-limited and Zn²⁺-replete conditions in used in this study have been achieved.

6.3 The importance of Zn²⁺ in *A. baumannii* ATCC 17978

Various strategies to maintain intracellular Zn²⁺ levels have been identified in pathogenic bacteria in order to survive in the environment or during course of infection (see Section 1.7). This is particularly important as the host generally limits Zn²⁺ by such mechanisms as the use of calprotectin to reduce the growth of the pathogen (see Section 1.8.1). In this study, It was revealed that Zn²⁺ limitation affected bacterial growth, in particular, there was a lag in entering the exponential growth phase and the culture exhibited a lower final cell density value (see Figure 3.3). This result is similar to that seen for *E. coli* grown in GGM medium, where an increase in the doubling time in Zn²⁺-limited medium compared to the growth in

Zn²⁺-replete medium was observed (Graham *et al.* 2009). The slower growth rate in Zn²⁺-limited culture may be due to the lack of Zn²⁺ for the cells to grow at a maximal rate. In addition, activation of Zn²⁺-scavenging systems as well as liberation of stored Zn²⁺ may account for this lag. Transcriptomic data confirmed that the Zn²⁺-limited condition led to a down-regulation of a vast number of metabolic genes (Figures 3.6 and 3.8).

A similar study analysing *P. protegens* grown in Zn²⁺-limited conditions also showed that a great number of metabolic genes were responsive to Zn²⁺ limitation (Lim *et al.* 2013). A study by De Nicola and co workers (De Nicola *et al.* 2007) in *S. cerevisiae* responding to Zn²⁺ deprivation also revealed a similar finding. Similarly, it has been shown here that a number of genes which showed decreased expression in Zn²⁺-limiting conditions encode proteins that require Zn²⁺ as a catalytic or structural component, *e.g.* the A1S_1697-1705 gene cluster (see Figure 3.9). As discussed in Section 3.2.5.7, genes within A1S_1881-1887 which have been suggested to contain a Zn²⁺-binding motif were also down-regulated under Zn²⁺-limiting conditions (see Figure 3.10). This indicated that Zn²⁺ availability is crucial to maintaining the function of these proteins as it has been shown previously that the deletion of Zn²⁺-finger motif in these proteins completely abolishes their enzymatic activity (Bilder *et al.* 2006).

RNA-seq analysis also showed that there was a 2- to 5-fold increase in the expression of *znuABC*, as well as other Zur-regulated genes including *rpmE2*, *tonB-exbB-exbD* and TBDR, with concomitant down-regulation of *czcABC* (see Table 3.3). Similar results have been reported in *E. coli* (Sigdel *et al.* 2006) and *P. protegens* (Lim *et al.* 2013) when grown in Zn²⁺-limited condition. Besides activating Zn²⁺ uptake and reducing Zn²⁺ efflux, in a low Zn²⁺ environment cells attempt to maintain sufficient Zn²⁺ for essential processes by mobilising it from storage systems such as the 50S ribosomal protein L31 RpmE1 (see Section 1.9). The qRT-PCR and RNA-seq data confirmed the role of L31 protein in Zn²⁺ homeostasis, as the expression of *rpmE2* was up-regulated by more than 400-fold (Table 3.3). This high increase in expression of *rpmE2* suggested that cells are attempting to liberate Zn²⁺ via displacing RpmE1 which contains bound Zn²⁺ in the 50S ribosome (see Section 1.9.2). It has also been suggested that the greater amount of RpmE2 produced, the

more Zn²⁺-bound RpmE1 can be displaced, allowing the release of significant Zn²⁺ reserves (Akanuma *et al.* 2006) (see Section 1.9). In addition, ICP-MS analysis undertaken in this project revealed that the level of Zn²⁺ in *A. baumannii* grown in Zn²⁺-limited culture was 25% lower than in Zn²⁺-replete culture. This would indicate that since the level of Zn²⁺ in the medium is very low, the cell has depleted its stored Zn²⁺ to maintain its essential metabolic processes.

A number of phenotypic characteristics were examined under Zn²⁺-replete and Zn²⁺-limited conditions, including the ability to form a biofilm. Under Zn²⁺-limited conditions a 25% reduction in biofilm produced by ATCC 17978 was observed. This finding is supported at a genetic level by the RNA-seq data (Figure 3.5) which revealed a decrease in the expression of A1S_2724 and A1S_2696 by approximately 2-fold (see Appendix 2); these two genes code for proteins previously proposed to be involved in biofilm formation (Loehfelm *et al.* 2008). Additionally, A1S_2160-2162 were shown to also be influenced by Zn²⁺ limitation albeit only marginally (data not shown). The products of these genes show similarity to genes present in *E. coli* and have been shown to be responsible for biofilm formation in that organism (Choi *et al.* 2009). Other factors previously identified as playing a role in *A. baumannii* biofilm formation were also down-regulated. This includes the CsuABABCDE pilus chaperone-usher assembly system (A1S_2214-2219) shown to be an essential factor for attachment to abiotic surfaces in ATCC 19606^T (Tomaras *et al.* 2008) and and OmpA (A1S_1193) (Gaddy *et al.* 2009) (Table 3.3). The decrease seen in biofilm formation under Zn²⁺-limited conditions is perhaps not surprising given that this effect has also been shown in *E. coli* and *A. pleuropneumoniae* (Gunasekera *et al.* 2009; Labrie *et al.* 2010). Furthermore, it has been shown that in *E. coli* the mutation of Zn²⁺-associated genes including the Zur-regulated *ykgM* and *zitA* greatly affected biofilm formation (Lim *et al.* 2011). Other studies in *S. epidermidis* and MRSA have also shown that Zn²⁺ depletion via metal chelation specifically prevented biofilm formation (Conrady *et al.* 2008). It has been suggested that Zn²⁺ limitation in bacteria can affect the ability to form biofilms through its roles in bacterial pilus assembly and curli production (Lim *et al.* 2011).

On the otherhand, as previously discussed, addition of Zn^{2+} in the medium has been shown to reduce the ability of several bacteria to form biofilms (see Section 3.2.3.2 (Gunasekera *et al.* 2009; Lim *et al.* 2011; Wu *et al.* 2013). These differences are possibly due to each bacterial species/strain having a different optimum cell concentration of Zn^{2+} required for cellular processes as high concentrations of Zn^{2+} are toxic and in some instances could hinder biofilm formation.

A study by Rumbo-Feal *et al.* (2013) in *A. baumannii* showed that 1621 genes were up-regulated in biofilms compared to planktonic cells; and 55 out of those genes were expressed only in biofilms (Rumbo-Feal *et al.* 2013). Many of those are involved in various processes including acyl carrier protein biosynthetic processes, amino acid metabolism, fatty acid metabolism, ion transport, carbohydrate biosynthesis, translation, transmembrane transport, and the stress response (Rumbo-Feal *et al.* 2013). Thus, although studies investigating the transcriptomic changes in the biofilm stage in bacteria have been conducted (Dötsch *et al.* 2012; Rumbo-Feal *et al.* 2013; Schoolnik 2001) there is no information of the effect that certain conditions, such as Zn^{2+} -limited conditions, have on the transcriptomic response of an organism in a biofilm, therefore future study in this subject is essential.

Related to this, Zn^{2+} availability has been demonstrated to influence motility in several bacteria (Section 3.2.3.1). However, in this study no difference in motility was observed when cells grown in semisolid medium with the addition of Zn^{2+} chelator TPEN (Section 2.3.6). This was unexpected as the RNA-seq data indicated that there was a decrease in expression of genes that were allocated to the respective motility COG group (see Figure 3.8). Despite the transcriptomic analysis which potentially supports the role of Zn^{2+} in motility of *A. baumannii*, this could not be phenotypically demonstrated in Zn^{2+} -limited conditions. Thus, although metal ions such as Zn^{2+} , Fe^{2+} , and Mn^{2+} have all been reported to contribute to bacterial motility, it appears that the limitation of Zn^{2+} alone under these study conditions is not adequate to significantly inhibit the motility of *A. baumannii*. Additionally, this may be due to the complexities of the motility phenotype and the difficulty to

create a Zn^{2+} -limited medium to observe motility in *A. baumannii* ATCC 17978. It should be noted that ATCC 17978 is not a very motile strain in comparison with other *A. baumannii* strains in our collection (Eijkelkamp *et al.*, 2011b).

Zn^{2+} is an essential cofactor for multiple enzymes including some involved in antibiotic resistance. Analysis of the antibiotic resistance profile exhibited by *A. baumannii* ATCC 17978 showed that this isolate is significantly more susceptible to chloramphenicol, Amp, amoxicillin clavulanic acid, cefotaxime, and ceftriaxone in MH with the addition of TPEN compared to MH agar alone (see Table 3.1). The role of Zn^{2+} in β -lactamase activity is well known, especially for MBLs, where the MBL enzymes are inactive in the absence of Zn^{2+} . Furthermore, removal of Zn^{2+} has been previously shown to reverse the antibiotic resistance of a carbapenem-resistant strain of *A. baumannii* (Hood *et al.* 2012). However, the effect on antibiotic susceptibility in these strains may also indicate that Zn^{2+} indirectly influences other mechanisms which can affect susceptibility to β -lactam antibiotics. Surprisingly the addition of TPEN led to an increase in resistance to aminoglycoside antibiotics (see Table 3.1), even though there is no clear explanation as to why this increase occurred. Various mechanisms that may explain this feature have been discussed previously (Section 3.2.3.3) including alteration of the ribosomal binding site (Poole 2005). In fact, under Zn^{2+} limitation, modulation in a multiple systems can occur. Based on the RNA-seq data, there are many proteins differentially expressed in Zn^{2+} -limited conditions with unknown functions which may potentially be involved in these characteristics. Because of the time constrains, this study only tested a limited number of aminoglycoside drugs. Therefore, further study is required to examine whether the alteration to aminoglycoside resistance is a general phenomenon under Zn^{2+} limited conditions in ATCC 17978 and could be extended to other bacteria obtained from clinical samples. As both Zn^{2+} (Section 3.2.3.3) and also Fe^{2+} levels (Eijkelkamp *et al.* 2011a) have a significant effect on the antibiotic resistance spectrum, it would be interesting to mimic human plasma which is low in both of these cations to see if in this scenario the changes in resistance profile are also seen.

Transcriptomic analysis revealed that Zn^{2+} limitation affected the transcription of various genes involved in virulence, including genes encoding;

surface antigen (A1S_1383), catalase (A1S_1386), lipases (A1S_3159-3160), and a VGR-like protein (A1S_3220) (see Table 3.3). Additionally, other virulence genes, such as A1S_1702-1703 were also down-regulated by 11- and 13-fold (Figure 3.9). These DLDH proteins have been shown to be involved in the survival of pneumococci within host cells (Smith *et al.* 2002). In addition, a PQQ gene (A1S_1880) (see Figure 3.10) which has been shown to play a role in protection against oxidative stress (Misra *et al.* 2004) showed decreased expression. Furthermore, Zn²⁺-limitation resulted in the down-regulation of many transcriptional regulators and signal peptides.

6.4 The role of RpmE1 and RpmE2 in *A. baumannii* ATCC 17978

One mechanism utilised by bacteria in Zn²⁺-starvation conditions is by increasing the expression of non-Zn-requiring proteins to replace essential Zn²⁺-dependent enzymes and proteins (see Section 1.9.1). The L31 ribosomal proteins have been shown to be one example of such a mechanism (Nanamiya *et al.* 2004). As previously discussed, L31 ribosomal proteins are encoded by two paralogous genes (see Section 1.9.2); the ability to alternate between two forms of these L31 proteins is effectively able to increase the concentration of free Zn²⁺ ions in Zn²⁺-limited conditions which are then available for use in metabolically critical cell functions (Akanuma *et al.* 2006; Nanamiya *et al.* 2004) (see Section 1.9.2). Evidence that these two proteins are interchangeable comes from experiments which revealed that they are co-fractionated with the 50S subunits of the ribosome albeit at different growth phases (Akanuma *et al.* 2006). Studies in bacteria such as *B. subtilis* (Akanuma *et al.* 2006; Gabriel and Helmann 2009), *E. coli* (Hensley *et al.* 2012) and *S. coelicolor* (Shin *et al.* 2007), confirmed that these proteins are involved in the bacterial response to Zn²⁺-limiting environments (Section 1.9). Despite the potential role of these proteins in Zn²⁺ homeostasis, there is little information about their function in *A. baumannii*. This present study, revealed for the first time the potential role of these two proteins in *A. baumannii* ATCC 17978 in response to Zn²⁺-limiting conditions. Two mutants were constructed, $\Delta rpmE1$ and $\Delta rpmE2$ (Section 4.2.1), and subsequently the effect of this gene inactivation on the

intracellular Zn²⁺ level (Section 4.2.5), selected phenotypic characteristics (Section 4.2.6) and global transcriptome (Section 5.2) was established.

The RNA-seq data of these *A. baumannii* ATCC 17978 mutants grown in Zn²⁺-limited and Zn²⁺-replete medium revealed that deletion of *rpmE1* or *rpmE2* affected *A. baumannii* global transcriptome (Figures 5.1 and 5.8). It is noted that most of the genes showed a decrease in expression in both mutants when grown in either Zn²⁺-replete or Zn²⁺-limited conditions compared to the WT. These two mutants also shared a great number of differentially-expressed genes, including gene encoding CsuABABCDE (A1S_2214-2219), T6SS (A1S_1292-1310), A1S_1669-1705, and A1S_1880-1894 (Figures 5.13, 5.14, 5.17, and 5.18) which indicates that these *rpmE1* and *rpmE2* have similar functions.

One aspect unique to the deletion of *rpmE1* is the reduction in *zur* expression both in Zn²⁺-limited and Zn²⁺-replete media. The RNA-seq data showed ~12-fold down-regulation of *zur* expression in the $\Delta rpmE1$ mutant compared to the WT (Figure 5.1). This reduction in *zur* expression has a knockon effect leading to the derepression of known Zur-regulated genes such as *znuA*, *rpmE2*, *tonB-ExbB-exbD*, and A1S_4311 (see Figure 5.1). The reduction of *zur* transcripts in this mutant led to a hypothesis that *rpmE1* plays a role as a Zn²⁺ sensor in *A. baumannii* ATCC 17978; the loss of RpmE1 causes the cells to mistakenly sense a low Zn²⁺ condition even in Zn²⁺-replete conditions. In fact, the deletion of *rpmE1* mirrors in many respects the changes seen in a *zur* knockout (Mortensen *et al.* 2014). Thus, one hypothesis may be that there is an unknown indirect mechanism between the regulation of *zur* and *rpmE1* which needs further investigation.

In contrast, in the $\Delta rpmE2$ mutant the Zn²⁺-regulated genes were not affected in either Zn²⁺-limited or Zn²⁺-replete conditions. However, under Zn²⁺-replete conditions, the deletion of *rpmE2* caused the up-regulation of a set of genes encoding ribosomal proteins (between 2- to 3-fold). Other genes that showed increased expression included genes encoding enzymes involved in methionine metabolism which require Zn²⁺ as a cofactor. Similarly, under Zn²⁺-limited conditions the loss of *rpmE2* led to an up-regulation of a set of genes encoding ribosomal proteins, including A1S_r01 to A1S_r15, which were up-regulated between 40- and

50-fold (Appendix 9). This may indicate that RpmE2 plays a role in ribosome-ribosome interactions or that the cell is attempting to compensate for the loss of RpmE2.

In this study, $\Delta rpmE1$ or $\Delta rpmE2$ grown in Zn^{2+} -limited culture showed a lower Zn^{2+} level compared to the WT grown in the same medium (see Figure 4.9). This indicates that the loss of *rpmE1* abrogates an intracellular Zn^{2+} -storage system (Nanamiya *et al.* 2004). Examination of the Zn^{2+} -binding capacity of RmpE1 has shown that in *B. subtilis* each RpmE1 polypeptide contained 0.82 atoms of Zn^{2+} (Nanamiya *et al.* 2004). Therefore, in *B. subtilis* cells, in order to maintain RpmE1 protein stability one Zn^{2+} ion is required to be bound to the CxxC motif (Nanamiya *et al.* 2004). In *E. coli*, however, RpmE1 appears to bind 0.3 ± 0.1 equivalents of Zn; which in metal-loaded conditions increases to 1.2 ± 0.1 (Hensley *et al.* 2012). Analysis of the ratio of Zn^{2+} bound per RpmE1 in *A. baumannii* should be considered in future studies.

Similarly, intracellular Zn^{2+} levels within the $\Delta rpmE2$ mutant were observed to be decreased by approximately 25% in Zn^{2+} -limited conditions compared to the WT (see Figure 4.9). This may be because when cells without *rpmE2* are grown in Zn^{2+} -limited medium, RpmE1 cannot be replaced by RpmE2 thereby severely limiting the ability to liberate Zn^{2+} from the RpmE1-containing ribosome. This result is similar to that seen in a previous study using an *E. coli* $\Delta ykgm$ mutant (Lim *et al.* 2011). Therefore, it is suggested that the lower Zn^{2+} levels seen in the $\Delta rpmE2$ mutant may be due to a disturbance of the Zn^{2+} recycling process, as the Zn^{2+} bound to RmpE1 cannot be utilised unless the ribosome complex is degraded which over time would lead to a reduced Zn^{2+} level within the cells. This suggestion is also supported by the previous study in *B. subtilis* where RpmE2 did not contain Zn^{2+} or other metal ions (Nanamiya *et al.* 2004) and was required to displace RpmE1 which contained bound Zn^{2+} from already assembled ribosomes, allowing the metal ion to be recycled within the cell (Akanuma *et al.* 2006). Based on this, the result obtained in this study indicated that the lower Zn^{2+} concentrations in the $\Delta rpmE2$ mutant may be due to the disturbance of this Zn^{2+} recycling process. Thus, it is likely that in order for the cells to survive and to obtain Zn^{2+} , the cell may start to degrade the ribosomes and over time this would lead to a reduced Zn^{2+} level within the cells.

Interestingly, the level of Mn^{2+} in these two mutants was higher in Zn^{2+} -limited compared to Zn^{2+} -replete culture (see Figure 4.10). The increase in the level of Mn^{2+} is inversely proportional to that of Zn^{2+} , i.e. when the level of Zn^{2+} dropped, the level of Mn^{2+} increased. A higher concentration of Mn^{2+} has also been seen in *S. pneumoniae* grown in Zn^{2+} -limited conditions (Jacobsen *et al.* 2011; McDevitt *et al.* 2011). *S. pneumoniae* has a unique Mn^{2+} transporter which is not found in *A. baumannii*, therefore further study on the mechanism of Mn^{2+} regulation in *A. baumannii* and the association with the concentration of Zn^{2+} needs to be undertaken.

The influence of the deletion of RpmE1 or RpmE2 in *A. baumannii* ATCC 17978 could be visualised in a number of phenotypes, including bacterial growth, biofilm production, motility, and antibiotic resistance (Section 4.2.3 and 4.2.6.1). The loss of RpmE1 or RpmE2 has an impact on bacterial growth in both Zn^{2+} -limited and Zn^{2+} -replete media compared to the WT (Figures 4.7 and 4.8). As discussed previously (Section 6.3), the slower growth rate of the mutants in both conditions compared to the WT may be due to the cells requirement for Zn^{2+} to grow at a maximal rate. Even though the ICP-MS results showed that in Zn^{2+} -replete medium the level of intracellular Zn^{2+} does not significantly differ to the level in the WT (Figure 4.10), the loss of RpmE1 seems to impair other biological processes in the cells. Additionally, it is suggested that RpmE1 may function as a Zn^{2+} sensor; thus, the loss of this protein essentially reprograms the cells to act as if they are in Zn^{2+} -limited conditions resulting in the activation of Zn^{2+} -responsive genes which may contribute to the lag in growth.

Another phenotypic change observed in the $\Delta rpmE1$ and $\Delta rpmE2$ strains are that they produced less biofilm (decrease of 25%) than the WT (Figure 4.12). This reduction in both motility and biofilm formation in both mutants may be as a result of the slower growth as discussed above. Additionally, genes that may play a role in these characteristics showed a decrease in expression, including *ompA* (2.6-fold) and *csuABABCDE* (A1S_2214-2219, 2- to 3-fold) (Appendix 4). In addition to the changes phenotypes above, the deletion of $\Delta rpmE1$ and $\Delta rpmE2$ did not appear to significantly affect antibiotic resistance. However, similar to the WT, $\Delta rpmE1$ and

$\Delta rpmE2$ mutants became more resistant to aminoglycosides when tested in medium where TPEN had been added (Table 4.5).

Finally, this study showed that the L31 genes may be involved indirectly in the oxidative stress response. It has been previously stated that many bacterial enzymes and regulatory proteins possess a Zn^{2+} -containing redox centre, C-X-X-C, providing an ability to sense the redox status of the cell (see Section 4.2.6.5). Here, it is shown that deletion of *rpmE1* and *rpmE2* reduced bacterial growth under paraquat stress (Figure 4.13). Additionally, the expression of oxidative stress genes, *fumC* (A1S_1986), *sodA* (A1S_2343), *katB* (A1S_3382) and *ahpC* (A1S_1205) (Figure 4.14) examined by qRT-PCR were altered in the $\Delta rpmE1$ and $\Delta rpmE2$ mutants compared to WT. The expression of *katB* and *ahpC* were higher in both mutant strains, while the expression of *fumC* and *sodA* was lower (see Figure 4.14). A study in *N. gonorrhoeae* also indicated that RpmE1 is negatively regulated by PerR and responds to oxidative stress (Wu *et al.* 2006). Based on the data obtained for sensitivity to paraquat, as well as the transcriptomic level of paraquat-responsive genes (Figure 4.14), it is possible that the loss of *rpmE1* and *rpmE2* may indirectly affect the oxidative stress response in *A. baumannii* ATCC 17978.

Thus, these studies provide a comprehensive picture of the effects that the deletion of *rpmE1* or *rpmE2* had on multiple phenotypes, intracellular Zn^{2+} levels, oxidative stress response and global transcriptomic changes.

6.5 Conclusions

In summary, this study has explored the effect of both Zn^{2+} limitation and the alternative deletion of two paralogous ribosomal proteins on *A. baumannii* ATCC 17978. The removal of Zn^{2+} from the media has produced numerous changes in gene transcription as well as affecting a number of phenotypic characteristics. Changes in gene expression in the $\Delta rpmE1$ mutant in the presence of Zn^{2+} appear to mimic many of the changes seen in the WT parent when grown under Zn^{2+} -limited conditions, whereas this was not the case for the $\Delta rpmE2$ strain. Furthermore, both mutants showed similar but also distinct changes in their transcriptomic response and also shared a number of phenotypic alterations. In essence this indicates that

there is a link between these two L32 proteins as to how the cell responds to their loss. Thus, this study has provided insight into how the loss of these two ribosomal proteins affects *A. baumannii* both in the presence and absence of Zn^{2+} . Furthermore, many of the changes seen are supported in the literature by similar studies in other bacteria yet it still highlights the very distinct difference seen in *A. baumannii* and warrants further investigation.

APPENDICES

Appendix 1 – Genes significantly up-regulated in *A. baumannii* ATCC 17978 under Zn²⁺-limited conditions (CP000521.1)

| Locus-tag^a | Gene product^b | Differential expression (Log₂) |
|------------------------------|--------------------------------------------------|--------------------------------------------------|
| A1S_0040 | Oxidoreductase | 1.0 |
| A1S_0145 | Zinc uptake regulator | 1.0 |
| A1S_0143 | High affinity Zn ²⁺ transport protein | 1.0 |
| A1S_2511 | Phenylacetic acid degradation-related protein | 1.0 |
| A1S_1681 | Methyltransferase | 1.0 |
| A1S_1794 | Hypothetical protein | 1.1 |
| A1S_2408 | Hypothetical protein | 1.1 |
| A1S_2909 | tRNA-Leu | 1.1 |
| A1S_1944 | Alpha/beta hydrolase | 1.1 |
| A1S_1712 | DMT family permease | 1.1 |
| A1S_2169 | Cytochrome o ubiquinol oxidase subunit IV | 1.1 |
| A1S_2016 | Phage-related lysozyme | 1.1 |
| A1S_0454 | Biopolymer transport protein ExbD | 1.1 |
| A1S_2217 | Protein CsuA | 1.2 |
| A1S_0144 | High affinity Zn ²⁺ transport protein | 1.2 |
| A1S_1143 | Hypothetical protein | 1.2 |
| A1S_1583 | Hypothetical protein | 1.2 |
| A1S_2038 | Hypothetical protein | 1.2 |
| A1S_0738 | Flavoprotein oxidoreductase | 1.2 |
| A1S_1276 | Hypothetical protein | 1.2 |
| A1S_2039 | Hypothetical protein | 1.2 |
| A1S_2893 | hypothetical protein | 1.2 |
| A1S_1925 | Cytochrome d ubiquinol oxidase subunit II | 1.3 |
| A1S_1908 | Phospho-2-dehydro-3-deoxyheptonate aldolase | 1.3 |
| A1S_0453 | Biopolymer transport protein (ExbB) | 1.6 |
| A1S_1719 | 4Fe-4S ferredoxin | 1.7 |
| A1S_0737 | Homocysteine methyltransferase | 1.9 |
| A1S_0180 | Hypothetical protein | 2.1 |
| A1S_1435 | Hypothetical protein | 2.1 |
| A1S_0561 | Hypothetical protein | 2.2 |
| A1S_0452 | Periplasmic protein TonB | 2.4 |
| A1S_0146 | High affinity Zn ²⁺ transport protein | 2.5 |
| A1S_0653 | Fe-transport protein B | 2.6 |
| A1S_0652 | Fe-transport protein A | 3.2 |
| A1S_3412 | Hypothetical protein | 4.2 |
| A1S_2892 | TonB-dependent receptor protein | 5.9 |

| Locus-tag^a | Gene product^b | Differential expression (Log₂) |
|------------------------------|-------------------------------------|--------------------------------------------------|
| A1S_0093 | Hypothetical protein | 6.1 |
| A1S_0092 | Ferric siderophore receptor protein | 6.2 |
| A1S_3411 | G3E family GTPase | 8.3 |
| A1S_0391 | 50S ribosomal protein L31, RpmE2 | 8.7 |

^a. Sequence was obtained from ATCC 17978 GenBank accession number CP000521.1

^b. The predicted function of the protein based on the data from KEGG: Kyoto Encyclopaedia of Genes and Genomes.

Appendix 2 – Genes significantly down-regulated in *A. baumannii* ATCC 17978 under Zn²⁺-limited conditions (CP000521.1)

| Locus-tag^a | Gene product^b | Differential expression (Log₂) |
|------------------------------|---------------------------------------------|--------------------------------------------------|
| A1S_3219 | RND efflux transporter | -5.0 |
| A1S_1383 | Surface antigen | -4.4 |
| A1S_3218 | RND efflux transporter | -4.6 |
| A1S_3220 | VGR-like protein | -4.3 |
| A1S_1701 | Dihydrolipoamide acetyltransferase | -4.0 |
| A1S_3217 | RND efflux transporter | -3.9 |
| A1S_1700 | 2,6-dichlorophenolindophenol oxidoreductase | -3.9 |
| A1S_1887 | 4-hydroxybenzoate transporter | -3.8 |
| A1S_1699 | 26-dichlorophenolindophenol oxidoreductase | -3.7 |
| A1S_1703 | Dihydrolipoamide dehydrogenase | -3.7 |
| A1S_1341 | Enoyl-CoA hydratase/carnithine racemase | -3.6 |
| A1S_0169 | Hypothetical protein | -3.6 |
| A1S_1704 | Acetoin dehydrogenase | -3.6 |
| A1S_1886 | Gamma-carboxymuconolactone decarboxylase | -3.5 |
| A1S_2082 | Transcriptional regulator | -3.5 |
| A1S_1702 | Dihydrolipoamide dehydrogenase | -3.5 |
| A1S_1384 | CinA-like protein | -3.1 |
| A1S_3043 | Hypothetical protein | -3.0 |
| A1S_0745 | Hypothetical protein | -3.0 |
| A1S_1890 | 3-carboxy-cis,cis-muconate cycloisomerase | -3.0 |
| A1S_3160 | Lipase | -2.9 |
| A1S_1705 | (RR)-butanediol dehydrogenase | -2.9 |
| A1S_1045 | Co/Zn/Cd efflux system | -2.8 |
| A1S_0170 | Outer membrane Cu-receptor (OprC) | -2.7 |
| A1S_1888 | MFS transporter | -2.7 |
| A1S_1889 | 3-oxoadipate enol-lactonase | -2.7 |
| A1S_1480 | Hypothetical protein | -2.7 |
| A1S_1894 | 3-oxoacid CoA-transferase subunit A | -2.6 |
| A1S_2823 | Hypothetical protein | -2.5 |
| A1S_3159 | Lipase chaperone | -2.5 |
| A1S_r07 | 5S ribosomal RNA | -2.5 |
| A1S_r03 | 5S ribosomal RNA | -2.5 |
| A1S_r04 | 5S ribosomal RNA | -2.5 |
| A1S_r10 | 5S ribosomal RNA | -2.5 |
| A1S_r13 | 5S ribosomal RNA | -2.5 |
| A1S_1846 | 3-oxoacid CoA-transferase subunit A | -2.5 |

| Locus-tag^a | Gene product^b | Differential expression (Log₂) |
|------------------------------|------------------------------------------------|--------------------------------------------------|
| A1S_2230 | Hypothetical protein | -2.4 |
| A1S_1882 | 3-dehydroshikimate dehydratase | -2.3 |
| A1S_0945 | Ferredoxin | -2.3 |
| A1S_3404 | Proline transport protein (APC family) | -2.3 |
| A1S_1697 | Transcriptional regulator | -2.3 |
| A1S_2451 | AsnC family transcriptional regulator | -2.3 |
| A1S_1724 | Dicarboxylic acid transport protein | -2.3 |
| A1S_1491 | Glutamate/aspartate transport protein | -2.2 |
| A1S_0951 | Ferredoxin reductase | -2.2 |
| A1S_1368 | Pyruvate ferredoxin/flavodoxin oxidoreductase | -2.2 |
| A1S_1847 | 3-oxoadipate CoA-transferase sub unit B | -2.2 |
| A1S_1893 | 3-oxoadipate CoA-transferase sub unit B | -2.2 |
| A1S_1380 | Putative protein (DcaP-like) | -2.2 |
| A1S_1387 | Oxidoreductase | -2.2 |
| A1S_1493 | Glutamate/aspartate transport protein | -2.1 |
| A1S_1467 | Glutamate symport transmembrane protein | -2.1 |
| A1S_2093 | Hypothetical protein | -2.1 |
| A1S_1885 | Protocatechuate 3 ₄ -dioxygenase | -2.1 |
| A1S_1492 | Glutamate/aspartate transport protein | -2.1 |
| A1S_1044 | Co/Zn/Cd efflux transporter | -2.0 |
| A1S_1883 | AroD; 3-dehydroquinone dehydratase | -2.0 |
| A1S_1490 | Glutamate/aspartate transport protein | -2.0 |
| A1S_0804 | Hypothetical protein | -2.0 |
| A1S_1340 | phenylacetate-CoA oxygenase/reductase PaaK | -2.0 |
| A1S_1193 | OmpA/MotB protein | -1.9 |
| A1S_1266 | Hypothetical protein/MntH | -1.9 |
| A1S_0009 | putative RND type efflux pump | -1.9 |
| A1S_0171 | Hypothetical protein | -1.9 |
| A1S_1336 | PaaA; phenylacetate-CoA oxygenase subunit PaaA | -1.9 |
| A1S_0803 | Trehalose-6-phosphate synthase | -1.8 |
| A1S_1880 | Pyrrroloquinoline-quinone QuiA | -1.8 |
| A1S_1337 | PaaB; phenylacetate-CoA oxygenase subunit PaaB | -1.8 |
| A1S_3264 | Transcriptional regulator | -1.8 |
| A1S_2423 | 50S ribosomal protein L31 | -1.8 |
| A1S_1881 | Porin | -1.8 |
| A1S_1730 | Short-chain fatty acid transporter | -1.8 |
| A1S_3418 | 4-hydroxyphenylpyruvate dioxygenase | -1.8 |
| A1S_1233 | Hypothetical protein | -1.8 |
| A1S_1268 | Hypothetical protein | -1.8 |

| Locus-tag^a | Gene product^b | Differential expression (Log₂) |
|------------------------------|-----------------------------------------------------|--------------------------------------------------|
| A1S_0918 | Hypothetical protein | -1.7 |
| A1S_1738 | Transcriptional regulator | -1.7 |
| A1S_2041 | Hypothetical protein | -1.7 |
| A1S_2159 | Hypothetical protein | -1.7 |
| A1S_1342 | Enoyl-CoA hydratase | -1.7 |
| A1S_1369 | Putative oxidoreductase protein | -1.7 |
| A1S_3406 | Urocanate hydratase | -1.7 |
| A1S_1345 | Hypothetical protein | -1.7 |
| A1S_1775 | Transcriptional activator | -1.7 |
| A1S_3253 | Putative signal peptide | -1.7 |
| A1S_2843 | Hypothetical protein | -1.7 |
| A1S_1349 | Thioesterase domain-containing protein | -1.7 |
| A1S_0996 | Hypothetical protein | -1.7 |
| A1S_2228 | Hypothetical protein | -1.6 |
| A1S_2602 | Hypothetical protein | -1.6 |
| A1S_1370 | Oxidoreductase | -1.6 |
| A1S_1500 | tRNA-Met | -1.6 |
| A1S_2373 | Acinetobactin biosynthesis protein | -1.6 |
| A1S_1732 | Acetoacetyl-CoA transferase subunit α | -1.6 |
| A1S_3300 | Cation/acetate symporter | -1.6 |
| A1S_0721 | Glutaryl-CoA dehydrogenase | -1.6 |
| A1S_2196 | Membrane-associated dicarboxylate transport protein | -1.6 |
| A1S_1385 | Hypothetical protein | -1.6 |
| A1S_2091 | Putative exported protein | -1.6 |
| A1S_3403 | Imidazolonepropionase | -1.5 |
| A1S_0104 | Putative acetyl-coA synthetase | -1.5 |
| A1S_0517 | Hypothetical protein | -1.5 |
| A1S_1758 | Short-chain dehydrogenase/reductase SDR | -1.5 |
| A1S_2415 | tRNA-Val | -1.5 |
| A1S_0010 | RND type efflux pump | -1.5 |
| A1S_0674 | Putative transposase | -1.5 |
| A1S_1094 | D-serine/D-alanine/glycine transporter | -1.5 |
| A1S_1884 | Protocatechuate 3,4-dioxygenase alpha chain | -1.5 |
| A1S_1339 | Phenylacetate-CoA oxygenase PaaJ subunit | -1.5 |
| A1S_1862 | Hypothetical protein | -1.5 |
| A1S_0690 | FilA | -1.4 |
| A1S_0708 | Cu-resistance protein B precursor | -1.4 |
| A1S_3407 | Urocanase | -1.4 |
| A1S_1376 | Acyl-CoA dehydrogenase | -1.4 |

| Locus-tag^a | Gene product^b | Differential expression (Log₂) |
|------------------------------|--------------------------------------------|--------------------------------------------------|
| A1S_0788 | Hypothetical protein | -1.4 |
| A1S_1378 | Putative long chain fatty-acid CoA ligase | -1.4 |
| A1S_3309 | Acetyl-CoA synthetase | -1.4 |
| A1S_3301 | Putative membrane protein | -1.4 |
| A1S_0910 | Gamma-glutamyltranspeptidase precursor | -1.4 |
| A1S_1386 | Catalase | -1.4 |
| A1S_1736 | Putative membrane protein | -1.4 |
| A1S_0855 | Dioxygenase beta subunit | -1.4 |
| A1S_1151 | Hypothetical protein | -1.4 |
| A1S_0566 | Pyridine nucleotide transhydrogenase | -1.4 |
| A1S_1687 | Transcriptional regulator | -1.3 |
| A1S_0850 | Betaine/choline/glycine transport | -1.3 |
| A1S_0946 | Hypothetical protein | -1.3 |
| A1S_3402 | Arginase hydrolase | -1.3 |
| A1S_1158 | Putative signal peptide | -1.3 |
| A1S_3135 | APC family S-methylmethionine transporter | -1.3 |
| A1S_1726 | Aspartate ammonia-lyase (aspartase) | -1.3 |
| A1S_2148 | Putative acetyl-CoA synthetase | -1.3 |
| A1S_0101 | Pseudogene | -1.3 |
| A1S_0490 | Putative hydrolase | -1.3 |
| A1S_2601 | Putative outer membrane protein A | -1.3 |
| A1S_0852 | Dioxygenase alpha subunit | -1.3 |
| A1S_0787 | Putative signal peptide | -1.3 |
| A1S_3129 | Succinylarginine dihydrolase | -1.3 |
| A1S_1335 | Phenylacetic acid degradation protein PaaN | -1.3 |
| A1S_3405 | Histidine ammonia-lyase | -1.3 |
| A1S_0949 | Putative dioxygenase | -1.3 |
| A1S_2224 | Threonine efflux protein | -1.3 |
| A1S_2346 | tRNA-Asn | -1.2 |
| A1S_1954 | Serine proteinase | -1.2 |
| A1S_3049 | Putative integral membrane protein | -1.2 |
| A1S_2348 | Hypothetical protein | -1.2 |
| A1S_2318 | Putative membrane protein | -1.2 |
| A1S_1745 | Putative signal peptide | -1.2 |
| A1S_2850 | Putative acyl-CoA transferase | -1.2 |
| A1S_0691 | FilB | -1.2 |
| A1S_0786 | Putative signal peptide | -1.2 |
| A1S_0785 | Hypothetical protein | -1.2 |
| A1S_2325 | Putative outer membrane protein | -1.2 |

| Locus-tag^a | Gene product^b | Differential expression (Log₂) |
|------------------------------|---------------------------------------------|--------------------------------------------------|
| A1S_2345 | tRNA-Asn | -1.2 |
| A1S_0853 | Succinate-semialdehyde dehydrogenase | -1.2 |
| A1S_1857 | Vanillate O-demethylase oxidoreductase | -1.2 |
| A1S_1860 | (2Fe-2S) protein | -1.2 |
| A1S_0482 | Acetate kinase | -1.2 |
| A1S_1529 | Leucine-responsive regulatory protein | -1.2 |
| A1S_0184 | Hypothetical protein | -1.1 |
| A1S_1466 | Glutaminase-asparaginase | -1.1 |
| A1S_0567 | Pyridine nucleotide transhydrogenase | -1.1 |
| A1S_1746 | Putative transcriptional regulator | -1.1 |
| A1S_1104 | Chlorogenate esterase | -1.1 |
| A1S_3458 | Na ⁺ -dependent transporters | -1.1 |
| A1S_r02 | Ribosomal protein | -1.1 |
| A1S_r05 | Ribosomal protein | -1.1 |
| A1S_r14 | Ribosomal protein | -1.1 |
| A1S_r11 | Ribosomal protein | -1.1 |
| A1S_2513 | tRNA-Asn | -1.1 |
| A1S_1004 | Citrate transporter | -1.1 |
| A1S_r08 | 23S ribosomal RNA | -1.1 |
| A1S_0732 | Transcriptional Regulator (AraC family) | -1.1 |
| A1S_1091 | Succinylornithine transaminase | -1.1 |
| A1S_1588 | Phage terminase-like protein large subunit | -1.1 |
| A1S_2401 | Hypothetical protein | -1.1 |
| A1S_2678 | tRNA-Leu | -1.1 |
| A1S_2744 | SAM-dependent methyltransferase | -1.1 |
| A1S_2229 | Putative acyl-CoA dehydrogenase | -1.1 |
| A1S_2452 | NAD-dependent aldehyde dehydrogenase | -1.1 |
| A1S_1696 | Hypothetical protein | -1.1 |
| A1S_1858 | Short-chain dehydrogenase SDR | -1.1 |
| A1S_2308 | Hypothetical protein | -1.1 |
| A1S_3343 | Hypothetical protein | -1.1 |
| A1S_2183 | Putative signal peptide | -1.1 |
| A1S_2101 | Putative transcriptional regulator | -1.1 |
| A1S_1731 | Acetoacetyl-CoA transferase beta subunit | -1.1 |
| A1S_3051 | Hypothetical protein | -1.1 |
| A1S_2755 | Putative acyltransferase | -1.1 |
| A1S_1008 | Isocitrate lyase | -1.1 |
| A1S_3130 | Succinylglutamic semialdehyde dehydrogenase | -1.1 |

| Locus-tag^a | Gene product^b | Differential expression (Log₂) |
|------------------------------|--------------------------------------------------|--------------------------------------------------|
| A1S_3355 | Hypothetical protein | -1.0 |
| A1S_2149 | Putative acyl CoA dehydrogenase | -1.0 |
| A1S_0779 | Hypothetical protein | -1.0 |
| A1S_1737 | 3-hydroxybutyrate dehydrogenase | -1.0 |
| A1S_1274 | Alcohol dehydrogenase GroES-like protein | -1.0 |
| A1S_0408 | putative glutathione S-transferase | -1.0 |
| A1S_1379 | Putative SAM-dependent methyltransferase | -1.0 |
| A1S_0848 | Transcriptional regulator | -1.0 |
| A1S_1160 | Hypothetical protein | -1.0 |
| A1S_0399 | Putative transcriptional regulator (LysR family) | -1.0 |
| A1S_2696 | Hypothetical protein | -1.0 |
| A1S_3214 | Cation efflux protein | -1.0 |
| A1S_2179 | Hypothetical protein | -1.0 |
| A1S_2527 | Putative thioesterase protein | -1.0 |
| A1S_2507 | Hypothetical protein | -1.0 |
| A1S_1261 | Putative 3-hydroxyacyl-CoA dehydrogenase | -1.0 |
| A1S_1156 | Hypothetical protein | -1.0 |
| A1S_1424 | Malonate decarboxylase beta subunit | -1.0 |
| A1S_2724 | Putative hemagglutinin/hemolysin | -1.0 |
| A1S_2344 | tRNA-Asn | -1.0 |
| A1S_1698 | Lipoate synthase | -1.0 |
| A1S_1338 | Hypothetical protein | -1.0 |
| A1S_0106 | Putative acyl CoA hydratase | -1.0 |
| A1S_2089 | Hypothetical protein | -1.0 |
| A1S_0108 | MFS metabolite/H ⁺ symporter | -1.0 |

^a. Sequence was obtained from ATCC 17978 GenBank accession number CP000521.1

^b. The predicted function of the protein based on the data from KEGG: Kyoto Encyclopaedia of Genes and Genomes.

Appendix 3 – Genes significantly up-regulated in *A. baumannii* ATCC 17978 Δ *rpmE1* under Zn²⁺-replete conditions (CP000521.1)

| Locus-tag ^a | Gene product ^b | Differential expression (Log ₂) |
|------------------------|--------------------------------------------------|---------------------------------------------|
| A1S_1121 | Lipase/esterase | 1.0 |
| A1S_1719 | 4Fe-4S ferredoxin | 1.0 |
| A1S_3226 | tRNA-Ser | 1.0 |
| A1S_1794 | Hypothetical protein | 1.1 |
| A1S_2334 | S-adenosyl-L-homocysteine hydrolase | 1.1 |
| A1S_0453 | Biopolymer transport protein (ExbB) | 1.2 |
| A1S_0214 | Universal stress protein | 1.2 |
| A1S_0215 | Sul1delta fusion protein | 1.3 |
| A1S_1813 | Transcriptional regulator | 1.4 |
| A1S_2335 | Methylenetetrahydrofolate reductase (NADPH) | 1.5 |
| A1S_0738 | Flavoprotein oxidoreductase | 1.5 |
| A1S_0736 | Hypothetical protein | 1.6 |
| A1S_0561 | Hypothetical protein | 1.6 |
| A1S_0452 | Periplasmic protein TonB | 1.8 |
| A1S_2310 | tRNA-Arg | 1.8 |
| A1S_0146 | High affinity Zn ²⁺ transport protein | 2.1 |
| A1S_1045 | Co/Zn/Cd efflux system | 2.2 |
| A1S_1044 | Co/Zn/Cd efflux system | 2.7 |
| A1S_0737 | Homocysteine methyltransferase | 2.7 |
| A1S_3412 | Hypothetical protein | 3.4 |
| A1S_2892 | TonB-dependent receptor protein | 5.4 |
| A1S_0092 | Ferric siderophore receptor protein | 5.6 |
| A1S_0093 | Hypothetical protein | 5.6 |
| A1S_0391 | L31 ribosomal protein, RpmE2 | 7.1 |
| A1S_3411 | G3E family GTPase | 7.2 |

^a. Sequence was obtained from ATCC 17978 GenBank accession number CP000521.1

^b. The predicted function of the protein based on the data from KEGG: Kyoto Encyclopaedia of Genes and Genomes.

Appendix 4 – Genes significantly down-regulated in *A. baumannii* ATCC 17978 $\Delta rpmE1$ under Zn²⁺-replete conditions (CP000521.1)

| Locus-tag^a | Gene product^b | Differential expression (Log₂) |
|------------------------------|----------------------------------------------------------------|--------------------------------------------------|
| A1S_1701 | Dihydrolipoamide acetyltransferase | -4.4 |
| A1S_2423 | L31 ribosomal protein, RpmE1 | -4.3 |
| A1S_1700 | Acetoin:26-dichlorophenolindophenol oxidoreductase | -4.0 |
| A1S_1699 | Acetoin:26-dichlorophenolindophenol oxidoreductase | -4.0 |
| A1S_1702 | Dihydrolipoamide dehydrogenase | -3.8 |
| A1S_1703 | Dihydrolipoamide dehydrogenase | -3.8 |
| A1S_1337 | Phenylacetic acid degradation B | -3.7 |
| A1S_0145 | Transcriptional repressor of Zn ²⁺ transport system | -3.6 |
| A1S_1704 | Acetoin dehydrogenase | -3.3 |
| A1S_1887 | 4-hydroxybenzoate transporter (MFS superfamily) | -3.3 |
| A1S_1890 | 3-carboxy-cis-cis-muconate cycloisomerase | -3.2 |
| A1S_3160 | Lipase | -3.2 |
| A1S_1894 | 3-oxoacid CoA-transferase subunit A | -2.9 |
| A1S_2093 | Hypothetical protein | -2.9 |
| A1S_1705 | (RR)-butanediol dehydrogenase | -2.7 |
| A1S_1467 | Glutamate symport transmembrane protein | -2.7 |
| A1S_1888 | Putative transport protein | -2.7 |
| A1S_1846 | 3-oxoacid CoA-transferase subunit A | -2.7 |
| A1S_1383 | Surface antigen | -2.7 |
| A1S_1885 | Protocatechuate 34-dioxygenase beta chain | -2.6 |
| A1S_3159 | Lipase foldase | -2.6 |
| A1S_1384 | CinA-like protein | -2.6 |
| A1S_2823 | Hypothetical protein | -2.6 |
| A1S_1697 | Putative transcriptional regulator | -2.5 |
| A1S_1884 | Protocatechuate 34-dioxygenase alpha chain (| -2.5 |
| A1S_1889 | 3-oxoadipate enol-lactonase I | -2.5 |
| A1S_1883 | Catabolic dehydroquinone dehydratase | -2.4 |
| A1S_1848 | Beta-ketoadipyl CoA thiolase | -2.3 |
| A1S_1892 | Beta-ketoadipyl CoA thiolase | -2.3 |
| A1S_1295 | Hypothetical protein | -2.3 |
| A1S_1886 | Gamma-carboxymuconolactone decarboxylase | -2.3 |
| A1S_1293 | Hypothetical protein | -2.3 |
| A1S_1882 | 3-dehydroshikimate dehydratase | -2.3 |
| A1S_1368 | Pyruvate ferredoxin/ferredoxin oxidoreductase | -2.2 |
| A1S_1292 | Putative signal peptide | -2.2 |
| A1S_1296 | Hypothetical protein | -2.2 |

| Locus-tag^a | Gene product^b | Differential expression (Log₂) |
|------------------------------|--------------------------------------------------------------------|--------------------------------------------------|
| A1S_1108 | Acyl coenzyme A dehydrogenase | -2.2 |
| A1S_1862 | Hypothetical protein | -2.2 |
| A1S_1369 | Putative oxidoreductase protein | -2.1 |
| A1S_1726 | Aspartate ammonia-lyase (aspartase) | -2.1 |
| A1S_2216 | CsuB | -2.1 |
| A1S_1294 | Hypothetical protein | -2.1 |
| A1S_2159 | Hypothetical protein | -2.1 |
| A1S_1724 | Dicarboxylic acid transport protein | -2.0 |
| A1S_1491 | Glutamate/aspartate transport protein | -2.0 |
| A1S_2843 | Hypothetical protein | -2.0 |
| A1S_2415 | tRNA-Val | -2.0 |
| A1S_2218 | CsuAB | -2.0 |
| A1S_1881 | Porin | -2.0 |
| A1S_1493 | Glutamate/aspartate transport protein | -2.0 |
| A1S_1301 | Putative membrane protein | -1.9 |
| A1S_0144 | High affinity Zn ²⁺ transport protein | -1.9 |
| A1S_0803 | Trehalose-6-phosphate synthase | -1.9 |
| A1S_1490 | Glutamate/aspartate transport protein | -1.9 |
| A1S_1380 | Putative protein (DcaP-like) | -1.9 |
| A1S_0804 | Hypothetical protein | -1.9 |
| A1S_1370 | Oxidoreductase | -1.9 |
| A1S_3445 | Putative RND family efflux pump | -1.9 |
| A1S_1738 | Putative transcriptional regulator | -1.8 |
| A1S_2217 | CsuA | -1.8 |
| A1S_1746 | Putative transcriptional regulator | -1.8 |
| A1S_1492 | Glutamate/aspartate transport protein | -1.8 |
| A1S_1341 | Enoyl-CoA hydratase/carnithine racemase | -1.8 |
| A1S_2033 | Hypothetical protein | -1.8 |
| A1S_1730 | Short-chain fatty acid transporter | -1.8 |
| A1S_3404 | Proline transport protein (APC family) | -1.8 |
| A1S_2451 | Transcriptional regulator AsnC family | -1.7 |
| A1S_0690 | FilA | -1.7 |
| A1S_2196 | Dicarboxylate transport protein | -1.7 |
| A1S_2214 | CsuD | -1.7 |
| A1S_1336 | Hypothetical protein | -1.7 |
| A1S_1300 | Hypothetical protein | -1.7 |
| A1S_1742 | Putative oxidoreductase short-chain Dehydrogenase/reductase family | -1.7 |
| A1S_2074 | Hypothetical protein | -1.7 |

| Locus-tag^a | Gene product^b | Differential expression (Log₂) |
|------------------------------|--------------------------------------------------|--------------------------------------------------|
| A1S_2215 | CsuC | -1.7 |
| A1S_0996 | Hypothetical protein | -1.7 |
| A1S_0184 | Hypothetical protein | -1.7 |
| A1S_3174 | Putative regulatory or redox component | -1.6 |
| A1S_1600 | Lysozyme | -1.6 |
| A1S_2325 | Putative outer membrane protein | -1.6 |
| A1S_2230 | Hypothetical protein | -1.6 |
| A1S_0721 | Glutaryl-CoA dehydrogenase | -1.6 |
| A1S_1349 | Thioesterase domain protein | -1.6 |
| A1S_0104 | Putative acetyl-coA synthetase/AMP- | -1.6 |
| A1S_1687 | Transcriptional regulator | -1.6 |
| A1S_1338 | Hypothetical protein | -1.6 |
| A1S_1297 | Hypothetical protein | -1.6 |
| A1S_2363 | Xanthine dehydrogenase large subunit | -1.6 |
| A1S_3446 | Putative RND family efflux pump | -1.6 |
| A1S_1342 | Putative enoyl-CoA hydratase II | -1.6 |
| A1S_0745 | Hypothetical protein | -1.6 |
| A1S_1298 | Hypothetical protein | -1.6 |
| A1S_3253 | Putative signal peptide | -1.6 |
| A1S_1151 | Hypothetical protein | -1.6 |
| A1S_1210 | Major facilitator superfamily MFS_1 | -1.6 |
| A1S_1838 | MFS family permease | -1.6 |
| A1S_2183 | Putative signal peptide | -1.5 |
| A1S_1847 | 3-oxoadipate CoA-transferase subunit B | -1.5 |
| A1S_1893 | 3-oxoadipate CoA-transferase subunit B | -1.5 |
| A1S_1880 | Pyrrroquinoline-quinone QuiA | -1.5 |
| A1S_0683 | Putative sigma(54) modulation protein RpoX | -1.5 |
| A1S_0009 | Putative RND type efflux pump | -1.5 |
| A1S_2308 | Hypothetical protein | -1.5 |
| A1S_1335 | Phenylacetic acid degradation protein PaaN | -1.5 |
| A1S_1386 | Catalase | -1.5 |
| A1S_0788 | Hypothetical protein | -1.5 |
| A1S_0490 | Putative hydrolase | -1.5 |
| A1S_2213 | CsuE | -1.5 |
| A1S_0143 | High affinity Zn ²⁺ transport protein | -1.5 |
| A1S_0099 | D-serine/D-alanine/glycine transport protein | -1.5 |
| A1S_0103 | 3-hydroxyisobutyrate dehydrogenase | -1.5 |
| A1S_0919 | Putative permease transmembrane protein | -1.5 |

| Locus-tag^a | Gene product^b | Differential expression (Log₂) |
|------------------------------|--------------------------------------------|--------------------------------------------------|
| A1S_0674 | Putative transposase | -1.4 |
| A1S_1680 | Hypothetical protein | -1.4 |
| A1S_0010 | RND type efflux pump | -1.4 |
| A1S_1340 | Phenylacetate-CoA oxygenase/reductase PaaK | -1.4 |
| A1S_0918 | Hypothetical protein | -1.4 |
| A1S_1149 | Hypothetical protein | -1.4 |
| A1S_1865 | Glu-tRNA amidotransferase | -1.4 |
| A1S_2031 | Hypothetical protein | -1.4 |
| A1S_1193 | OmpA/MotB | -1.4 |
| A1S_1844 | CatC3 | -1.4 |
| A1S_1736 | Putative membrane protein | -1.4 |
| A1S_3283 | Gamma-aminobutyrate permease | -1.4 |
| A1S_0910 | Gamma-glutamyltranspeptidase precursor | -1.4 |
| A1S_2148 | Ligase | -1.4 |
| A1S_1308 | Hypothetical protein | -1.3 |
| A1S_0853 | Succinate-semialdehyde dehydrogenase | -1.3 |
| A1S_2228 | Hypothetical protein | -1.3 |
| A1S_1104 | Chlorogenate esterase | -1.3 |
| A1S_2601 | Putative outer membrane protein A | -1.3 |
| A1S_1215 | Benzoate 12 dioxygenase alpha subunit | -1.3 |
| A1S_1302 | Putative membrane protein | -1.3 |
| A1S_1499 | Hypothetical protein | -1.3 |
| A1S_1378 | Putative long chain fatty-acid CoA ligase | -1.3 |
| A1S_0081 | Putative signal peptide | -1.3 |
| A1S_3418 | 4-hydroxyphenylpyruvate dioxygenase | -1.3 |
| A1S_0086 | Hypothetical protein | -1.3 |
| A1S_2027 | Hypothetical protein | -1.3 |
| A1S_1857 | Vanillate O-demethylase oxidoreductase | -1.3 |
| A1S_1385 | Hypothetical protein | -1.3 |
| A1S_1339 | Phenylacetate-CoA oxygenase PaaJ subunit | -1.3 |
| A1S_3043 | Hypothetical protein | -1.3 |
| A1S_1309 | Hypothetical protein | -1.3 |
| A1S_1731 | Acetoacetyl-CoA transferase beta subunit | -1.3 |
| A1S_1360 | ABC transporter | -1.3 |
| A1S_1841 | Hypothetical protein | -1.2 |
| A1S_0732 | Transcriptional Regulator | -1.2 |
| A1S_0720 | Putative transcriptional regulator | -1.2 |
| A1S_1387 | Oxidoreductase | -1.2 |

| Locus-tag^a | Gene product^b | Differential expression (Log₂) |
|------------------------------|-------------------------------------------|--------------------------------------------------|
| A1S_3300 | Putative sodium:solute symporter | -1.2 |
| A1S_2975 | Putative membrane protein | -1.2 |
| A1S_1526 | tRNA (uracil-5-)-methyltransferase | -1.2 |
| A1S_1125 | Putative transferase | -1.2 |
| A1S_0847 | Putative signal peptide | -1.2 |
| A1S_0787 | Putative signal peptide | -1.2 |
| A1S_2231 | Gamma-aminobutyrate permease | -1.2 |
| A1S_0108 | MFS metabolite/H ⁺ symporter | -1.2 |
| A1S_1312 | Putative membrane protein | -1.2 |
| A1S_3416 | Glyoxalase/bleomycin resistance protein | -1.2 |
| A1S_0786 | Putative signal peptide | -1.2 |
| A1S_2179 | Hypothetical protein | -1.2 |
| A1S_1233 | Hypothetical protein | -1.2 |
| A1S_1304 | Hypothetical protein | -1.2 |
| A1S_3327 | Dihydrolipoamide S-acetyltransferase | -1.2 |
| A1S_1440 | Putative transporter (MFS superfamily) | -1.2 |
| A1S_1109 | Coenzyme A ligase | -1.2 |
| A1S_1504 | YyaM | -1.2 |
| A1S_3143 | Cu/ Zn ²⁺ superoxide dismutase | -1.2 |
| A1S_1333 | Putative amino acid transporter | -1.2 |
| A1S_2104 | Ethanolamine ammonia-lyase heavy chain | -1.2 |
| A1S_0951 | Ferredoxin reductase | -1.2 |
| A1S_2602 | Hypothetical protein | -1.2 |
| A1S_2026 | Hypothetical protein | -1.2 |
| A1S_2452 | NAD-dependent aldehyde dehydrogenase | -1.2 |
| A1S_2082 | Transcriptional regulator | -1.2 |
| A1S_2210 | Hypothetical protein | -1.2 |
| A1S_0101 | Pseudogene | -1.2 |
| A1S_3309 | Acetyl-CoA synthetase | -1.2 |
| A1S_1299 | Hypothetical protein | -1.2 |
| A1S_1810 | Putative tartrate transporter | -1.2 |
| A1S_1311 | Putative membrane protein | -1.2 |
| A1S_3301 | Putative membrane protein | -1.2 |
| A1S_3343 | Hypothetical protein | -1.2 |
| A1S_2318 | Putative membrane protein | -1.2 |
| A1S_3415 | Maleylacetoacetate isomerase | -1.2 |
| A1S_2289 | Putative signal peptide | -1.1 |
| A1S_2826 | Putative signal peptide | -1.1 |

| Locus-tag^a | Gene product^b | Differential expression (Log₂) |
|------------------------------|------------------------------------------------------|--------------------------------------------------|
| A1S_2162 | Hypothetical protein YcdS precursor | -1.1 |
| A1S_0779 | Hypothetical protein | -1.1 |
| A1S_1760 | Hypothetical protein | -1.1 |
| A1S_1814 | Putative transporter | -1.1 |
| A1S_1932 | Hypothetical protein | -1.1 |
| A1S_3135 | Putative APC family S-methylmethionine transporter | -1.1 |
| A1S_3402 | Arginase hydrolase | -1.1 |
| A1S_1163 | Hypothetical protein | -1.1 |
| A1S_2557 | Hypothetical protein | -1.1 |
| A1S_3403 | Imidazolonepropionase | -1.1 |
| A1S_1594 | Hypothetical protein | -1.1 |
| A1S_1751 | AdeA membrane fusion protein | -1.1 |
| A1S_2160 | Haemin storage system HmsR protein | -1.1 |
| A1S_0850 | Betaine/choline/glycine transport | -1.1 |
| A1S_3278 | Hydrolase isochorismatase family | -1.1 |
| A1S_1737 | 3-hydroxybutyrate dehydrogenase | -1.1 |
| A1S_2406 | Hypothetical protein | -1.1 |
| A1S_2820 | Hypothetical protein | -1.1 |
| A1S_0591 | Putative AMP-dependent synthetase/ligase | -1.1 |
| A1S_1303 | Putative membrane protein | -1.1 |
| A1S_0929 | Putative choline/carnitine/betaine transporter | -1.1 |
| A1S_1356 | Transcriptional activator | -1.1 |
| A1S_1094 | D-serine/D-alanine/glycine transporter | -1.1 |
| A1S_1891 | Beta-ketoadipyl CoA thiolase | -1.1 |
| A1S_0802 | Putative transport protein (permease) | -1.1 |
| A1S_0917 | Transcriptional regulator | -1.1 |
| A1S_1951 | Hypothetical protein | -1.1 |
| A1S_1503 | Purine-cytosine permease | -1.1 |
| A1S_0441 | Putative membrane protein | -1.1 |
| A1S_3049 | Putative integral membrane protein | -1.1 |
| A1S_0960 | Putative permease (MFS superfamily) | -1.1 |
| A1S_1377 | Transcriptional regulator acrR family | -1.1 |
| A1S_0140 | NAD-linked malate dehydrogenase | -1.0 |
| A1S_0889 | Hypothetical protein | -1.0 |
| A1S_2809 | Bacteriolytic lipoprotein entericidin B | -1.0 |
| A1S_1287 | ABC nitrate/sulfonate/bicarbonate family transporter | -1.0 |
| A1S_1776 | Transcriptional regulatory protein | -1.0 |
| A1S_2484 | Putative membrane protein | -1.0 |

| Locus-tag^a | Gene product^b | Differential expression (Log₂) |
|------------------------------|------------------------------------------------|--------------------------------------------------|
| A1S_1209 | Putative benzoate transport porin (BenP) | -1.0 |
| A1S_2850 | Putative acyl-CoA transferase | -1.0 |
| A1S_1345 | PaaK | -1.0 |
| A1S_3120 | Hypothetical protein | -1.0 |
| A1S_1363 | Hypothetical protein | -1.0 |
| A1S_0464 | Sec-independent protein translocase protein | -1.0 |
| A1S_1430 | Transcriptional regulator (LysR family) | -1.0 |
| A1S_2028 | Phage putative head morphogenesis protein | -1.0 |
| A1S_1868 | Porin for benzoate transport (BenP) | -1.0 |
| A1S_2649 | Putative regulatory protein | -1.0 |
| A1S_1954 | Serine proteinase | -1.0 |
| A1S_3139 | Putative signal peptide | -1.0 |
| A1S_0785 | Hypothetical protein | -1.0 |
| A1S_3051 | Hypothetical protein | -1.0 |
| A1S_1585 | EsvK1 | -1.0 |
| A1S_0482 | Acetate kinase (propionate kinase) | -1.0 |
| A1S_0855 | Dioxygenase beta subunit | -1.0 |
| A1S_1376 | Acyl-CoA dehydrogenase | -1.0 |
| A1S_3155 | Hypothetical protein | -1.0 |
| A1S_1227 | Transporter LysE family | -1.0 |
| A1S_1797 | Aldehyde dehydrogenase | -1.0 |
| A1S_2388 | Putative ferric acinetobactin transport system | -1.0 |
| A1S_0959 | Putative signal peptide | -1.0 |

^a. Sequence was obtained from ATCC 17978 GenBank accession number CP000521.1

^b. The predicted function of the protein based on the data from KEGG: Kyoto Encyclopaedia of Genes and Genomes.

Appendix 5 – Genes significantly up-regulated in *A. baumannii* ATCC 17978 Δ *rpmE1* under Zn²⁺-limited conditions (CP000521.1)

| Locus-tag^a | Gene product^b | Differential expression (Log₂) |
|------------------------------|---------------------------------------------|--------------------------------------------------|
| A1S_0737 | Homocysteine-S- methyltransferase | 1.0 |
| A1S_2334 | S-adenosyl-L-homocysteine hydrolase | 1.0 |
| A1S_3043 | Hypothetical protein | 1.0 |
| A1S_0951 | Putative ferredoxin reductase | 1.0 |
| A1S_0918 | Hypothetical protein | 1.0 |
| A1S_1121 | Putative short-chain dehydrogenase | 1.0 |
| A1S_1663 | Cobalamin-5-phosphate synthase CobS | 1.0 |
| A1S_1500 | tRNA-Met | 1.1 |
| A1S_1339 | Phenylacetate-CoA oxygenase PaaJ subunit | 1.2 |
| A1S_1384 | CinA-like protein | 1.2 |
| A1S_0214 | Universal stress protein | 1.2 |
| A1S_2105 | Ethanolamine ammonia-lyase | 1.3 |
| A1S_0215 | Sul1delta fusion protein | 1.3 |
| A1S_0946 | Hypothetical protein | 1.3 |
| A1S_2224 | Threonine efflux protein | 1.3 |
| A1S_2558 | Putative transposase | 1.3 |
| A1S_3122 | Putative membrane protein | 1.4 |
| A1S_1588 | Phage terminase-like protein large subunit | 1.5 |
| A1S_1341 | Enoyl-CoA hydratase/carnithine racemase | 1.5 |
| A1S_2373 | Putative acinetobactin biosynthesis protein | 1.7 |
| A1S_1480 | Hypothetical protein | 1.8 |
| A1S_r03 | 5S ribosomal RNA | 1.9 |
| A1S_r04 | 5S ribosomal RNA | 1.9 |
| A1S_r10 | 5S ribosomal RNA | 1.9 |
| A1S_r13 | 5S ribosomal RNA | 1.9 |
| A1S_r07 | 5S ribosomal RNA | 2.0 |
| A1S_1758 | Short-chain dehydrogenase SDR | 2.0 |
| A1S_0945 | Ferredoxin | 3.0 |
| A1S_2082 | Transcriptional regulator | 3.0 |

^a. Sequence was obtained from ATCC 17978 GenBank accession number CP000521.1

^b. The predicted function of the protein based on the data from KEGG: Kyoto Encyclopaedia of Genes and Genomes.

Appendix 6 – Genes significantly down-regulated in *A. baumannii* ATCC 17978 $\Delta rpmE1$ under Zn^{2+} -limited conditions (CP000521.1)

| Locus-tag^a | Gene product^b | Differential expression (Log₂) |
|------------------------------|--------------------------------------------------|--------------------------------------------------|
| A1S_0145 | Zinc uptake regulator | -4.1 |
| A1S_0144 | High affinity Zn^{2+} transport protein | -3.2 |
| A1S_2423 | L31 ribosomal protein, RpmE1 | -3.0 |
| A1S_1294 | Type VI secretion system protein ImpB | -2.9 |
| A1S_3445 | RND family cation/multidrug efflux pump | -2.9 |
| A1S_0143 | High affinity Zn^{2+} transport protein | -2.6 |
| A1S_1293 | Hypothetical protein | -2.5 |
| A1S_1295 | Type VI secretion system protein ImpC | -2.5 |
| A1S_2217 | CsuA | -2.5 |
| A1S_1296 | Type VI secretion system secreted protein Hcp | -2.4 |
| A1S_1292 | Signal peptide | -2.3 |
| A1S_2310 | tRNA-Arg | -2.3 |
| A1s_2027 | Hypothetical protein | -2.2 |
| A1S_2218 | CsuAB | -2.1 |
| A1S_2216 | CsuB | -2.0 |
| A1S_1297 | Hypothetical protein | -2.0 |
| A1S_2021 | Hypothetical protein | -2.0 |
| A1S_1311 | Putative membrane protein | -1.9 |
| A1S_1301 | Putative membrane protein | -1.8 |
| A1S_1298 | Hypothetical protein | -1.7 |
| A1S_2557 | Hypothetical protein | -1.7 |
| A1S_3446 | Putative RND family cation/multidrug efflux pump | -1.7 |
| A1S_2016 | Phage-related lysozyme | -1.7 |
| A1S_3215 | tRNA-Phe | -1.7 |
| A1S_2214 | CsuD | -1.6 |
| A1S_1309 | Hypothetical protein | -1.6 |
| A1S_1151 | Hypothetical protein | -1.6 |
| A1S_2215 | CsuC | -1.5 |
| A1S_1300 | Hypothetical protein | -1.5 |
| A1S_1310 | Hypothetical protein | -1.5 |
| A1S_1299 | Hypothetical protein | -1.5 |
| A1S_1303 | Putative membrane protein | -1.5 |
| A1S_2213 | CsuE | -1.4 |
| A1S_0991 | Hypothetical protein | -1.4 |
| A1S_1302 | Putative membrane protein | -1.3 |

| Locus-tag^a | Gene product^b | Differential expression (Log₂) |
|------------------------------|--------------------------------------------------------------------|--------------------------------------------------|
| A1S_0086 | Hypothetical protein | -1.3 |
| A1S_1147 | Site-specific DNA methylase-like protein | -1.3 |
| A1S_1308 | Hypothetical protein | -1.3 |
| A1S_1304 | Hypothetical protein | -1.2 |
| A1S_1161 | Hypothetical protein | -1.2 |
| A1S_0727 | Putative substrate-binding protein | -1.2 |
| A1S_0233 | Type 4 fimbriae expression regulatory protein | -1.2 |
| A1S_2026 | Hypothetical protein | -1.2 |
| A1S_2031 | Hypothetical protein | -1.2 |
| A1S_2652 | tRNA-Ser | -1.1 |
| A1S_0915 | Putative MFS transporter | -1.1 |
| A1S_2030 | Hypothetical protein | -1.1 |
| A1S_1719 | 4Fe-4S ferredoxin iron-sulfur binding | -1.1 |
| A1S_1681 | Putative methyltransferase | -1.1 |
| A1S_1081 | Hypothetical protein | -1.1 |
| A1S_1742 | Putative oxidoreductase short-chain dehydrogenase/reductase family | -1.1 |
| A1S_1278 | Allophanate hydrolase subunit 2 | -1.1 |
| A1S_1594 | Hypothetical protein | -1.1 |
| A1S_3286 | Putative inner membrane protein | -1.0 |
| A1S_2029 | Hypothetical protein | -1.0 |
| A1S_2033 | Hypothetical protein | -1.0 |
| A1S_0819 | Acyl carrier protein (ACP) | -1.0 |
| A1S_2675 | tRNA-Cys | -1.0 |
| A1S_1305 | Putative outer membrane lipoprotein | -1.0 |
| A1S_1592 | Putative Phage head-tail adaptor | -1.0 |

^a. Sequence was obtained from ATCC 17978 GenBank accession number CP000521.1

^b. The predicted function of the protein based on the data from KEGG: Kyoto Encyclopaedia of Genes and Genomes.

Appendix 7 – Genes significantly up-regulated in *A. baumannii* ATCC 17978 $\Delta rpmE2$ under Zn^{2+} -replete conditions (CP000521.1)

| Locus-tag ^a | Gene product ^b | Differential expression (Log ₂) |
|------------------------|-----------------------------------------------|---------------------------------------------|
| A1S_2068 | Putative magnesium transporter | 1.0 |
| A1S_1794 | Dihydroxy-acid dehydratase | 1.0 |
| A1S_1715 | Chromate transporter | 1.0 |
| A1S_2744 | SAM-dependent methyltransferase | 1.0 |
| A1S_0097 | Hypothetical protein | 1.0 |
| A1S_2646 | Putative metal hydrolase | 1.1 |
| A1S_3059 | Ribosomal protein S13 | 1.3 |
| A1S_3058 | 30S ribosomal protein S11 | 1.3 |
| A1S_2334 | 510-methylenetetrahydrofolate reductase | 1.3 |
| A1S_1435 | Putative acyl-CoA dehydrogenase | 1.4 |
| A1S_2016 | Hypothetical protein | 1.4 |
| A1S_3056 | DNA-directed RNA polymerase subunit alpha | 1.4 |
| A1S_3057 | 30S ribosomal protein S4 ribosomal protein S4 | 1.4 |
| A1S_3055 | Ribosomal protein L17 | 1.5 |
| A1S_2335 | Hypothetical protein | 1.6 |
| A1S_0736 | Hypothetical protein | 1.6 |
| A1S_0738 | Putative flavoprotein oxidoreductase | 1.6 |
| A1S_2573 | 23-dihydroxybenzoate-AMP ligase | 1.9 |
| A1S_0737 | Homocysteine-S- methyltransferase | 2.4 |

^a. Sequence was obtained from ATCC 17978 GenBank accession number CP000521.1

^b. The predicted function of the protein based on the data from KEGG: Kyoto Encyclopaedia of Genes and Genomes.

Appendix 8 – Genes significantly down-regulated in *A. baumannii* ATCC 17978 Δ *rpmE2* under Zn²⁺-replete conditions (CP000521.1)

| Locus-tag^a | Gene product^b | Differential expression (Log₂) |
|------------------------------|------------------------------------------------------------------|--------------------------------------------------|
| A1S_0391 | L31 ribosomal protein, RpmE2 | -3.0 |
| A1S_1890 | 3-carboxy-cis,cis-muconate cycloisomerase | -2.8 |
| A1S_1888 | Transport protein MFS transporter | -2.8 |
| A1S_1889 | 3-oxoadipate enol-lactonase | -2.7 |
| A1S_3160 | Lipase | -2.7 |
| A1S_1701 | Dihydrolipoamide acetyltransferase | -2.7 |
| A1S_1383 | Surface antigen | -2.7 |
| A1S_1894 | 3-oxoacid CoA-transferase subunit A | -2.6 |
| A1S_1293 | Hypothetical protein | -2.6 |
| A1S_1292 | Signal peptide | -2.6 |
| A1S_1704 | Acetoin dehydrogenase | -2.5 |
| A1S_2093 | Hypothetical protein | -2.5 |
| A1S_1886 | Gamma-carboxymuconolactone decarboxylase (CMD) | -2.5 |
| A1S_1700 | Acetoin:26-dichlorophenolindophenol oxidoreductase subunit beta | -2.5 |
| A1S_1846 | 3-oxoacid CoA-transferase subunit A | -2.4 |
| A1S_1702 | Dihydrolipoamide dehydrogenase | -2.4 |
| A1S_1294 | Hypothetical protein | -2.4 |
| A1S_1703 | Dihydrolipoamide dehydrogenase | -2.3 |
| A1S_1699 | Acetoin:26-dichlorophenolindophenol oxidoreductase subunit alpha | -2.3 |
| A1S_1705 | (RR)-butanediol dehydrogenase | -2.3 |
| A1S_2823 | Hypothetical protein | -2.2 |
| A1S_1467 | Gutamate symport transmembrane protein | -2.2 |
| A1S_1885 | Protocatechuate 34-dioxygenase subunit beta | -2.2 |
| A1S_1887 | 4-hydroxybenzoate transporter | -2.2 |
| A1S_1193 | OmpA/MotB protein | -2.2 |
| A1S_1349 | Thioesterase domain-containing protein | -2.1 |
| A1S_1295 | Hypothetical protein | -2.1 |
| A1S_1847 | 3-oxoadipate CoA-transferase subunit B | -2.1 |
| A1S_1893 | 3-oxoadipate CoA-transferase subunit B | -2.1 |
| A1S_1883 | AroD; 3-dehydroquinate dehydratase | -2.1 |
| A1S_3159 | Lipase chaperone | -2.1 |
| A1S_1884 | Protocatechuate 34-dioxygenase subunit alpha | -1.9 |
| A1S_1296 | Hypothetical protein | -1.9 |
| A1S_0803 | Trehalose-6-phosphate synthase] | -1.9 |
| A1S_0804 | Trehalose-6-phosphate phosphatase | -1.9 |

| Locus-tag^a | Gene product^b | Differential expression (Log₂) |
|------------------------------|-----------------------------------------------------|--------------------------------------------------|
| A1S_1697 | Transcriptional regulator | -1.8 |
| A1S_0674 | Intracellular multiplication protein lcmO | -1.8 |
| A1S_1386 | Catalase | -1.8 |
| A1S_3043 | Hypothetical protein | -1.8 |
| A1S_2196 | Membrane-associated dicarboxylate transport protein | -1.8 |
| A1S_1297 | Hypothetical protein | -1.7 |
| A1S_1337 | Phenylacetate-CoA oxygenase subunit PaaB | -1.7 |
| A1S_2230 | Hypothetical protein | -1.7 |
| A1S_1848 | Protocatechuate 3,4-dioxygenase subunit alpha | -1.7 |
| A1S_1892 | Beta-ketoadipyl CoA thiolase | -1.7 |
| A1S_3174 | Bacterioferritin-associated ferredoxin | -1.7 |
| A1S_1341 | Enoyl-CoA hydratase/carnithine racemase | -1.7 |
| A1S_1301 | Hypothetical protein | -1.7 |
| A1S_1726 | Aspartate ammonia-lyase (aspartase) | -1.7 |
| A1S_1724 | Dicarboxylic acid transport protein | -1.6 |
| A1S_0745 | Hypothetical protein | -1.6 |
| A1S_1385 | Hypothetical protein | -1.6 |
| A1S_1336 | Ring-1,2-phenylacetyl-CoA epoxidase subunit PaaA | -1.6 |
| A1S_1881 | Porin | -1.6 |
| A1S_1882 | 3-dehydroshikimate dehydratase | -1.6 |
| A1S_2843 | Hypothetical protein | -1.6 |
| A1S_1384 | CinA-like protein | -1.6 |
| A1S_2451 | Transcriptional regulator AsnC family | -1.6 |
| A1S_3297 | Putative outer membrane protein | -1.6 |
| A1S_2183 | Putative signal peptide | -1.5 |
| A1S_1492 | Glutamate/aspartate transport protein | -1.5 |
| A1S_1369 | Putative oxidoreductase protein | -1.5 |
| A1S_0721 | Glutaryl-CoA dehydrogenase | -1.5 |
| A1S_1491 | Glutamate/aspartate transport protein | -1.5 |
| A1S_1738 | Putative transcriptional regulator | -1.5 |
| A1S_1880 | Pyrrroquinoline-quinone QuiA | -1.4 |
| A1S_1368 | Pyruvate ferredoxin/flavodoxin oxidoreductase | -1.4 |
| A1S_2228 | Hypothetical protein | -1.4 |
| A1S_1490 | Glutamate/aspartate transport protein | -1.4 |
| A1S_3404 | Proline transport protein (APC family) | -1.4 |
| A1S_3327 | Dihydrolipoamide S-acetyltransferase E2 | -1.4 |
| A1S_0104 | Acetyl-CoA synthetase | -1.4 |
| A1S_2159 | Hypothetical protei | -1.4 |
| A1S_2216 | CsuB | -1.4 |
| A1S_1730 | Short-chain fatty acid transporter (scFAT family) | -1.3 |

| Locus-tag^a | Gene product^b | Differential expression (Log₂) |
|------------------------------|---------------------------------------------------------------|--------------------------------------------------|
| A1S_0490 | Putative hydrolase | -1.3 |
| A1S_1308 | Hypothetical protein | -1.3 |
| A1S_1310 | Type VI secretion system protein ImpK | -1.3 |
| A1S_2217 | CsuA | -1.3 |
| A1S_1300 | Type VI secretion system protein ImpH | -1.3 |
| A1S_3253 | Putative signal peptide | -1.3 |
| A1S_0788 | Hypothetical protein | -1.3 |
| A1S_3248 | Glycerol uptake facilitator | -1.3 |
| A1S_1687 | Hypothetical protein | -1.3 |
| A1S_1340 | Enoyl-CoA hydratase/carnithine racemase | -1.3 |
| A1S_1298 | Hypothetical protein | -1.2 |
| A1S_1309 | Hypothetical protein | -1.2 |
| A1S_0771 | Putative membrane protein | -1.2 |
| A1S_3143 | Cu/ Zn ²⁺ superoxide dismutase | -1.2 |
| A1S_2849 | Putative glucose-sensitive porin (OprB-like) | -1.2 |
| A1S_0690 | FilA | -1.2 |
| A1S_1493 | Glutamate/aspartate transport protein | -1.2 |
| A1S_1746 | Hypothetical protein | -1.2 |
| A1S_3428 | Putative glucose dehydrogenase precursor | -1.2 |
| A1S_1932 | Hypothetical protein | -1.2 |
| A1S_1302 | Putative membrane protein | -1.2 |
| A1S_0558 | Aconitate hydratase 1 | -1.2 |
| A1S_0561 | Hypothetical protein | -1.2 |
| A1S_2218 | CsuAB | -1.2 |
| A1S_1304 | Hypothetical protein | -1.2 |
| A1S_1303 | Hypothetical protein | -1.2 |
| A1S_0996 | Hypothetical protein | -1.2 |
| A1S_1339 | Phenylacetate-CoA oxygenase PaaJ subunit | -1.1 |
| A1S_1732 | Acetoacetyl-CoA transferase subunit α | -1.1 |
| A1S_1104 | Chlorogenate esterase | -1.1 |
| A1S_2975 | Putative membrane protein | -1.1 |
| A1S_0683 | Putative sigma(54) modulation protein RpoX | -1.1 |
| A1S_1335 | Hypothetical protein | -1.1 |
| A1S_0929 | Putative choline/carnitine/betaine transporter family protein | -1.1 |
| A1S_1342 | PaaC | -1.1 |
| A1S_1387 | Hypothetical protein | -1.1 |
| A1S_2215 | CsuB | -1.1 |
| A1S_2847 | Glucose dehydrogenase | -1.1 |
| A1S_1891 | Beta-ketoadipyl CoA thiolase | -1.1 |
| A1S_1858 | Short-chain dehydrogenase SDR | -1.1 |

| Locus-tag^a | Gene product^b | Differential expression (Log₂) |
|------------------------------|--------------------------------------------------------|--------------------------------------------------|
| A1S_1860 | (2Fe-2S) protein | -1.1 |
| A1S_2179 | Hypothetical protein | -1.1 |
| A1S_2452 | NAD-dependent aldehyde dehydrogenase | -1.1 |
| A1S_0099 | D-serine/D-alanine/glycine transport protein | -1.0 |
| A1S_2308 | Hypothetical protein | -1.0 |
| A1S_3328 | Pyruvate decarboxylase E1 component | -1.0 |
| A1S_2848 | Glucose dehydrogenase | -1.0 |
| A1S_1731 | Acetoacetyl-CoA transferase alpha subunit | -1.0 |
| A1S_0394 | Putative acyl-CoA dehydrogenase | -1.0 |
| A1S_1220 | Hypothetical protein | -1.0 |
| A1S_1760 | Acetyltransferase | -1.0 |
| A1S_2331 | Putative 4-carboxymuconolactone decarboxylase | -1.0 |
| A1S_2148 | Putative acyl CoA dehydrogenase oxidoreductase protein | -1.0 |
| A1S_2364 | Xanthine dehydrogenase small subunit | -1.0 |
| A1S_1574 | Putative membrane protein | -1.0 |
| A1S_0140 | NAD-linked malate dehydrogenase | -1.0 |
| A1S_3406 | Urocanate hydratase | -1.0 |
| A1S_1370 | Transcriptional regulator LysR family | -1.0 |
| A1S_0786 | Putative signal peptide | -1.0 |
| A1S_2487 | Hypothetical protein | -1.0 |
| A1S_2640 | Putative oxidoreductase molybdopterin | -1.0 |

^a. Sequence was obtained from ATCC 17978 GenBank accession number CP000521.1

^b. The predicted function of the protein based on the data from KEGG: Kyoto Encyclopaedia of Genes and Genomes.

Appendix 9 – Genes significantly up-regulated in *A. baumannii* ATCC 17978 Δ rpmE2 under Zn²⁺-limited conditions (CP000521.1)

| Locus-tag ^a | Gene product ^b | Differential expression (Log ₂) |
|------------------------|------------------------------------|---------------------------------------------|
| A1S_2224 | Threonine efflux protein | 1.0 |
| A1S_1121 | Lipase/esterase | 1.0 |
| A1S_2744 | SAM-dependent methyltransferase | 1.0 |
| A1S_0517 | Hypothetical protein | 1.0 |
| A1S_2573 | 23-dihydroxybenzoate-AMP ligase | 1.1 |
| A1S_2885 | putative signal peptide | 1.1 |
| A1S_0032 | Putative signal peptide | 1.1 |
| A1S_0595 | Putative membrane protein | 1.2 |
| A1S_3264 | Putative transcriptional regulator | 1.2 |
| A1S_2347 | Hypothetical protein | 1.2 |
| A1S_3059 | 30S ribosomal protein S13 | 1.3 |
| A1S_3058 | 30S ribosomal protein S11 | 1.3 |
| A1S_3056 | RNA polymerase alpha subunit | 1.4 |
| A1S_3055 | 50S ribosomal protein L17 | 1.4 |
| A1S_3057 | 30S ribosomal protein S4 | 1.5 |
| A1S_0945 | Putative Ferredoxin reductase | 1.5 |
| A1S_0951 | Putative ferredoxin reductase | 1.6 |
| A1S_1480 | Hypothetical protein | 1.6 |
| A1S_2889 | Putative signal peptide | 1.7 |
| A1S_1384 | CinA-like protein | 1.7 |
| A1S_1500 | tRNA-Meth | 1.8 |
| A1S_2423 | 50S ribosomal protein L31 | 2.2 |
| A1S_2082 | Transcriptional regulator | 2.6 |
| A1S_r08 | 23S ribosomal RNA | 5.5 |
| A1S_r11 | 23S ribosomal RNA | 5.5 |
| A1S_r02 | 23S ribosomal RNA | 5.5 |
| A1S_r05 | 23S ribosomal RNA | 5.5 |
| A1S_r14 | 23S ribosomal RNA | 5.5 |
| A1S_r01 | 16S ribosomal RNA | 5.6 |
| A1S_r06 | 16S ribosomal RNA | 5.6 |
| A1S_r09 | 16S ribosomal RNA | 5.6 |
| A1S_r12 | 16S ribosomal RNA | 5.6 |
| A1S_r15 | 16S ribosomal RNA | 5.6 |

^a. Sequence was obtained from ATCC 17978 GenBank accession number CP000521.1

^b. The predicted function of the protein based on the data from KEGG: Kyoto Encyclopaedia of Genes and Genomes.

Appendix 10 – Genes significantly down-regulated in *A. baumannii* ATCC 17978 Δ *rpmE2* under Zn²⁺-limited conditions (CP000521.1)

| Locus-tag^a | Gene product^b | Differential expression (Log₂) |
|------------------------------|--------------------------------------------------|--------------------------------------------------|
| A1S_0391 | 50S ribosomal protein L31, RpmE2 | -11.3 |
| A1S_1292 | Hypothetical protein | -2.3 |
| A1S_1294 | Hypothetical protein | -2.2 |
| A1S_1295 | Hypothetical protein | -2.2 |
| A1S_1148 | Hypothetical protein | -2.2 |
| A1S_1296 | Hypothetical protein | -2.1 |
| A1S_1293 | Hypothetical protein | -2.1 |
| A1S_2218 | CsuAB | -2.1 |
| A1S_1297 | Hypothetical protein | -2.0 |
| A1S_2217 | CsuA | -2.0 |
| A1S_2216 | CsuB | -1.9 |
| A1S_1147 | Site-specific DNA methylase-like protein | -1.9 |
| A1S_0561 | Hypothetical protein | -1.8 |
| A1S_3297 | Putative high affinity choline transport protein | -1.7 |
| A1S_2215 | CsuC | -1.7 |
| A1S_1152 | Putative phage-related protein | -1.7 |
| A1S_1422 | Malonate decarboxylase alpha subunit | -1.6 |
| A1S_1894 | 3-oxoacid CoA-transferase subunit A | -1.6 |
| A1S_1309 | Hypothetical protein | -1.5 |
| A1S_1302 | Putative membrane protein | -1.5 |
| A1S_1301 | Putative membrane protein | -1.5 |
| A1S_1308 | Hypothetical protein | -1.4 |
| A1S_1303 | Putative membrane protein | -1.4 |
| A1S_1304 | Hypothetical protein | -1.4 |
| A1S_3272 | Putative peptide signal | -1.4 |
| A1S_1276 | Hypothetical protein | -1.3 |
| A1S_1846 | 3-oxoacid CoA-transferase subunit A | -1.3 |
| A1S_2408 | Hypothetical protein | -1.3 |
| A1S_2214 | CsuD | -1.3 |
| A1S_1163 | Putative phage tail tape measure protein | -1.3 |
| A1S_1300 | Hypothetical protein | -1.3 |
| A1S_1486 | Putative monooxygenase (DszA-like) | -1.3 |

^a. Sequence was obtained from ATCC 17978 GenBank accession number CP000521.1

^b. The predicted function of the protein based on the data from KEGG: Kyoto Encyclopaedia of Genes and Genomes.

Appendix 11 – Genes significantly up-regulated in *A. baumannii* ATCC 17978 under Zn²⁺-limited conditions (CP012004)

| Locus-tag^a | Gene product | Differential expression (Log₂) |
|------------------------------|---------------------------------------------------------------------------|--------------------------------------------------|
| ACX60_16160 | 50S ribosomal protein L31 | 8.5 |
| ACX60_00360 | Hypothetical protein | 8.1 |
| ACX60_17610 | Ligand-gated channel protein | 6.2 |
| ACX60_03050 | TonB-dependent receptor | 6.1 |
| ACX60_17605 | Membrane protein | 6.1 |
| ACX60_00355 | Peptidase M15 | 4.2 |
| A1S_3475 | Hypothetical protein | 3.5 |
| A1S_3476 | Secretory lipase | 3.1 |
| ACX60_18595 | Iron transporter | 3.0 |
| ACX60_17350 | DNA repair protein | 2.9 |
| ACX60_18600 | Iron transporter FeoB | 2.7 |
| ACX60_15845 | TonB-dependent receptor | 2.5 |
| ACX60_15315 | Hypothetical protein | 2.2 |
| ACX60_10955 | Hypothetical protein | 2.2 |
| ACX60_17175 | Membrane protein | 2.1 |
| ACX60_14705 | 5-methyltetrahydropteroyltriglutamate-- Homocysteine methyltransferase | 1.9 |
| ACX60_11735 | Hypothetical protein | 1.8 |
| ACX60_10160 | Hypothetical protein | 1.8 |
| ACX60_11065 | Murein hydrolase transporter LrgA | 1.7 |
| ACX60_15840 | Biopolymer transporter ExbB | 1.7 |
| ACX60_07415 | Hypothetical protein | 1.6 |
| ACX60_09315 | 4Fe-4S ferredoxin | 1.5 |
| ACX60_10595 | Hypothetical protein | 1.5 |
| ACX60_08185 | Cytochrome bd biosynthesis protein | 1.5 |
| ACX60_01975 | Hypothetical protein | 1.5 |
| ACX60_00800 | Hypothetical protein | 1.4 |
| ACX60_08200 | Cytochrome d terminal oxidase subunit 1 | 1.3 |
| ACX60_08195 | Cytochrome d ubiquinol oxidase subunit 2 | 1.3 |
| ACX60_07410 | ATPase AAA | 1.3 |
| ACX60_08295 | Phospho-2-dehydro-3-deoxyheptonate aldolase | 1.3 |
| ACX60_07440 | Hypothetical protein | 1.2 |
| ACX60_08190 | Membrane protein | 1.2 |
| ACX60_14700 | Flavin reductase | 1.2 |
| ACX60_03045 | Zn ²⁺ dependent phospholipase C | 1.2 |
| ACX60_07420 | Hypothetical protein | 1.2 |
| ACX60_12605 | Hypothetical protein | 1.2 |
| ACX60_17360 | Zn ²⁺ ABC transporter ATP-binding protein | 1.2 |

| Locus-tag^a | Gene product | Differential expression (Log₂) |
|------------------------------|-------------------------------------------|--------------------------------------------------|
| ACX60_00085 | tRNA-Ala | 1.2 |
| ACX60_02440 | tRNA-Ala | 1.2 |
| ACX60_02605 | tRNA-Ala | 1.2 |
| ACX60_14995 | tRNA-Ala | 1.2 |
| ACX60_17210 | tRNA-Ala | 1.2 |
| ACX60_18015 | tRNA-Ala | 1.2 |
| ACX60_09350 | Multidrug DMT transporter permease | 1.2 |
| ACX60_05605 | Iron ABC transporter permease | 1.1 |
| ACX60_08090 | Alpha/beta hydrolase | 1.1 |
| ACX60_06720 | Cytochrome o ubiquinol oxidase subunit IV | 1.1 |
| ACX60_01460 | tRNA-Ala | 1.1 |
| ACX60_15835 | Biopolymer transporter ExbD | 1.1 |
| ACX60_07390 | Hypothetical protein | 1.1 |
| ACX60_09615 | Membrane protein | 1.1 |
| ACX60_12610 | Hypothetical protein | 1.1 |
| ACX60_13810 | Hypothetical protein | 1.1 |
| ACX60_10155 | Hypothetical protein | 1.1 |
| ACX60_06485 | Protein CsuA | 1.0 |
| ACX60_08875 | Fumarylacetoacetate hydrolase | 1.0 |
| ACX60_12635 | Hypothetical protein | 1.0 |
| ACX60_17885 | Oxidoreductase | 1.0 |
| ACX60_17865 | Hypothetical protein | 1.0 |
| ACX60_17365 | DNA repair protein | 1.0 |
| ACX60_09515 | SAM-dependent methyltransferase | 1.0 |
| ACX60_17355 | Fur family transcriptional regulator | 1.0 |
| ACX60_01020 | branched-chain amino acid transport | 1.0 |
| ACX60_00085 | tRNA-Ala | 1.2 |
| ACX60_02440 | tRNA-Ala | 1.2 |
| ACX60_02605 | tRNA-Ala | 1.2 |
| ACX60_14995 | tRNA-Ala | 1.2 |
| ACX60_17210 | tRNA-Ala | 1.2 |
| ACX60_18015 | tRNA-Ala | 1.2 |
| ACX60_09350 | Multidrug DMT transporter permease | 1.2 |
| ACX60_05605 | Iron ABC transporter permease | 1.1 |
| ACX60_08090 | Alpha/beta hydrolase | 1.1 |
| ACX60_06720 | Cytochrome o ubiquinol oxidase subunit IV | 1.1 |
| ACX60_01460 | tRNA-Ala | 1.1 |

| Locus-tag^a | Gene product | Differential expression (Log₂) |
|------------------------------|--------------------------------------|--------------------------------------------------|
| ACX60_15835 | Biopolymer transporter ExbD | 1.1 |
| ACX60_07390 | Hypothetical protein | 1.1 |
| ACX60_09615 | Membrane protein | 1.1 |
| ACX60_12610 | Hypothetical protein | 1.1 |
| ACX60_13810 | Hypothetical protein | 1.1 |
| ACX60_10155 | Hypothetical protein | 1.1 |
| ACX60_06485 | Protein CsuA | 1.0 |
| ACX60_08875 | Fumarylacetoacetate hydrolase | 1.0 |
| ACX60_12635 | Hypothetical protein | 1.0 |
| ACX60_17885 | Oxidoreductase | 1.0 |
| ACX60_17865 | Hypothetical protein | 1.0 |
| ACX60_17365 | DNA repair protein | 1.0 |
| ACX60_09515 | SAM-dependent methyltransferase | 1.0 |
| ACX60_17355 | Fur family transcriptional regulator | 1.0 |
| ACX60_01020 | Branched-chain amino acid transport | 1.0 |

^a Sequence was obtained from ATCC 17978 GenBank accession number CP012004

Appendix 12 – Genes significantly down-regulated in *A. baumannii* ATCC 17978 under Zn²⁺-limited conditions (CP012004)

| Locus-tag^a | Gene product | Differential expression (Log₂) |
|------------------------------|-----------------------------------------|--------------------------------------------------|
| ACX60_06405 | Acyl-CoA dehydrogenase | -1.0 |
| ACX60_12105 | Hypothetical protein | -1.0 |
| ACX60_00260 | Membrane protein | -1.0 |
| ACX60_12455 | Hypothetical protein | -1.0 |
| ACX60_17575 | Amino acid transporter | -1.0 |
| ACX60_16080 | Glutathione S-transferase | -1.0 |
| ACX60_14105 | Succinate-semialdehyde dehydrogenase | -1.0 |
| ACX60_09195 | 3-hydroxybutyrate dehydrogenase | -1.0 |
| ACX60_01420 | Cation transporter | -1.0 |
| ACX60_12040 | Hypothetical protein | -1.0 |
| ACX60_04030 | Type I secretion protein | -1.0 |
| ACX60_12830 | Esterase | -1.0 |
| ACX60_05560 | Hypothetical protein | -1.0 |
| ACX60_05890 | Signal peptide protein | -1.0 |
| ACX60_02250 | Hypothetical protein | -1.0 |
| ACX60_06675 | Hypothetical protein | -1.0 |
| ACX60_09425 | TENA/THI-4 domain protein | -1.0 |
| ACX60_00670 | Ion channel protein Tsx | -1.0 |
| ACX60_06825 | Acyl-CoA dehydrogenase | -1.0 |
| ACX60_12280 | Hypothetical protein | -1.0 |
| ACX60_01530 | Membrane protein | -1.1 |
| ACX60_14470 | Hypothetical protein | -1.1 |
| ACX60_13345 | Isocitrate lyase | -1.1 |
| ACX60_00615 | Hypothetical protein | -1.1 |
| ACX60_12480 | Hypothetical protein | -1.1 |
| ACX60_18940 | Hypothetical protein | -1.1 |
| ACX60_09240 | Succinyl-CoA:3-ketoacid-CoA transferase | -1.1 |
| ACX60_12805 | Feruloyl-CoA synthase | -1.1 |
| ACX60_11850 | 3-hydroxyacyl-CoA dehydrogenase | -1.1 |
| ACX60_05035 | Hypothetical protein | -1.1 |
| ACX60_14115 | Lipase | -1.1 |
| ACX60_05315 | Aldehyde dehydrogenase | -1.1 |
| ACX60_01840 | Succinylglutamate desuccinylase | -1.1 |
| ACX60_04310 | Hypothetical protein | -1.1 |
| ACX60_05000 | tRNA-Asn | -1.1 |
| ACX60_05805 | tRNA-Asn | -1.1 |

| Locus-tag^a | Gene product | Differential expression (Log₂) |
|------------------------------|---------------------------------------|--------------------------------------------------|
| ACX60_05815 | tRNA-Asn | -1.1 |
| ACX60_05810 | tRNA-Asn | -1.1 |
| ACX60_05945 | Hypothetical protein | -1.1 |
| ACX60_03790 | SAM-dependent methyltransferase | -1.1 |
| ACX60_08515 | Polyketide cyclase | -1.1 |
| ACX60_09090 | Short-chain dehydrogenase | -1.1 |
| ACX60_09960 | Hypothetical protein | -1.1 |
| ACX60_11235 | Hypothetical protein | -1.1 |
| ACX60_13650 | Hypothetical protein | -1.1 |
| ACX60_17640 | Hypothetical protein | -1.1 |
| ACX60_00725 | Hypothetical protein | -1.1 |
| ACX60_06655 | Hypothetical protein | -1.1 |
| ACX60_03735 | Acyltransferase | -1.1 |
| ACX60_13360 | Citrate transporter | -1.1 |
| ACX60_08520 | (2Fe-2S) protein | -1.1 |
| ACX60_07060 | Transcriptional regulator | -1.1 |
| ACX60_09160 | Phenol degradation protein meta | -1.1 |
| ACX60_15285 | NAD(P) transhydrogenase subunit alpha | -1.1 |
| ACX60_00090 | 23S ribosomal RNA | -1.1 |
| ACX60_02445 | 23S ribosomal RNA | -1.1 |
| ACX60_02610 | 23S ribosomal RNA | -1.1 |
| ACX60_14990 | 23S ribosomal RNA | -1.1 |
| ACX60_17205 | 23S ribosomal RNA | -1.1 |
| ACX60_18010 | 23S ribosomal RNA | -1.1 |
| ACX60_15690 | Acetate kinase | -1.1 |
| ACX60_10460 | ArsR family transcriptional regulator | -1.1 |
| ACX60_05945 | Hypothetical protein | -1.1 |
| ACX60_03790 | SAM-dependent methyltransferase | -1.1 |
| ACX60_08515 | Polyketide cyclase | -1.1 |
| ACX60_09090 | Short-chain dehydrogenase | -1.1 |
| ACX60_09960 | Hypothetical protein | -1.1 |
| ACX60_11235 | Hypothetical protein | -1.1 |
| ACX60_13650 | Hypothetical protein | -1.1 |
| ACX60_17640 | Hypothetical protein | -1.1 |
| ACX60_00725 | Hypothetical protein | -1.1 |
| ACX60_06655 | Hypothetical protein | -1.1 |
| ACX60_03735 | Acyltransferase | -1.1 |
| ACX60_13360 | Citrate transporter | -1.1 |
| ACX60_08520 | (2Fe-2S) protein | -1.1 |

| Locus-tag^a | Gene product | Differential expression (Log₂) |
|------------------------------|-------------------------------------------|--------------------------------------------------|
| ACX60_00950 | Acetate permease | -1.6 |
| ACX60_06600 | C4-dicarboxylate transporter | -1.6 |
| ACX60_08005 | Hypothetical protein | -1.6 |
| ACX60_08580 | 3-oxoadipate CoA-transferase | -1.7 |
| ACX60_08410 | Protocatechuate 3%2C4-dioxygenase | -1.7 |
| ACX60_12495 | Hypothetical protein | -1.7 |
| ACX60_01220 | Hypothetical protein | -1.7 |
| ACX60_07370 | Hypothetical protein | -1.7 |
| ACX60_11450 | Enoyl-CoA hydratase | -1.7 |
| ACX60_06775 | Flavoprotein | -1.7 |
| ACX60_13400 | ATPase | -1.7 |
| ACX60_03280 | Glyoxalase | -1.7 |
| ACX60_11310 | MFS transporter | -1.8 |
| ACX60_11195 | Hypothetical protein | -1.8 |
| ACX60_12005 | Hypothetical protein | -1.8 |
| ACX60_11420 | Phenylacetic acid degradation protein | -1.8 |
| ACX60_09190 | AraC family transcriptional regulator | -1.8 |
| ACX60_11460 | Phenylacetic acid degradation protein | -1.8 |
| ACX60_00325 | 4-hydroxyphenylpyruvate dioxygenase | -1.8 |
| ACX60_08415 | 3-dehydroquinate dehydratase | -1.8 |
| ACX60_01135 | TetR family transcriptional regulator | -1.8 |
| ACX60_17235 | Hypothetical protein | -1.8 |
| ACX60_05445 | 50S ribosomal protein L31 | -1.9 |
| ACX60_17555 | AMP-binding protein | -1.9 |
| ACX60_08430 | Quinate dehydrogenase | -1.9 |
| ACX60_11805 | Hypothetical protein | -1.9 |
| ACX60_11475 | Phenylacetate-CoA oxygenase | -1.9 |
| ACX60_14355 | Trehalose-6-phosphate synthase | -1.9 |
| ACX60_14420 | Hypothetical protein | -1.9 |
| ACX60_08425 | Porin | -1.9 |
| ACX60_00425 | Hypothetical protein | -1.9 |
| ACX60_12000 | Glycine zipper | -1.9 |
| ACX60_00045 | RND transporter | -1.9 |
| ACX60_10745 | Hypothetical protein | -1.9 |
| ACX60_09245 | Short chain fatty acid transporter | -1.9 |
| ACX60_12255 | Membrane protein | -1.9 |
| ACX60_10685 | ABC transporter substrate-binding protein | -2.0 |
| ACX60_13655 | (2Fe-2S) protein | -2.0 |
| ACX60_11815 | Membrane protein | -2.0 |
| ACX60_08405 | Protocatechuate C4-dioxygenase | -2.0 |

| Locus-tag ^a | Gene product | Differential expression (Log ₂) |
|------------------------|---------------------------------------------------------|---------------------------------------------|
| ACX60_11480 | ATPase AAA | -2.0 |
| ACX60_08375 | 3-oxoadipate CoA-transferase | -2.0 |
| ACX60_07155 | TetR family transcriptional regulator | -2.0 |
| ACX60_12520 | Hypothetical protein | -2.0 |
| ACX60_07095 | Hypothetical protein | -2.1 |
| ACX60_01700 | Lipase chaperone | -2.1 |
| ACX60_10810 | Na ⁺ :H ⁺ dicarboxylate symporter | -2.1 |
| ACX60_12535 | Hypothetical protein | -2.1 |
| ACX60_10675 | Amino acid ABC transporter permease | -2.1 |
| ACX60_07000 | Homocysteine methyltransferase | -2.1 |
| ACX60_10680 | Amino acid transporter | -2.1 |
| ACX60_10670 | Hypothetical protein | -2.1 |
| ACX60_11190 | Stress-induced protein | -2.2 |
| ACX60_11260 | DcaP-like protein | -2.2 |
| ACX60_16650 | DNA transfer protein p32 | -2.2 |
| ACX60_11200 | Short-chain dehydrogenase | -2.2 |
| ACX60_14350 | Trehalose phosphatase | -2.2 |
| ACX60_05320 | AsnC family transcriptional regulator | -2.2 |
| ACX60_09420 | Transcriptional regulator | -2.2 |
| ACX60_08420 | 3-dehydroshikimate dehydratase | -2.3 |
| ACX60_00390 | Proline-specific permease | -2.3 |
| ACX60_09285 | Alpha-ketoglutarate permease | -2.3 |
| ACX60_08585 | 3-oxoadipate CoA-transferase | -2.3 |
| ACX60_03385 | Toxin | -2.4 |
| ACX60_06400 | Hypothetical protein | -2.4 |
| ACX60_08370 | 3-oxoadipate CoA-transferase | -2.6 |
| ACX60_13160 | Cobalt transporter | -2.6 |
| ACX60_00600 | Hypothetical protein | -2.7 |
| ACX60_18475 | Hypothetical protein | -2.7 |
| ACX60_16645 | DNA transfer protein p32 | -2.8 |
| ACX60_08390 | 3-oxoadipate enol-lactonase | -2.8 |
| ACX60_17240 | TonB-dependent receptor | -2.8 |
| ACX60_09385 | Butanediol dehydrogenase | -2.9 |
| ACX60_08385 | 3-carboxy-cis-2Cis-muconate cycloisomerase | -2.9 |
| ACX60_08395 | 4-hydroxybenzoate transporter | -3.0 |
| ACX60_01695 | Lipase | -3.0 |
| ACX60_02305 | Membrane protein | -3.0 |
| ACX60_14660 | Membrane protein | -3.0 |
| ACX60_11215 | Damage-inducible protein CinA | -3.3 |
| ACX60_11455 | C3-dehydroadipyl-CoA hydratase | -3.3 |

| Locus-tag^a | Gene product | Differential expression (Log₂) |
|------------------------------|-------------------------------------------------------|--------------------------------------------------|
| ACX60_09395 | Dihydrolipoamide dehydrogenase | -3.6 |
| ACX60_08400 | 4-carboxymuconolactone decarboxylase | -3.6 |
| ACX60_09410 | ABC transporter substrate-binding protein | -3.6 |
| ACX60_09390 | Diacetyl reductase | -3.8 |
| ACX60_09405 | Pyruvate dehydrogenase | -3.8 |
| ACX60_01415 | Cation transporter | -4.0 |
| ACX60_09400 | diaminohydroxyphosphoribosylaminopyrimidine Deaminase | -4.0 |
| ACX60_11220 | Hypothetical protein | -4.1 |
| ACX60_01410 | Hemolysin D | -4.4 |
| ACX60_11225 | Hypothetical protein | -4.4 |
| ACX60_01400 | Cation transporter | -4.6 |
| ACX60_00095 | 5S ribosomal RNA | -4.9 |
| ACX60_02450 | 5S ribosomal RNA | -4.9 |
| ACX60_02615 | 5S ribosomal RNA | -4.9 |
| ACX60_14985 | 5S ribosomal RNA | -4.9 |
| ACX60_17200 | 5S ribosomal RNA | -4.9 |
| ACX60_18005 | 5S ribosomal RNA | -4.9 |
| ACX60_01405 | RND transporter | -5.1 |

^a. Sequence was obtained from ATCC 17978 GenBank accession number CP012004

Appendix 13 – Genes significantly up-regulated in *A. baumannii* ATCC 17978 Δ *rpmE1* under Zn²⁺-replete conditions (CP012004)

| Locus-tag ^a | Gene product | Differential expression (Log ₂) |
|------------------------|-----------------------------------------------------------------------|---------------------------------------------|
| ACX60_00360 | Hypothetical protein | 7.0 |
| ACX60_16160 | 50S ribosomal protein L31 | 6.9 |
| ACX60_17605 | Membrane protein | 5.6 |
| ACX60_03050 | TonB-dependent receptor | 5.6 |
| ACX60_17610 | Ligand-gated channel protein | 5.5 |
| ACX60_00355 | Peptidase M15 | 3.5 |
| ACX60_14705 | 5-methyltetrahydropteroyltriglutamate--Homocysteine methyltransferase | 2.7 |
| ACX60_17350 | High affinity Zn ²⁺ transport protein | 2.4 |
| ACX60_08790 | Hypothetical protein | 2.4 |
| ACX60_13160 | Cobalt transporter | 2.3 |
| ACX60_15845 | TonB-dependent receptor | 1.8 |
| ACX60_14710 | Hypothetical protein | 1.6 |
| ACX60_15315 | Hypothetical protein | 1.6 |
| ACX60_05855 | 5%2C10-methylenetetrahydrofolate reductase | 1.5 |
| ACX60_14700 | Flavin reductase | 1.5 |
| ACX60_09525 | Hypothetical protein | 1.5 |
| ACX60_10125 | Hypothetical protein | 1.4 |
| ACX60_11735 | Hypothetical protein | 1.4 |
| ACX60_08750 | TetR family transcriptional regulator | 1.3 |
| ACX60_17005 | Sulfate transporter | 1.3 |
| ACX60_18810 | Sulfate transporter | 1.3 |
| ACX60_15840 | Biopolymer transporter ExbB | 1.3 |
| ACX60_17020 | Hypothetical protein | 1.2 |
| ACX60_18825 | Hypothetical protein | 1.2 |
| ACX60_17010 | Universal stress protein | 1.2 |
| ACX60_18815 | Universal stress protein | 1.2 |
| ACX60_17015 | Hypothetical protein | 1.2 |
| ACX60_18820 | Hypothetical protein | 1.2 |
| ACX60_00800 | Hypothetical protein | 1.2 |
| ACX60_08875 | Fumarylacetoacetate hydrolase | 1.2 |
| ACX60_05860 | Adenosylhomocysteinase | 1.2 |
| ACX60_01460 | tRNA-Ala | 1.1 |
| ACX60_02710 | hypothetical protein | 1.1 |
| ACX60_09315 | 4Fe-4S ferredoxin | 1.0 |
| ACX60_10080 | Hypothetical protein | 1.0 |

^a. The sequence were obtained from ATCC 17978 GenBank accession number CP012004

Appendix 14 – Genes significantly down-regulated in *A. baumannii* ATCC 17978 Δ *rpmE1* under Zn²⁺-replete conditions (CP012004)

| Locus-tag ^a | Gene product | Differential expression (Log ₂) |
|------------------------|--------------------------------------------|---------------------------------------------|
| ACX60_08885 | NAD-dependent epimerase | -1.0 |
| ACX60_05935 | Amino acid ABC transporter permease | -1.0 |
| ACX60_01790 | Hypothetical protein | -1.0 |
| ACX60_14105 | Succinate-semialdehyde dehydrogenase | -1.0 |
| ACX60_02250 | Hypothetical protein | -1.0 |
| ACX60_04330 | TetR family transcriptional regulator | -1.0 |
| ACX60_12280 | Hypothetical protein | -1.0 |
| ACX60_10940 | MFS transporter | -1.0 |
| ACX60_09165 | Flavin reductase | -1.0 |
| ACX60_12885 | Hypothetical protein | -1.0 |
| ACX60_09195 | 3-hydroxybutyrate dehydrogenase | -1.0 |
| ACX60_07575 | Stress-responsive nuclear envelope protein | -1.0 |
| ACX60_17380 | Malate dehydrogenase | -1.0 |
| ACX60_02260 | Membrane protein | -1.0 |
| ACX60_14115 | Lipase | -1.0 |
| ACX60_11445 | 3-hydroxyacyl-CoA dehydrogenase | -1.0 |
| ACX60_06415 | Methyltransferase | -1.0 |
| ACX60_11280 | Isovaleryl-CoA dehydrogenase | -1.0 |
| ACX60_10620 | Membrane protein | -1.0 |
| ACX60_06770 | Transporter | -1.0 |
| ACX60_11335 | Monomeric sarcosine oxidase | -1.0 |
| ACX60_15175 | Acyl-CoA synthetase | -1.0 |
| ACX60_14120 | Transporter | -1.0 |
| ACX60_08050 | Quinoprotein glucose dehydrogenase | -1.1 |
| ACX60_06765 | N-glycosyltransferase | -1.1 |
| ACX60_07105 | Spore coat protein SpoU | -1.1 |
| ACX60_14790 | LysR family transcriptional regulator | -1.1 |
| ACX60_05515 | Nicotinamidase | -1.1 |
| ACX60_01060 | Hypothetical protein | -1.1 |
| ACX60_00280 | formate transporter | -1.1 |
| ACX60_12895 | Amino acid transporter | -1.1 |
| ACX60_11600 | D-Ala-D-Ala carboxypeptidase | -1.1 |
| ACX60_13630 | Ferredoxin reductase | -1.1 |
| ACX60_03400 | Hypothetical protein | -1.1 |

| Locus-tag^a | Gene product | Differential expression (Log₂) |
|------------------------------|-----------------------------------------------------|--------------------------------------------------|
| ACX60_00400 | Formimidoylglutamase | -1.1 |
| ACX60_00395 | Imidazolonepropionase | -1.1 |
| ACX60_11600 | D-Ala-D-Ala carboxypeptidase | -1.1 |
| ACX60_13630 | Ferredoxin reductase | -1.1 |
| ACX60_03400 | Hypothetical protein | -1.1 |
| ACX60_00400 | Formimidoylglutamase | -1.1 |
| ACX60_00395 | Imidazolonepropionase | -1.1 |
| ACX60_01810 | Amino acid transporter | -1.1 |
| ACX60_01320 | tRNA-Phe | -1.1 |
| ACX60_01325 | tRNA-Phe | -1.1 |
| ACX60_02245 | Membrane protein | -1.1 |
| ACX60_03370 | Hypothetical protein | -1.1 |
| ACX60_00945 | Membrane protein | -1.1 |
| ACX60_14470 | Hypothetical protein | -1.1 |
| ACX60_05315 | Aldehyde dehydrogenase | -1.1 |
| ACX60_08380 | Beta-ketoadipyl CoA thiolase | -1.1 |
| ACX60_08005 | Hypothetical protein | -1.1 |
| ACX60_05945 | Hypothetical protein | -1.1 |
| ACX60_11365 | 4-hydroxybenzoate 3-monooxygenase | -1.1 |
| ACX60_00725 | Hypothetical protein | -1.1 |
| ACX60_08155 | Hypothetical protein | -1.1 |
| ACX60_06525 | Phosphohydrolase | -1.1 |
| ACX60_09070 | Membrane protein | -1.1 |
| ACX60_00625 | Hypothetical protein | -1.1 |
| ACX60_13585 | MFS transporter permease | -1.1 |
| ACX60_00905 | Acetyl-CoA synthetase | -1.1 |
| ACX60_04545 | Rhombotarget A | -1.1 |
| ACX60_05770 | Peptide permease | -1.1 |
| ACX60_10615 | sulfonate ABC transporter substrate-binding Protein | -1.1 |
| ACX60_06755 | Biofilm synthesis protein | -1.1 |
| ACX60_01770 | Superoxide dismutase | -1.1 |
| ACX60_06675 | Hypothetical protein | -1.1 |
| ACX60_06395 | Gamma-aminobutyrate transporter | -1.2 |
| ACX60_10020 | Hypothetical protein | -1.2 |
| ACX60_08525 | Aromatic-ring-hydroxylating dioxygenase | -1.2 |
| ACX60_14435 | Hypothetical protein | -1.2 |
| ACX60_08805 | MFS transporter permease | -1.2 |
| ACX60_07690 | Hypothetical protein | -1.2 |

| Locus-tag^a | Gene product | Differential expression (Log₂) |
|------------------------------|-------------------------------------------|--------------------------------------------------|
| ACX60_17535 | Major facilitator transporter | -1.2 |
| ACX60_00815 | Dihydrolipoamide acetyltransferase | -1.2 |
| ACX60_12005 | Hypothetical protein | -1.2 |
| ACX60_14430 | Hypothetical protein | -1.2 |
| ACX60_12560 | HNH endonuclease | -1.2 |
| ACX60_11640 | Type VI secretion protein | -1.2 |
| ACX60_11495 | Aspartate:proton symporter | -1.2 |
| ACX60_13500 | Lipoprotein precursor | -1.2 |
| ACX60_17950 | ABC transporter permease | -1.2 |
| ACX60_11210 | Hypothetical protein | -1.2 |
| ACX60_07630 | Hypothetical protein | -1.2 |
| ACX60_06095 | Hypothetical protein | -1.2 |
| ACX60_14135 | Hypothetical protein | -1.2 |
| ACX60_17660 | Triacylglycerol lipase | -1.2 |
| ACX60_00335 | Glyoxalase | -1.2 |
| ACX60_12435 | Hypothetical protein | -1.2 |
| ACX60_00950 | Acetate permease | -1.2 |
| ACX60_17565 | Methylmalonate-semialdehyde dehydrogenase | -1.2 |
| ACX60_01640 | Fimbrial protein | -1.2 |
| ACX60_07615 | Hypothetical protein | -1.2 |
| ACX60_11605 | Hypothetical protein | -1.2 |
| ACX60_11615 | Type VI secretion protein | -1.2 |
| ACX60_11465 | Phenylacetate-CoA oxygenase | -1.2 |
| ACX60_11200 | Short-chain dehydrogenase | -1.2 |
| ACX60_07155 | TetR family transcriptional regulator | -1.2 |
| ACX60_09240 | Succinyl-CoA:3-ketoacid-CoA transferase | -1.2 |
| ACX60_02305 | Membrane protein | -1.2 |
| ACX60_18155 | Transglycosylase | -1.2 |
| ACX60_08610 | Hypothetical protein | -1.2 |
| ACX60_11645 | Type VI secretion protein | -1.2 |
| ACX60_12830 | Esterase | -1.3 |
| ACX60_10745 | Hypothetical protein | -1.3 |
| ACX60_12805 | Feruloyl-CoA synthase | -1.3 |
| ACX60_00325 | 4-hydroxyphenylpyruvate dioxygenase | -1.3 |
| ACX60_08580 | 3-oxoadipate CoA-transferase | -1.3 |
| ACX60_08740 | Bile acid:sodium symporter | -1.3 |
| ACX60_10480 | Hypothetical protein | -1.3 |
| ACX60_12155 | Benzene 1%2C2-dioxygenase | -1.3 |
| ACX60_07680 | Holin | -1.3 |
| ACX60_10880 | Hypothetical protein | -1.3 |

| Locus-tag^a | Gene product | Differential expression (Log₂) |
|------------------------------|----------------------------------------|--------------------------------------------------|
| ACX60_11520 | Hypothetical protein | -1.3 |
| ACX60_12730 | Transferase | -1.3 |
| ACX60_17670 | Hypothetical protein | -1.3 |
| ACX60_10640 | Hypothetical protein | -1.3 |
| ACX60_07205 | Hypothetical protein | -1.3 |
| ACX60_07565 | Hypothetical protein | -1.3 |
| ACX60_11620 | Type VI secretion protein | -1.3 |
| ACX60_04550 | Membrane protein | -1.3 |
| ACX60_08500 | Glutamyl-tRNA amidotransferase | -1.3 |
| ACX60_07045 | Ethanolamine ammonia-lyase | -1.3 |
| ACX60_01035 | Gamma-aminobutyrate transporter | -1.3 |
| ACX60_06410 | LmbE protein | -1.3 |
| ACX60_04780 | Hypothetical protein | -1.3 |
| ACX60_12790 | MFS transporter | -1.3 |
| ACX60_12530 | Hypothetical protein | -1.3 |
| ACX60_11270 | Fatty acid--CoA ligase | -1.3 |
| ACX60_14730 | AraC family transcriptional regulator | -1.3 |
| ACX60_14525 | Hypothetical protein | -1.3 |
| ACX60_08595 | Muconolactone delta-isomerase | -1.4 |
| ACX60_17560 | 3-hydroxyisobutyrate dehydrogenase | -1.4 |
| ACX60_11460 | Phenylacetic acid degradation protein | -1.4 |
| ACX60_13835 | Gamma-glutamyltransferase | -1.4 |
| ACX60_09530 | Hypothetical protein | -1.4 |
| ACX60_12255 | Membrane protein | -1.4 |
| ACX60_06110 | Hemin transporter HemP | -1.4 |
| ACX60_14130 | LysR family transcriptional regulator | -1.4 |
| ACX60_09470 | Transcriptional regulator | -1.4 |
| ACX60_08375 | 3-oxoadipate CoA-transferase | -1.4 |
| ACX60_07370 | Hypothetical protein | -1.4 |
| ACX60_09200 | Transporter | -1.4 |
| ACX60_06535 | TetR family transcriptional regulator | -1.4 |
| ACX60_07175 | Hypothetical protein | -1.4 |
| ACX60_11660 | Type VI secretion system protein ImpG | -1.4 |
| ACX60_06830 | AMP-binding protein | -1.4 |
| ACX60_10515 | Hypothetical protein | -1.4 |
| ACX60_00050 | Hypothetical protein | -1.4 |
| ACX60_08545 | AraC family transcriptional regulator | -1.4 |
| ACX60_07555 | Hypothetical protein | -1.4 |
| ACX60_16645 | DNA transfer protein p32 | -1.5 |
| ACX60_08535 | Vanillate O-demethylase oxidoreductase | -1.5 |

| Locus-tag^a | Gene product | Differential expression (Log₂) |
|------------------------------|-----------------------------------------|--------------------------------------------------|
| ACX60_03420 | Hypothetical protein | -1.5 |
| ACX60_17575 | Amino acid transporter | -1.5 |
| ACX60_18045 | Hypothetical protein | -1.5 |
| ACX60_11205 | Hydroperoxidase | -1.5 |
| ACX60_07520 | Hypothetical protein | -1.5 |
| ACX60_12180 | Major facilitator transporter | -1.5 |
| ACX60_17365 | DNA repair protein | -1.5 |
| ACX60_06425 | DNA-binding protein | -1.5 |
| ACX60_06655 | Hypothetical protein | -1.5 |
| ACX60_14425 | Heme utilisation protein | -1.5 |
| ACX60_15655 | Hydrolase | -1.5 |
| ACX60_08430 | Quinate dehydrogenase | -1.5 |
| ACX60_05070 | MFS transporter | -1.5 |
| ACX60_09235 | Succinyl-CoA:3-ketoacid-CoA transferase | -1.5 |
| ACX60_14975 | Ribosome hibernation promoting factor | -1.5 |
| ACX60_00045 | RND transporter | -1.5 |
| ACX60_07530 | Hypothetical protein | -1.5 |
| ACX60_11420 | Phenylacetic acid degradation protein | -1.5 |
| ACX60_12535 | Hypothetical protein | -1.5 |
| ACX60_12550 | Hypothetical protein | -1.5 |
| ACX60_06000 | Triacylglycerol lipase | -1.5 |
| ACX60_11470 | Phenylacetic acid degradation protein | -1.6 |
| ACX60_01220 | Hypothetical protein | -1.6 |
| ACX60_14660 | Membrane protein | -1.6 |
| ACX60_05905 | Membrane protein | -1.6 |
| ACX60_06505 | Protein CsuE | -1.6 |
| ACX60_09955 | Lysozyme | -1.6 |
| ACX60_11450 | Enoyl-CoA hydratase | -1.6 |
| ACX60_14785 | Acyl-CoA dehydrogenase | -1.6 |
| ACX60_07510 | Hypothetical protein | -1.6 |
| ACX60_11485 | Enoyl-CoA hydratase | -1.6 |
| ACX60_06400 | Hypothetical protein | -1.6 |
| ACX60_00425 | Hypothetical protein | -1.6 |
| ACX60_13400 | ATPase | -1.6 |
| ACX60_17155 | Hypothetical protein | -1.6 |
| ACX60_12325 | Membrane protein | -1.6 |
| ACX60_11455 | C3-dehydroadipyl-CoA hydratase | -1.6 |
| ACX60_06495 | Protein CsuC | -1.7 |
| ACX60_11480 | ATPase AAA | -1.7 |
| ACX60_06485 | Protein CsuA | -1.7 |

| Locus-tag ^a | Gene product | Differential expression (Log ₂) |
|------------------------|------------------------------------------------------------------------------------|---------------------------------------------|
| ACX60_07210 | DNA breaking-rejoining protein | -1.7 |
| ACX60_06500 | Protein CsuD | -1.7 |
| ACX60_09870 | Hypothetical protein | -1.7 |
| ACX60_14940 | Protein FilA | -1.7 |
| ACX60_17555 | AMP-binding protein | -1.7 |
| ACX60_12520 | Hypothetical protein | -1.7 |
| ACX60_09175 | Short-chain dehydrogenase | -1.7 |
| ACX60_05320 | AsnC family transcriptional regulator | -1.7 |
| ACX60_06600 | C4-dicarboxylate transporter | -1.7 |
| ACX60_00170 | Multidrug transporter AcrB | -1.7 |
| ACX60_00390 | Proline-specific permease | -1.7 |
| ACX60_12810 | Acyl-CoA dehydrogenase | -1.8 |
| ACX60_09155 | AraC family transcriptional regulator | -1.8 |
| ACX60_10675 | Amino acid ABC transporter permease | -1.8 |
| ACX60_11655 | Type VI secretion protein | -1.8 |
| ACX60_09190 | AraC family transcriptional regulator | -1.8 |
| ACX60_00260 | Membrane protein | -1.8 |
| ACX60_10970 | Hypothetical protein | -1.8 |
| ACX60_11665 | Type VI secretion protein | -1.8 |
| ACX60_10685 | ABC transporter substrate-binding protein | -1.8 |
| ACX60_11650 | Membrane protein | -1.8 |
| ACX60_01610 | regulatory or redox protein complexing with Bfr in iron storage and mobility (BFD) | -1.8 |
| ACX60_09245 | Short chain fatty acid transporter | -1.9 |
| ACX60_14350 | Trehalose phosphatase | -1.9 |
| ACX60_11260 | DcaP-like protein | -1.9 |
| ACX60_14355 | Trehalose-6-phosphate synthase | -1.9 |
| ACX60_08415 | 3-dehydroquinone dehydratase | -1.9 |
| ACX60_14420 | Hypothetical protein | -1.9 |
| ACX60_10680 | Amino acid transporter | -1.9 |
| ACX60_08425 | Porin | -2.0 |
| ACX60_10635 | tRNA-Met | -2.0 |
| ACX60_10670 | Hypothetical protein | -2.0 |
| ACX60_06480 | Protein CsuA/B | -2.0 |
| ACX60_11310 | MFS transporter | -2.0 |
| ACX60_03280 | Glyoxalase | -2.0 |
| ACX60_06775 | Flavoprotein | -2.0 |
| ACX60_11680 | Type VI secretion protein | -2.0 |
| ACX60_11235 | Hypothetical protein | -2.1 |
| ACX60_17360 | Zn ²⁺ ABC transporter | -2.1 |
| ACX60_09285 | Alpha-ketoglutarate permease | -2.1 |

| Locus-tag ^a | Gene product | Differential expression (Log ₂) |
|------------------------|---------------------------------------------------------|---------------------------------------------|
| ACX60_13715 | Hypothetical protein | -2.1 |
| ACX60_14095 | tRNA-Met | -2.1 |
| ACX60_14140 | tRNA-Met | -2.1 |
| ACX60_08420 | 3-dehydroshikimate dehydratase | -2.1 |
| ACX60_11670 | Hypothetical protein | -2.2 |
| ACX60_09275 | Aspartate ammonia-lyase | -2.2 |
| ACX60_07485 | Hypothetical protein | -2.2 |
| ACX60_11685 | Hypothetical protein | -2.2 |
| ACX60_06490 | Protein CsuB | -2.2 |
| ACX60_01700 | Lipase chaperone | -2.2 |
| ACX60_08400 | 4-carboxymuconolactone decarboxylase | -2.2 |
| ACX60_11675 | EvpB family type VI secretion protein | -2.3 |
| ACX60_08405 | Protocatechuate 3%2C4-dioxygenase | -2.3 |
| ACX60_07580 | Hypothetical protein | -2.3 |
| ACX60_11220 | Hypothetical protein | -2.4 |
| ACX60_03385 | Toxin | -2.4 |
| ACX60_08390 | 3-oxoadipate enol-lactonase | -2.4 |
| ACX60_08410 | Protocatechuate 3%2C4-dioxygenase | -2.5 |
| ACX60_09420 | Transcriptional regulator | -2.5 |
| ACX60_11225 | Hypothetical protein | -2.7 |
| ACX60_09385 | Butanediol dehydrogenase | -2.7 |
| ACX60_07660 | Bacteriophage protein | -2.8 |
| ACX60_10810 | Na ⁺ :H ⁺ dicarboxylate symporter | -2.8 |
| ACX60_07095 | Hypothetical protein | -2.8 |
| ACX60_08395 | 4-hydroxybenzoate transporter | -2.9 |
| ACX60_08585 | 3-oxoadipate CoA-transferase | -3.0 |
| ACX60_08515 | Polyketide cyclase | -3.1 |
| ACX60_08385 | 3-carboxy-cis%2Ccis-muconate cycloisomerase | -3.1 |
| ACX60_01695 | Lipase | -3.2 |
| ACX60_08370 | 3-oxoadipate CoA-transferase | -3.3 |
| ACX60_17355 | Fur family transcriptional regulator | -3.5 |
| ACX60_09390 | Diacetyl reductase | -3.5 |
| ACX60_11475 | Phenylacetate-CoA oxygenase | -3.6 |
| ACX60_11215 | Damage-inducible protein CinA | -3.8 |
| ACX60_09395 | Dihydrolipoamide dehydrogenase | -3.8 |
| ACX60_09410 | ABC transporter substrate-binding protein | -4.0 |
| ACX60_09405 | Pyruvate dehydrogenase | -4.0 |
| ACX60_09400 | diaminohydroxyphosphoribosylaminopyrimidine Deaminase | -4.4 |
| ACX60_05445 | 50S ribosomal protein L31, RpmE1 | -9.7 |

^a. Sequence was obtained from ATCC 17978 GenBank accession number CP012004.

Appendix 15 – Genes significantly up-regulated in *A. baumannii* ATCC 17978 $\Delta rpmE2$ under Zn^{2+} -replete conditions (CP012004)

| Locus-tag^a | Gene product | Differential expression (Log₂) |
|------------------------------|--------------------------------------------|--------------------------------------------------|
| ACX60_14705 | Homocysteine methyltransferase | 2.4 |
| ACX60_14700 | Flavin reductase | 1.6 |
| ACX60_05855 | 5%2C10-methylenetetrahydrofolate reductase | 1.6 |
| ACX60_14710 | Hypothetical protein | 1.6 |
| ACX60_10160 | Hypothetical protein | 1.6 |
| ACX60_02225 | 50S ribosomal protein L17 | 1.6 |
| ACX60_00185 | Hypothetical protein | 1.5 |
| ACX60_02215 | 30S ribosomal protein S4 | 1.5 |
| ACX60_02220 | DNA-directed RNA polymerase subunit alpha | 1.5 |
| ACX60_10955 | Hypothetical protein | 1.4 |
| ACX60_10100 | Hypothetical protein | 1.4 |
| ACX60_05860 | Adenosylhomocysteinase | 1.3 |
| ACX60_02210 | 30S ribosomal protein S11 | 1.3 |
| ACX60_07685 | Lysozyme | 1.3 |
| ACX60_11560 | Hypothetical protein | 1.3 |
| ACX60_02205 | 30S ribosomal protein S13 | 1.3 |
| ACX60_01370 | Hypothetical protein | 1.3 |
| ACX60_14810 | tRNA-His | 1.2 |
| ACX60_00215 | Hypothetical protein | 1.1 |
| ACX60_17585 | Endoribonuclease L-PSP | 1.1 |
| ACX60_09335 | FMN-dependent NADH-azoreductase | 1.1 |
| ACX60_09525 | Hypothetical protein | 1.1 |
| ACX60_04325 | Metal-dependent hydrolase | 1.1 |
| ACX60_18535 | Hypothetical protein | 1.1 |
| ACX60_08875 | Fumarylacetoacetate hydrolase | 1.0 |

^a Sequence was obtained from ATCC 17978 GenBank accession number CP012004

Appendix 16 – Genes significantly down-regulated in *A. baumannii* ATCC 17978 Δ *rpmE2* under Zn²⁺-replete conditions (CP012004)

| Locus-tag^a | Gene product | Differential expression (Log₂) |
|------------------------------|-----------------------------------------|--------------------------------------------------|
| ACX60_04355 | CbbBc protein | -1.0 |
| ACX60_00810 | Pyruvate dehydrogenase | -1.0 |
| ACX60_17575 | Amino acid transporter | -1.0 |
| ACX60_18725 | Transposase | -1.0 |
| ACX60_10515 | Hypothetical protein | -1.0 |
| ACX60_07485 | Hypothetical protein | -1.0 |
| ACX60_08595 | Muconolactone delta-isomerase | -1.0 |
| ACX60_09240 | Succinyl-CoA:3-ketoacid-CoA transferase | -1.0 |
| ACX60_06110 | Hemin transporter HemP | -1.0 |
| ACX60_12805 | Feruloyl-CoA synthase | -1.0 |
| ACX60_11660 | Type VI secretion system protein ImpG | -1.0 |
| ACX60_05725 | Xanthine dehydrogenase | -1.0 |
| ACX60_03260 | Glucose dehydrogenase | -1.0 |
| ACX60_06830 | AMP-binding protein | -1.0 |
| ACX60_11730 | Transcriptional regulator | -1.1 |
| ACX60_05315 | Aldehyde dehydrogenase | -1.1 |
| ACX60_00425 | Hypothetical protein | -1.1 |
| ACX60_13735 | Choline transporter | -1.1 |
| ACX60_06000 | Triacylglycerol lipase | -1.1 |
| ACX60_12830 | Esterase | -1.1 |
| ACX60_06495 | Protein CsuC | -1.1 |
| ACX60_06675 | Hypothetical protein | -1.1 |
| ACX60_11200 | Short-chain dehydrogenase | -1.1 |
| ACX60_09470 | Transcriptional regulator | -1.1 |
| ACX60_18155 | Transglycosylase | -1.1 |
| ACX60_11460 | Phenylacetic acid degradation protein | -1.1 |
| ACX60_09155 | AraC family transcriptional regulator | -1.1 |
| ACX60_00280 | Formate transporter | -1.1 |
| ACX60_09235 | Succinyl-CoA:3-ketoacid-CoA transferase | -1.1 |
| ACX60_14975 | Ribosome hibernation promoting factor | -1.1 |
| ACX60_13400 | ATPase | -1.1 |
| ACX60_04260 | tRNA-Ser | -1.1 |
| ACX60_08525 | Aromatic-ring-hydroxylating dioxygenase | -1.1 |
| ACX60_10595 | Hypothetical protein | -1.1 |
| ACX60_12535 | Hypothetical protein | -1.1 |

| Locus-tag^a | Gene product | Differential expression (Log₂) |
|------------------------------|------------------------------------------------------------------------------------|--------------------------------------------------|
| ACX60_13035 | tRNA-Ser | -1.1 |
| ACX60_14680 | Hypothetical protein | -1.1 |
| ACX60_15330 | Aconitate hydratase | -1.1 |
| ACX60_11485 | Enoyl-CoA hydratase | -1.2 |
| ACX60_06490 | Protein CsuB | -1.2 |
| ACX60_15315 | Hypothetical protein | -1.2 |
| ACX60_08530 | 3-oxoacyl-ACP reductase | -1.2 |
| ACX60_07205 | Hypothetical protein | -1.2 |
| ACX60_06480 | Protein CsuA/B | -1.2 |
| ACX60_11450 | Enoyl-CoA hydratase | -1.2 |
| ACX60_11645 | Type VI secretion protein | -1.2 |
| ACX60_11610 | hypothetical protein | -1.2 |
| ACX60_01770 | Superoxide dismutase | -1.2 |
| ACX60_04780 | Hypothetical protein | -1.2 |
| ACX60_03255 | Porin | -1.2 |
| ACX60_08155 | Hypothetical protein | -1.2 |
| ACX60_14940 | Protein FilA | -1.2 |
| ACX60_05320 | AsnC family transcriptional regulator | -1.2 |
| ACX60_11640 | Type VI secretion protein | -1.2 |
| ACX60_14520 | Hypothetical protein | -1.2 |
| ACX60_11465 | Phenylacetate-CoA oxygenase | -1.2 |
| ACX60_11310 | MFS transporter | -1.2 |
| ACX60_11655 | Type VI secretion protein | -1.2 |
| ACX60_10670 | Hypothetical protein | -1.2 |
| ACX60_11620 | Type VI secretion protein | -1.2 |
| ACX60_00270 | Glucose dehydrogenase | -1.2 |
| ACX60_11615 | Type VI secretion protein | -1.2 |
| ACX60_10970 | Hypothetical protein | -1.3 |
| ACX60_01240 | Porin | -1.3 |
| ACX60_01220 | Hypothetical protein | -1.3 |
| ACX60_14425 | Heme utilisation protein | -1.3 |
| ACX60_06485 | Protein CsuA | -1.3 |
| ACX60_14095 | tRNA-Met | -1.3 |
| ACX60_14140 | tRNA-Met | -1.3 |
| ACX60_15655 | Hydrolase | -1.3 |
| ACX60_06775 | Flavoprotein | -1.3 |
| ACX60_00260 | Membrane protein | -1.3 |
| ACX60_10685 | ABC transporter substrate-binding protein | -1.4 |
| ACX60_00815 | dihydrolipoamide acetyltransferase | -1.4 |
| ACX60_00390 | Proline-specific permease | -1.4 |
| ACX60_01610 | Regulatory or redox protein complexing with Bfr in iron storage and mobility (BFD) | -1.4 |

| Locus-tag^a | Gene product | Differential expression (Log₂) |
|------------------------------|---------------------------------------|--------------------------------------------------|
| ACX60_06410 | LmbE protein | -1.4 |
| ACX60_11420 | Phenylacetic acid degradation protein | -1.4 |
| ACX60_14420 | Hypothetical protein | -1.4 |
| ACX60_17555 | AMP-binding protein | -1.4 |
| ACX60_14525 | Hypothetical protein | -1.4 |
| ACX60_10680 | Amino acid transporter | -1.4 |
| ACX60_08430 | Quinate dehydrogenase | -1.4 |
| ACX60_09190 | AraC family transcriptional regulator | -1.4 |
| ACX60_01135 | TetR family transcriptional regulator | -1.4 |
| ACX60_14785 | Acyl-CoA dehydrogenase | -1.4 |
| ACX60_06655 | Hypothetical protein | -1.5 |
| ACX60_09245 | Short chain fatty acid transporter | -1.5 |
| ACX60_08420 | 3-dehydroshikimate dehydratase | -1.5 |
| ACX60_10675 | Amino acid ABC transporter permease | -1.5 |
| ACX60_11475 | Phenylacetate-CoA oxygenase | -1.5 |
| ACX60_11210 | Hypothetical protein | -1.5 |
| ACX60_00965 | Membrane protein | -1.6 |
| ACX60_06425 | DNA-binding protein | -1.6 |
| ACX60_11650 | Membrane protein | -1.6 |
| ACX60_14660 | Membrane protein | -1.6 |
| ACX60_03280 | Glyoxalase | -1.6 |
| ACX60_11215 | Damage-inducible protein CinA | -1.6 |
| ACX60_08425 | Porin | -1.6 |
| ACX60_01390 | Sel1 repeat protein | -1.6 |
| ACX60_06400 | Hypothetical protein | -1.7 |
| ACX60_09275 | Aspartate ammonia-lyase | -1.7 |
| ACX60_09420 | Transcriptional regulator | -1.7 |
| ACX60_11480 | ATPase AAA | -1.7 |
| ACX60_06410 | LmbE protein | -1.4 |
| ACX60_11420 | Phenylacetic acid degradation protein | -1.4 |
| ACX60_14420 | Hypothetical protein | -1.4 |
| ACX60_17555 | AMP-binding protein | -1.4 |
| ACX60_14525 | Hypothetical protein | -1.4 |
| ACX60_10680 | Amino acid transporter | -1.4 |
| ACX60_08430 | Quinate dehydrogenase | -1.4 |
| ACX60_09190 | AraC family transcriptional regulator | -1.4 |
| ACX60_01135 | TetR family transcriptional regulator | -1.4 |
| ACX60_14785 | Acyl-CoA dehydrogenase | -1.4 |
| ACX60_06655 | Hypothetical protein | -1.5 |

| Locus-tag^a | Gene product | Differential expression (Log₂) |
|------------------------------|---------------------------------------|--------------------------------------------------|
| ACX60_09245 | Short chain fatty acid transporter | -1.5 |
| ACX60_08420 | 3-dehydroshikimate dehydratase | -1.5 |
| ACX60_10675 | Amino acid ABC transporter permease | -1.5 |
| ACX60_11475 | phenylacetate-CoA oxygenase | -1.5 |
| ACX60_11210 | Hypothetical protein | -1.5 |
| ACX60_00965 | membrane protein | -1.6 |
| ACX60_06425 | DNA-binding protein | -1.6 |
| ACX60_11650 | Membrane protein | -1.6 |
| ACX60_14660 | Membrane protein | -1.6 |
| ACX60_03280 | Glyoxalase | -1.6 |
| ACX60_11215 | Damage-inducible protein CinA | -1.6 |
| ACX60_08425 | Porin | -1.6 |
| ACX60_01390 | Sel1 repeat protein | -1.6 |
| ACX60_06400 | Hypothetical protein | -1.7 |
| ACX60_09275 | Aspartate ammonia-lyase | -1.7 |
| ACX60_09420 | Transcriptional regulator | -1.7 |
| ACX60_11480 | ATPase AAA | -1.7 |
| ACX60_09285 | Alpha-ketoglutarate permease | -1.7 |
| ACX60_08415 | 3-dehydroquininate dehydratase | -1.7 |
| ACX60_08580 | 3-oxoadipate CoA-transferase | -1.7 |
| ACX60_11190 | Stress-induced protein | -1.8 |
| ACX60_02305 | Membrane protein | -1.8 |
| ACX60_11205 | Hydroperoxidase | -1.8 |
| ACX60_06600 | C4-dicarboxylate transporter | -1.8 |
| ACX60_13715 | Hypothetical protein | -1.8 |
| ACX60_11665 | Type VI secretion protein | -1.8 |
| ACX60_14355 | Trehalose-6-phosphate synthase | -1.8 |
| ACX60_11670 | Hypothetical protein | -1.8 |
| ACX60_11455 | 2%2C3-dehydroadipyl-CoA hydratase | -1.9 |
| ACX60_01700 | Lipase chaperone | -1.9 |
| ACX60_16645 | DNA transfer protein p32 | -1.9 |
| ACX60_14350 | Trehalose phosphatase | -1.9 |
| ACX60_08410 | Protocatechuate 3%2C4-dioxygenase | -2.0 |
| ACX60_08375 | 3-oxoadipate CoA-transferase | -2.0 |
| ACX60_11235 | Hypothetical protein | -2.0 |
| ACX60_08405 | Protocatechuate 3%2C4-dioxygenase | -2.1 |
| ACX60_03385 | Toxin | -2.1 |
| ACX60_11675 | EvpB family type VI secretion protein | -2.1 |
| ACX60_12255 | Membrane protein | -2.1 |

| Locus-tag^a | Gene product | Differential expression (Log₂) |
|------------------------------|---------------------------------------------------------|--------------------------------------------------|
| ACX60_09410 | ABC transporter substrate-binding protein | -2.2 |
| ACX60_09385 | Butanediol dehydrogenase | -2.2 |
| ACX60_10810 | Na ⁺ :H ⁺ dicarboxylate symporter | -2.3 |
| ACX60_12490 | Hypothetical protein | -2.3 |
| ACX60_09395 | Dihydrolipoamide dehydrogenase | -2.4 |
| ACX60_11680 | Type VI secretion protein | -2.4 |
| ACX60_08585 | 3-oxoadipate CoA-transferase | -2.4 |
| ACX60_07095 | Hypothetical protein | -2.4 |
| ACX60_09405 | pyruvate dehydrogenase | -2.4 |
| ACX60_11220 | Hypothetical protein | -2.5 |
| ACX60_08400 | 4-carboxymuconolactone decarboxylase | -2.5 |
| ACX60_08395 | 4-hydroxybenzoate transporter | -2.5 |
| ACX60_09390 | Diacetyl reductase | -2.6 |
| ACX60_08370 | 3-oxoadipate CoA-transferase | -2.6 |
| ACX60_09400 | Diaminohydroxyphosphoribosylaminopyrimidine deaminase | -2.6 |
| ACX60_11225 | Hypothetical protein | -2.7 |
| ACX60_01695 | Lipase | -2.7 |
| ACX60_08390 | 3-oxoadipate enol-lactonase | -2.7 |
| ACX60_11685 | Hypothetical protein | -2.7 |
| ACX60_08385 | 3-carboxy-cis%2Ccis-muconate cycloisomerase | -2.8 |
| ACX60_16160 | 50S ribosomal protein L31 | -3.2 |
| ACX60_09410 | ABC transporter substrate-binding protein | -2.2 |
| ACX60_09385 | Butanediol dehydrogenase | -2.2 |
| ACX60_10810 | Na ⁺ :H ⁺ dicarboxylate symporter | -2.3 |
| ACX60_12490 | Hypothetical protein | -2.3 |
| ACX60_09395 | Dihydrolipoamide dehydrogenase | -2.4 |
| ACX60_11680 | Type VI secretion protein | -2.4 |
| ACX60_08585 | 3-oxoadipate CoA-transferase | -2.4 |
| ACX60_07095 | Hypothetical protein | -2.4 |
| ACX60_09405 | Pyruvate dehydrogenase | -2.4 |
| ACX60_11220 | Hypothetical protein | -2.5 |
| ACX60_08400 | 4-carboxymuconolactone decarboxylase | -2.5 |
| ACX60_08395 | 4-hydroxybenzoate transporter | -2.5 |
| ACX60_09390 | Diacetyl reductase | -2.6 |
| ACX60_08370 | 3-oxoadipate CoA-transferase | -2.6 |
| ACX60_09400 | Diaminohydroxyphosphoribosylaminopyrimidine deaminase | -2.6 |
| ACX60_11225 | Hypothetical protein | -2.7 |

| Locus-tag^a | Gene product | Differential expression (Log₂) |
|------------------------------|---------------------------------------------|--------------------------------------------------|
| ACX60_01695 | Lipase | -2.7 |
| ACX60_08390 | 3-oxoadipate enol-lactonase | -2.7 |
| ACX60_11685 | Hypothetical protein | -2.7 |
| ACX60_08385 | 3-carboxy-cis%2Ccis-muconate cycloisomerase | -2.8 |
| ACX60_16160 | 50S ribosomal protein L31 | -3.2 |

^a. Sequence was obtained from ATCC 17978 GenBank accession number CP012004

Appendix 17 – Abbreviations

| | |
|-------------------|----------------------------------------------------------------------------|
| ABC | Adenosine-triphosphate binding cassette |
| Amp | Ampicillin resistance |
| ATCC | American type culture collection |
| ATP | Adenosine triphosphate |
| Bap | Biofilm-associated protein |
| Blastn | Basic local alignment search tool for nucleotide sequences |
| Blastp | Basic local alignment search tool for protein sequences |
| BSH | Bacillithiol |
| bp | Base pair |
| C | Cysteine |
| °C | Degree Celsius |
| Cd | Cadmium |
| CDF | Cation Diffusion Facilitator transporter |
| cDNA | Complimentary deoxyribonucleic acid |
| CFU | Colony forming units |
| Cm | Chloramphenicol |
| Co | Cobalt |
| COG | Clusters of orthologous groups |
| CPS | Capsular polysaccharide |
| Cr | Chromium |
| Cu | Copper |
| DEPC | Diethylpyrocarbonate |
| dH ₂ O | Distilled H ₂ O |
| DLDH | Dihydrolipoamide dehydrogenase |
| DNAse | Deoxyribonuclease |
| Ery | Erythromycin resistance cassette |
| EDTA | Ethylenediaminetetraacetic acid |
| EGTA | Ethylene glycol-bis(β -aminoethyl ether)-N,N,N',N'-tetraacetic acid |
| ESBL | Extended spectrum β -lactamase |
| DNA | Deoxyribonucleic acid |
| Fe | Iron |
| Fur | Ferric uptake regulator |
| <i>g</i> | Centrifugal force |
| GGM | Glycerol-glycerophosphate medium |
| GSH | Gluthathione |
| ICU | Intensive care unit |
| IPTG | Isopropyl β -D-1-thiogalactopyranoside |
| ICP-MS | Inductively coupled plasma mass spectrometry |
| Kb | Kilo base |
| KEGG | Kyoto encyclopaedia of genes and genomes |

| | |
|---------|-------------------------------------------------------------|
| I | Litre |
| LB | Luria-Bertani |
| LOS | Lipooligosaccharide |
| LPS | Lipopolysaccharide |
| M | Molar |
| mA | Milliampere |
| MBL | Metallo β -lactamases |
| MDR | Multidrug resistant |
| mg | Milligram |
| Mg | Magnesium |
| MH | Mueller-Hinton |
| MIC | Minimal inhibitory concentration |
| ml | Millilitre |
| mM | Millimolar |
| mm | Millimetre |
| Mn | Manganese |
| mQ | MilliQ |
| mRNA | Messenger ribonucleic acid |
| MRSA | Methicillin resistant <i>Staphylococcus aureus</i> |
| Ni | Nickel |
| NCBI | National centre for biotechnology information |
| ng | Nanogram |
| nm | Nanometre |
| OD | Optical density |
| OMP | Outer membrane protein |
| OMV | Outer membrane vesicle |
| ON | Overnight |
| ORF | Open reading frame |
| p-value | Probability value |
| PBS | Phosphate buffered saline |
| PCR | Polymerase chain reaction |
| PQQ | Pyrroloquinoline-quinone |
| qRT-PCR | Quantitive reverse transcription polymerase chain reaction |
| RNA | Ribonucleic acid |
| RNAse | Ribonuclease |
| RND | Resistance nodulation division |
| rpm | Rotations per minute |
| R | Resistance |
| ROS | Reactive oxygen species |
| RT | Room temperature |
| SOD | Superoxide Dismutase |
| T6SS | Type VI secretion system |
| TPEN | <i>N,N,N',N'</i> -tetrakis-(2-pyridylmethyl)ethylenediamine |

| | |
|-----|-----------------------|
| Tet | Tetracycline |
| U | Units |
| V | Volt |
| v/v | Volume/volume |
| w/v | Weight/volume |
| WT | WT |
| Zn | Zinc |
| Zur | Zinc uptake regulator |
| µg | Microgram |
| µl | Microlitre |
| µM | Micromolar |

REFERENCES

- Abrantes, MC, Lopes Mde, F, and Kok, J.** (2011). Impact of manganese, copper and zinc ions on the transcriptome of the nosocomial pathogen *Enterococcus faecalis* V583. *PLoS One*, *6*, e26519.
- Abu Kwaik, Y, and Bumann, D.** (2013). Microbial quest for food in vivo: 'nutritional virulence' as an emerging paradigm. *Cell Microbiology*, *15*, 882-890.
- Akanuma, G, Nanamiya, H, Natori, Y, Nomura, N, and Kawamura, F.** (2006). Liberation of zinc-containing L31 (RpmE) from ribosomes by its paralogous gene product, YtiA, in *Bacillus subtilis*. *Journal of Bacteriology*, *188*, 2715-2720.
- Alting-Mees, MA, and Short, JM.** (1989). pBluescript II: gene mapping vectors. *Nucleic Acids Research*, *17*, 9494.
- Ammendola, S, Pasquali, P, Pistoia, C, Petrucci, P, Petrarca, P, Rotilio, G, and Battistoni, A.** (2007). High-affinity Zn²⁺ uptake system ZnuABC is required for bacterial zinc homeostasis in intracellular environments and contributes to the virulence of *Salmonella enterica*. *Infection and Immunity*, *75*, 5867-5876.
- Ansaldi, F, Canepa, P, Bassetti, M, Zancolli, M, Molinari, MP, Talamini, A, Ginocchio, F, Durando, P, Mussap, M, Orengo, G, Viscoli, C, and Icardi, G.** (2011). Sequential outbreaks of multidrug-resistant *Acinetobacter baumannii* in intensive care units of a tertiary referral hospital in Italy: combined molecular approach for epidemiological investigation. *The Journal of Hospital Infection*, *79*, 134-140.
- Anton, A, Grosse, C, Reissmann, J, Pribyl, T, and Nies, DH.** (1999). CzcD is a heavy metal ion transporter involved in regulation of heavy metal resistance in *Ralstonia sp.* strain CH34. *Journal of Bacteriology*, *181*, 6876-6881.
- Apell, HJ.** (2004). How do P-type ATPases transport ions? *Bioelectrochemistry*, *63*, 149-156.
- Aranda, J, Poza, M, Pardo, BG, Rumbo, S, Rumbo, C, Parreira, JR, Rodriguez-Velo, P, and Bou, G.** (2010). A rapid and simple method for constructing stable mutants of *Acinetobacter baumannii*. *BMC Microbiology*, *10*, 279.
- Bayle, L, Chimalapati, S, Schoehn, G, Brown, J, Vernet, T, and Durmort, C.** (2011). Zinc uptake by *Streptococcus pneumoniae* depends on both AdcA and AdcAll and is essential for normal bacterial morphology and virulence. *Molecular Microbiology*, *82*, 904-916.
- Beringer, M.** (2008). Modulating the activity of the peptidyl transferase center of the ribosome. *RNA*, *14*, 795-801.

- Bilder, P, Lightle, S, Bainbridge, G, Ohren, J, Finzel, B, Sun, F, Holley, S, Al-Kassim, L, Spessard, C, Melnick, M, Newcomer, M, and Waldrop, GL.** (2006). The structure of the carboxyltransferase component of acetyl-coA carboxylase reveals a zinc-binding motif unique to the bacterial enzyme. *Biochemistry*, *45*, 1712-1722.
- Blindauer, CA, Harrison, MD, Parkinson, JA, Robinson, AK, Cavet, JS, Robinson, NJ, and Sadler, PJ.** (2001). A metallothionein containing a zinc finger within a four-metal cluster protects a bacterium from zinc toxicity. *Proceedings of the National Academy of Sciences of the United States of America*, *98*, 9593-9598.
- Bonnin, RA, Nordmann, P, and Poirel, L.** (2013). Screening and deciphering antibiotic resistance in *Acinetobacter baumannii*: a state of the art. *Expert Review of Anti-Infective Therapy*, *11*, 571-583.
- Bou, G, and Martinez-Beltran, J.** (2000). Cloning, nucleotide sequencing, and analysis of the gene encoding an AmpC beta-lactamase in *Acinetobacter baumannii*. *Antimicrobial Agents and Chemotherapy*, *44*, 428-432.
- Braun, V, and Braun, M.** (2002). Iron transport and signaling in *Escherichia coli*. *FEBS Letters*, *529*, 78-85.
- Bray, TM, and Bettger, WJ.** (1990). The physiological role of zinc as an antioxidant. *Free Radical Biology & Medicine*, *8*, 281-291.
- Brodersen, DE, and Nissen, P.** (2005). The social life of ribosomal proteins. *The FEBS Journal*, *272*, 2098-2108.
- Brooks, MJ, Rajasimha, HK, Roger, JE, and Swaroop, A.** (2011). Next-generation sequencing facilitates quantitative analysis of wild-type and Nrl(-/-) retinal transcriptomes. *Molecular Vision*, *17*, 3034-3054.
- Brossard, KA, and Campagnari, AA.** (2012). The *Acinetobacter baumannii* biofilm-associated protein plays a role in adherence to human epithelial cells. *Infection and Immunity*, *80*, 228-233.
- Brown, NL, Stoyanov, JV, Kidd, SP, and Hobman, JL.** (2003). The MerR family of transcriptional regulators. *FEMS Microbiology Reviews*, *27*, 145-163.
- Butland, G, Peregrin-Alvarez, JM, Li, J, Yang, W, Yang, X, Canadien, V, Starostine, A, Richards, D, Beattie, B, Krogan, N, Davey, M, Parkinson, J, Greenblatt, J, and Emili, A.** (2005). Interaction network containing conserved and essential protein complexes in *Escherichia coli*. *Nature*, *433*, 531-537.
- Cabiscol, E, Tamarit, J, and Ros, J.** (2000). Oxidative stress in bacteria and protein damage by reactive oxygen species. *International Microbiology*, *3*, 3-8.

- Cai, Y, Chai, D, Wang, R, Liang, B, and Bai, N.** (2012). Colistin resistance of *Acinetobacter baumannii*: clinical reports, mechanisms and antimicrobial strategies. *The Journal of Antimicrobial Chemotherapy*, 67, 1607-1615.
- Calhoun, JH, Murray, CK, and Manning, MM.** (2008). Multidrug-resistant organisms in military wounds from Iraq and Afghanistan. *Clinical Orthopaedics Related Research*, 466, 1356-1362.
- Capdevila, DA, Wang, J, and Giedroc, DP.** (2016). Bacterial strategies to maintain zinc metallostasis at the host-pathogen interface. *The Journal of Biological Chemistry*, 291, 20858-20868.
- Carrasco-Lopez, C, Godoy, C, de Las Rivas, B, Fernandez-Lorente, G, Palomo, JM, Guisan, JM, Fernandez-Lafuente, R, Martinez-Ripoll, M, and Hermoso, JA.** (2009). Activation of bacterial thermoalkalophilic lipases is spurred by dramatic structural rearrangements. *The Journal of Biological Chemistry*, 284, 4365-4372.
- Carruthers, MD, Nicholson, PA, Tracy, EN, and Munson, RS, Jr.** (2013). *Acinetobacter baumannii* utilizes a type VI secretion system for bacterial competition. *PLoS One*, 8, e59388.
- Cerasi, M, Ammendola, S, and Battistoni, A.** (2013). Competition for zinc binding in the host-pathogen interaction. *Frontiers in Cellular and Infection Microbiology*, 3, 108.
- Cerasi, M, Liu, JZ, Ammendola, S, Poe, AJ, Petrarca, P, Pesciaroli, M, Pasquali, P, Raffatellu, M, and Battistoni, A.** (2014). The ZupT transporter plays an important role in zinc homeostasis and contributes to *Salmonella enterica* virulence. *Metallomics*, 6, 845-853.
- Cersini, A, Salvia, AM, and Bernardini, ML.** (1998). Intracellular multiplication and virulence of *Shigella flexneri* auxotrophic mutants. *Infection and Immunity*, 66, 549-557.
- Chandra, BR, Yogavel, M, and Sharma, A.** (2007). Structural analysis of ABC-family periplasmic zinc binding protein provides new insights into mechanism of ligand uptake and release. *Journal of Molecular Biology*, 367, 970-982.
- Chen, MZ, Hsueh, PR, Lee, LN, Yu, CJ, Yang, PC, and Luh, KT.** (2001). Severe community-acquired pneumonia due to *Acinetobacter baumannii*. *Chest*, 120, 1072-1077.
- Chen, Q, Cao, H, Lu, H, Qiu, ZH, and He, JJ.** (2015). Bioprosthetic tricuspid valve endocarditis caused by *Acinetobacter baumannii* complex, a case report and brief review of the literature. *Journal of Cardiothoracic Surgery*, 10, 149.
- Chiang, WC, Su, CP, Hsu, CY, Chen, SY, Chen, YC, Chang, SC, and Hsueh, PR.** (2003). Community-acquired bacteremic cellulitis caused by *Acinetobacter baumannii*. *Journal of the Formosan Medical Association*, 102, 650-652.

- Choi, AH, Slamti, L, Avci, FY, Pier, GB, ., and Maira-Litran, T.** (2009). The *pgaABCD* locus of *Acinetobacter baumannii* encodes the production of poly- β -1-6-N-acetylglucosamine, which is critical for biofilm formation. *Journal of Bacteriology*, 191, 5953-5963.
- Choi, CH, Lee, EY, Lee, YC, Park, TI, Kim, HJ, Hyun, SH, Kim, SA, Lee, SK, and Lee, JC.** (2005). Outer membrane protein 38 of *Acinetobacter baumannii* localizes to the mitochondria and induces apoptosis of epithelial cells. *Cellular Microbiology*, 7, 1127-1138.
- Choi, CH, Lee, JS, Lee, YC, Park, TI, and Lee, JC.** (2008). *Acinetobacter baumannii* invades epithelial cells and outer membrane protein A mediates interactions with epithelial cells. *BMC Microbiology*, 8, 216.
- Choudhury, R, and Srivastava, S.** (2001). Zinc resistance mechanisms in bacteria. *Current Science*, 81, 768-775.
- Chuang, YC, Sheng, WH, Lauderdale, TL, Li, SY, Wang, JT, Chen, YC, and Chang, SC.** (2014). Molecular epidemiology, antimicrobial susceptibility and carbapenemase resistance determinants among *Acinetobacter baumannii* clinical isolates in Taiwan. *Journal of Microbiology, Immunology and Infection*, 47, 324-332.
- Chuang, YC, Sheng, WH, Li, SY, Lin, YC, Wang, JT, Chen, YC, and Chang, SC.** (2011). Influence of genospecies of *Acinetobacter baumannii* complex on clinical outcomes of patients with acinetobacter bacteremia. *Clinical Infectious Diseases* 52, 352-360.
- Clarke, TE, Tari, LW, and Vogel, HJ.** (2001). Structural biology of bacterial iron uptake systems. *Current Topics in Medicinal Chemistry*, 1, 7-30.
- CLSI.** (2014). Performance Standards For Antimicrobial Susceptibility Testing; 24th Informational Supplement. *Clinical and Laboratory Standards Institute*.
- Colvin, RA, Holmes, WR, Fontaine, CP, and Maret, W.** (2010). Cytosolic zinc buffering and muffling: their role in intracellular zinc homeostasis. *Metallomics*, 2, 306-317.
- Conrady, DG, Brescia, CC, Horii, K, Weiss, AA, Hasset, DJ, and Herr, AB.** (2008). A zinc-dependent adhesion module is responsible for intercellular adhesion in staphylococcal biofilms. *Proceedings of the National Academy of Sciences of the United States of America*, 105, 19456-19461.
- Consales, G, Gramigni, E, Zamidei, L, Bettocchi, D, and De Gaudio, AR.** (2011). A multidrug-resistant *Acinetobacter baumannii* outbreak in intensive care unit: antimicrobial and organizational strategies. *Journal of Critical Care*, 26, 453-459.

- Corbett, D, Wang, J, Schuler, S, Lopez-Castejon, G, Glenn, S, Brough, D, Andrew, PW, Cavet, JS, and Roberts, IS.** (2012). Two zinc uptake systems contribute to the full virulence of *Listeria monocytogenes* during growth *in vitro* and *in vivo*. *Infection and Immunity*, *80*, 14-21.
- Corbin, BD, Seeley, EH, Raab, A, Feldmann, J, Miller, MR, Torres, VJ, Anderson, KL, Dattilo, BM, Dunman, PM, Gerads, R, Caprioli, RM, Nacken, W, Chazin, WJ, and Skaar, EP.** (2008). Metal chelation and inhibition of bacterial growth in tissue abscesses. *Science*, *319*, 962-965.
- Coulthurst, SJ.** (2013). The Type VI secretion system - a widespread and versatile cell targeting system. *Research in Microbiology*, *164*, 640-654.
- Coyne, S, Courvalin, P, and Perichon, B.** (2011). Efflux-mediated antibiotic resistance in *Acinetobacter* spp. *Antimicrobial Agents and Chemotherapy*, *55*, 947-953.
- Dalet, K, Gouin, E, Cenatiempo, Y, Cossart, P, and Hechard, Y.** (1999). Characterisation of a new operon encoding a Zur-like protein and an associated ABC zinc permease in *Listeria monocytogenes*. *FEMS Microbiology Letters*, *174*, 111-116.
- de Berardinis, V, Vallenet, D, Castelli, V, Besnard, M, Pinet, A, Cruaud, C, Samair, S, Lechaplais, C, Gyapay, G, Richez, C, Durot, M, Kreimeyer, A, Le Fevre, F, Schachter, V, Pezo, V, Doring, V, Scarpelli, C, Medigue, C, Cohen, GN, Marliere, P, Salanoubat, M, and Weissenbach, J.** (2008). A complete collection of single-gene deletion mutants of *Acinetobacter baylyi* ADP1. *Molecular Systems Biology*, *4*, 174.
- De Nicola, R, Hazelwood, LA, De Hulster, EA, Walsh, MC, Knijnenburg, TA, Reinders, MJ, Walker, GM, Pronk, JT, Daran, JM, and Daran-Lapujade, P.** (2007). Physiological and transcriptional responses of *Saccharomyces cerevisiae* to zinc limitation in chemostat cultures. *Applied and Environmental Microbiology*, *73*, 7680-7692.
- Decoin, V, Barbey, C, Bergeau, D, Latour, X, Feuilloley, MG, Orange, N, and Merieau, A.** (2014). A type VI secretion system is involved in *Pseudomonas fluorescens* bacterial competition. *PLoS One*, *9*, e89411.
- Dexter, C, Murray, GL, Paulsen, IT, and Peleg, AY.** (2015). Community-acquired *Acinetobacter baumannii*: clinical characteristics, epidemiology and pathogenesis. *Expert Review of Anti-Infective Therapy*, *13*, 567-573.
- Diancourt, L, Passet, V, Nemec, A, Dijkshoorn, L, and Brisse, S.** (2010). The population structure of *Acinetobacter baumannii*: expanding multiresistant clones from an ancestral susceptible genetic pool. *PLoS One*, *5*, e10034.

- Dorsey, CW, Tomaras, AP, Connerly, PL, Tolmasky, ME, Crosa, JH, and Actis, LA.** (2004). The siderophore-mediated iron acquisition systems of *Acinetobacter baumannii* ATCC 19606 and *Vibrio anguillarum* 775 are structurally and functionally related. *Microbiology*, 150, 3657-3667.
- Dötsch, A, Eckweiler, D, Schniederjans, M, Zimmermann, A, Jensen, V, Scharfe, M, Geffers, R, and Häussler, S.** (2012). The *Pseudomonas aeruginosa* transcriptome in planktonic cultures and static biofilms using RNA sequencing. *PLoS One*, 7, 1-11.
- Eide, DJ.** (2006). Zinc transporters and the cellular trafficking of zinc. *Biochimica et Biophysica Acta*, 1763, 711-722.
- Eijkelkamp, BA.** (2011). *Factors contributing to the success of Acinetobacter baumannii as a human pathogen.* (PhD), Flinders University, Australia.
- Eijkelkamp, BA, Hassan, KA, Paulsen, IT, and Brown, MH.** (2011a). Investigation of the human pathogen *Acinetobacter baumannii* under iron limiting conditions. *BMC Genomics*, 12, 126.
- Eijkelkamp, BA, Morey, JR, Ween, MP, Ong, CL, McEwan, AG, Paton, JC, and McDevitt, CA.** (2014a). Extracellular zinc competitively inhibits manganese uptake and compromises oxidative stress management in *Streptococcus pneumoniae*. *PLoS One*, 9, e89427.
- Eijkelkamp, BA, Stroehler, UH, Hassan, KA, Papadimitriou, MS, Paulsen, IT, and Brown, MH.** (2011b). Adherence and motility characteristics of clinical *Acinetobacter baumannii* isolates. *FEMS Microbiology Letters*, 323, 44-51.
- Eijkelkamp, BA, Stroehler, UH, Hassan, KA, Paulsen, IT, and Brown, MH.** (2014b). Comparative analysis of surface-exposed virulence factors of *Acinetobacter baumannii*. *BMC Genomics*, 15, 1020.
- Ellis, TN, and Kuehn, MJ.** (2010). Virulence and immunomodulatory roles of bacterial outer membrane vesicles. *Microbiology and Molecular Biology Reviews* 74, 81-94.
- Ellison, ML, Farrow, JM, 3rd, Parrish, W, Danell, AS, and Pesci, EC.** (2013). The transcriptional regulator Np20 is the zinc uptake regulator in *Pseudomonas aeruginosa*. *PLoS One*, 8, e75389.
- Espinal, P, Marti, S, and Vila, J.** (2012). Effect of biofilm formation on the survival of *Acinetobacter baumannii* on dry surfaces. *The Journal of Hospital Infection*, 80, 56-60.
- Eugenin, EA.** (2013). Community-acquired pneumonia infections by *Acinetobacter baumannii*: how does alcohol impact the antimicrobial functions of macrophages? *Virulence*, 4, 435-436.

- Eveillard, M, Kempf, M, Belmonte, O, Pailhories, H, and Joly-Guillou, ML.** (2013). Reservoirs of *Acinetobacter baumannii* outside the hospital and potential involvement in emerging human community-acquired infections. *International Journal of Infectious Diseases*, 17, e802-805.
- Feng, Y, Li, M, Zhang, H, Zheng, B, Han, H, Wang, C, Yan, J, Tang, J, and Gao, GF.** (2008). Functional definition and global regulation of Zur, a zinc uptake regulator in a *Streptococcus suis* serotype 2 strain causing streptococcal toxic shock syndrome. *Journal of Bacteriology*, 190, 7567-7578.
- Fournier, PE, and Richet, H.** (2006). The epidemiology and control of *Acinetobacter baumannii* in health care facilities. *Clinical Infectious Diseases*, 42, 692-699.
- Fukushima, T, Tanaka, K, Lim, H, and Moriyama, M.** (2002). Mechanism of cytotoxicity of paraquat. *Environmental Health and Preventive Medicine* 7, 89-94.
- Gaballa, A, and Helmann, JD.** (1998). Identification of a zinc-specific metalloregulatory protein, Zur, controlling zinc transport operons in *Bacillus subtilis*. *Journal of Bacteriology*, 180, 5815-5821.
- Gaballa, A, and Helmann, JD.** (2002). A peroxide-induced zinc uptake system plays an important role in protection against oxidative stress in *Bacillus subtilis*. *Molecular Microbiology*, 45, 997-1005.
- Gabriel, SE, and Helmann, JD.** (2009). Contributions of Zur-controlled ribosomal proteins to growth under zinc starvation conditions. *Journal of Bacteriology*, 191, 6116-6122.
- Gabriel, SE, Miyagi, F, Gaballa, A, and Helmann, JD.** (2008). Regulation of the *Bacillus subtilis* *yciC* gene and insights into the DNA-binding specificity of the zinc-sensing metalloregulator Zur. *Journal of Bacteriology*, 190, 3482-3488.
- Gaddy, JA, Tomaras, AP, and Actis, LA.** (2009). The *Acinetobacter baumannii* 19606 OmpA protein plays a role in biofilm formation on abiotic surfaces and in the interaction of this pathogen with eukaryotic cells. *Infection and Immunity*, 77, 3150-3160.
- Garneau-Tsodikova, S, and Labby, KJ.** (2016). Mechanisms of Resistance to Aminoglycoside Antibiotics: Overview and Perspectives. *Medicinal Chemical Communications*, 7, 11-27.
- Geisinger, E, and Isberg, RR.** (2015). Antibiotic modulation of capsular exopolysaccharide and virulence in *Acinetobacter baumannii*. *PLoS Pathogens*, 11, e1004691.
- Gentile, V, Frangipani, E, Bonchi, C, Minandri, F, Runci, F, and Visca, P.** (2014). Iron and *Acinetobacter baumannii* biofilm formation. *Pathogens*, 3, 704-719.

- Geoghegan, JA, Corrigan, RM, Gruszka, DT, Speziale, P, O'Gara, JP, Potts, JR, and Foster, TJ.** (2010). Role of surface protein SasG in biofilm formation by *Staphylococcus aureus*. *Journal of Bacteriology*, *192*, 5663-5673.
- Giannouli, M, Antunes, LC, Marchetti, V, Triassi, M, Visca, P, and Zarrilli, R.** (2013). Virulence-related traits of epidemic *Acinetobacter baumannii* strains belonging to the international clonal lineages I-III and to the emerging genotypes ST25 and ST78. *BMC Infectious Diseases*, *13*, 282.
- Giard, DJ, Aaronson, SA, Todaro, GJ, Arnstein, P, Kersey, JH, Dosik, H, and Parks, WP.** (1973). *In vitro* cultivation of human tumors: establishment of cell lines derived from a series of solid tumors. *Journal of the National Cancer Institute*, *51*, 1417-1423.
- Giedroc, DP, and Arunkumar, AI.** (2007). Metal sensor proteins: nature's metalloregulated allosteric switches. *Dalton Transactions*, 3107-3120.
- Giles, SK, Stroehler, UH, Eijkelkamp, BA, and Brown, MH.** (2015). Identification of genes essential for pellicle formation in *Acinetobacter baumannii*. *BMC Microbiology*, *15*, 116.
- Gilston, BA, Wang, S, Marcus, MD, Canalizo-Hernandez, MA, Swindell, EP, Xue, Y, Mondragon, A, and O'Halloran, TV.** (2014). Structural and mechanistic basis of zinc regulation across the *E. coli* Zur regulon. *PLoS Biology*, *12*, e1001987.
- Gohl, O, Friedrich, A, Hoppert, M, and Averhoff, B.** (2006). The thin pili of *Acinetobacter sp.* strain BD413 mediate adhesion to biotic and abiotic surfaces. *Applied and Environmental Microbiology*, *72*, 1394-1401.
- Graham, AI, Hunt, S, Stokes, SL, Bramall, N, Bunch, J, Cox, AG, McLeod, CW, and Poole, RK.** (2009). Severe zinc depletion of *Escherichia coli*: roles for high affinity zinc binding by ZinT, zinc transport and zinc-independent proteins. *The Journal of Biological Chemistry*, *284*, 18377-18389.
- Grass, G, Fan, B, Rosen, BP, Franke, S, Nies, DH, and Rensing, C.** (2001). ZitB (YbgR), a member of the cation diffusion facilitator family, is an additional zinc transporter in *Escherichia coli*. *Journal of Bacteriology*, *183*, 4664-4667.
- Grass, G, Franke, S, Taudte, N, Nies, DH, Kucharski, LM, Maguire, ME, and Rensing, C.** (2005). The metal permease ZupT from *Escherichia coli* is a transporter with a broad substrate spectrum. *Journal of Bacteriology*, *187*, 1604-1611.
- Grass, G, Wong, MD, Rosen, BP, Smith, RL, and Rensing, C.** (2002). ZupT is a Zn(II) uptake system in *Escherichia coli*. *Journal of Bacteriology*, *184*, 864-866.
- Greene, C, Vadlamudi, G, Newton, D, Foxman, B, and Xi, C.** (2016). The influence of biofilm formation and multidrug resistance on environmental survival of clinical and environmental isolates of *Acinetobacter baumannii*. *American Journal of Infection Control* *44*, e65-71.

- Guilhen, C, Taha, MK, and Veyrier, FJ.** (2013). Role of transition metal exporters in virulence: the example of *Neisseria meningitidis*. *Frontiers in Cellular and Infection Microbiology*, 3, 102.
- Gulen, TA, Guner, R, Celikbilek, N, Keske, S, and Tasyaran, M.** (2015). Clinical importance and cost of bacteremia caused by nosocomial multi drug resistant *Acinetobacter baumannii*. *International Journal of Infectious Diseases*.
- Gunasekera, TS, Herre, AH, and Crowder, MW.** (2009). Absence of ZnuABC-mediated zinc uptake affects virulence-associated phenotypes of uropathogenic *Escherichia coli* CFT073 under Zn(II)-depleted conditions. *FEMS Microbiology Letters*, 300, 36-41.
- Gurung, J, Khyriem, AB, Banik, A, Lyngdoh, WV, Choudhury, B, and Bhattacharyya, P.** (2013). Association of biofilm production with multidrug resistance among clinical isolates of *Acinetobacter baumannii* and *Pseudomonas aeruginosa* from intensive care unit. *Indian Journal of Critical Care Medicine*, 17, 214-218.
- Haas, CE, Rodionov, DA, Kropat, J, Malasarn, D, Merchant, SS, and de Crecy-Lagard, V.** (2009). A subset of the diverse COG0523 family of putative metal chaperones is linked to zinc homeostasis in all kingdoms of life. *BMC Genomics*, 10, 470.
- Hakansson, AP, and Smith, AW.** (2007). Enzymatic characterization of dihydrolipoamide dehydrogenase from *Streptococcus pneumoniae* harboring its own substrate. *The Journal of Biological Chemistry*, 282, 29521-29530.
- Hamidian, M, and Hall, RM.** (2014). Resistance to third-generation cephalosporins in *Acinetobacter baumannii* due to horizontal transfer of a chromosomal segment containing ISAbal-ampC. *The Journal of Antimicrobial Chemotherapy*, 69, 2865-2866.
- Hanahan, D.** (1983). Studies on transformation of *Escherichia coli* with plasmids. *Molecular Biology*, 166, 557-580.
- Hancock, V, Dahl, M, and Klemm, P.** (2010). Abolition of biofilm formation in urinary tract *Escherichia coli* and *Klebsiella* isolates by metal interference through competition for fur. *Applied and Environmental Microbiology*, 76, 3836-3841.
- Hantke, K.** (2001a). Bacterial zinc transporters and regulators. *Biometals*, 14, 239-249.
- Hantke, K.** (2001b). Iron and metal regulation in bacteria. *Current Opinion in Microbiology*, 4, 172-177.
- Hantke, K.** (2005). Bacterial zinc uptake and regulators. *Current Opinion in Microbiology*, 8, 196-202.

- Harding, CM, Tracy, EN, Carruthers, MD, Rather, PN, Actis, LA, and Munson, RS, Jr.** (2013). *Acinetobacter baumannii* strain M2 produces type IV pili which play a role in natural transformation and twitching motility but not surface-associated motility. *MBio*, *4*, e00360-00313.
- Hare, NJ, Scott, NE, Shin, EH, Connolly, AM, Larsen, MR, Palmisano, G, and Cordwell, SJ.** (2011). Proteomics of the oxidative stress response induced by hydrogen peroxide and paraquat reveals a novel AhpC-like protein in *Pseudomonas aeruginosa*. *Proteomics*, *11*, 3056-3069.
- Hassan, MT, van der Lelie, D, Springael, D, Romling, U, Ahmed, N, and Mergeay, M.** (1999). Identification of a gene cluster, *czr*, involved in cadmium and zinc resistance in *Pseudomonas aeruginosa*. *Gene*, *238*, 417-425.
- Hazard, D, Liaubet, L, Sancristobal, M, and Mormede, P.** (2008). Gene array and real time PCR analysis of the adrenal sensitivity to adrenocorticotrophic hormone in pig. *BMC Genomics*, *9*, 101.
- Heath, C, H. , Orrell, T, C., Lee, R, C., Pearman, J, W. , McCullough, C, and Christiansen, K, J.** (2003). A review of the Royal Perth Hospital Bali experience: an infection control perspective. *Australian Infection Control*, *8*, 43-54
- Heindorf, M, Kadari, M, Heider, C, Skiebe, E, and Wilharm, G.** (2014). Impact of *Acinetobacter baumannii* superoxide dismutase on motility, virulence, oxidative stress resistance and susceptibility to antibiotics. *PLoS One*, *9*, e101033.
- Helbig, K, Bleuel, C, Krauss, GJ, and Nies, DH.** (2008). Glutathione and transition-metal homeostasis in *Escherichia coli*. *Journal of Bacteriology*, *190*, 5431-5438.
- Hensley, MP, Gunasekera, TS, Easton, JA, Sigdel, TK, Sugarbaker, SA, Klingbeil, L, Breece, RM, Tierney, DL, and Crowder, MW.** (2012). Characterization of Zn(II)-responsive ribosomal proteins YkgM and L31 in *E. coli*. *Journal of Inorganic Biochemistry*, *111*, 164-172.
- Higgins, VJ, Rogers, PJ, and Dawes, IW.** (2003). Application of genome-wide expression analysis to identify molecular markers useful in monitoring industrial fermentations. *Applied and Environmental Microbiology*, *69*, 7535-7540.
- Ho, YH, Wang, LS, Chao, HJ, Chang, KC, and Su, CF.** (2007). Successful treatment of meningitis caused by multidrug-resistant *Acinetobacter baumannii* with intravenous and intrathecal colistin. *Journal of Microbiology, Immunology, and Infection*, *40*, 537-540.

- Hoang, TT, Karkhoff-Schweizer, RR, Kutchma, AJ, and Schweizer, HP.** (1998). A broad-host-range Flp-FRT recombination system for site-specific excision of chromosomally-located DNA sequences: application for isolation of unmarked *Pseudomonas aeruginosa* mutants. *Gene*, 212, 77-78.
- Hood, MI, Mortensen, BL, Moore, JL, Zhang, Y, Kehl-Fie, TE, Sugitani, N, Chazin, WJ, Caprioli, RM, and Skaar, EP.** (2012). Identification of an *Acinetobacter baumannii* zinc acquisition system that facilitates resistance to calprotectin-mediated zinc sequestration. *PLoS Pathogens*, 8, e1003068.
- Hood, MI, Skaar, E.P.** (2012). Nutritional immunity: transition metals at the pathogen–host interface. *Nature Reviews Microbiology* 10, 525-537.
- Hood, RD, Singh, P, Hsu, F, Guvener, T, Carl, MA, Trinidad, RR, Silverman, JM, Ohlson, BB, Hicks, KG, Plemel, RL, Li, M, Schwarz, S, Wang, WY, Merz, AJ, Goodlett, DR, and Mougous, JD.** (2010). A type VI secretion system of *Pseudomonas aeruginosa* targets a toxin to bacteria. *Cell Host & Microbe*, 7, 25-37.
- Hu, D, Liu, B, Dijkshoorn, L, Wang, L, and Reeves, PR.** (2013). Diversity in the major polysaccharide antigen of *Acinetobacter baumannii* assessed by DNA sequencing, and development of a molecular serotyping scheme. *PLoS One*, 8, e70329.
- Huang, M, Oppermann-Sanio, FB, and Steinbuchel, A.** (1999). Biochemical and molecular characterization of the *Bacillus subtilis* acetoin catabolic pathway. *Journal of Bacteriology*, 181, 3837-3841.
- Hunger, M, Schmucker, R, Kishan, V, and Hillen, W.** (1990). Analysis and nucleotide sequence of an origin of DNA replication in *Acinetobacter calcoaceticus* and its use for *Escherichia coli* shuttle plasmids. *Gene*, 87, 45-51.
- Iwig, JS, Rowe, JL, and Chivers, PT.** (2006). Nickel homeostasis in *Escherichia coli* - the *rcnR-rcnA* efflux pathway and its linkage to NikR function. *Molecular Microbiology*, 62, 252-262.
- Jacobsen, FE, Kazmierczak, KM, Lisher, JP, Winkler, ME, and Giedroc, DP.** (2011). Interplay between manganese and zinc homeostasis in the human pathogen *Streptococcus pneumoniae*. *Metallomics*, 3, 38-41.
- Jacoby, GA.** (2009). AmpC β -lactamases. *Clinical Microbiology Reviews*, 22, 161-182.
- Jaeger, KE, Ransac, S, Dijkstra, BW, Colson, C, van Heuvel, M, and Misset, O.** (1994). Bacterial lipases. *FEMS Microbiology Reviews*, 15, 29-63.
- Jawad, A, Seifert, H, Snelling, AM, Heritage, J, and Hawkey, PM.** (1998). Survival of *Acinetobacter baumannii* on dry surfaces: comparison of outbreak and sporadic isolates. *Journal of Clinical Microbiology*, 36, 1938-1941.

- Jin, JS, Kwon, SO, Moon, DC, Gurung, M, Lee, JH, Kim, SI, and Lee, JC.** (2011). *Acinetobacter baumannii* secretes cytotoxic outer membrane protein A via outer membrane vesicles. *PLoS One*, *6*, e17027.
- Jomova, K, and Valko, M.** (2011). Advances in metal-induced oxidative stress and human disease. *Toxicology*, *283*, 65-87.
- Jun, SH, Lee, JH, Kim, BR, Kim, SI, Park, TI, Lee, JC, and Lee, YC.** (2013). *Acinetobacter baumannii* outer membrane vesicles elicit a potent innate immune response via membrane proteins. *PLoS One*, *8*, e71751.
- Kearns, DB, Bonner, PJ, Smith, DR, and Shimkets, LJ.** (2002). An extracellular matrix-associated zinc metalloprotease is required for dilauroyl phosphatidylethanolamine chemotactic excitation in *Myxococcus xanthus*. *Journal of Bacteriology*, *184*, 1678-1684.
- Kehl-Fie, TE, Zhang, Y, Moore, JL, Farrand, AJ, Hood, MI, Rathi, S, Chazin, WJ, Caprioli, RM, and Skaar, EP.** (2013). MntABC and MntH contribute to systemic *Staphylococcus aureus* infection by competing with calprotectin for nutrient manganese. *Infection and Immunity*, *81*, 3395-3405.
- Kenyon, JJ, and Hall, RM.** (2013). Variation in the complex carbohydrate biosynthesis loci of *Acinetobacter baumannii* genomes. *PLoS One*, *8*, e62160.
- Kenyon, JJ, Marzaioli, AM, Hall, RM, and De Castro, C.** (2014a). Structure of the K2 capsule associated with the KL2 gene cluster of *Acinetobacter baumannii*. *Glycobiology*, *24*, 554-563.
- Kenyon, JJ, Marzaioli, AM, Hall, RM, and De Castro, C.** (2015). Structure of the K12 capsule containing 5,7-di-N-acetylacinetaminic acid from *Acinetobacter baumannii* isolate D36. *Glycobiology*, *25*, 881-887.
- Kenyon, JJ, Nigro, SJ, and Hall, RM.** (2014b). Variation in the OC locus of *Acinetobacter baumannii* genomes predicts extensive structural diversity in the lipooligosaccharide. *PLoS One*, *9*, e107833.
- Kenyon, JJ, Shneider, MM, Senchenkova, SN, Shashkov, AS, Siniagina, MN, Malanin, SY, Popova, AV, Miroshnikov, KA, Hall, RM, and Knirel, YA.** (2016). K19 capsular polysaccharide of *Acinetobacter baumannii* is produced via a Wzy polymerase encoded in a small genomic island rather than the KL19 capsule gene cluster. *Microbiology*, *162*, 1479-1489.
- Khan, S, Brocklehurst, KR, Jones, GW, and Morby, AP.** (2002). The functional analysis of directed amino-acid alterations in ZntR from *Escherichia coli*. *Biochemical and Biophysical Research Communications*, *299*, 438-445.
- Kim, SW, Choi, CH, Moon, DC, Jin, JS, Lee, JH, Shin, JH, Kim, JM, Lee, YC, Seol, SY, Cho, DT, and Lee, JC.** (2009). Serum resistance of *Acinetobacter baumannii* through the binding of factor H to outer membrane proteins. *FEMS Microbiology Letters*, *301*, 224-231.

- Kolaj-Robin, O, Russell, D, Hayes, KA, Pembroke, JT, and Soulimane, T.** (2015). Cation Diffusion Facilitator family: Structure and function. *FEBS Letters*, *589*, 1283-1295.
- Korobeinikova, AV, Garber, MB, and Gongadze, GM.** (2012). Ribosomal proteins: structure, function, and evolution. *Biochemistry. Biokhimiia*, *77*, 562-574.
- Koster, W.** (2005). Cytoplasmic membrane iron permease systems in the bacterial cell envelope. *Frontiers in Bioscience*, *10*, 462-477.
- Kuroda, M, Hayashi, H, and Ohta, T.** (1999). Chromosome-determined zinc-responsive operon *czr* in *Staphylococcus aureus* strain 912. *Microbiology and Immunology*, *43*, 115-125.
- Labrie, J, Pelletier-Jacques, G, Deslandes, V, Ramjeet, M, Auger, E, Nash, JH, and Jacques, M.** (2010). Effects of growth conditions on biofilm formation by *Actinobacillus pleuropneumoniae*. *Veterinary Research*, *41*, 3.
- Lazureanu, V, Porosnicu, M, Gandac, C, Moisil, T, Baditoiu, L, Laza, R, Musta, V, Crisan, A, and Marinescu, AR.** (2016). Infection with *Acinetobacter baumannii* in an intensive care unit in the Western part of Romania. *BMC Infectious Diseases*, *16*, 95.
- Lee, CW, Chakravorty, DK, Chang, FM, Reyes-Caballero, H, Ye, Y, Merz, KM, Jr., and Giedroc, DP.** (2012a). Solution structure of *Mycobacterium tuberculosis* NmtR in the apo state: insights into Ni(II)-mediated allostery. *Biochemistry*, *51*, 2619-2629.
- Lee, HW, Koh, YM, Kim, J, Lee, JC, Lee, YC, Seol, SY, Cho, DT, and Kim, J.** (2008). Capacity of multidrug-resistant clinical isolates of *Acinetobacter baumannii* to form biofilm and adhere to epithelial cell surfaces. *Clinical Microbiology and Infection*, *14*, 49-54.
- Lee, YC, Huang, YT, Tan, CK, Kuo, YW, Liao, CH, Lee, PI, and Hsueh, PR.** (2011). *Acinetobacter baumannii* and *Acinetobacter* genospecies 13TU and 3 bacteraemia: comparison of clinical features, prognostic factors and outcomes. *The Journal of Antimicrobial Chemotherapy*, *66*, 1839-1846.
- Lee, YT, Fung, CP, Wang, FD, Chen, CP, Chen, TL, and Cho, WL.** (2012b). Outbreak of imipenem-resistant *Acinetobacter calcoaceticus*-*Acinetobacter baumannii* complex harboring different carbapenemase gene-associated genetic structures in an intensive care unit. *Journal of Microbiology, Immunology, and Infection*, *45*, 43-51.
- Leichert, LI, Scharf, C, and Hecker, M.** (2003). Global characterization of disulfide stress in *Bacillus subtilis*. *Journal of Bacteriology*, *185*, 1967-1975.

- Lemos, EV, de la Hoz, FP, Alvis, N, Einarson, TR, Quevedo, E, Castaneda, C, Leon, Y, Amado, C, Canon, O, and Kawai, K.** (2014). Impact of carbapenem resistance on clinical and economic outcomes among patients with *Acinetobacter baumannii* infection in Colombia. *Clinical Microbiology and Infection*, *20*, 174-180.
- Leon-Kempis, MR, Guccione, E, Mulholland, F, Williamson, MP, and Kelly, DJ.** (2006). The *Campylobacter jejuni* PEB1a adhesin is an aspartate/glutamate-binding protein of an ABC transporter essential for microaerobic growth on dicarboxylic amino acids. *Molecular Microbiology*, *60*, 1262-1275.
- Leseva, M, Arguirova, M, Nashev, D, Zamfirova, E, and Hadzhyiski, O.** (2013). Nosocomial infections in burn patients: etiology, antimicrobial resistance, means to control. *Annals of Burns and Fire Disasters*, *26*, 5-11.
- Li, Y, Qiu, Y, Gao, H, Guo, Z, Han, Y, Song, Y, Du, Z, Wang, X, Zhou, D, and Yang, R.** (2009). Characterization of Zur-dependent genes and direct Zur targets in *Yersinia pestis*. *BMC Microbiology*, *9*, 128.
- Lim, C, Hassan, KA, Penesyan, A, Loper, JE, and Paulsen, IT.** (2013). The effect of zinc limitation on the transcriptome of *Pseudomonas protegens* Pf-5. *Environmental Microbiology*, *15*, 702-715.
- Lim, C, Hassan, KA, Tetu, SG, Loper, JE, and Paulsen, IT.** (2012). The effect of iron limitation on the transcriptome and proteome of *Pseudomonas fluorescens* Pf-5. *PLoS One*, *7*, e39139.
- Lim, J, Lee, KM, Kim, SH, Kim, Y, Kim, SH, Park, W, and Park, S.** (2011). YkgM and ZinT proteins are required for maintaining intracellular zinc concentration and producing curli in enterohemorrhagic *Escherichia coli* (EHEC) O157:H7 under zinc deficient conditions. *International Journal of Food Microbiology*, *149*, 159-170.
- Lin, L, Tan, B, Pantapalangkoor, P, Ho, T, Baquir, B, Tomaras, A, Montgomery, JI, Reilly, U, Barbacci, EG, Hujer, K, Bonomo, RA, Fernandez, L, Hancock, RE, Adams, MD, French, SW, Buslon, VS, and Spellberg, B.** (2012). Inhibition of LpxC protects mice from resistant *Acinetobacter baumannii* by modulating inflammation and enhancing phagocytosis. *MBio*, *3*, e00312-00312.
- Lindsay, JA, and Foster, SJ.** (2001). Zur: a Zn(2+)-responsive regulatory element of *Staphylococcus aureus*. *Microbiology*, *147*, 1259-1266.
- Liu, Q, Li, W, Du, X, Li, W, Zhong, T, Tang, Y, Feng, Y, Tao, C, and Xie, Y.** (2015). Risk and prognostic factors for multidrug-resistant *Acinetobacter baumannii* complex bacteremia: A retrospective study in a tertiary hospital of West China. *PLoS One*, *10*, e0130701.
- Liu, T, Ramesh, A, Ma, Z, Ward, SK, Zhang, L, George, GN, Talaat, AM, Sacchettini, JC, and Giedroc, DP.** (2007). CsoR is a novel *Mycobacterium tuberculosis* copper-sensing transcriptional regulator. *Nature Chemical Biology*, *3*, 60-68.

- Livak, KJ, and Schmittgen, TD.** (2001). Analysis of relative gene expression data using real-time quantitative PCR and the $2^{-(\Delta\Delta C(T))}$ method. *Methods*, 25, 402-408.
- Loehfelm, TW, Luke, NR, and Campagnari, AA.** (2008). Identification and characterization of an *Acinetobacter baumannii* biofilm-associated protein. *Journal of Bacteriology*, 190, 1036-1044.
- Lutsenko, S, and Kaplan, JH.** (1995). Organization of P-type ATPases: significance of structural diversity. *Biochemistry*, 34, 15607-15613.
- Ma, Z, Chandrangu, P, Helmann, TC, Romsang, A, Gaballa, A, and Helmann, JD.** (2014). Bacillithiol is a major buffer of the labile zinc pool in *Bacillus subtilis*. *Molecular Microbiology*, 94, 756-770.
- Ma, Z, Jacobsen, FE, and Giedroc, DP.** (2009). Coordination chemistry of bacterial metal transport and sensing. *Chemical Reviews*, 109, 4644-4681.
- Maciag, A, Dainese, E, Rodriguez, GM, Milano, A, Provvedi, R, Pasca, MR, Smith, I, Palu, G, Riccardi, G, and Manganeli, R.** (2007). Global analysis of the *Mycobacterium tuberculosis* Zur (FurB) regulon. *Journal of Bacteriology*, 189, 730-740.
- MacIntyre, DL, Miyata, ST, Kitaoka, M, and Pukatzki, S.** (2010). The *Vibrio cholerae* type VI secretion system displays antimicrobial properties. *Proceedings of the National Academy of Sciences of the United States of America*, 107, 19520-19524.
- Makarova, KS, Ponomarev, VA, and Koonin, EV.** (2001). Two C or not two C: recurrent disruption of Zn-ribbons, gene duplication, lineage-specific gene loss, and horizontal gene transfer in evolution of bacterial ribosomal proteins. *Genome Biology*, 2, 1-12.
- Marchler-Bauer, A, Lu, S, Anderson, JB, Chitsaz, F, Derbyshire, MK, DeWeese-Scott, C, and Bryant, SH.** (2011). A Conserved Domain Database for the functional annotation of proteins. *Nucleic Acids Research*, 39, D225-229.
- Maret, W.** (2013). Zinc biochemistry: from a single zinc enzyme to a key element of life. *Advances in Nutrition*, 4, 82-91.
- Marti, S, Nait Chabane, Y, Alexandre, S, Coquet, L, Vila, J, Jouenne, T, and De, E.** (2011). Growth of *Acinetobacter baumannii* in pellicle enhanced the expression of potential virulence factors. *PLoS One*, 6, e26030.
- Matsushita, K, Arents, JC, Bader, R, Yamada, M, Adachi, O, and Postma, PW.** (1997). *Escherichia coli* is unable to produce pyrroloquinoline quinone (PQQ). *Microbiology*, 143 3149-3156.

- McConnell, MJ, Actis, L, and Pachon, J.** (2013). *Acinetobacter baumannii*: human infections, factors contributing to pathogenesis and animal models. *FEMS Microbiology Reviews*, 37, 130-155.
- McConnell, MJ, Perez-Ordóñez, A, Perez-Romero, P, Valencia, R, Lepe, JA, Vázquez-Barba, I, and Pachon, J.** (2012). Quantitative real-time PCR for detection of *Acinetobacter baumannii* colonization in the hospital environment. *Journal of Clinical Microbiology*, 50, 1412-1414.
- McDevitt, CA, Ogunniyi, AD, Valkov, E, Lawrence, MC, Kobe, B, McEwan, AG, and Paton, JC.** (2011). A molecular mechanism for bacterial susceptibility to zinc. *PLoS pathogens*, 7, e1002357.
- McQueary, CN, Kirkup, BC, Si, Y, Barlow, M, Actis, LA, Craft, DW, and Zurawski, DV.** (2012). Extracellular stress and lipopolysaccharide modulate *Acinetobacter baumannii* surface-associated motility. *Journal of Microbiology*, 50, 434-443.
- Membrillo-Hernandez, J, Kim, SO, Cook, GM, and Poole, RK.** (1997). Paraquat regulation of *hmp* (flavo-hemoglobin) gene expression in *Escherichia coli* K-12 is SoxRS independent but modulated by δ . *Journal of Bacteriology*, 179, 3164-3170.
- Misbah, S, Hassan, H, Yusof, MY, Hanifah, YA, and AbuBakar, S.** (2005). Genomic species identification of *Acinetobacter* of clinical isolates by 16S rDNA sequencing. *Singapore Medical Journal*, 46, 461-464.
- Misra, HS, Khairnar, NP, Barik, A, Indira Priyadarsini, K, Mohan, H, and Apte, SK.** (2004). Pyrroloquinoline-quinone: a reactive oxygen species scavenger in bacteria. *FEBS Letters*, 578, 26-30.
- Montanini, B, Blaudez, D, Jeandroz, S, Sanders, D, and Chalot, M.** (2007). Phylogenetic and functional analysis of the Cation Diffusion Facilitator (CDF) family: improved signature and prediction of substrate specificity. *BMC Genomics*, 8, 107.
- Mortensen, BL, Rathi, S, Chazin, WJ, and Skaar, EP.** (2014). *Acinetobacter baumannii* response to host-mediated zinc limitation requires the transcriptional regulator Zur. *Journal of Bacteriology*, 196, 2616-2626.
- Mortensen, BL, and Skaar, EP.** (2013). The contribution of nutrient metal acquisition and metabolism to *Acinetobacter baumannii* survival within the host. *Frontiers in Cellular and Infection Microbiology*, 3, 95.
- Motojima-Miyazaki, Y, Yoshida, M, and Motojima, F.** (2010). Ribosomal protein L2 associates with *E. coli* HtpG and activates its ATPase activity. *Biochemical and Biophysical Research Communications*, 400, 241-245.

- Muller, A, Leon-Kempis Mdel, R, Dodson, E, Wilson, KS, Wilkinson, AJ, and Kelly, DJ.** (2007). A bacterial virulence factor with a dual role as an adhesin and a solute-binding protein: the crystal structure at 1.5 Å resolution of the PEB1a protein from the food-borne human pathogen *Campylobacter jejuni*. *Journal of Molecular Biology*, 372, 160-171.
- Munoz-Price, LS, Fajardo-Aquino, Y, Arheart, KL, Cleary, T, DePascale, D, Pizano, L, Namias, N, Rivera, JI, O'Hara, JA, and Doi, Y.** (2013). Aerosolization of *Acinetobacter baumannii* in a trauma ICU. *Critical Care Medicine*, 41, 1915-1918.
- Murakami, S.** (2008). Multidrug efflux transporter, AcrB-the pumping mechanism. *Current Opinion in Structural Biology*, 18, 459-465.
- Naas, T, Coignard, B, Carbonne, A, Blanckaert, K, Bajolet, O, Bernet, C, Verdeil, X, Astagneau, P, Desenclos, JC, and Nordmann, P.** (2006). VEB-1 Extended-spectrum β -lactamase-producing *Acinetobacter baumannii*, France. *Emerging Infectious Diseases*, 12, 1214-1222.
- Nairn, BL, Lonergan, ZR, Wang, J, Braymer, JJ, Zhang, Y, Calcutt, MW, Lisher, JP, Gilston, BA, Chazin, WJ, de Crecy-Lagard, V, Giedroc, DP, and Skaar, EP.** (2016). The response of *Acinetobacter baumannii* to zinc starvation. *Cell Host & Microbe*, 19, 826-836.
- Nait Chabane, Y, Marti, S, Rihouey, C, Alexandre, S, Hardouin, J, Lesouhaitier, O, Vila, J, Kaplan, JB, Jouenne, T, and De, E.** (2014). Characterisation of pellicles formed by *Acinetobacter baumannii* at the air-liquid interface. *PLoS One*, 9, e111660.
- Nakamoto, H, Fujita, K, Ohtaki, A, Watanabe, S, Narumi, S, Maruyama, T, Suenaga, E, Misono, TS, Kumar, PK, Goloubinoff, P, and Yoshikawa, H.** (2014). Physical interaction between bacterial heat shock protein (Hsp) 90 and Hsp70 chaperones mediates their cooperative action to refold denatured proteins. *The Journal of Biological Chemistry*, 289, 6110-6119.
- Nanamiya, H, Akanuma, G, Natori, Y, Murayama, R, Kosono, S, Kudo, T, Kobayashi, K, Ogasawara, N, Park, SM, Ochi, K, and Kawamura, F.** (2004). Zinc is a key factor in controlling alternation of two types of L31 protein in the *Bacillus subtilis* ribosome. *Molecular Microbiology*, 52, 273-283.
- Nanamiya, H, Kawamura, F, and Kosono, S.** (2006). Proteomic study of the *Bacillus subtilis* ribosome: Finding of zinc-dependent replacement for ribosomal protein L31 paralogues. *The Journal of General and Applied Microbiology*, 52, 249-258.
- Napolitano, M, Rubio, MA, Santamaria-Gomez, J, Olmedo-Verd, E, Robinson, NJ, and Luque, I.** (2012). Characterization of the response to zinc deficiency in the cyanobacterium *Anabaena sp.* strain PCC 7120. *Journal of Bacteriology*, 194, 2426-2436.

- Natori, Y, Nanamiya, H, Akanuma, G, Kosono, S, Kudo, T, Ochi, K, and Kawamura, F.** (2007). A fail-safe system for the ribosome under zinc-limiting conditions in *Bacillus subtilis*. *Molecular Microbiology*, *63*, 294-307.
- Nevo, Y, and Nelson, N.** (2006). The NRAMP family of metal-ion transporters. *Biochimica et Biophysica Acta*, *1763*, 609-620.
- Ni, S, Li, S, Yang, N, Zhang, S, Hu, D, Li, Q, and Lu, M.** (2015). Post-neurosurgical meningitis caused by *Acinetobacter baumannii*: case series and review of the literature. *International Journal of Clinical and Experimental Medicine*, *8*, 21833-21838.
- Nielubowicz, GR, Smith, SN, and Mobley, HL.** (2010). Zinc uptake contributes to motility and provides a competitive advantage to *Proteus mirabilis* during experimental urinary tract infection. *Infection and Immunity*, *78*, 2823-2833.
- Nies, DH.** (1995). The cobalt, zinc, and cadmium efflux system CzcABC from *Alcaligenes eutrophus* functions as a cation-proton antiporter in *Escherichia coli*. *Journal of Bacteriology*, *177*, 2707-2712.
- Nigro, S, and Hall, RM.** (2015). Distribution of the blaOXA-23-containing transposons Tn2006 and Tn2008 in Australian carbapenem-resistant *Acinetobacter baumannii* isolates. *The Journal of Antimicrobial Chemotherapy*, *70*, 2409-2411.
- Nigro, SJ, and Hall, RM.** (2016). Loss and gain of aminoglycoside resistance in global clone 2 *Acinetobacter baumannii* in Australia via modification of genomic resistance islands and acquisition of plasmids. *The Journal of Antimicrobial Chemotherapy*, *71*, 2432-2440.
- Nikaido, H.** (2003). Molecular basis of bacterial outer membrane permeability revisited. *Microbiology and Molecular Biology Reviews*, *67*, 593-656.
- Norton, MD, Spilka, AJ, and Godoy, VG.** (2013). Antibiotic resistance acquired through a DNA damage-inducible response in *Acinetobacter baumannii*. *Journal of Bacteriology*, *195*, 1335-1345.
- Ong, CL, Walker, MJ, and McEwan, AG.** (2015). Zinc disrupts central carbon metabolism and capsule biosynthesis in *Streptococcus pyogenes*. *Scientific Reports*, *5*, 10799.
- Outten, CE, and O'Halloran, TV.** (2001). Femtomolar sensitivity of metalloregulatory proteins controlling zinc homeostasis. *Science*, *292*, 2488-2492.
- Outten, CE, Tobin, DA, Penner-Hahn, JE, and O'Halloran, TV.** (2001). Characterization of the metal receptor sites in *Escherichia coli* Zur, an ultrasensitive zinc(II) metalloregulatory protein. *Biochemistry*, *40*, 10417-10423.

- Owen, GA, Pascoe, B, Kallifidas, D, and Paget, MS. (2007). Zinc-responsive regulation of alternative ribosomal protein genes in *Streptomyces coelicolor* involves zur and δR . *Journal of Bacteriology*, 189, 4078-4086.
- Ozaki, T, Nishimura, N, Arakawa, Y, Suzuki, M, Narita, A, Yamamoto, Y, Koyama, N, Nakane, K, Yasuda, N, and Funahashi, K. (2009). Community-acquired *Acinetobacter baumannii* meningitis in a previously healthy 14-month-old boy. *Journal of Infection and Chemotherapy*, 15, 322-324.
- Paget, MS, Kang, JG, Roe, JH, and Buttner, MJ. (1998). δR , an RNA polymerase sigma factor that modulates expression of the thioredoxin system in response to oxidative stress in *Streptomyces coelicolor* A3(2). *The EMBO Journal*, 17, 5776-5782.
- Palmieri, M, Russo, L, Malgieri, G, Esposito, S, Baglivo, I, Rivellino, A, Farina, B, de Paola, I, Zaccaro, L, Milardi, D, Isernia, C, Pedone, PV, and Fattorusso, R. (2014). Deciphering the zinc coordination properties of the prokaryotic zinc finger domain: The solution structure characterization of Ros87 H42A functional mutant. *Journal of Inorganic Biochemistry*, 131, 30-36.
- Pandey, A, Benjamin, S, Soccol, CR, Nigam, P, Krieger, N, and Soccol, VT. (1999). The realm of microbial lipases in biotechnology. *Biotechnology and Applied Biochemistry*, 29 119-131.
- Panina, EM, Mironov, AA, and Gelfand, MS. (2003). Comparative genomics of bacterial zinc regulons: enhanced ion transport, pathogenesis, and rearrangement of ribosomal proteins. *Proceedings of the National Academy of Sciences of the United States of America*, 100, 9912-9917.
- Parish, T, and Stoker, NG. (2002). The common aromatic amino acid biosynthesis pathway is essential in *Mycobacterium tuberculosis*. *Microbiology*, 148, 3069-3077.
- Patel, R, J., Sahgal, S, P., Mortazavi, Vyas, Y, K, , Adam, R, J., and Antonios, V, S. (2011). Hematogenous osteomyelitis by *Acinetobacter Baumannii*: Case report and literature review. *Scientific Research*, 1, 23-27.
- Patzer, SI, and Hantke, K. (1998). The ZnuABC high-affinity zinc uptake system and its regulator Zur in *Escherichia coli*. *Molecular Microbiology*, 28, 1199-1210.
- Patzer, SI, and Hantke, K. (2000). The zinc-responsive regulator Zur and its control of the znu gene cluster encoding the ZnuABC zinc uptake system in *Escherichia coli*. *The Journal of Biological Chemistry*, 275, 24321-24332.
- Pawlik, MC, Hubert, K, Joseph, B, Claus, H, Schoen, C, and Vogel, U. (2012). The zinc-responsive regulon of *Neisseria meningitidis* comprises 17 genes under control of a Zur element. *Journal of Bacteriology*, 194, 6594-6603.

- Pederick, VG, Eijkelkamp, BA, Begg, SL, Ween, MP, McAllister, LJ, Paton, JC, and McDevitt, CA.** (2015). ZnuA and zinc homeostasis in *Pseudomonas aeruginosa*. *Scientific Reports*, 5, 13139.
- Peleg, AY, de Breij, A, Adams, MD, Cerqueira, GM, Mocali, S, Galardini, M, Nibbering, PH, Earl, AM, Ward, DV, Paterson, DL, Seifert, H, and Dijkshoorn, L.** (2012). The success of *Acinetobacter* species; genetic, metabolic and virulence attributes. *PLoS One*, 7, e46984.
- Peleg, AY, Seifert, H, and Paterson, DL.** (2008). *Acinetobacter baumannii*: emergence of a successful pathogen. *Clinical Microbiology Reviews*, 21, 538-582.
- Perez, F, Hujer, AM, Hujer, KM, Decker, BK, Rather, PN, and Bonomo, RA.** (2007). Global challenge of multidrug-resistant *Acinetobacter baumannii*. *Antimicrobial Agents and Chemotherapy*, 51, 3471-3484.
- Perron, K, Caille, O, Rossier, C, Van Delden, C, Dumas, JL, and Kohler, T.** (2004). CzcR-CzcS, a two-component system involved in heavy metal and carbapenem resistance in *Pseudomonas aeruginosa*. *The Journal of Biological Chemistry*, 279, 8761-8768.
- Poole, K.** (2005). Aminoglycoside resistance in *Pseudomonas aeruginosa*. *Antimicrobial Agents and Chemotherapy*, 49, 479-487.
- Porcheron, G, Garenaux, A, Proulx, J, Sabri, M, and Dozois, CM.** (2013). Iron, copper, zinc, and manganese transport and regulation in pathogenic Enterobacteria: correlations between strains, site of infection and the relative importance of the different metal transport systems for virulence. *Frontiers in Cellular and Infection Microbiology*, 3, 90.
- Pour, NK, Dusane, DH, Dhakephalkar, PK, Zamin, FR, Zinjarde, SS, and Chopade, BA.** (2011). Biofilm formation by *Acinetobacter baumannii* strains isolated from urinary tract infection and urinary catheters. *FEMS Immunology and Medical Microbiology*, 62, 328-338.
- Price, CT, Richards, AM, and Abu Kwaik, Y.** (2014). Nutrient generation and retrieval from the host cell cytosol by intra-vacuolar *Legionella pneumophila*. *Frontiers in Cellular and Infection Microbiology*, 4, 111.
- Raad, I, Reitzel, R, Jiang, Y, Chemaly, RF, Dvorak, T, and Hachem, R.** (2008). Anti-adherence activity and antimicrobial durability of anti-infective-coated catheters against multidrug-resistant bacteria. *The Journal of Antimicrobial chemotherapy*, 62, 746-750.
- Raedts, J, Siemerink, MA, Levisson, M, van der Oost, J, and Kengen, SW.** (2014). Molecular characterization of an NADPH-dependent acetoin reductase/2,3-butanediol dehydrogenase from *Clostridium beijerinckii* NCIMB 8052. *Applied and Environmental Microbiology*, 80, 2011-2020.

- Rao, RS, Karthika, RU, Singh, SP, Shashikala, P, Kanungo, R, Jayachandran, S, and Prashanth, K. (2008). Correlation between biofilm production and multiple drug resistance in imipenem resistant clinical isolates of *Acinetobacter baumannii*. *Indian Journal of Medical Microbiology*, 26, 333-337.
- Ray, A, Perez, F, Beltramini, AM, Jakubowycz, M, Dimick, P, Jacobs, MR, Roman, K, Bonomo, RA, and Salata, RA. (2010). Use of vaporized hydrogen peroxide decontamination during an outbreak of multidrug-resistant *Acinetobacter baumannii* infection at a long-term acute care hospital. *Infection Control and Hospital Epidemiology*, 31, 1236-1241.
- Ray, PD, Huang, BW, and Tsuji, Y. (2012). Reactive oxygen species (ROS) homeostasis and redox regulation in cellular signaling. *Cell Signal*, 24, 981-990.
- Rensing, C, Mitra, B, and Rosen, BP. (1997). The *zntA* gene of *Escherichia coli* encodes a Zn(II)-translocating P-type ATPase. *Proceedings of the National Academy of Sciences of the United States of America*, 94, 14326-14333.
- Reyes-Caballero, H, Campanello, GC, and Giedroc, DP. (2011). Metalloregulatory proteins: metal selectivity and allosteric switching. *Biophysical Chemistry*, 156, 103-114.
- Roca, I, Espinal, P, Vila-Farres, X, and Vila, J. (2012). The *Acinetobacter baumannii* oxymoron: commensal hospital dweller turned pan-drug-resistant menace. *Frontiers in Microbiology*, 3, 148.
- Rosenau, F, and Jaeger, K. (2000). Bacterial lipases from *Pseudomonas*: regulation of gene expression and mechanisms of secretion. *Biochimie*, 82, 1023-1032.
- Ruiz, FM, Santillana, E, Spinola-Amilibia, M, Torreira, E, Culebras, E, and Romero, A. (2015). Crystal Structure of Hcp from *Acinetobacter baumannii*: a component of the Type VI secretion system. *PLoS One*, 10, e0129691.
- Rumbo-Feal, S, Gomez, MJ, Gayoso, C, Alvarez-Fraga, L, Cabral, MP, Aransay, AM, Rodriguez-Ezpeleta, N, Fullaondo, A, Valle, J, Tomas, M, Bou, G, and Poza, M. (2013). Whole transcriptome analysis of *Acinetobacter baumannii* assessed by RNA-sequencing reveals different mRNA expression profiles in biofilm compared to planktonic cells. *PLoS One*, 8, e72968.
- Rumbo, C, Fernandez-Moreira, E, Merino, M, Poza, M, Mendez, JA, Soares, NC, Mosquera, A, Chaves, F, and Bou, G. (2011). Horizontal transfer of the OXA-24 carbapenemase gene via outer membrane vesicles: a new mechanism of dissemination of carbapenem resistance genes in *Acinetobacter baumannii*. *Antimicrobial Agents and Chemotherapy*, 55, 3084-3090.
- Russo, TA, Luke, NR, Beanan, JM, Olson, R, Sauberan, SL, MacDonald, U, Schultz, LW, Umland, TC, and Campagnari, AA. (2010). The K1 capsular polysaccharide of *Acinetobacter baumannii* strain 307-0294 is a major virulence factor. *Infection and Immunity*, 78, 3993-4000.

- Sabri, M, Houle, S, and Dozois, CM.** (2009). Roles of the extraintestinal pathogenic *Escherichia coli* ZnuACB and ZupT zinc transporters during urinary tract infection. *Infection and Immunity*, 77, 1155-1164.
- Salameh, MA, and Wiegel, J.** (2007). Purification and characterization of two highly thermophilic alkaline lipases from *Thermosyntropha lipolytica*. *Applied and Environmental Microbiology*, 73, 7725-7731.
- Schmitt, MP, Twiddy, EM, and Holmes, RK.** (1992). Purification and characterization of the diphtheria toxin repressor. *Proceedings of the National Academy of Sciences of the United States of America*, 89, 7576-7580.
- Schoolnik, GK, Martin I. Voskuil, Dirk Schnappinger, Fitnat H. yildiz, Karin Meibom, Nadia A. Dolganov, Michael A. Wilson, Kimberly H. Chong.** (2001). Whole genome DNA microarray expression analysis of biofilm development by *Vibrio cholerae* O1 El Tor. *Methods in Enzymology*, 336, 3-18.
- Schwarz, S, Singh, P, Robertson, JD, LeRoux, M, Skerrett, SJ, Goodlett, DR, West, TE, and Mougous, JD.** (2014). VgrG-5 is a *Burkholderia* type VI secretion system-exported protein required for multinucleated giant cell formation and virulence. *Infection and Immunity*, 82, 1445-1452.
- Schwarz, S, West, TE, Boyer, F, Chiang, WC, Carl, MA, Hood, RD, Rohmer, L, Tolker-Nielsen, T, Skerrett, SJ, and Mougous, JD.** (2010). *Burkholderia* type VI secretion systems have distinct roles in eukaryotic and bacterial cell interactions. *PLoS Pathogens*, 6, e1001068.
- Sebkova, A, Karasova, D, Crhanova, M, Budinska, E, and Rychlik, I.** (2008). *aro* mutations in *Salmonella enterica* cause defects in cell wall and outer membrane integrity. *Journal of Bacteriology*, 190, 3155-3160.
- Seifert, H, Dijkshoorn, L, Gerner-Smidt, P, Pelzer, N, Tjernberg, I, and Vanechoutte, M.** (1997). Distribution of *Acinetobacter* species on human skin: comparison of phenotypic and genotypic identification methods. *Journal of Clinical Microbiology*, 35, 2819-2825.
- Sein-Echaluce, VC, Gonzalez, A, Napolitano, M, Luque, I, Barja, F, Peleato, ML, and Fillat, MF.** (2015). Zur (FurB) is a key factor in the control of the oxidative stress response in *Anabaena* sp. PCC 7120. *Environmental Microbiology*, 17, 2006-2017.
- Sganga, MW, Aksamit, RR, Cantoni, GL, and Bauer, CE.** (1992). Mutational and nucleotide sequence analysis of S-adenosyl-L-homocysteine hydrolase from *Rhodobacter capsulatus*. *Proceedings of the National Academy of Sciences of the United States of America*, 89, 6328-6332.
- Shafeeq, S, Kloosterman, TG, and Kuipers, OP.** (2011). Transcriptional response of *Streptococcus pneumoniae* to Zn²⁺ limitation and the repressor/activator function of AdcR. *Metallomics*, 3, 609-618.

- Shin, JH, Oh, SY, Kim, SJ, and Roe, JH.** (2007). The zinc-responsive regulator Zur controls a zinc uptake system and some ribosomal proteins in *Streptomyces coelicolor* A3(2). *Journal of Bacteriology*, 189, 4070-4077.
- Sigdel, TK, Easton, JA, and Crowder, MW.** (2006). Transcriptional response of *Escherichia coli* to TPEN. *Journal of Bacteriology*, 188, 6709-6713.
- Singh, VK, Xiong, A, Usgaard, TR, Chakrabarti, S, Deora, R, Misra, TK, and Jayaswal, RK.** (1999). ZntR is an autoregulatory protein and negatively regulates the chromosomal zinc resistance operon znt of *Staphylococcus aureus*. *Molecular Microbiology*, 33, 200-207.
- Smani, Y, McConnell, MJ, and Pachon, J.** (2012). Role of fibronectin in the adhesion of *Acinetobacter baumannii* to host cells. *PLoS One*, 7, e33073.
- Smith, AW, Roche, H, Trombe, MC, Briles, DE, and Hakansson, A.** (2002). Characterization of the dihydrolipoamide dehydrogenase from *Streptococcus pneumoniae* and its role in pneumococcal infection. *Molecular Microbiology*, 44, 431-448.
- Smith, KF, Bibb, LA, Schmitt, MP, and Oram, DM.** (2009). Regulation and activity of a zinc uptake regulator, Zur, in *Corynebacterium diphtheriae*. *Journal of Bacteriology*, 191, 1595-1603.
- Smith, MG, Gianoulis, TA, Pukatzki, S, Mekalanos, JJ, Ornston, LN, Gerstein, M, and Snyder, M.** (2007). New insights into *Acinetobacter baumannii* pathogenesis revealed by high-density pyrosequencing and transposon mutagenesis. *Genes & Development*, 21, 601-614.
- Snitkin, ES, Zelazny, AM, Montero, CI, Stock, F, Mijares, L, Program, NCS, Murray, PR, and Segre, JA.** (2011). Genome-wide recombination drives diversification of epidemic strains of *Acinetobacter baumannii*. *Proceedings of the National Academy of Sciences of the United States of America*, 108, 13758-13763.
- Solak, Y, Atalay, H, Turkmen, K, Biyik, Z, Genc, N, and Yeksan, M.** (2011). Community-acquired carbapenem-resistant *Acinetobacter baumannii* urinary tract infection just after marriage in a renal transplant recipient. *Transplant Infectious Disease* 13, 638-640.
- Somerville, GA, and Proctor, RA.** (2009). At the crossroads of bacterial metabolism and virulence factor synthesis in Staphylococci. *Microbiology and Molecular Biology Reviews*, 73, 233-248.
- Sowmiya, M, Umashankar, V, Muthukumaran, S, Madhavan, HN, and Malathi, J.** (2012). Studies on New Delhi Metallo-Beta-Lactamase-1 producing *Acinetobacter baumannii* isolated from donor swab in a tertiary eye care centre, India and structural analysis of its antibiotic binding interactions. *Bioinformation*, 8, 445-452.

- Stahler, FN, Odenbreit, S, Haas, R, Wilrich, J, Van Vliet, AH, Kusters, JG, Kist, M, and Bereswill, S.** (2006). The novel *Helicobacter pylori* CznABC metal efflux pump is required for cadmium, zinc, and nickel resistance, urease modulation, and gastric colonization. *Infection and Immunity*, 74, 3845-3852.
- Stehra, F, Kretschmarb, M, Krögera, C, Hubea, B, and Schäfera, W.** (2003). Microbial lipases as virulence factors. *Journal of Molecular Catalysis B: Enzymatic*, 22, 347–355.
- Stojiljkovic, I, Baumler, AJ, and Hantke, K.** (1994). Fur regulon in gram-negative bacteria. Identification and characterization of new iron-regulated *Escherichia coli* genes by a *fur* titration assay. *Journal of Molecular Biology*, 236, 531-545.
- Stork, M, Bos, MP, Jongerius, I, de Kok, N, Schilders, I, Weynants, VE, Poolman, JT, and Tommassen, J.** (2010). An outer membrane receptor of *Neisseria meningitidis* involved in zinc acquisition with vaccine potential. *PLoS Pathogens*, 6, e1000969.
- Tamilselvi, A, and Mugesh, G.** (2008). Zinc and antibiotic resistance: metallo- β -lactamases and their synthetic analogues. *Journal of Biological Inorganic Chemistry*, 13, 1039-1053.
- Tekin, R, Dal, T, Bozkurt, F, Deveci, O, Palanc, Y, Arslan, E, Selcuk, CT, and Hosoglu, S.** (2014). Risk factors for nosocomial burn wound infection caused by multidrug resistant *Acinetobacter baumannii*. *Journal of Burn Care & Research* 35, e73-80.
- Tomaras, AP, Dorsey, CW, Edelmann, RE, and Actis, LA.** (2003). Attachment to and biofilm formation on abiotic surfaces by *Acinetobacter baumannii*: involvement of a novel chaperone-usher pili assembly system. *Microbiology*, 149, 3473-3484.
- Tomaras, AP, Flagler, MJ, Dorsey, CW, Gaddy, JA, and Actis, LA.** (2008). Characterization of a two-component regulatory system from *Acinetobacter baumannii* that controls biofilm formation and cellular morphology. *Microbiology*, 154, 3398-3409.
- Towner, KJ.** (2009). *Acinetobacter*: an old friend, but a new enemy. *The Journal of Hospital Infection*, 73, 355-363.
- Valencia, EY, Braz, VS, Guzzo, C, and Marques, MV.** (2013). Two RND proteins involved in heavy metal efflux in *Caulobacter crescentus* belong to separate clusters within proteobacteria. *BMC Microbiology*, 13, 79.

- Valentine, SC, Contreras, D, Tan, S, Real, LJ, Chu, S, and Xu, HH.** (2008). Phenotypic and molecular characterization of *Acinetobacter baumannii* clinical isolates from nosocomial outbreaks in Los Angeles County, California. *Journal of Clinical Microbiology*, 46, 2499-2507.
- Vassinova, N, and Kozyrev, D.** (2000). A method for direct cloning of *fur*-regulated genes: identification of seven new *fur*-regulated loci in *Escherichia coli*. *Microbiology*, 146 Pt 12, 3171-3182.
- Vila, J, and Pachon, J.** (2011). *Acinetobacter baumannii* resistant to everything: what should we do? *Clinical Microbiology and Infection*, 17, 955-956.
- Villegas, MV, and Hartstein, AI.** (2003). *Acinetobacter* outbreaks, 1977-2000. *Infection Control and Hospital Epidemiology*, 24, 284-295.
- Waldron, KJ, and Robinson, NJ.** (2009). How do bacterial cells ensure that metalloproteins get the correct metal? *Nature Reviews Microbiology*, 7, 25-35.
- Wang, D, Hosteen, O, and Fierke, CA.** (2012). ZntR-mediated transcription of *zntA* responds to nanomolar intracellular free zinc. *Journal of Inorganic Biochemistry*, 111, 173-181.
- Weber, Bruckner, C, Weinreb, S, Lehr, C, Essl, C, and Boles, E.** (2012). Biosynthesis of *cis,cis*-muconic acid and its aromatic precursors, catechol and protocatechuic acid, from renewable feedstocks by *Saccharomyces cerevisiae*. *Applied and Environmental Microbiology*, 78, 8421-8430.
- Weber, BS, Miyata, ST, Iwashkiw, JA, Mortensen, BL, Skaar, EP, Pukatzki, S, and Feldman, MF.** (2013). Genomic and functional analysis of the type VI secretion system in *Acinetobacter*. *PLoS One*, 8, e55142.
- Weinberg, ED.** (2009). Iron availability and infection. *Biochimica et Biophysica Acta*, 1790, 600-605.
- Wilson, DN.** (2014). Ribosome-targeting antibiotics and mechanisms of bacterial resistance. *Nature Reviews Microbiology*, 12, 35-48.
- Wu, C, Labrie, J, Tremblay, YD, Haine, D, Mourez, M, and Jacques, M.** (2013). Zinc as an agent for the prevention of biofilm formation by pathogenic bacteria. *Journal of Applied Microbiology*, 115, 30-40.
- Wu, HJ, Seib, KL, Srihanta, YN, Kidd, SP, Edwards, JL, Maguire, TL, Grimmond, SM, Apicella, MA, McEwan, AG, and Jennings, MP.** (2006). PerR controls Mn-dependent resistance to oxidative stress in *Neisseria gonorrhoeae*. *Molecular Microbiology*, 60, 401-416.

- Xiao, Z, and Xu, P.** (2007). Acetoin metabolism in bacteria. *Critical Reviews in Microbiology*, 33, 127-140.
- Yamamoto, S, Okujo, N, and Sakakibara, Y.** (1994). Isolation and structure elucidation of acinetobactin, a novel siderophore from *Acinetobacter baumannii*. *Archive Microbiology*, 162, 249-254.
- Yan, L, Cerny, RL, and Cirillo, JD.** (2004). Evidence that *hsp90* is involved in the altered interactions of *Acanthamoeba castellanii* variants with bacteria. *Eukaryotic Cell*, 3, 567-578.
- Yan, LJ, Thangthaeng, N, Sumien, N, and Forster, MJ.** (2013). Serum dihydrolipoamide dehydrogenase is a labile enzyme. *Journal of Biochemical and Pharmacological Research*, 1, 30-42.
- Yoneyama, H, and Nakae, T.** (1996). Protein C (OprC) of the outer membrane of *Pseudomonas aeruginosa* is a copper-regulated channel protein. *Microbiology*, 142 (Pt 8), 2137-2144.
- Zarrilli, R, Pournaras, S, Giannouli, M, and Tsakris, A.** (2013). Global evolution of multidrug-resistant *Acinetobacter baumannii* clonal lineages. *International Journal of Antimicrobial Agents*, 41, 11-19.
- Zhou, Y, Tao, J, Yu, H, Ni, J, Zeng, L, Teng, Q, Kim, KS, Zhao, GP, Guo, X, and Yao, Y.** (2012). Hcp family proteins secreted via the type VI secretion system coordinately regulate *Escherichia coli* K1 interaction with human brain microvascular endothelial cells. *Infection and Immunity*, 80, 1243-1251.